UNIVERSIDADE DE SÃO PAULO
CENTRO DE ENERGIA NUCLEAR NA AGRICULTURA

HENRIQUE NERY CIPRIANI

Soil quality and microbiota associated with integrated production and pasture systems in Western Amazonia

Piracicaba, SP
2026

HENRIQUE NERY CIPRIANI

Soil quality and microbiota associated with integrated production and pasture systems in Western Amazonia

Versão revisada de acordo com a Resolução CoPGr 6018 de 2011

Thesis presented to the Centro de Energia Nuclear na Agricultura, Universidade de São Paulo, in partial fulfillment of the requirements for the degree of Doctor in Sciences.

Concentration Area: Biology in Agriculture and Environment

Advisor: Dr. Tsai Siu Mui

Piracicaba, SP

2026

Dados Internacionais de Catalogação na Publicação (CIP)

Seção Técnica de Biblioteca - CENA/USP

Cipriani, Henrique Nery

Qualidade do solo e microbiota associada a sistemas integrados de produção e pastagens na Amazônia Ocidental / Soil quality and microbiota associated with integrated production and pasture systems in Western Amazonia / Henrique Nery Cipriani; orientadora Tsai Siu Mui. - - Versão revisada de acordo com a Resolução CoPGr 6018 de 2011. - - Piracicaba, 2026.

163 p.

Tese (Doutorado – Programa de Pós-Graduação em Ciências. Área de Concentração: Biologia na Agricultura e no Ambiente) – Centro de Energia Nuclear na Agricultura da Universidade de São Paulo.

1. Microbiologia do solo 2. Pastagens 3. Produção agrícola 4. Qualidade do solo 5. Sequestro de carbono 6. Sistemas agrossilvopastoris I. Título

CDU 631.41 : 631.153.7

Elaborada por:
Marilia Ribeiro Garcia Henyei
CRB-8/3631
Resolução CFB Nº 184 de 29 de setembro de 2017

ACKNOWLEDGEMENTS

I give thanks to the Sacred Hearts of Jesus and Mary, sources of Life, consolation in times of tribulation, and the foundation and reason of my existence.

I am deeply grateful to my parents who, after God, were responsible for the gift of my life.

I thank my wife and children, my inseparable companions, who supported me both physically and psychologically throughout the course of my doctoral studies.

I sincerely thank Prof. Tsai Siu Mui for her academic guidance and friendship throughout my doctoral studies.

I am grateful to the technicians of the Laboratório de Biologia Celular e Molecular, Andreia and Fabio, for their guidance and assistance on several occasions during laboratory work, and especially to Wagner for his help with soil sampling in April 2024. I also thank the laboratory trainees Giovanna, Júlia, Laura, Letícia, Yuri, Teresa and Vitor for the assistance with DNA extraction and enzyme activity assays.

I am thankful to Prof. Lucas Mendes and the many colleagues I met in Laboratório de Biologia Celular between 2022 and 2025 (Ana Vitória, Anderson, Beatriz, Caciara, Camille, Danielle, Deisi, Dominique, Eduardo, Fabiana, Franciele, Gabriel, Guilherme, Gustavo, Iara, Izadora, Jéssica, Juan, Lara, Luana, Luís Felipe, Luís Merlotti, Maike, Maycon, Rafael Destro, Rafael do Açúcar, Sayuri, Solange, Thierry and Wanderlei) for the constant exchange of knowledge and for their patience and companionship in daily interactions. The lab was like a second home for me.

I thank the staff of the Campo Experimental de Porto Velho (Embrapa Rondônia), Aldenir, Aldoir, Adauto, Celso, Claudir, Delvino, Deniz, Francisco, Hebson, Iraque, Jânio, José Augusto, José Ribamar, Judivaldo, Manoel, Marcelo, Ricardo, Sally, Walfredo e Wanderley, for maintaining the experimental areas and for their support during the field sampling campaigns of 2022, 2023, and 2024, particularly the technician Paulo Marcante for coordinating the fieldwork activities. I also thank Dr. Ana Karina, for the supervision of the experimental areas and collaborative research, and her doctoral students, Elaine and Wéllen, for their aid in sample collection and data sharing.

I am grateful to Mr. Laércio Monteiro Filho for preparing the original sketch used in Figure 2.1, which served as the basis for the final illustrative figure presented in this thesis.

I thank Ms. Marília Henyei, from the CENA Library, for formatting, revising the layout, and preparing the cataloging-in-publication (CIP) data for the thesis.

I thank M.Sc. Vanderlei dos Reis, from Embrapa Pantanal, for his assistance with the thesis submission.

I am grateful to CENA, ESALQ, and USP for providing such a rich and rewarding doctoral experience, specially to the Laboratório de Biologia Celular e Molecular, which provided, space, material, and financial resources to most of the analysis.

I thank Embrapa for granting me the opportunity and institutional support to pursue my doctoral studies through its Corporate Stricto Sensu Graduate Program.

I thank the Laboratório Nacional de Agro-Fotônica (LANAF, Embrapa Instrumentação), especially Dr. Ladislau Martin Neto and Dr. Vitor Freitas, for enabling the analyses of the humification index (H_{LIFS}).

I thank the Laboratório de Isótopos Estáveis (LIE, USP/CENA) for conducting the analyses of total C and $\delta^{13}C$.

I acknowledge the financial support provided by FAPERO, FAPESP, and CNPq for the development of this research.

Finally, I thank all those who will read this work.

ABSTRACT

CIPRIANI, H. N. **Soil quality and microbiota associated with integrated production and pasture systems in Western Amazonia**. 2026. 163 p. Thesis (PhD in Sciences) – Centro de Energia Nuclear na Agricultura, Universidade de São Paulo, Piracicaba, 2026.

The conversion of Amazonian forests into extensive pastures has driven soil degradation, biotic homogenization and carbon losses. To tackle these challenges, integrated production systems have emerged as an important strategy. This thesis analyzed the impact of different land-use systems, including integrated livestock-forestry (ILF) with native (*Samanea tubulosa*) and exotic (*Eucalyptus pellita*) trees, integrated crop-livestock (ICL), integrated crop-livestock-forestry (ICLF), and treeless pastures, on the structure and function of the soil microbiome, soil quality indices (SQI), and carbon (C) sequestration potential in Western Amazonia (Porto Velho, Rondônia State, Brazil). The first study characterized the soil microbiota in vertical profiles (up to 40 cm). Results showed that the integration of the native legume *S. tubulosa* (ILF-ST) promoted greater recovery of microbial diversity and functional connectivity compared to eucalyptus and monoculture pastures. The ILF-ST system was enriched with nitrogen-fixing bacteria and favored complex carbon degradation pathways. In contrast, ILF with *E. pellita* (ILF-EP) created a niche dominated by ectomycorrhizal fungi, reflecting niche filtering rather than broad ecosystem restoration. Cross-kingdom co-occurrence networks indicated that, although monoculture pasture exhibited high connectivity, it lacked the modular stability and fungi/prokaryote ratio seen in integrated systems and native forest, suggesting greater structural fragility. The second study assessed soil health by integrating chemical, physical and biological indicators into composite SQIs over two years (2023 and 2024). All systems maintained high functional stability, decoupling livestock production from the traditional cycle of soil exhaustion. In 2024, the ILF-ST system stood out as the most resilient, with better scores for acidity regulation and organic matter, avoiding compaction observed near eucalyptus in ILF-EP. Well-managed treeless pastures (e.g., 'Ipyporã') demonstrated competitive quality, indicating viability for sustainable intensification when well managed. The third study assessed the potential for soil C sequestration. The ILF-ST system, at 21 m from the tree line, achieved the highest C content (4.35 dag kg^{-1}) and stocks (95.3 t ha^{-1}), surpassing the native forest (78.1 t ha^{-1}) in deeper layers. The Carbon Management Index (CMI) confirmed that only ILF-ST reached or exceeded the carbon quality of native forests (CMI ≥ 100). The

isotopic composition ($\delta^{13}C$) indicated faster carbon renewal in ICLF, while ILF systems provided more stable environments. In summary, although all systems evaluated offer improvements over degraded pastures, the choice of tree species is crucial. The integration of native legumes such as *S. tubulosa* is superior for restoring soil biological quality, maintaining spatial resilience, and optimizing carbon sequestration. These results indicate that the transition to sustainable livestock in the Amazon must prioritize native species and maintain the conservation of natural ecosystems to ensure long-term ecological resilience.

Keywords: Carbon sequestration. *Samanea tubulosa*. Soil health. Soil microbiome. Silvopastoral systems.

RESUMO

CIPRIANI, H. N. **Qualidade do solo e microbiota associada a sistemas integrados de produção e pastagens na Amazônia Ocidental**. 2026. 163 p. Tese (Doutorado em Ciências) – Centro de Energia Nuclear na Agricultura, Universidade de São Paulo, Piracicaba, 2026.

A conversão de florestas amazônicas em pastagens extensivas tem impulsionado a degradação do solo, homogeneização biótica e perdas de carbono. Para enfrentar esses desafios, sistemas integrados de produção surgem como estratégia importante. Esta tese analisou o impacto de diferentes sistemas de uso da terra, incluindo integração pecuária-floresta (IPF) com árvores nativas (*Samanea tubulosa*) e exóticas (*Eucalyptus pellita*), integração lavoura-pecuária (ILP), integração lavoura-pecuária-floresta (ILPF) e pastagens sem árvores, sobre a estrutura e função do microbioma do solo, índices de qualidade do solo (IQS) e potencial de sequestro de carbono (C) na Amazônia Ocidental (Porto Velho, Rondônia, Brasil). O primeiro estudo caracterizou a microbiota do solo em perfis verticais (até 40 cm). Os resultados mostraram que a integração da leguminosa nativa *S. tubulosa* (IPF-ST) promoveu maior recuperação da diversidade microbiana e conectividade funcional em relação ao eucalipto e às pastagens em monocultivo. O sistema IPF-ST foi enriquecido com bactérias fixadoras de nitrogênio e favoreceu vias complexas de degradação de carbono. Em contraste, a IPF com *E. pellita* (IPF-EP) criou um nicho dominado por fungos ectomicorrízicos, refletindo filtragem de nicho em vez de restauração ecossistêmica ampla. Redes de coocorrência multirreinos indicaram que, embora a pastagem em monocultivo apresentasse alta conectividade, faltava estabilidade modular e relação fungos/procariontes vistas nos sistemas integrados e floresta nativa, sugerindo maior fragilidade estrutural. O segundo estudo avaliou a saúde do solo integrando indicadores químicos, físicos e biológicos em IQS compostos durante dois anos (2023 and 2024). Todos os sistemas mantiveram alta estabilidade funcional, desvinculando a produção pecuária do ciclo tradicional de exaustão do solo. Em 2024, o sistema IPF-ST destacou-se como o mais resiliente, com melhores escores de regulação de acidez e matéria orgânica, evitando compactação observada próximo ao eucalipto no IPF-EP. Pastagens sem árvores, bem manejadas (ex.: 'Ipyporã'), demonstraram qualidade competitiva, indicando viabilidade para intensificação sustentável quando bem manejadas. O terceiro estudo avaliou o potencial de sequestro de C no solo. O sistema IPF-ST, a 21 m da linha de árvores, atingiu o maior teor de C (4,35 dag kg^{-1}) e estoques (95,3 t ha^{-1}), superando a floresta nativa (78,1 t ha^{-1}) nas camadas

profundas. O Índice de Manejo de Carbono (IMC) confirmou que apenas o IPF-ST atingiu ou superou a qualidade de carbono das florestas nativas (IMC ≥ 100). A composição isotópica ($\delta^{13}C$) indicou renovação mais rápida de carbono no ILPF, enquanto os sistemas IPF proporcionaram ambientes mais estáveis. Em síntese, embora todos os sistemas avaliados ofereçam melhorias sobre pastagens degradadas, a escolha da espécie arbórea é determinante. A integração de leguminosas nativas como *S. tubulosa* é superior para restaurar a qualidade biológica do solo, manter resiliência espacial e otimizar o sequestro de carbono. Esses resultados indicam que a transição para pecuária sustentável na Amazônia deve priorizar espécies nativas e manter a conservação dos ecossistemas naturais para garantir resiliência ecológica a longo prazo.

Palavras-chave: Microbioma do solo. *Samanea tubulosa*. Saúde do solo. Sequestro de carbono. Sistemas silvipastoris.

SUMMARY

1 INTRODUCTION

The Amazon rainforest plays a critical role in global climate regulation and biodiversity conservation. However, over the past decades, the expansion of extensive cattle ranching has been a primary driver of land-use change in the region. In states like Rondônia, in Western Amazonia, livestock production is not merely an agricultural activity but a cornerstone of the regional economy, providing livelihoods, food security, and driving local development. Given its socio-economic importance, the challenge is not to abolish cattle ranching, but to transition from traditional, low-productivity models to sustainable intensification strategies.

Historically, the conversion of primary forests into extensive, unmanaged pastures has led to severe environmental consequences, including soil degradation and significant losses of soil organic carbon. However, monoculture pasture systems should not be overlooked; when coupled with appropriate management practices, such as soil fertility correction, the use of improved forage cultivars, and controlled grazing, they can maintain high productivity and ensure soil stability. Therefore, sustainable intensification in the Amazon encompasses a spectrum of solutions, ranging from well-managed specialized pastures to high-complexity integrated systems.

A key element in these intensified systems is the inclusion of the forest component. While exotic species like *Eucalyptus* spp. are widely used due to their rapid growth, there is a growing interest in using native tree species, such as the legume *Samanea tubulosa* (bordão-de-velho). Native trees may offer superior ecological benefits, including nitrogen fixation and the creation of favorable microclimates for soil life, yet their specific impact on soil health and microbial dynamics compared to exotic species remains under-researched.

Soil health is a multi-dimensional concept, and the soil microbiome is a sensitive indicator of environmental change. Understanding how different integrated systems reshape the taxonomic and functional architecture of the soil microbiome, especially across vertical soil profiles, is essential to ensure the long-term viability of sustainable livestock. Furthermore, the potential for soil carbon (C) sequestration is a vital ecosystem service that can transform the image of Amazonian ranching from a source of emissions to a potential carbon sink.

Therefore, the general objective of this thesis is to evaluate the potential of sustainable intensification strategies, ranging from well-managed pastures to complex integrated crop-livestock-forestry systems, as a pathway to reconcile beef production with soil health

restoration, microbial diversity recovery, and carbon sequestration in Western Amazonia, with a special emphasis on the functional role of the native legume *S. tubulosa*.

To achieve this objective, three interconnected studies are presented: Chapter 1 explores how the transition from forest to integrated systems affects the diversity, functional potential, and co-occurrence networks of the soil microbiota; Chapter 2 integrates chemical, physical, and biological indicators into holistic soil quality indices (SQI) to assess the overall health and resilience of these systems over time; and Chapter 3 quantifies the potential for soil carbon sequestration and evaluates the quality of soil organic matter, comparing native forest fragments with intensified and conventional production models. By integrating these perspectives, this research seeks to demonstrate that sustainable intensification through integrated systems is a robust strategy to maintain the economic vitality of Amazonian ranching while restoring soil health and mitigating climate change.

2 STRUCTURE, DIVERSITY AND ECOLOGICAL FUNCTIONS OF SOIL MICROBIOTA IN INTEGRATED PRODUCTION AND PASTURE SYSTEMS IN WESTERN AMAZONIA

ABSTRACT

The conversion of primary Amazonian forests into extensive pastures has driven significant soil degradation and biotic homogenization. Integrated livestock-forestry (ILF) systems are emerging as sustainable alternatives to restore soil health, yet the specific role of different tree species, such as native legumes versus exotic eucalyptus, in reshaping the taxonomic and functional architecture of the soil microbiome remains poorly understood, especially across vertical soil profiles in Western Amazonia. This study aimed to evaluate the impact of land-use change and the integration of *Samanea tubulosa* (legume) and *Eucalyptus pellita* into pastures on the soil prokaryotic and fungal communities. We hypothesized that the native legume would promote a more robust recovery of microbial diversity and functional connectivity compared to eucalyptus and monoculture pastures. Soil samples were collected at three layers (0-10, 10-20, and 20-40 cm) across four systems: native forest (NF), monoculture pasture (MP), and two ILF systems (ILF-ST and ILF-EP). In addition, In the ILF systems, two distances from the tree rows were considered: 0.00 and 5.25 m. High-throughput sequencing of 16S rRNA and ITS regions was combined with LEfSe, FAPROTAX/FungalTraits, and co-occurrence network analysis to characterize the microbial community structure, potential functions, and interaction patterns. Alpha diversity analysis revealed that the prokaryotic diversity was higher in MP and ILF-ST, compared to NF and ILF-EP, whereas fungal diversity was higher in NF and ILF-ST, and lower in MP and ILF-EP. Beta diversity indicated a clear separation of microbial communities by land use, with the legume tree row exerting a spatially broader influence than the eucalyptus. Taxonomic biomarkers identified via LEfSe showed that ILF-ST was enriched with nitrogen-fixing bacteria (e.g., *Bradyrhizobium*) and soft rot decomposers, while ILF-EP was uniquely characterized by a symbiotic footprint of ectomycorrhizal fungi (e.g., *Tomentella* and *Pisolithus*), particularly in the subsoil (LDA > 4.0). Functional prediction confirmed that ILF-ST promoted complex carbon degradation and nitrate reduction pathways, contrasting with the simplified cellulolysis signature of the MP. Co-occurrence networks revealed a complexity-stability paradox: while the MP exhibited the highest connectivity (average degree of 86.665 in the topsoil), it lacked modularity and was dominated by positive correlations, suggesting structural fragility. Conversely, forested systems maintained more partitioned, modular

architectures. Notably, the universal core microbiota for fungi was only 0.5 %, highlighting the extreme sensitivity of fungal guilds to tree species selection. The integration of *S. tubulosa* is superior to *E. pellita* for restoring the biological quality of Amazonian soils. While eucalyptus creates a specialized niche for nutrient mining, the native legume fosters a more diverse and functionally integrated microbial network. These results emphasize that the transition to sustainable livestock intensification in the Amazon must prioritize native tree species, while comprising conservation of native ecosystems, to ensure the restoration of soil biodiversity and long-term ecosystem resilience.

Keywords: microbial networks, *Samanea tubulosa*, silvopastoral systems, soil health, soil microbiome.

2.1 Introduction

The Amazon rainforest is a global biodiversity hotspot where soil microbial communities, comprising bacteria, archaea, and fungi, act as the biological engine for nutrient cycling and organic matter decomposition (Danielson and Rodrigues 2022). However, Western Amazonia, particularly the state of Rondônia, has faced significant deforestation driven by the conversion of primary forests into cattle pastures and agricultural crops (P. C. S. de S. Oliveira et al. 2019; Piontekowski et al. 2019). This land-use change fundamentally alters soil physical and chemical properties, often leading to biotic homogenization (Danielson and Rodrigues 2022). In this process, the loss of forest-specialist taxa is accompanied by the proliferation of generalists, resulting in a net decline in regional microbial diversity and potential shifts in ecosystem functioning (Venturini et al. 2023; Mandro et al. 2026; Rodrigues et al. 2013).

In response to soil degradation, integrated production systems like integrated livestock-forestry (ILF) have emerged as promising alternatives for sustainable intensification. By incorporating trees into agricultural landscapes, these systems enhance organic matter inputs and increase habitat heterogeneity (Shi and Conway-Anderson 2022; Maracaípe et al. 2025; Perez-Alvarez et al. 2023). A critical factor in Western Amazonia is the choice between native tree species, such as *Samanea tubulosa*, and exotic species like *Eucalyptus pellita*. These species differ in shading, litter quality and root exudation patterns, which can differentially influence soil microbiota and their associated ecological functions (Bieluczyk et al. 2024; Kerdraon et al. 2019; Cipriani, Salman, Pellegrinetti, et al. 2025).

Beyond taxonomic diversity, the functional potential of these communities is vital for ecosystem services, including carbon sequestration and nitrogen fixation. Integrated systems have shown promise in enhancing microbial biomass and enzyme activities compared to degraded pastures, suggesting improved functional resilience through higher niche availability (Brewer and Gaudin 2020; Cipriani et al. 2025; Deng et al. 2022).

Moreover, the complexity of microbial interactions is a vital indicator of ecosystem stability. Co-occurrence networks identify microbial hubs and interaction patterns, such as cooperation (positive correlations) or competition (negative correlations), that are not visible through abundance metrics alone (Karimi et al. 2017; Gong et al. 2022). In integrated systems, environmental heterogeneity may foster more complex microbial networks compared to monocultures, potentially enhancing the resistance of the soil microbiome to environmental stressors (Peng et al. 2024; Tahir et al. 2026; Costa et al. 2024).

Despite the known benefits of integrated systems, significant gaps remain regarding their ability to maintain or restore microbial communities in Western Amazonia, particularly concerning the simultaneous response of bacterial and fungal communities across different depths, the comparative influence of native versus exotic tree species in integrated configurations, and the functional implications of these changes for sustainable agricultural intensification (Beule and Vaupel et al. 2022; Vaupel et al. 2025; Venturini et al. 2023).

Therefore, this study investigated the structure, diversity, and ecological functions of soil microbiota across various land-use systems (ILF, monoculture pasture, and native forest) to: characterize bacterial and fungal diversity across systems and soil depths; assess the functional potential of these communities in relation to soil health; evaluate the potential of integrated systems to enhance soil biodiversity and ecosystem functioning compared to conventional management; analyze the topological properties of microbial co-occurrence networks, identifying the influence of land-use change on stability and interaction patterns; and compare the relative performance of native (*S. tubulosa*) and exotic (*E. pellita*) tree species in maintaining soil microbial diversity.

2.2 Materials and Methods

2.2.1 Site description

Samples were taken from three cattle ranching experimental areas and a native forest (NF) fragment located within the Empresa Brasileira de Pesquisa Agropecuária (Embrapa)

experimental field in Porto Velho, Rondônia State, Brazil (8° 48’ S, 63° 51’ W; 95 m altitude). According to the Köppen climate classification system, the climate is Am, or tropical monsoon (Alvares et al. 2013). The area has an average annual rainfall of 2,216 mm, with average annual maximum and minimum temperatures of 30.4 °C and 23.3 °C, respectively (Climate-Data.org 2022).

The predominant soil in the area is classified as a Latossolo Vermelho-Amarelo distrófico (LVAd) according to the Brazilian soil classification system (Valente et al. 1998; H. G. dos Santos et al. 2025), which corresponds to a Ferralsol in the World Reference Base (WRB) soil classification system (IUSS Working Group WRB 2022), or a Hapludox under the USDA Soil Taxonomy (Soil Survey Staff 2022). The soil has a predominant clay texture (Table 2.1).

Table 2.1 – Mean ± standard deviation of soil pH_{H2O}, available phosphorus (P), base saturation (BS), organic matter (OM), bulk density (BD), and clay content for soil layers (0-10, 10-20 and 20-40 cm) in the studied land-use systems†. ILF-ST: integrated livestock-forestry with *Samanea tubulosa*; ILF-EP: integrated livestock-forestry with *Eucalyptus pellita*; MP: *Urochloa brizantha* ‘Marandu’ pasture; NF: native forest.

Distance‡	**Area**	**pH_{H2O}**	**P**	**BS**	**OM**	**BD**	**Clay**
			mg dm^{-3}	%	dag kg^{-1}	g cm^{-3}	dag kg^{-1}
		---------- 0-10 cm ----------					
0.00 m	ILF-ST	5.84±0.09	2.56±0.80	52.52±0.47	3.99±5.81	1.02±0.09	56.50±11.26
	ILF-EP	5.11±0.47	2.36±0.30	29.93±0.24	3.13±13.28	1.07±0.04	67.50±8.29
5.25 m	ILF-ST	5.56±0.42	1.60±1.17	41.02±0.29	3.39±14.95	1.11±0.15	54.50±6.94
	ILF-EP	5.35±0.43	0.83±0.37	35.88±0.15	2.88±13.97	1.10±0.09	63.50±5.76
	MP	4.90±0.58	1.39±0.47	22.25±1.16	4.02±16.44	0.98±0.20	59.50±4.47
	NF	4.46±0.09	1.74±0.34	4.46±0.69	3.19±0.24	0.83±0.14	54.00±3.35
		----------10-20cm----------					
0.00 m	ILF-ST	5.74±0.13	2.41±0.66	48.59±0.26	3.73±6.95	0.98±0.09	61.50±4.18
	ILF-EP	4.85±0.40	2.08±0.52	21.60±0.38	3.00±12.28	1.02±0.11	71.90±3.52
5.25 m	ILF-ST	5.40±0.47	1.60±1.15	34.50±0.30	3.00±18.36	1.05±0.09	58.50±5.48
	ILF-EP	4.85±0.38	0.93±0.23	19.04±0.19	2.63±11.72	1.03±0.09	66.50±6.98
	MP	4.92±0.44	1.15±0.66	18.84±0.93	3.40±16.71	1.04±0.05	61.50±5.48
	NF	4.45±0.08	1.53±0.27	4.39±0.61	3.08±0.76	0.90±0.08	58.50±4.18
		----------20-40cm----------					
0.00 m	ILF-ST	5.55±0.36	2.20±0.57	41.73±0.28	3.33±12.20	1.03±0.14	67.50±3.06
	ILF-EP	4.83±0.39	1.74±0.68	15.58±0.51	2.59±12.00	1.07±0.11	72.40±6.43
5.25 m	ILF-ST	4.94±0.51	1.17±0.47	20.73±0.35	2.58±18.30	1.12±0.13	65.50±4.11
	ILF-EP	4.69±0.12	0.83±0.55	9.27±0.33	2.26±3.15	1.16±0.18	70.00±5.30
	MP	4.69±0.08	1.08±0.37	9.90±0.38	2.71±5.42	1.01±0.06	65.00±3.95
	NF	4.40±0.02	1.25±0.11	5.04±0.56	2.68±0.50	0.87±0.09	50.00±7.71

† The soil properties were determined by the methods described in Teixeira et al. (2017). Clay contents for ILF-ST, ILF-EP and NF were sourced from Cipriani, Salman, da Cruz, et al. (2025), whereas MP values were directly measured. ‡ Distance from the trees in the tree-integrated systems.

The experiments were initiated in February 2018 with the establishment of trees in a palisade grass pasture [*Urochloa brizantha* (Hochst. Ex A. Rich.) R. Webster 'Marandu'], resulting in two low-tree-density integrated livestock–forestry (ILF) systems: one with *Eucalyptus pellita* F. Muell (ILF-EP) and another with *Samanea tubulosa* (Benth.) Barneby & J.W. Grimes (ILF-ST). The third system is composed solely of 'Marandu' pasture (MP).

In each ILF system, trees were planted in a single tree strip functioning primarily as a windbreak, composed of two rows approximately 300 m long, with spacing of 6.0 m between rows and 3.5 m between trees within rows, oriented along an azimuth of 320° (NW–SE). Considering the total area of each ILF system (12.8 ha), the initial tree density was approximately 13 trees ha^{-1}, with 171 trees planted in each system. The *E. pellita* and *S. tubulosa* strips were separated by approximately 240 m (Figure 2.1).

The planting was done manually, using post hole diggers and 30 cm-tall cuttings (*E. pellita*) and seedlings (*S. tubulosa*), 30 days after desiccating the pasture in the strip area with glyphosate. Fertilization was done with chemical NPK + micronutrients fertilizer (350 g $plant^{-1}$) applied in the holes, just before planting, and as top-dressing applications (twice annually in 2018 and 2019, and once annually from 2020 to 2023). The mean total height of the trees was 5.9 m (*S. tubulosa*), and 19.8 m (*E.* pellita), and mean canopy diameter was 8.4 m (*S. tubulosa*), and 5.8 m (*E. pellita*), at the time of soil sampling (Cipriani et al. 2023; Oliveira et al. 2021; Welke et al. 2022).

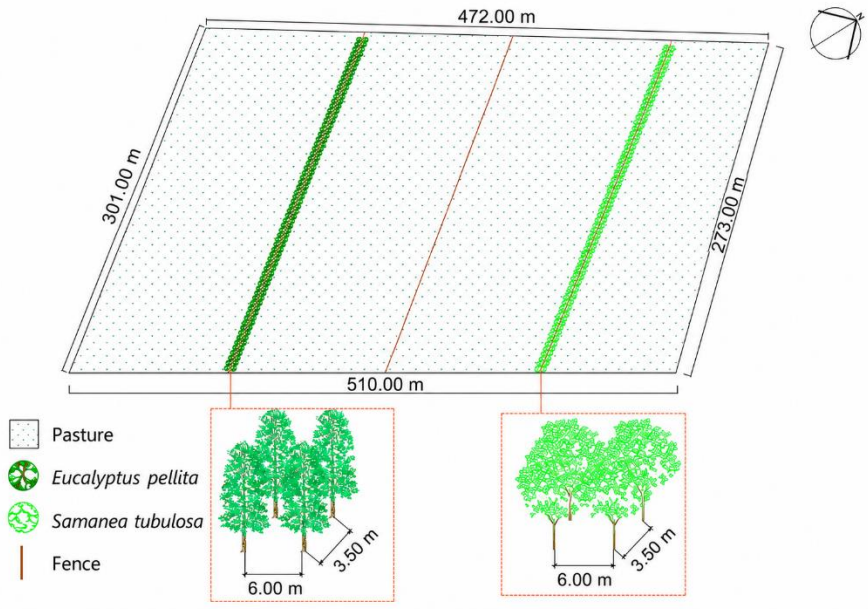

Figure 2.1 - Layout of the integrated livestock-forestry (ILF) systems. Left: ILF-EP (*Eucalyptus pellita*); right: ILF-ST (*Samanea tubulosa*).

The palisade grass was established before 1970, i.e., more than 40 years before tree planting, and its grazing management was carried out using 4 paddocks of 3.2 ha. The animals used were of the Girolando breed (dry cows and heifers) with ad libittum intake of salt and water. Grazing management followed a mob grazing strategy, in which animals were maintained at high stocking density for short occupation periods followed by adequate pasture recovery intervals. Average annual stocking rate was approximately two animal units per hectare in both ILF-ST and ILF-EP systems. Whole-area pasture fertilization and liming were rare, with the most recent application occurring five years before the planting of the trees.

An unmanaged NF fragment from the same experimental field was included as a reference area to represent baseline conditions without human intervention. The fragment spans 41 ha of primary tropical rainforest, containing 99 woody species and 258 individuals per hectare. *Sclerolobium paniculatum*, *Psidium araca*, *Eschweilera grandiflora*, *Licania heteromorpha*, and *Protium puncticulatum* comprise 35 % of the relative density in the fragment (Bentes-Gama et al. 2009). The NF soil was assigned the same classification as the ILFSs.

2.2.2 Soil sampling

Soil samples were collected with a Dutch auger in April 2024 (rainy season) from the 0-10, 10-20, and 20-40 cm layers. In the ILF systems, samples were taken at two distances from the tree rows: 0.00 m (the planting line) and 5.25 m, and 21.00 m. The 5.25 m distance was chosen for standardization, as it corresponds to one-eighth of the 42 m inter-row spacing used in previous studies conducted in an integrated crop-livestock-forestry system experimental area (Feitosa et al. 2019, 2022). Furthermore, this distance is representative of an intermediate zone among those adopted by studies assessing the influence of trees on pasture and soil attributes in integrated systems.

The spatial distribution of sampling points was planned to ensure representativeness and minimize edge effects within the experimental areas. In NF, the five sampling points were established along a transect parallel to the boundary road, with each point located more than 30 m from the edge to avoid external influences. Successive samples were collected approximately every 30 m along this transect to ensure spatial independence. In the treeless system (MP), the five sampling points were distributed randomly across the area, while maintaining a minimum distance of 30 m from the edges and between points. In the ILF systems, the five sampling points for each distance (0.00 and 5.25 m) were positioned along the

tree rows. A 30 m buffer zone was maintained from both the start and the end of the rows. Samples were collected at intervals of approximately 30 m along the row, alternating the collection between the NE and SW sides of the planting line.

Five composite samples (prepared from two simple samples each) were taken per area, depth and distance, summing up 90 composite samples per year. Specifically, MP and NF areas contributed with 15 samples each (3 depths x 5 replicates), while the two ILF areas contributed with 30 samples each, factoring in the two distance levels (2 distances x 3 depths x 5 replicates). Subsamples for DNA extraction were placed in a cooler and stored at -20 °C, while soil samples for chemical analysis were air-dried, ground, sieved (2 mm) and stored at room temperature.

2.2.3 Soil DNA extraction and sequencing

The total DNA from soil samples was extracted using the DNeasy PowerSoil Pro kit (Qiagen, Hilden, Germany) following the manufacturer's instructions. Briefly, the soil sample was homogenized, and the microbial cells were lysed by mechanical and chemical methods. After that, the total genomic DNA was captured on a silica membrane in a spin column format, washed, and eluted from the membrane to obtain the extract. In addition, the DNA concentration and quality were measured using the NanoDrop 2000c spectrophotometer (Thermo Scientific, Waltham, Massachusetts, EUA) according to the manufacturer's protocol.

The V3-V4 region of the 16S rDNA was amplified to access the abundance of prokaryotes (bacteria and archaea) from samples by using the updated primers 341F (5′-CCTAYGGGRBGCASCAG-3′) and 806R (5′-GGACTACNNGGGTATCTAAT-3′) (Caporaso et al. 2011). To determine the abundance of fungi, the ITS region was amplified using the primers ITS1F (5′-CTTGGTCATTTAGAGGAAGTAA-3') and ITS2R (5'-GCTGCGTTCTTCATCGATGC-3') (White et al. 1990). The paired-end sequencing with 2 x 250 bp reads was performed in Illumina NextSeq 2000 platform. Both amplification and sequencing were performed by Centro de Genômica Funcional (USP/ESALQ, Piracicaba, São Paulo, Brazil) using standard approaches as defined by the Earth Microbiome Project (Gilbert et al. 2014). The raw reads from this sequencing were deposited in the Sequence Read Archive (SRA) under the Bioproject PRJNA1215384.

Raw reads were analyzed using the DADA2 pipeline (Callahan et al. 2016), considering acceptable sequences with a quality score greater than 20, maximum expected errors per read of 2, and minimum length of 50. Filtered reads were grouped into amplicon sequence variants (ASVs) and matched to taxonomy using the databases SILVA v. 138.2 (Quast et al. 2013), for

prokaryotes, and UNITE 10.0 (Abarenkov et al. 2025), for fungi. The resulting ASV table was imported into a phyloseq object (McMurdie and Holmes 2013) for downstream analysis in the microeco package for R (Liu et al. 2021). For prokaryotes, ASVs not assigned to the *Bacteria* nor the *Archaea* kingdoms or classified as chloroplast or mitochondria, were removed. Count data was normalized by the scaling with ranked subsampling (SRS) method (Beule and Karlovsky 2020), using the minimum number of reads across samples: 40,096 for prokaryotes and 32,666 for fungi.

2.2.4 Data analysis

2.2.4.1 Alpha diversity

Richness and Shannon Index were calculated from the taxonomic relative abundance matrix at the ASV level. After checking for the assumptions of homoscedasticity and normality, outlier removal, and application of the Box-Cox transformation (when necessary), the means of alpha diversity (number of different ASVs and Shannon Index) were compared among areas through ANOVA or Dunnett's test (for comparisons of ILF systems with MP and NF), with the aid of Minitab 22 software and Tratamentos.ad package for R (Azevedo 2022). The following experimental design was used: 2 ILFSs (ILF-EP and ILF-ST) × 2 distances from the trees (0 and 5.25 m) + 2 additional treatments (MP and NF), with 5 replicates in CRD. Each soil layer (0-10, 10-20 and 20-40 cm) was analyzed separately.

2.2.4.2 Beta diversity

To visualize shifts in microbial community structure across treatments, Principal Coordinate Analysis (PCoA) was performed based on Weighted UniFrac distances at the ASV level using the microeco R package (Liu et al. 2021). Unlike non-phylogenetic metrics, Weighted UniFrac accounts for the relative abundance of taxa and their phylogenetic relationships, providing a deeper resolution of community transitions between land-use systems. The statistical significance of observed clusters (areas and distance from trees) was assessed using Permutational Multivariate Analysis of Variance (PERMANOVA) with 999 permutations, applied directly to the Weighted UniFrac distance matrix. The phylogenetic trees required for UniFrac distances were constructed using the Neighbor-Joining (NJ) method based on a Maximum Likelihood (ML) distance matrix calculated via the phangorn package

(Schliep 2011). Sequences were previously aligned using the DECIPHER R package (Berry and Widder 2014). To allow for phylogenetic distance calculations, the phylogenetic tree was rooted by the midpoint method using the *phytools* package (Revell 2024) in the R environment.

2.2.4.3 Taxonomic biomarkers and community composition

The linear discriminant analysis (LDA) effect size (LEfSe) method (Segata et al. 2011) was employed to identify differentially abundant ASVs (biomarkers) specific to each management area and soil layer. This analysis was performed using the microeco package in R, adopting a significance level of 0.05 (with FDR correction for multiple comparisons) and a minimum LDA score threshold of 2.000. To visualize the distribution of unique and shared ASVs among treatments across the three soil layers, Venn diagrams were generated using the InteractiVenn web tool (Heberle et al. 2015). Furthermore, the taxonomic composition was assessed through a descriptive visual analysis of relative abundance at the phylum level, separately for prokaryotes (including a detailed assessment of *Archaea*) and fungi.

2.2.4.4 Functional prediction and profile analysis

Functional profiles of the soil microbial communities were predicted based on the taxonomic data using automated functional classifiers within the microeco environment. For prokaryotes, ecological functions were assigned using the FAPROTAX v.1.2.6 database (Louca et al. 2016). For the fungal community, ecological traits and guilds were predicted using the FungalTraits database (Põlme et al. 2020). To generate the functional output tables, the trans_func class in microeco was utilized, with the abundance_weighted argument set to TRUE to calculate the functional percentages based on the relative abundance of each assigned taxon. Subsequently, the LEfSe test was applied to the predicted functional groups to identify significant functional biomarkers for each treatment (LDA score ≥ 2.000; p-adjusted < 0.05). This approach allowed for the identification of ecological functions and fungal lifestyles specifically enriched in response to management systems and soil layers.

2.2.4.5 Co-occurrence networks

To investigate the interactions between soil prokaryotic and fungal communities across different management systems and soil depths, co-occurrence networks were constructed using

the SparCC (Sparse Correlations for Compositional Data) algorithm (Friedman and Alm 2012). The analysis was performed at the ASV level using the microeco package in R (Liu et al. 2021), with the SpiecEasi method implementation (Kurtz et al. 2015).

A total of 18 networks were generated, representing each combination of area (ILF-ST 0.00 m, ILF-ST 5.25 m, ILF-EP 0.00 m, ILF-EP 5.25 m, MP, and NF) and soil layer (0-10, 10-20, and 20-40 cm). To ensure comparability between the domains, the prokaryotic and fungal ASV tables were first merged into a single global matrix. Subsequently, SRS normalization was applied to the integrated table to account for differences in sequencing depth while maintaining the relative abundance ratios between fungi and prokaryotes.

Following normalization, a filtering step was applied to reduce noise and computational complexity: only ASVs accounting for 90 % of the cumulative relative abundance (without discriminating between domains) and occurring in at least three replicates per treatment were retained. Only correlations with a SparCC coefficient (r) ≤ -0.7 or ≥ 0.7 and a p-value < 0.01 (after FDR correction) were considered for further analysis.

The topological properties of the networks, including nodes, edges, average degree, diameter, density, modularity, average clustering coefficient, and average path length, were calculated using Gephi software v. 0.10.1 (Bastian et al. 2009). Additionally, the ratios of fungi/prokaryote nodes and positive/negative correlations were determined to assess community balance and potential biotic interactions.

2.3 Results

2.3.1 Alpha diversity

The alpha diversity of soil prokaryotes and fungi was significantly influenced by the management systems, sampling distances, and soil depths (Table 2.2). In the surface layer (0-10 cm), prokaryotic richness was significantly higher in the ILF-ST system compared to ILF-EP at both 0.00 m and 5.25 m distances. At the tree row (0.00 m), ILF-ST reached a richness of 1,129.80 ASVs, while ILF-EP presented 937.00 ASVs. This pattern of superiority for the *S. tubulosa* system was maintained across the deeper layers (10-20 and 20-40 cm). Regarding the Shannon index, ILF-ST consistently outperformed ILF-EP at the 0.00 m distance in all layers, indicating a more even and diverse prokaryotic community under the legume tree. When compared to the controls, the prokaryotic diversity was generally lower in the native forest (NF) and higher in the treeless pasture (MP).

Table 2.2 - Alpha diversity measures (mean ± standard deviation) at the ASV level of soil prokaryotes and fungi across different management systems, sampling distances, and soil layers (0-10, 10-20, and 20-40 cm). ILF-ST: integrated livestock-forestry with *Samanea tubulosa*; ILF-EP: integrated livestock-forestry with *Eucalyptus pellita;* MP: *Urochloa brizantha* 'Marandu' pasture; NF: native forest.

Distance	Area	Prokaryotes		Fungi	
		Richness	**Shannon index**	**Richness**	**Shannon index**
		---------- 0-10 cm ----------			
0.00 m	ILF-ST	1,129.80±94.44 Aa‡	6.34±0.12 Aa‡	749.60±65.66 Aa†‡	5.21±0.13 Aa
	ILF-EP	937.00±43.98 Ab†	5.98±0.10 Ab†	692.20±43.01 Aa‡	4.79±0.42 Ab‡
5.25 m	ILF-ST	1,137.80±81.33 Aa‡	6.28±0.11 Aa‡	664.40±17.37 Ba‡	4.78±0.21 Ba‡
	ILF-EP	932.40±87.89 Ab†	5.96±0.17 Ab†	634.80±58.88 Aa‡	4.85±0.41 Aa‡
	MP	1,244.60±121.61 α	6.34±0.17 α	624.40±43.29 β	4.77±0.25 β
	NF	835.80±97.78 β	5.95±0.17 β	974.40±28.39 α	5.62±0.25 α
		---------- 10-20 cm ----------			
0.00 m	ILF-ST	1,136.20±65.97 Aa‡	6.33±0.05 Aa‡	835.40±170.35 Aa†	5.25±0.23 Aa
	ILF-EP	942.40±78.77 Ab†	5.98±0.10 Ab†	682.80±48.25 Ab‡	4.82±0.37 Ab‡
5.25 m	ILF-ST	1,023.00±42.40 Aa†‡	6.23±0.08 Aa‡	638.00±78.59 Ba‡	4.81±0.42 Ba‡
	ILF-EP	912.20±107.67 Aa†	5.91±0.16 Ab†	590.60±68.06 Ba‡	4.57±0.48 Aa‡
	MP	1,253.40±139.89 α	6.33±0.19 α	635.80±59.79 β	4.78±0.21 β
	NF	863.40±72.69 β	5.98±0.15 β	998.00±90.45 α	5.50±0.14 α
		---------- 20-40 cm ----------			
0.00 m	ILF-ST	1,111.20±81.24 Aa‡	6.26±0.11 Aa‡	785.00±65.43 Aa†	5.33±0.14 Aa†
	ILF-EP	939.00±16.99 Ab†	6.01±0.09 Ab	651.40±39.26 Ab‡	4.67±0.28 Ab‡
5.25 m	ILF-ST	1,012.40±108.16 Aa‡	6.14±0.12 Aa	671.60±82.28 Aa‡	4.88±0.34 Ba‡
	ILF-EP	899.60±81.88 Aa†	5.90±0.15 Ab†	607.20±69.45 Aa‡	4.83±0.26 Aa‡
	MP	1,139.20±180.08 α	6.19±0.21 α	608.20±128.67 β	4.69±0.52 β
	NF	798.20±98.07 β	5.91±0.15 β	878.00±124.25 α	5.44±0.20 α

Data were analyzed by factorial ANOVA at a 5 % significance level. Capital letters compare distances from the tree row (0.00 m vs. 5.25 m) within the same tree-integrated system and soil layer. Lowercase letters compare tree-integrated systems (ILF-ST vs. ILF-EP) within the same distance and soil layer. Greek letters compare the treeless system (MP) with the native forest (NF) within each soil layer. Systems followed by the same letter do not differ statistically. The symbols † and ‡ indicate a significant difference relative to MP and NF, respectively, according to Dunnett's test.

For the fungal community, the responses to distance and management were more variable. In the 0-10 cm layer, there were no significant differences in fungal richness between ILF-ST and ILF-EP at the 0.00 m distance. However, the Shannon index for fungi was significantly higher in ILF-ST (5.21) than in ILF-EP (4.79) at the tree row. In the intermediate layer (10-20 cm), a significant spatial effect was observed for ILF-EP, where fungal richness was higher at the 0.00 m distance (682.80 ASVs) compared to the 5.25 m distance (590.60 ASVs). In the deepest layer (20-40 cm), the ILF-ST system maintained significantly higher fungal richness and Shannon diversity at the 0.00 m distance compared to ILF-EP. Notably, fungal richness and Shannon index in NF was consistently superior to the managed

systems across all depths (except for ILF-ST at 0.00 m), while the Shannon index of the NF remained the highest overall, but equivalent to ILF-ST at 0.00 m.

2.3.2 Beta diversity

Principal Coordinate Analysis (PCoA) revealed distinct clustering patterns for both prokaryotic and fungal communities across the three soil layers (Figure 2.2). The first two principal coordinates explained a substantial portion of the total variance, with prokaryotes showing more pronounced segregation between management systems than fungi. The native forest (NF) formed a highly cohesive and isolated group in all depths, underscoring a unique microbial signature compared to all managed systems.

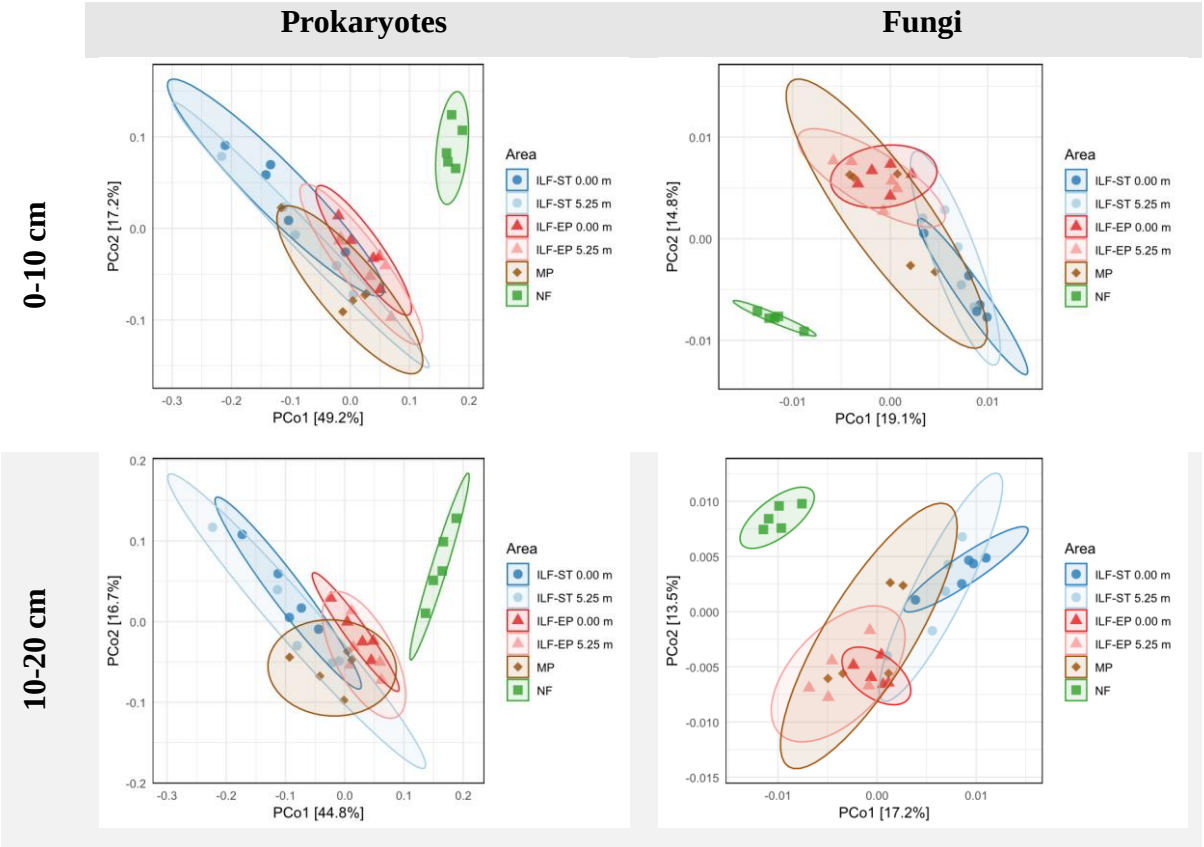

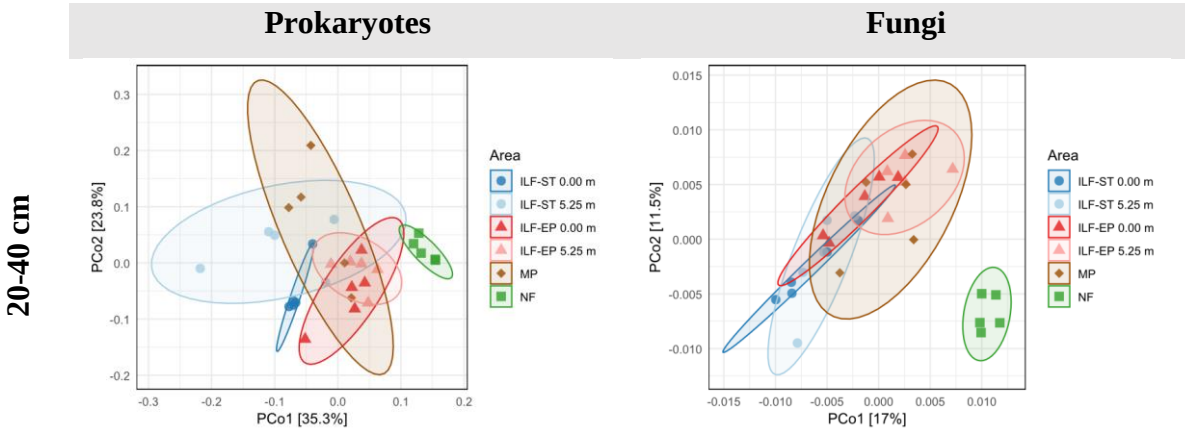

Figure 2.2 - Principal Coordinate Analysis (PCoA) based on weighted UniFrac distances for soil prokaryotic (*Archaea* and *Bacteria*) and fungal communities across three soil layers (0-10, 10-20, and 20-40 cm) under different management systems. Percentages on axes indicate the variance explained by each coordinate. Ellipses represent 95 % confidence intervals for each group). Statistical significance among groups can be found in Table 2.3. ILF-ST: integrated livestock-forestry with *Samanea tubulosa*; ILF-EP: integrated livestock-forestry with *Eucalyptus pellita*; MP: *Urochloa brizantha* 'Marandu' pasture; NF: native forest; 0.00 and 5.25 m: distance from the tree row in the ILF systems.

The PERMANOVA pairwise comparisons confirmed that the native vegetation supports a markedly different microbial assembly than the managed systems, since the microbial community composition of NF differed significantly from all managed systems across soil layers (Table 2.3). Moreover, ILF-ST at 0.00 and 5.25 m was significantly different from ILF-EP at 0.00 and 5.25 m in every soil layer for prokaryotes and fungi. The communities of ILF-ST did not differ significantly between the 0.00 m and 5.25 m distances across layers for prokaryotes and fungi, suggesting a more homogeneous influence of the *S. tubulosa* tree on the soil microbiome.

At 0.00 m from the tree row, prokaryotic and fungal communities of both ILF systems differed significantly from the treeless pasture (MP) across soil layers, except for ILF-EP at 20-40 cm (for prokaryotes). However, at 5.25 m from the tree row, fewer significant differences from MP were observed. For prokaryotic community, a significant difference was observed only for ILF-EP at the 10-20 cm layer. Whereas, for fungal communities, significant differences were observed for ILF-ST at the 0-10 and 20-40 cm layers.

Table 2.3 - Pairwise PERMANOVA comparisons of soil prokaryotic (*Archaea* and *Bacteria*) and fungal community compositions based on the weighted UniFrac distance matrix across management systems and sampling distances for three soil layers (0-10, 10-20, and 20-40 cm). The F-statistic indicates the strength of the separation between groups, and the R^2 value represents the proportion of variation explained by the specific comparison. ILF-ST: integrated livestock-forestry with *Samanea tubulosa*; ILF-EP: integrated livestock-forestry with *Eucalyptus pellita*; MP: *Urochloa brizantha* 'Marandu' pasture; NF: native forest; 0.00 and 5.25 m: distance from the tree row in the ILF systems.

Comparison			**Prokaryote**			**Fungi**		
			F	R^2	p adj.[†]	F	R^2	p adj.[†]
			---------- 0-10 cm ----------					
ILF-ST 0.00 m	vs.	ILF-ST 5.25 m	0.966	0.108	0.418	1.298	0.140	0.147
		ILF-EP 0.00 m	7.377	0.480	**0.023**	3.985	0.332	**0.021**
		ILF-EP 5.25 m	6.533	0.450	**0.039**	3.771	0.320	**0.021**
		MP	4.229	0.346	**0.023**	2.723	0.254	**0.021**
		NF	22.228	0.735	**0.023**	6.201	0.437	**0.021**
ILF-EP 0.00 m	vs.	ILF-EP 5.25 m	0.759	0.087	0.609	1.277	0.138	0.167
		ILF-ST 5.25 m	3.672	0.315	**0.023**	2.555	0.242	**0.021**
		MP	2.669	0.250	**0.023**	1.757	0.180	**0.030**
		NF	14.964	0.652	**0.023**	5.507	0.408	**0.021**
ILF-ST 5.25 m	vs.	ILF-EP 5.25 m	3.260	0.290	**0.040**	2.421	0.232	**0.021**
		MP	1.651	0.171	0.149	1.674	0.173	**0.043**
		NF	14.386	0.643	**0.023**	5.074	0.388	**0.021**
ILF-EP 5.25 m	vs.	MP	1.933	0.195	0.070	1.303	0.140	0.208
		NF	11.979	0.600	**0.023**	4.642	0.367	**0.021**
MP	vs.	NF	12.040	0.601	**0.023**	3.877	0.326	**0.021**
			---------- 10-20 cm ----------					
ILF-ST 0.00 m	vs.	ILF-ST 5.25 m	0.588	0.068	0.716	1.244	0.135	0.171
		ILF-EP 0.00 m	7.125	0.471	**0.016**	3.904	0.328	**0.015**
		ILF-EP 5.25 m	7.703	0.490	**0.015**	3.854	0.325	**0.015**
		MP	3.922	0.329	**0.025**	2.597	0.245	**0.015**
		NF	18.684	0.700	**0.015**	5.414	0.404	**0.015**
ILF-EP 0.00 m	vs.	ILF-EP 5.25 m	1.139	0.125	0.336	1.663	0.172	**0.033**
		ILF-ST 5.25 m	3.887	0.327	**0.015**	2.517	0.239	**0.015**
		MP	3.605	0.311	**0.015**	1.797	0.183	**0.015**
		NF	12.498	0.610	**0.015**	4.977	0.384	**0.015**
ILF-ST 5.25 m	vs.	ILF-EP 5.25 m	4.084	0.338	**0.015**	2.448	0.234	**0.015**
		MP	1.908	0.192	0.072	1.662	0.172	0.067
		NF	11.398	0.588	**0.015**	4.093	0.338	**0.015**
ILF-EP 5.25 m	vs.	MP	2.960	0.270	**0.025**	1.262	0.136	0.184
		NF	10.912	0.577	**0.015**	3.657	0.314	**0.015**
MP	vs.	NF	10.740	0.573	**0.015**	3.167	0.284	**0.020**
			---------- 20-40 cm ----------					
ILF-ST 0.00 m	vs.	ILF-ST 5.25 m	1.578	0.165	0.197	1.090	0.120	0.321
		ILF-EP 0.00 m	3.217	0.287	**0.026**	2.926	0.268	**0.023**
		ILF-EP 5.25 m	5.995	0.428	**0.026**	3.288	0.291	**0.027**
		MP	3.673	0.315	**0.036**	2.361	0.228	**0.023**
		NF	18.413	0.697	**0.026**	5.383	0.402	**0.023**
ILF-EP 0.00 m	vs.	ILF-EP 5.25 m	1.442	0.153	0.205	1.924	0.194	**0.030**
		ILF-ST 5.25 m	3.405	0.298	**0.033**	2.073	0.206	**0.023**
		MP	3.315	0.293	0.054	1.739	0.179	**0.031**
		NF	9.947	0.554	**0.026**	4.422	0.356	**0.023**
ILF-ST 5.25 m	vs.	ILF-EP 5.25 m	4.317	0.350	**0.026**	2.356	0.228	**0.023**
		MP	1.361	0.145	0.205	1.620	0.168	**0.026**
		NF	11.059	0.580	**0.026**	4.177	0.343	**0.023**
ILF-EP 5.25 m	vs.	MP	2.745	0.255	0.110	1.282	0.138	0.141
		NF	12.599	0.612	**0.026**	3.660	0.314	**0.023**
MP	vs.	NF	8.228	0.507	**0.026**	3.208	0.286	**0.023**

[†] Bold values indicate significant difference at the 5 % level with FDR correction for multiple comparisons.

2.3.3 Taxonomic biomarkers and community composition

The LEfSe analysis revealed significant taxonomic biomarkers (prokaryotic and fungal ASVs) that characterize each management system and the native forest (Table 2.4 and Table 2.5). There was a dramatic vertical stratification of microbial communities, with biomarker diversity declining sharply with depth: 148 >141 > 31 prokaryotic ASVs, and 130 > 106 > 37 fungal ASVs. Only 8.4 % of the prokaryotic biomarkers and 9.5 % of the fungal biomarkers were shared among the three layers, reinforcing vertical niche partitioning (most taxa are layer-specific). The native forest maintained dominance across all soil layers, with 84.1 % of total (320) prokaryotic biomarkers and 74.0 % of total (273) fungal biomarkers.

Table 2.4. Taxonomic biomarkers of soil prokaryotic communities across management systems, sampling distances from the trees in the ILF systems (0.00 and 5.25 m), and soil layers (0-10, 10-20 and 20–40 cm) [†]. LDA: linear discriminant analysis score. ILF-ST: integrated livestock-forestry with *Samanea tubulosa*; ILF-EP: integrated livestock-forestry with *Eucalyptus pellita*; MP: *Urochloa brizantha* 'Marandu' pasture; NF: native forest.

Area	Taxa	LDA
	---------- 0-10 cm ----------	
ILF-ST 0.00 m	k_Bacteria|p_Pseudomonadota|c_Alphaproteobacteria|o_Hyphomicrobiales|f_Methyloligellaceae|g_|s_|ASV_580	2.952
	k_Bacteria|p_Pseudomonadota|c_Alphaproteobacteria|o_|f_|g_Hypericibacter|s_|ASV_522	2.836
	k_Bacteria|p_Actinomycetota|c_Actinobacteria|o_Micromonosporales|f_Micromonosporaceae|g_|s_|ASV_576	2.800
	k_Bacteria|p_Acidobacteriota|c_Vicinamibacteria|o_Vicinamibacterales|f_|g_|s_|ASV_2453	2.707
	k_Bacteria|p_Acidobacteriota|c_Acidobacteriae|o_Terriglobales|f_Acidobacteriaceae (Subgroup 1)|g_|s_|ASV_1625	2.681
	k_Bacteria|p_Acidobacteriota|c_Vicinamibacteria|o_Vicinamibacterales|f_|g_|s_|ASV_1610	2.667
	k_Bacteria|p_Myxococcota|c_bacteriap25|o_|f_|g_|s_|ASV_1716	2.635
	k_Bacteria|p_Pseudomonadota|c_Alphaproteobacteria|o_Hyphomicrobiales|f_Hyphomicrobiaceae|g_Hyphomicrobium|s_|ASV_1481	2.631
ILF-ST 5.25 m	k_Bacteria|p_Actinomycetota|c_Acidimicrobiia|o_Acidimicrobiales|f_Acidimicrobiaceae|g_Acidiferrimicrobium|s_|ASV_1001	2.876
ILF-EP 0.00 m	k_Bacteria|p_Acidobacteriota|c_Acidobacteriae|o_Subgroup 2|f_|g_|s_|ASV_179	3.264
	k_Bacteria|p_Acidobacteriota|c_Acidobacteriae|o_Subgroup 2|f_|g_|s_|ASV_1171	2.921
	k_Bacteria|p_Chloroflexota|c_Ktedonobacteria|o_Ktedonobacterales|f_JG30-KF-AS9|g_|s_|ASV_518	2.653
ILF-EP 5.25 m	k_Bacteria|p_Pseudomonadota|c_Alphaproteobacteria|o_Hyphomicrobiales|f_Xanthobacteraceae|g_|s_|ASV_1	4.331
	k_Bacteria|p_Actinomycetota|c_Thermoleophilia|o_Solirubrobacterales|f_Solirubrobacteraceae|g_Conexibacter|s_|ASV_127	3.418
	k_Bacteria|p_Verrucomicrobiota|c_Verrucomicrobiia|o_Chthoniobacterales|f_Xiphinematobacteraceae|g_Candidatus Xiphinematobacter|s_|ASV_521	2.871
	k_Bacteria|p_Chloroflexota|c_Ktedonobacteria|o_B12-WMSP1|f_|g_|s_|ASV_284	2.850
	k_Bacteria|p_Chloroflexota|c_Ktedonobacteria|o_B12-WMSP1|f_|g_|s_|ASV_405	2.795
MP	k_Bacteria|p_Actinomycetota|c_Actinobacteria|o_Micromonosporales|f_Micromonosporaceae|g_|s_|ASV_53	3.337
	k_Bacteria|p_Chloroflexota|c_Ktedonobacteria|o_Ktedonobacterales|f_Ktedonobacteraceae|g_|s_|ASV_1978	2.507
NF	k_Bacteria|p_Pseudomonadota|c_Alphaproteobacteria|o_Hyphomicrobiales|f_Xanthobacteraceae|g_|s_|ASV_2	4.089

Area	Taxa	LDA
	k_Bacteria|p_Chloroflexota|c_Ktedonobacteria|o_Ktedonobacterales|f_JG30-KF-AS9|g_|s_|ASV_72	3.861
	k_Bacteria|p_Acidobacteriota|c_Acidobacteriae|o_Terriglobales|f_|g_|s_|ASV_65	3.756
	k_Bacteria|p_Pseudomonadota|c_Alphaproteobacteria|o_Elsterales|f_|g_|s_|ASV_31	3.602
	k_Bacteria|p_Pseudomonadota|c_Alphaproteobacteria|o_Hyphomicrobiales|f_Xanthobacteraceae|g_|s_|ASV_124	3.582
	k_Bacteria|p_Actinomycetota|c_Actinobacteria|o_Frankiales|f_Acidothermaceae|g_Acidothermus|s_|ASV_167	3.564
	k_Bacteria|p_Pseudomonadota|c_Alphaproteobacteria|o_Hyphomicrobiales|f_Xanthobacteraceae|g_|s_|ASV_129	3.562
	k_Bacteria|p_Pseudomonadota|c_Alphaproteobacteria|o_Hyphomicrobiales|f_Xanthobacteraceae|g_|s_|ASV_192	3.557
	k_Bacteria|p_Acidobacteriota|c_Acidobacteriae|o_Solibacterales|f_Solibacteraceae|g_Candidatus Solibacter|s_|ASV_82	3.557
	k_Bacteria|p_Pseudomonadota|c_Alphaproteobacteria|o_Hyphomicrobiales|f_Xanthobacteraceae|g_|s_|ASV_121	3.547
	k_Bacteria|p_Pseudomonadota|c_Alphaproteobacteria|o_Hyphomicrobiales|f_Xanthobacteraceae|g_|s_|ASV_207	3.544
	k_Bacteria|p_Pseudomonadota|c_Alphaproteobacteria|o_Hyphomicrobiales|f_Xanthobacteraceae|g_|s_|ASV_219	3.536
	k_Bacteria|p_Acidobacteriota|c_Acidobacteriae|o_Bryobacterales|f_Bryobacteraceae|g_Bryobacter|s_|ASV_61	3.522
	k_Bacteria|p_Pseudomonadota|c_Alphaproteobacteria|o_Hyphomicrobiales|f_Xanthobacteraceae|g_|s_|ASV_256	3.494
	k_Bacteria|p_Pseudomonadota|c_Gammaproteobacteria|o_|f_|g_Acidibacter|s_|ASV_164	3.446
	k_Bacteria|p_Acidobacteriota|c_Acidobacteriae|o_Terriglobales|f_|g_|s_|ASV_221	3.437
	k_Bacteria|p_Pseudomonadota|c_Alphaproteobacteria|o_Acetobacterales|f_Acetobacteraceae|g_Acidicaldus|s_|ASV_303	3.424
	k_Bacteria|p_Actinomycetota|c_Thermoleophilia|o_Solirubrobacterales|f_Solirubrobacteraceae|g_Conexibacter|s_|ASV_16	3.417
	k_Bacteria|p_Pseudomonadota|c_Alphaproteobacteria|o_Hyphomicrobiales|f_Xanthobacteraceae|g_|s_|ASV_253	3.389
	k_Bacteria|p_Actinomycetota|c_Acidimicrobiia|o_Acidimicrobiales|f_Acidimicrobiaceae|g_|s_|ASV_298	3.344
	k_Bacteria|p_Acidobacteriota|c_Acidobacteriae|o_Solibacterales|f_Solibacteraceae|g_Candidatus Solibacter|s_|ASV_144	3.321
	k_Bacteria|p_Pseudomonadota|c_Alphaproteobacteria|o_Hyphomicrobiales|f_Xanthobacteraceae|g_|s_|ASV_429	3.291
	k_Bacteria|p_Pseudomonadota|c_Alphaproteobacteria|o_Elsterales|f_|g_|s_|ASV_182	3.271
	k_Bacteria|p_Pseudomonadota|c_Alphaproteobacteria|o_Hyphomicrobiales|f_Xanthobacteraceae|g_|s_|ASV_338	3.248
	k_Bacteria|p_Acidobacteriota|c_Acidobacteriae|o_Terriglobales|f_|g_|s_|ASV_333	3.246
	k_Bacteria|p_Pseudomonadota|c_Alphaproteobacteria|o_Acetobacterales|f_Acetobacteraceae|g_Acidicaldus|s_|ASV_437	3.224
	k_Bacteria|p_Actinomycetota|c_Thermoleophilia|o_Solirubrobacterales|f_Solirubrobacteraceae|g_Conexibacter|s_|ASV_462	3.204
	k_Bacteria|p_Pseudomonadota|c_Alphaproteobacteria|o_Hyphomicrobiales|f_Xanthobacteraceae|g_|s_|ASV_328	3.203
	k_Bacteria|p_Pseudomonadota|c_Alphaproteobacteria|o_Elsterales|f_|g_|s_|ASV_473	3.198
	k_Bacteria|p_Pseudomonadota|c_Gammaproteobacteria|o_|f_|g_Acidibacter|s_|ASV_277	3.192
	k_Bacteria|p_Pseudomonadota|c_Alphaproteobacteria|o_Acetobacterales|f_Acetobacteraceae|g_Acidicaldus|s_|ASV_455	3.186
	k_Bacteria|p_Acidobacteriota|c_Acidobacteriae|o_Terriglobales|f_|g_|s_|ASV_412	3.178
	k_Bacteria|p_Acidobacteriota|c_Acidobacteriae|o_Solibacterales|f_Solibacteraceae|g_Candidatus Solibacter|s_|ASV_530	3.144
	k_Bacteria|p_Pseudomonadota|c_Gammaproteobacteria|o_|f_|g_Acidibacter|s_|ASV_485	3.138
	k_Bacteria|p_Actinomycetota|c_Actinobacteria|o_Frankiales|f_Acidothermaceae|g_Acidothermus|s_|ASV_588	3.123
	k_Bacteria|p_Acidobacteriota|c_Subgroup 5|o_|f_|g_|s_|ASV_551	3.120
	k_Bacteria|p_Actinomycetota|c_Actinobacteria|o_Frankiales|f_Acidothermaceae|g_Acidothermus|s_|ASV_356	3.116

Area	Taxa	LDA
	k_Bacteria|p_Chloroflexota|c_Ktedonobacteria|o_Ktedonobacterales|f_JG30-KF-AS9|g_|s_|ASV_382	3.102
	k_Bacteria|p_Pseudomonadota|c_Alphaproteobacteria|o_Hyphomicrobiales|f_Xanthobacteraceae|g_|s_|ASV_458	3.101
	k_Bacteria|p_Acidobacteriota|c_Acidobacteriae|o_Terriglobales|f_Acidobacteriaceae (Subgroup 1)|g_Terracidiphilus|s_|ASV_235	3.089
	k_Bacteria|p_Actinomycetota|c_Actinobacteria|o_Frankiales|f_Acidothermaceae|g_Acidothermus|s_|ASV_488	3.064
	k_Bacteria|p_Pseudomonadota|c_Alphaproteobacteria|o_Hyphomicrobiales|f_Xanthobacteraceae|g_|s_|ASV_675	3.059
	k_Bacteria|p_Bacillota|c_Bacilli|o_Paenibacillales|f_Paenibacillaceae|g_Cohnella|s_|ASV_553	3.055
	k_Bacteria|p_Chloroflexota|c_TK10|o_|f_|g_|s_|ASV_418	3.052
	k_Bacteria|p_Actinomycetota|c_Actinobacteria|o_Frankiales|f_Acidothermaceae|g_Acidothermus|s_|ASV_581	3.021
	k_Bacteria|p_Acidobacteriota|c_Acidobacteriae|o_Terriglobales|f_|g_|s_|ASV_716	3.013
	k_Bacteria|p_Acidobacteriota|c_Vicinamibacteria|o_Vicinamibacterales|f_|g_|s_|ASV_417	3.012
	k_Bacteria|p_Chloroflexota|c_TK10|o_|f_|g_|s_|ASV_568	3.011
	k_Bacteria|p_Acidobacteriota|c_Vicinamibacteria|o_Vicinamibacterales|f_|g_|s_|ASV_899	3.002
	k_Bacteria|p_Pseudomonadota|c_Alphaproteobacteria|o_Hyphomicrobiales|f_Xanthobacteraceae|g_|s_|ASV_620	2.992
	k_Bacteria|p_Actinomycetota|c_Actinobacteria|o_Frankiales|f_Acidothermaceae|g_Acidothermus|s_|ASV_613	2.989
	k_Bacteria|p_Pseudomonadota|c_Gammaproteobacteria|o_|f_|g_Acidibacter|s_|ASV_645	2.942
	k_Bacteria|p_Chloroflexota|c_TK10|o_|f_|g_|s_|ASV_626	2.940
	k_Bacteria|p_Pseudomonadota|c_Alphaproteobacteria|o_Acetobacterales|f_Acetobacteraceae|g_|s_|ASV_717	2.939
	k_Bacteria|p_Actinomycetota|c_Actinobacteria|o_Mycobacteriales|f_Mycobacteriaceae|g_Mycobacterium|s_|ASV_730	2.929
	k_Bacteria|p_Chloroflexota|c_Ktedonobacteria|o_Ktedonobacterales|f_JG30-KF-AS9|g_|s_|ASV_857	2.927
	k_Bacteria|p_Actinomycetota|c_Actinobacteria|o_Frankiales|f_Acidothermaceae|g_Acidothermus|s_|ASV_803	2.902
	k_Bacteria|p_Pseudomonadota|c_Alphaproteobacteria|o_Elsterales|f_|g_|s_|ASV_701	2.894
	k_Bacteria|p_Pseudomonadota|c_Alphaproteobacteria|o_Elsterales|f_|g_|s_|ASV_797	2.893
	k_Bacteria|p_Chloroflexota|c_Ktedonobacteria|o_Ktedonobacterales|f_JG30-KF-AS9|g_|s_|ASV_531	2.870
	k_Bacteria|p_GAL15|c_|o_|f_|g_|s_|ASV_614	2.865
	k_Bacteria|p_Acidobacteriota|c_Acidobacteriae|o_Bryobacterales|f_Bryobacteraceae|g_Bryobacter|s_|ASV_1007	2.854
	k_Bacteria|p_Candidatus Eremiobacterota|c_Eremiobacteria|o_|f_|g_|s_|ASV_959	2.820
	k_Bacteria|p_Pseudomonadota|c_Alphaproteobacteria|o_Elsterales|f_|g_|s_|ASV_1015	2.804
	k_Bacteria|p_Acidobacteriota|c_Acidobacteriae|o_Terriglobales|f_|g_|s_|ASV_1028	2.779
	k_Bacteria|p_Chloroflexota|c_Ktedonobacteria|o_Ktedonobacterales|f_Ktedonobacteraceae|g_|s_|ASV_1367	2.774
	k_Bacteria|p_Acidobacteriota|c_Acidobacteriae|o_Bryobacterales|f_Bryobacteraceae|g_Bryobacter|s_|ASV_1023	2.771
	k_Bacteria|p_Acidobacteriota|c_Acidobacteriae|o_Terriglobales|f_|g_|s_|ASV_974	2.749
	k_Bacteria|p_Actinomycetota|c_Acidimicrobiia|o_Acidimicrobiales|f_Acidimicrobiaceae|g_|s_|ASV_1156	2.745
	k_Bacteria|p_Chloroflexota|c_Ktedonobacteria|o_Ktedonobacterales|f_JG30-KF-AS9|g_|s_|ASV_808	2.745
	k_Bacteria|p_Actinomycetota|c_Acidimicrobiia|o_Acidimicrobiales|f_Acidimicrobiaceae|g_Acidiferrimicrobium|s_|ASV_1457	2.734
	k_Bacteria|p_Acidobacteriota|c_Acidobacteriae|o_Terriglobales|f_|g_|s_|ASV_513	2.727
	k_Bacteria|p_Chloroflexota|c_Ktedonobacteria|o_Ktedonobacterales|f_JG30-KF-AS9|g_|s_|ASV_1679	2.710
	k_Bacteria|p_Pseudomonadota|c_Alphaproteobacteria|o_Elsterales|f_|g_|s_|ASV_905	2.709

Area	Taxa	LDA
	k_Bacteria|p_Actinomycetota|c_Acidimicrobiia|o_Acidimicrobiales|f_Acidimicrobiaceae|g_Acidiferrimicrobium|s_|ASV_1214	2.704
	k_Archaea|p_Thermoproteota|c_Nitrososphaeria|o_Nitrososphaerales|f_Nitrososphaeraceae|g_|s_|ASV_927	2.703
	k_Bacteria|p_Pseudomonadota|c_Alphaproteobacteria|o_Elsterales|f_|g_|s_|ASV_997	2.695
	k_Bacteria|p_Actinomycetota|c_Acidimicrobiia|o_Acidimicrobiales|f_Acidimicrobiaceae|g_Acidiferrimicrobium|s_|ASV_1201	2.693
	k_Bacteria|p_Pseudomonadota|c_Gammaproteobacteria|o_|f_|g_Acidibacter|s_|ASV_1022	2.689
	k_Bacteria|p_Actinomycetota|c_Acidimicrobiia|o_Acidimicrobiales|f_Acidimicrobiaceae|g_Acidiferrimicrobium|s_|ASV_1264	2.680
	k_Bacteria|p_Chloroflexota|c_Ktedonobacteria|o_Ktedonobacterales|f_|g_|s_|ASV_943	2.676
	k_Bacteria|p_Acidobacteriota|c_Acidobacteriae|o_Subgroup 2|f_|g_|s_|ASV_956	2.667
	k_Bacteria|p_Candidatus Eremiobacterota|c_Eremiobacteria|o_|f_|g_|s_|ASV_1270	2.665
	k_Bacteria|p_Chloroflexota|c_Ktedonobacteria|o_Ktedonobacterales|f_JG30-KF-AS9|g_|s_|ASV_1189	2.664
	k_Bacteria|p_Actinomycetota|c_Actinobacteria|o_Frankiales|f_Acidothermaceae|g_Acidothermus|s_|ASV_1274	2.662
	k_Bacteria|p_Pseudomonadota|c_Alphaproteobacteria|o_Elsterales|f_|g_|s_|ASV_1192	2.657
	k_Bacteria|p_Chloroflexota|c_Ktedonobacteria|o_Ktedonobacterales|f_Ktedonobacteraceae|g_G12-WMSP1|s_|ASV_1068	2.647
	k_Bacteria|p_Acidobacteriota|c_Acidobacteriae|o_Terriglobales|f_Acidobacteriaceae (Subgroup 1)|g_Edaphobacter|s_|ASV_1090	2.646
	k_Bacteria|p_Chloroflexota|c_Ktedonobacteria|o_Ktedonobacterales|f_|g_|s_|ASV_1313	2.614
	k_Bacteria|p_Chloroflexota|c_Ktedonobacteria|o_Ktedonobacterales|f_JG30-KF-AS9|g_|s_|ASV_1622	2.611
	k_Bacteria|p_Chloroflexota|c_Ktedonobacteria|o_Ktedonobacterales|f_JG30-KF-AS9|g_|s_|ASV_1281	2.606
	k_Bacteria|p_Chloroflexota|c_Ktedonobacteria|o_Ktedonobacterales|f_Ktedonobacteraceae|g_HSB OF53-F07|s_|ASV_1605	2.604
	k_Bacteria|p_Pseudomonadota|c_Gammaproteobacteria|o_|f_|g_Acidibacter|s_|ASV_1528	2.588
	k_Bacteria|p_Chloroflexota|c_Ktedonobacteria|o_Ktedonobacterales|f_|g_|s_|ASV_1749	2.571
	k_Bacteria|p_Pseudomonadota|c_Alphaproteobacteria|o_Elsterales|f_|g_|s_|ASV_1265	2.564
	k_Bacteria|p_Acidobacteriota|c_Acidobacteriae|o_Solibacterales|f_Solibacteraceae|g_Candidatus Solibacter|s_|ASV_1569	2.563
	k_Bacteria|p_Chloroflexota|c_Ktedonobacteria|o_Ktedonobacterales|f_JG30-KF-AS9|g_|s_|ASV_1419	2.551
	k_Bacteria|p_Pseudomonadota|c_Alphaproteobacteria|o_Micropepsales|f_Micropepsaceae|g_|s_|ASV_1588	2.547
	k_Bacteria|p_Pseudomonadota|c_Alphaproteobacteria|o_Acetobacterales|f_Acetobacteraceae|g_Acidicaldus|s_|ASV_1660	2.547
	k_Bacteria|p_Bacillota|c_Bacilli|o_Bacillales|f_Bacillaceae|g_Gottfriedia|s_|ASV_1840	2.537
	k_Bacteria|p_Pseudomonadota|c_Gammaproteobacteria|o_|f_|g_Acidibacter|s_|ASV_1774	2.528
	k_Bacteria|p_Chloroflexota|c_Ktedonobacteria|o_Ktedonobacterales|f_JG30-KF-AS9|g_|s_|ASV_1436	2.516
	k_Bacteria|p_Actinomycetota|c_Actinobacteria|o_Frankiales|f_Acidothermaceae|g_Acidothermus|s_|ASV_1487	2.509
	k_Bacteria|p_Actinomycetota|c_Actinobacteria|o_Mycobacteriales|f_Mycobacteriaceae|g_Mycobacterium|s_celatum|ASV_1630	2.503
	k_Bacteria|p_Actinomycetota|c_Actinobacteria|o_Frankiales|f_Acidothermaceae|g_Acidothermus|s_|ASV_938	2.485
	k_Bacteria|p_Pseudomonadota|c_Alphaproteobacteria|o_Reyranellales|f_Reyranellaceae|g_Reyranella|s_|ASV_1444	2.480
	k_Bacteria|p_Chloroflexota|c_Ktedonobacteria|o_Ktedonobacterales|f_JG30-KF-AS9|g_|s_|ASV_1757	2.479
	k_Bacteria|p_Bacillota|c_Bacilli|o_Paenibacillales|f_Paenibacillaceae|g_Gorillibacterium|s_|ASV_1268	2.474
	k_Bacteria|p_Chloroflexota|c_AD3|o_|f_|g_|s_|ASV_1165	2.450
	k_Bacteria|p_Chloroflexota|c_Ktedonobacteria|o_Ktedonobacterales|f_JG30-KF-AS9|g_|s_|ASV_1533	2.448

Area	Taxa	LDA
	k_Bacteria|p_Pseudomonadota|c_Gammaproteobacteria|o_|f_|g_Acidibacter|s_|ASV_1368	2.437
	k_Bacteria|p_Candidatus Eremiobacterota|c_Eremiobacteria|o_|f_|g_|s_|ASV_1963	2.425
	k_Bacteria|p_Chloroflexota|c_Ktedonobacteria|o_Ktedonobacterales|f_Ktedonobacteraceae|g_|s_|ASV_2241	2.390
	k_Bacteria|p_Candidatus Eremiobacterota|c_Eremiobacteria|o_|f_|g_|s_|ASV_1844	2.388
	k_Bacteria|p_Pseudomonadota|c_Alphaproteobacteria|o_Hyphomicrobiales|f_Devosiaceae|g_Devosia|s_|ASV_1905	2.387
	k_Bacteria|p_Chloroflexota|c_Ktedonobacteria|o_Ktedonobacterales|f_Ktedonobacteraceae|g_|s_|ASV_1951	2.381
	k_Bacteria|p_Acidobacteriota|c_Acidobacteriae|o_Subgroup 2|f_|g_|s_|ASV_2154	2.370
	k_Bacteria|p_Gemmatimonadota|c_Gemmatimonadia|o_Gemmatimonadales|f_Gemmatimonadaceae|g_Gemmatimonas|s_|ASV_1897	2.369
	k_Bacteria|p_Candidatus Eremiobacterota|c_Eremiobacteria|o_|f_|g_|s_|ASV_1346	2.358
	k_Bacteria|p_Pseudomonadota|c_Alphaproteobacteria|o_Elsterales|f_|g_|s_|ASV_2284	2.355
	k_Bacteria|p_Acidobacteriota|c_Acidobacteriae|o_Solibacterales|f_Solibacteraceae|g_Candidatus Solibacter|s_|ASV_1787	2.317
	k_Bacteria|p_Pseudomonadota|c_Gammaproteobacteria|o_|f_|g_Candidatus Berkiella|s_|ASV_2988	2.309
	k_Bacteria|p_Actinomycetota|c_Actinobacteria|o_Frankiales|f_Acidothermaceae|g_Acidothermus|s_|ASV_2428	2.294
	k_Bacteria|p_Chloroflexota|c_Ktedonobacteria|o_Ktedonobacterales|f_JG30-KF-AS9|g_|s_|ASV_3707	2.223
	k_Bacteria|p_Chloroflexota|c_Ktedonobacteria|o_Ktedonobacterales|f_JG30-KF-AS9|g_|s_|ASV_2780	2.212
	k_Bacteria|p_Pseudomonadota|c_Alphaproteobacteria|o_Elsterales|f_|g_|s_|ASV_2519	2.199
	k_Bacteria|p_Chloroflexota|c_Ktedonobacteria|o_Ktedonobacterales|f_JG30-KF-AS9|g_|s_|ASV_2400	2.177
	k_Bacteria|p_Chloroflexota|c_Ktedonobacteria|o_Ktedonobacterales|f_JG30-KF-AS9|g_|s_|ASV_2763	2.166
	k_Bacteria|p_Candidatus Eremiobacterota|c_Eremiobacteria|o_|f_|g_|s_|ASV_3819	2.142
	---------- 10-20 cm ----------	
	k_Bacteria|p_Actinomycetota|c_Thermoleophilia|o_Solirubrobacterales|f_67-14|g_|s_|ASV_363	3.077
	k_Bacteria|p_Acidobacteriota|c_Blastocatellia|o_11-24|f_|g_|s_|ASV_362	3.066
	k_Bacteria|p_Chloroflexota|c_TK10|o_|f_|g_|s_|ASV_2633	3.001
	k_Bacteria|p_Actinomycetota|c_Thermoleophilia|o_Gaiellales|f_|g_|s_|ASV_396	2.985
	k_Bacteria|p_Actinomycetota|c_Actinobacteria|o_Propionibacteriales|f_Nocardioidaceae|g_Nocardioides|s_|ASV_595	2.959
	k_Bacteria|p_Pseudomonadota|c_Gammaproteobacteria|o_Burkholderiales|f_Nitrosomonadaceae|g_Ellin6067|s_|ASV_753	2.942
	k_Bacteria|p_Pseudomonadota|c_Alphaproteobacteria|o_Hyphomicrobiales|f_Xanthobacteraceae|g_|s_|ASV_587	2.916
ILF-ST 0.00 m	k_Bacteria|p_Verrucomicrobiota|c_Verrucomicrobiia|o_Chthoniobacterales|f_Chthoniobacteraceae|g_Candidatus Udaeobacter|s_|ASV_456	2.914
	k_Bacteria|p_Pseudomonadota|c_Gammaproteobacteria|o_Burkholderiales|f_A21b|g_|s_|ASV_567	2.886
	k_Bacteria|p_Actinomycetota|c_Thermoleophilia|o_Gaiellales|f_Gaiellaceae|g_Gaiella|s_|ASV_647	2.863
	k_Bacteria|p_Pseudomonadota|c_Gammaproteobacteria|o_Steroidobacterales|f_Steroidobacteraceae|g_Steroidobacter|s_|ASV_610	2.863
	k_Bacteria|p_Actinomycetota|c_Acidimicrobiia|o_Acidimicrobiales|f_Acidimicrobiaceae|g_Acidiferrimicrobium|s_|ASV_1001	2.859
	k_Bacteria|p_Actinomycetota|c_Thermoleophilia|o_|f_|g_|s_|ASV_1141	2.852
	k_Bacteria|p_Myxococcota|c_bacteriap25|o_|f_|g_|s_|ASV_778	2.812
	k_Bacteria|p_Acidobacteriota|c_Vicinamibacteria|o_Vicinamibacterales|f_Vicinamibacteraceae|g_|s_|ASV_755	2.767
ILF-ST 5.25 m	k_Bacteria|p_Pseudomonadota|c_Alphaproteobacteria|o_Hyphomicrobiales|f_Xanthobacteraceae|g_Bradyrhizobium|s_|ASV_122	3.130

Area	Taxa	LDA
	k_Bacteria|p_Actinomycetota|c_Actinobacteria|o_Pseudonocardiales|f_Pseudonocardiaceae|g_Pseudonocardia|s_|ASV_563	2.907
	k_Bacteria|p_Pseudomonadota|c_Alphaproteobacteria|o_Elsterales|f_|g_|s_|ASV_1600	2.674
ILF-EP 0.00 m	k_Bacteria|p_Acidobacteriota|c_Acidobacteriae|o_Subgroup 2|f_|g_|s_|ASV_179	3.292
	k_Bacteria|p_Acidobacteriota|c_Vicinamibacteria|o_Vicinamibacterales|f_|g_|s_|ASV_148	3.166
	k_Bacteria|p_Pseudomonadota|c_Alphaproteobacteria|o_Elsterales|f_|g_|s_|ASV_212	3.102
	k_Bacteria|p_Actinomycetota|c_Actinobacteria|o_Frankiales|f_Acidothermaceae|g_Acidothermus|s_|ASV_459	2.779
ILF-EP 5.25 m	k_Bacteria|p_Actinomycetota|c_Thermoleophilia|o_Solirubrobacterales|f_Solirubrobacteraceae|g_Conexibacter|s_|ASV_127	3.384
	k_Bacteria|p_Acidobacteriota|c_Acidobacteriae|o_Terriglobales|f_|g_|s_|ASV_300	3.048
	k_Bacteria|p_Chloroflexota|c_Ktedonobacteria|o_B12-WMSP1|f_|g_|s_|ASV_284	3.036
	k_Bacteria|p_Acidobacteriota|c_Acidobacteriae|o_Terriglobales|f_Koribacteraceae|g_Candidatus Koribacter|s_|ASV_150	2.990
	k_Bacteria|p_Chloroflexota|c_Ktedonobacteria|o_B12-WMSP1|f_|g_|s_|ASV_405	2.845
	k_Bacteria|p_Chloroflexota|c_Ktedonobacteria|o_Ktedonobacterales|f_JG30-KF-AS9|g_|s_|ASV_518	2.759
MP	k_Bacteria|p_Chloroflexota|c_Ktedonobacteria|o_Ktedonobacterales|f_Ktedonobacteraceae|g_HSB OF53-F07|s_|ASV_108	3.146
NF	k_Bacteria|p_Pseudomonadota|c_Alphaproteobacteria|o_Hyphomicrobiales|f_Xanthobacteraceae|g_|s_|ASV_2	4.052
	k_Bacteria|p_Pseudomonadota|c_Alphaproteobacteria|o_Elsterales|f_|g_|s_|ASV_31	3.653
	k_Bacteria|p_Actinomycetota|c_Actinobacteria|o_Frankiales|f_Acidothermaceae|g_Acidothermus|s_|ASV_167	3.564
	k_Bacteria|p_Pseudomonadota|c_Alphaproteobacteria|o_Hyphomicrobiales|f_Xanthobacteraceae|g_|s_|ASV_192	3.559
	k_Bacteria|p_Pseudomonadota|c_Alphaproteobacteria|o_Hyphomicrobiales|f_Xanthobacteraceae|g_|s_|ASV_207	3.537
	k_Bacteria|p_Pseudomonadota|c_Alphaproteobacteria|o_Hyphomicrobiales|f_Xanthobacteraceae|g_|s_|ASV_121	3.503
	k_Bacteria|p_Pseudomonadota|c_Alphaproteobacteria|o_Hyphomicrobiales|f_Xanthobacteraceae|g_|s_|ASV_219	3.495
	k_Bacteria|p_Pseudomonadota|c_Gammaproteobacteria|o_|f_|g_Acidibacter|s_|ASV_164	3.461
	k_Bacteria|p_Pseudomonadota|c_Alphaproteobacteria|o_Acetobacterales|f_Acetobacteraceae|g_Acidicaldus|s_|ASV_303	3.416
	k_Bacteria|p_Acidobacteriota|c_Acidobacteriae|o_Bryobacterales|f_Bryobacteraceae|g_Bryobacter|s_|ASV_61	3.407
	k_Bacteria|p_Pseudomonadota|c_Alphaproteobacteria|o_Hyphomicrobiales|f_Xanthobacteraceae|g_|s_|ASV_253	3.406
	k_Bacteria|p_Actinomycetota|c_Thermoleophilia|o_Solirubrobacterales|f_Solirubrobacteraceae|g_Conexibacter|s_|ASV_16	3.361
	k_Bacteria|p_Acidobacteriota|c_Acidobacteriae|o_Bryobacterales|f_Bryobacteraceae|g_Bryobacter|s_|ASV_71	3.332
	k_Bacteria|p_Pseudomonadota|c_Alphaproteobacteria|o_Elsterales|f_|g_|s_|ASV_182	3.329
	k_Bacteria|p_Actinomycetota|c_Acidimicrobiia|o_Acidimicrobiales|f_Acidimicrobiaceae|g_|s_|ASV_298	3.314
	k_Bacteria|p_Pseudomonadota|c_Alphaproteobacteria|o_Hyphomicrobiales|f_Xanthobacteraceae|g_|s_|ASV_338	3.263
	k_Bacteria|p_Pseudomonadota|c_Alphaproteobacteria|o_Acetobacterales|f_Acetobacteraceae|g_Acidicaldus|s_|ASV_437	3.228
	k_Bacteria|p_Acidobacteriota|c_Acidobacteriae|o_Terriglobales|f_|g_|s_|ASV_333	3.227
	k_Bacteria|p_Pseudomonadota|c_Gammaproteobacteria|o_|f_|g_Acidibacter|s_|ASV_277	3.226
	k_Bacteria|p_Pseudomonadota|c_Alphaproteobacteria|o_Acetobacterales|f_Acetobacteraceae|g_Acidicaldus|s_|ASV_455	3.217
	k_Bacteria|p_Acidobacteriota|c_Acidobacteriae|o_Solibacterales|f_Solibacteraceae|g_Candidatus Solibacter|s_|ASV_144	3.204
	k_Bacteria|p_Chloroflexota|c_Ktedonobacteria|o_Ktedonobacterales|f_JG30-KF-AS9|g_|s_|ASV_382	3.198
	k_Bacteria|p_Pseudomonadota|c_Gammaproteobacteria|o_|f_|g_Acidibacter|s_|ASV_485	3.193

Area	Taxa	LDA
	k_Bacteria|p_Pseudomonadota|c_Alphaproteobacteria|o_Hyphomicrobiales|f_Xanthobacteraceae|g_|s_|ASV_429	3.149
	k_Bacteria|p_Pseudomonadota|c_Alphaproteobacteria|o_Elsterales|f_|g_|s_|ASV_473	3.149
	k_Bacteria|p_Actinomycetota|c_Actinobacteria|o_Frankiales|f_Acidothermaceae|g_Acidothermus|s_|ASV_356	3.130
	k_Bacteria|p_Acidobacteriota|c_Acidobacteriae|o_Solibacterales|f_Solibacteraceae|g_Candidatus Solibacter|s_|ASV_530	3.126
	k_Bacteria|p_Pseudomonadota|c_Alphaproteobacteria|o_Hyphomicrobiales|f_Xanthobacteraceae|g_|s_|ASV_458	3.113
	k_Bacteria|p_Actinomycetota|c_Thermoleophilia|o_Solirubrobacterales|f_Solirubrobacteraceae|g_Conexibacter|s_|ASV_462	3.095
	k_Bacteria|p_Actinomycetota|c_Actinobacteria|o_Frankiales|f_Acidothermaceae|g_Acidothermus|s_|ASV_581	3.092
	k_Bacteria|p_Actinomycetota|c_Actinobacteria|o_Frankiales|f_Acidothermaceae|g_Acidothermus|s_|ASV_488	3.083
	k_Bacteria|p_Acidobacteriota|c_Vicinamibacteria|o_Vicinamibacterales|f_|g_|s_|ASV_417	3.073
	k_Bacteria|p_Acidobacteriota|c_Acidobacteriae|o_Terriglobales|f_Acidobacteriaceae (Subgroup 1)|g_Terracidiphilus|s_|ASV_235	3.066
	k_Bacteria|p_Actinomycetota|c_Actinobacteria|o_Frankiales|f_Acidothermaceae|g_Acidothermus|s_|ASV_297	3.055
	k_Bacteria|p_Pseudomonadota|c_Gammaproteobacteria|o_|f_|g_Acidibacter|s_|ASV_645	3.035
	k_Bacteria|p_Pseudomonadota|c_Alphaproteobacteria|o_Hyphomicrobiales|f_Xanthobacteraceae|g_|s_|ASV_620	3.019
	k_Bacteria|p_Chloroflexota|c_TK10|o_|f_|g_|s_|ASV_568	3.015
	k_Bacteria|p_Actinomycetota|c_Actinobacteria|o_Frankiales|f_Acidothermaceae|g_Acidothermus|s_|ASV_588	3.013
	k_Bacteria|p_Actinomycetota|c_Thermoleophilia|o_Solirubrobacterales|f_Solirubrobacteraceae|g_Conexibacter|s_|ASV_365	2.999
	k_Bacteria|p_Candidatus Eremiobacterota|c_Eremiobacteria|o_|f_|g_|s_|ASV_229	2.974
	k_Bacteria|p_Pseudomonadota|c_Alphaproteobacteria|o_Hyphomicrobiales|f_Xanthobacteraceae|g_|s_|ASV_675	2.963
	k_Bacteria|p_Actinomycetota|c_Actinobacteria|o_Mycobacteriales|f_Mycobacteriaceae|g_Mycobacterium|s_|ASV_730	2.957
	k_Bacteria|p_Pseudomonadota|c_Alphaproteobacteria|o_Elsterales|f_|g_|s_|ASV_701	2.951
	k_Bacteria|p_Actinomycetota|c_Actinobacteria|o_Frankiales|f_Acidothermaceae|g_Acidothermus|s_|ASV_613	2.945
	k_Bacteria|p_Acidobacteriota|c_Acidobacteriae|o_Terriglobales|f_|g_|s_|ASV_716	2.942
	k_Bacteria|p_Pseudomonadota|c_Alphaproteobacteria|o_Elsterales|f_|g_|s_|ASV_797	2.921
	k_Bacteria|p_Pseudomonadota|c_Alphaproteobacteria|o_Acetobacterales|f_Acetobacteraceae|g_|s_|ASV_717	2.912
	k_Bacteria|p_Candidatus Eremiobacterota|c_Eremiobacteria|o_|f_|g_|s_|ASV_537	2.885
	k_Bacteria|p_Acidobacteriota|c_Vicinamibacteria|o_Vicinamibacterales|f_|g_|s_|ASV_899	2.876
	k_Bacteria|p_Chloroflexota|c_Ktedonobacteria|o_Ktedonobacterales|f_JG30-KF-AS9|g_|s_|ASV_857	2.874
	k_Bacteria|p_Actinomycetota|c_Thermoleophilia|o_Solirubrobacterales|f_Solirubrobacteraceae|g_Conexibacter|s_|ASV_407	2.834
	k_Bacteria|p_Actinomycetota|c_Acidimicrobiia|o_Acidimicrobiales|f_Acidimicrobiaceae|g_|s_|ASV_1156	2.815
	k_Bacteria|p_Actinomycetota|c_Actinobacteria|o_Frankiales|f_Acidothermaceae|g_Acidothermus|s_|ASV_803	2.807
	k_Bacteria|p_RCP2-54|c_|o_|f_|g_|s_|ASV_1013	2.807
	k_Bacteria|p_Acidobacteriota|c_Acidobacteriae|o_Terriglobales|f_Acidobacteriaceae (Subgroup 1)|g_Edaphobacter|s_|ASV_1090	2.794
	k_Bacteria|p_Pseudomonadota|c_Gammaproteobacteria|o_|f_|g_Acidibacter|s_|ASV_1022	2.779
	k_Bacteria|p_Acidobacteriota|c_Acidobacteriae|o_Subgroup 2|f_|g_|s_|ASV_956	2.776
	k_Bacteria|p_Pseudomonadota|c_Gammaproteobacteria|o_|f_|g_Acidibacter|s_|ASV_1368	2.771
	k_Bacteria|p_Chloroflexota|c_Ktedonobacteria|o_Ktedonobacterales|f_JG30-KF-AS9|g_|s_|ASV_808	2.757

Area	Taxa	LDA
	k_Bacteria|p_Chloroflexota|c_AD3|o_|f_|g_|s_|ASV_1165	2.752
	k_Bacteria|p_Bacillota|c_Bacilli|o_Paenibacillales|f_Paenibacillaceae|g_Paenibacillus|s_cellulosilyticus|ASV_928	2.751
	k_Bacteria|p_Acidobacteriota|c_Acidobacteriae|o_Terriglobales|f_|g_|s_|ASV_1028	2.746
	k_Bacteria|p_Actinomycetota|c_Acidimicrobiia|o_Acidimicrobiales|f_Acidimicrobiaceae|g_Acidiferrimicrobium|s_|ASV_1264	2.742
	k_Bacteria|p_Acidobacteriota|c_Acidobacteriae|o_Bryobacterales|f_Bryobacteraceae|g_Bryobacter|s_|ASV_1007	2.736
	k_Bacteria|p_Candidatus Eremiobacterota|c_Eremiobacteria|o_|f_|g_|s_|ASV_959	2.734
	k_Bacteria|p_Pseudomonadota|c_Alphaproteobacteria|o_Hyphomicrobiales|f_Xanthobacteraceae|g_|s_|ASV_1197	2.719
	k_Bacteria|p_Chloroflexota|c_Ktedonobacteria|o_Ktedonobacterales|f_JG30-KF-AS9|g_|s_|ASV_1189	2.716
	k_Bacteria|p_Actinomycetota|c_Acidimicrobiia|o_Acidimicrobiales|f_Acidimicrobiaceae|g_Acidiferrimicrobium|s_|ASV_1201	2.710
	k_Bacteria|p_Chloroflexota|c_Ktedonobacteria|o_Ktedonobacterales|f_Ktedonobacteraceae|g_G12-WMSP1|s_|ASV_1068	2.705
	k_Bacteria|p_Actinomycetota|c_Actinobacteria|o_Frankiales|f_Acidothermaceae|g_Acidothermus|s_|ASV_1495	2.701
	k_Bacteria|p_Candidatus Eremiobacterota|c_Eremiobacteria|o_|f_|g_|s_|ASV_1270	2.694
	k_Archaea|p_Thermoproteota|c_Nitrososphaeria|o_Nitrososphaerales|f_Nitrososphaeraceae|g_|s_|ASV_932	2.687
	k_Bacteria|p_Actinomycetota|c_Acidimicrobiia|o_Acidimicrobiales|f_Acidimicrobiaceae|g_Acidiferrimicrobium|s_|ASV_1214	2.684
	k_Bacteria|p_Acidobacteriota|c_Acidobacteriae|o_Terriglobales|f_|g_|s_|ASV_1554	2.682
	k_Bacteria|p_Acidobacteriota|c_Acidobacteriae|o_Bryobacterales|f_Bryobacteraceae|g_Bryobacter|s_|ASV_1023	2.677
	k_Bacteria|p_Pseudomonadota|c_Alphaproteobacteria|o_Hyphomicrobiales|f_KF-JG30-B3|g_|s_|ASV_1338	2.673
	k_Bacteria|p_Chloroflexota|c_Ktedonobacteria|o_Ktedonobacterales|f_JG30-KF-AS9|g_|s_|ASV_1281	2.670
	k_Archaea|p_Thermoproteota|c_Nitrososphaeria|o_Nitrososphaerales|f_Nitrososphaeraceae|g_|s_|ASV_927	2.669
	k_Bacteria|p_Acidobacteriota|c_Acidobacteriae|o_Terriglobales|f_|g_|s_|ASV_1032	2.667
	k_Bacteria|p_Actinomycetota|c_Actinobacteria|o_Frankiales|f_Acidothermaceae|g_Acidothermus|s_|ASV_1516	2.640
	k_Bacteria|p_Actinomycetota|c_Actinobacteria|o_Kitasatosporales|f_Streptomycetaceae|g_|s_|ASV_1061	2.626
	k_Bacteria|p_Acidobacteriota|c_Acidobacteriae|o_Subgroup 2|f_|g_|s_|ASV_1541	2.622
	k_Bacteria|p_Pseudomonadota|c_Alphaproteobacteria|o_Elsterales|f_|g_|s_|ASV_1752	2.607
	k_Bacteria|p_Chloroflexota|c_Ktedonobacteria|o_Ktedonobacterales|f_JG30-KF-AS9|g_|s_|ASV_1419	2.596
	k_Bacteria|p_Pseudomonadota|c_Alphaproteobacteria|o_Micropepsales|f_Micropepsaceae|g_|s_|ASV_1588	2.591
	k_Bacteria|p_Chloroflexota|c_Ktedonobacteria|o_Ktedonobacterales|f_JG30-KF-AS9|g_|s_|ASV_1436	2.578
	k_Bacteria|p_Pseudomonadota|c_Alphaproteobacteria|o_Elsterales|f_|g_|s_|ASV_1265	2.577
	k_Bacteria|p_Pseudomonadota|c_Alphaproteobacteria|o_Reyranellales|f_Reyranellaceae|g_Reyranella|s_|ASV_1444	2.574
	k_Bacteria|p_Actinomycetota|c_Actinobacteria|o_Frankiales|f_Frankiaceae|g_Frankia|s_|ASV_1470	2.567
	k_Bacteria|p_Actinomycetota|c_Actinobacteria|o_Frankiales|f_Acidothermaceae|g_Acidothermus|s_|ASV_2056	2.564
	k_Bacteria|p_Actinomycetota|c_Actinobacteria|o_Frankiales|f_Acidothermaceae|g_Acidothermus|s_|ASV_1598	2.557
	k_Bacteria|p_Pseudomonadota|c_Gammaproteobacteria|o_|f_|g_Acidibacter|s_|ASV_1774	2.556
	k_Bacteria|p_Pseudomonadota|c_Alphaproteobacteria|o_Caulobacterales|f_Caulobacteraceae|g_Phenylobacterium|s_|ASV_1718	2.539
	k_Bacteria|p_Acidobacteriota|c_Blastocatellia|o_11-24|f_|g_|s_|ASV_1746	2.535
	k_Bacteria|p_Acidobacteriota|c_Acidobacteriae|o_Subgroup 2|f_|g_|s_|ASV_1922	2.513

Area	Taxa	LDA
	k_Bacteria|p_Chloroflexota|c_Ktedonobacteria|o_Ktedonobacterales|f_Ktedonobacteraceae|g_|s_|ASV_1951	2.494
	k_Bacteria|p_Candidatus Eremiobacterota|c_Eremiobacteria|o_|f_|g_|s_|ASV_1844	2.482
	k_Bacteria|p_Chloroflexota|c_Ktedonobacteria|o_Ktedonobacterales|f_Ktedonobacteraceae|g_HSB OF53-F07|s_|ASV_1605	2.482
	k_Bacteria|p_Chloroflexota|c_Ktedonobacteria|o_Ktedonobacterales|f_JG30-KF-AS9|g_|s_|ASV_1757	2.475
	k_Bacteria|p_Gemmatimonadota|c_Gemmatimonadia|o_Gemmatimonadales|f_Gemmatimonadaceae|g_Gemmatimonas|s_|ASV_1897	2.471
	k_Bacteria|p_Candidatus Eremiobacterota|c_Eremiobacteria|o_|f_|g_|s_|ASV_1963	2.469
	k_Bacteria|p_Actinomycetota|c_Actinobacteria|o_Frankiales|f_Acidothermaceae|g_Acidothermus|s_|ASV_3176	2.466
	k_Bacteria|p_Pseudomonadota|c_Alphaproteobacteria|o_Elsterales|f_|g_|s_|ASV_2563	2.453
	k_Bacteria|p_Chloroflexota|c_Ktedonobacteria|o_Ktedonobacterales|f_Ktedonobacteraceae|g_FCPS473|s_|ASV_1691	2.446
	k_Bacteria|p_Chloroflexota|c_Ktedonobacteria|o_Ktedonobacterales|f_JG30-KF-AS9|g_|s_|ASV_1581	2.438
	k_Bacteria|p_Chloroflexota|c_Ktedonobacteria|o_Ktedonobacterales|f_|g_|s_|ASV_1749	2.433
	k_Bacteria|p_Pseudomonadota|c_Alphaproteobacteria|o_Elsterales|f_|g_|s_|ASV_2284	2.431
	k_Bacteria|p_Pseudomonadota|c_Alphaproteobacteria|o_Elsterales|f_URHD0088|g_|s_|ASV_1919	2.400
	k_Bacteria|p_Acidobacteriota|c_Vicinamibacteria|o_Vicinamibacterales|f_|g_|s_|ASV_1880	2.338
	k_Bacteria|p_Chloroflexota|c_Ktedonobacteria|o_B12-WMSP1|f_|g_|s_|ASV_2861	2.314
	k_Bacteria|p_Pseudomonadota|c_Alphaproteobacteria|o_Hyphomicrobiales|f_Devosiaceae|g_Devosia|s_|ASV_1905	2.300
	k_Bacteria|p_Bacillota|c_Sulfobacillia|o_Sulfobacillales|f_Sulfobacillaceae|g_|s_|ASV_3069	2.185
	---------- 20-40 cm ----------	
ILF-ST 0.00 m	k_Bacteria|p_Actinomycetota|c_Actinobacteria|o_Frankiales|f_Acidothermaceae|g_Acidothermus|s_|ASV_820	2.884
	k_Bacteria|p_Pseudomonadota|c_Alphaproteobacteria|o_Hyphomicrobiales|f_Xanthobacteraceae|g_Pseudolabrys|s_|ASV_741	2.837
ILF-EP 5.25 m	k_Bacteria|p_Actinomycetota|c_Thermoleophilia|o_Solirubrobacterales|f_Solirubrobacteraceae|g_Conexibacter|s_|ASV_127	3.458
NF	k_Bacteria|p_Actinomycetota|c_Actinobacteria|o_Frankiales|f_Acidothermaceae|g_Acidothermus|s_|ASV_167	3.495
	k_Bacteria|p_Pseudomonadota|c_Alphaproteobacteria|o_Hyphomicrobiales|f_Xanthobacteraceae|g_|s_|ASV_129	3.427
	k_Bacteria|p_Pseudomonadota|c_Alphaproteobacteria|o_Hyphomicrobiales|f_Xanthobacteraceae|g_|s_|ASV_121	3.425
	k_Bacteria|p_Pseudomonadota|c_Alphaproteobacteria|o_Hyphomicrobiales|f_Xanthobacteraceae|g_|s_|ASV_192	3.401
	k_Bacteria|p_Pseudomonadota|c_Alphaproteobacteria|o_Hyphomicrobiales|f_Xanthobacteraceae|g_|s_|ASV_207	3.353
	k_Bacteria|p_Pseudomonadota|c_Alphaproteobacteria|o_Elsterales|f_|g_|s_|ASV_182	3.346
	k_Bacteria|p_Pseudomonadota|c_Alphaproteobacteria|o_Hyphomicrobiales|f_Xanthobacteraceae|g_|s_|ASV_219	3.339
	k_Bacteria|p_Actinomycetota|c_Acidimicrobiia|o_Acidimicrobiales|f_Acidimicrobiaceae|g_|s_|ASV_298	3.338
	k_Bacteria|p_Acidobacteriota|c_Acidobacteriae|o_Solibacterales|f_Solibacteraceae|g_Candidatus Solibacter|s_|ASV_144	3.282
	k_Bacteria|p_Pseudomonadota|c_Alphaproteobacteria|o_Hyphomicrobiales|f_Xanthobacteraceae|g_|s_|ASV_429	3.102
	k_Bacteria|p_Pseudomonadota|c_Alphaproteobacteria|o_Elsterales|f_|g_|s_|ASV_1265	3.061
	k_Bacteria|p_Pseudomonadota|c_Alphaproteobacteria|o_Acetobacterales|f_Acetobacteraceae|g_Acidicaldus|s_|ASV_437	3.051
	k_Bacteria|p_Actinomycetota|c_Thermoleophilia|o_Solirubrobacterales|f_Solirubrobacteraceae|g_Conexibacter|s_|ASV_462	3.041
	k_Bacteria|p_Pseudomonadota|c_Gammaproteobacteria|o_|f_|g_Acidibacter|s_|ASV_485	3.025

Area	Taxa	LDA
	k_Bacteria|p_Actinomycetota|c_Actinobacteria|o_Frankiales|f_Acidothermaceae|g_Acidothermus|s_|ASV_581	2.998
	k_Bacteria|p_Acidobacteriota|c_Acidobacteriae|o_Solibacterales|f_Solibacteraceae|g_Candidatus Solibacter|s_|ASV_530	2.990
	k_Bacteria|p_Actinomycetota|c_Actinobacteria|o_Frankiales|f_Acidothermaceae|g_Acidothermus|s_|ASV_588	2.966
	k_Bacteria|p_Acidobacteriota|c_Acidobacteriae|o_Subgroup 2|f_|g_|s_|ASV_956	2.909
	k_Bacteria|p_Acidobacteriota|c_Vicinamibacteria|o_Vicinamibacterales|f_|g_|s_|ASV_1880	2.891
	k_Bacteria|p_Pseudomonadota|c_Alphaproteobacteria|o_Elsterales|f_|g_|s_|ASV_797	2.877
	k_Bacteria|p_Acidobacteriota|c_Acidobacteriae|o_Bryobacterales|f_Bryobacteraceae|g_Bryobacter|s_|ASV_1007	2.854
	k_Bacteria|p_Acidobacteriota|c_Acidobacteriae|o_Terriglobales|f_|g_|s_|ASV_1028	2.817
	k_Bacteria|p_Chloroflexota|c_Ktedonobacteria|o_Ktedonobacterales|f_JG30-KF-AS9|g_|s_|ASV_1419	2.795
	k_Bacteria|p_Gemmatimonadota|c_Gemmatimonadia|o_Gemmatimonadales|f_Gemmatimonadaceae|g_Gemmatimonas|s_|ASV_1897	2.791
	k_Bacteria|p_Acidobacteriota|c_Acidobacteriae|o_Bryobacterales|f_Bryobacteraceae|g_Bryobacter|s_|ASV_1023	2.776
	k_Bacteria|p_Pseudomonadota|c_Alphaproteobacteria|o_Hyphomicrobiales|f_Devosiaceae|g_Devosia|s_|ASV_1905	2.762
	k_Bacteria|p_Chloroflexota|c_Ktedonobacteria|o_Ktedonobacterales|f_JG30-KF-AS9|g_|s_|ASV_857	2.745
	k_Bacteria|p_Acidobacteriota|c_Acidobacteriae|o_Terriglobales|f_Acidobacteriaceae (Subgroup 1)|g_Edaphobacter|s_|ASV_1090	2.736

† Significant (adjusted $p < 0.05$) taxa identified by Linear Discriminant Analysis Effect Size (LEfSe) with an LDA score threshold of ≥ 2.000. Positive LDA scores indicate significantly higher relative abundance of the taxon within the respective area compared to other treatments in that soil layer. Taxonomic levels: p, phylum; c, class; o, order; f, family; g, genus; s, species; ASV, amplicon sequence variant.

Table 2.5 - Taxonomic biomarkers of soil fungal communities across management systems, sampling distances from the tree row in the ILF systems (0.00 and 5.25 m), and soil layers (0-10, 10-20 and 20–40 cm) †. LDA: linear discriminant analysis score. ILF-ST: integrated livestock-forestry with *Samanea tubulosa*; ILF-EP: integrated livestock-forestry with *Eucalyptus pellita*; MP: *Urochloa brizantha* 'Marandu' pasture; NF: native forest.

Area	Taxa	LDA
	---------- 0-10 cm ----------	
ILF-ST 0.00 m	k_Fungi|p_Ascomycota|c_Sordariomycetes|o_Hypocreales|f_Nectriaceae|g_Fusarium|s_variasi|ASV_5	4.324
	k_Fungi|p_Rozellomycota|c_|o_GS11|f_|g_|s_|ASV_24	4.065
	k_Fungi|p_Ascomycota|c_Eurotiomycetes|o_Eurotiales|f_Aspergillaceae|g_Penicillium|s_shearii|ASV_39	3.868
	k_Fungi|p_Mortierellomycota|c_Mortierellomycetes|o_Mortierellales|f_Mortierellaceae|g_Actinomortierella|s_|ASV_27	3.842
	k_Fungi|p_Ascomycota|c_Sordariomycetes|o_Sordariales|f_Chaetomiaceae|g_Humicola|s_|ASV_167	3.408
	k_Fungi|p_Ascomycota|c_Eurotiomycetes|o_Onygenales|f_Onygenaceae|g_Auxarthron|s_|ASV_193	3.260
	k_Fungi|p_|c_|o_|f_|g_|s_|ASV_393	3.256
	k_Fungi|p_Ascomycota|c_Sordariomycetes|o_Hypocreales|f_|g_|s_|ASV_347	3.169
	k_Fungi|p_Ascomycota|c_Sordariomycetes|o_Hypocreales|f_Nectriaceae|g_Volutella|s_consors|ASV_459	3.012
	k_Fungi|p_Ascomycota|c_Sordariomycetes|o_Hypocreales|f_|g_|s_|ASV_1102	2.709
	k_Fungi|p_Ascomycota|c_Sordariomycetes|o_Myrmecridiales|f_Myrmecridiaceae|g_Myrmecridium|s_schulzeri|ASV_992	2.643
	k_Fungi|p_Ascomycota|c_Sordariomycetes|o_Hypocreales|f_|g_|s_|ASV_771	2.640
	k_Fungi|p_Ascomycota|c_Sordariomycetes|o_Sordariales|f_Neoschizotheciaceae|g_Cercophora|s_fici|ASV_5375	2.584
	k_Fungi|p_Ascomycota|c_Dothideomycetes|o_Pleosporales|f_Dacampiaceae|g_Aaosphaeria|s_arxii|ASV_797	2.559
	k_Fungi|p_Basidiomycota|c_|o_|f_|g_|s_|ASV_1703	2.500
	k_Fungi|p_|c_|o_|f_|g_|s_|ASV_2124	2.412
ILF-ST 5.25 m	k_Fungi|p_Ascomycota|c_Sordariomycetes|o_Hypocreales|f_|g_Bulbithecium|s_pinkertoniae|ASV_16	3.898
	k_Fungi|p_Ascomycota|c_Sordariomycetes|o_Sordariales|f_Chaetomiaceae|g_Staphylotrichum|s_acaciicola|ASV_258	3.292
	k_Fungi|p_Ascomycota|c_Dothideomycetes|o_Pleosporales|f_Phaeosphaeriaceae|g_Setophoma|s_|ASV_1738	2.402
ILF-EP 0.00 m	k_Fungi|p_Ascomycota|c_Archaeorhizomycetes|o_Archaeorhizomycetales|f_Archaeorhizomycetaceae|g_|s_|ASV_15	4.427
	k_Fungi|p_Basidiomycota|c_Agaricomycetes|o_Thelephorales|f_Thelephoraceae|g_Tomentella|s_|ASV_6	4.365
	k_Fungi|p_Basidiomycota|c_Agaricomycetes|o_Thelephorales|f_Thelephoraceae|g_|s_|ASV_33	4.061
	k_Fungi|p_Ascomycota|c_Eurotiomycetes|o_Eurotiales|f_Trichocomaceae|g_Talaromyces|s_|ASV_68	3.919
	k_Fungi|p_Ascomycota|c_Pezizomycetes|o_Pezizales|f_Pezizaceae|g_Ruhlandiella|s_|ASV_69	3.639
	k_Fungi|p_Basidiomycota|c_Agaricomycetes|o_Boletales|f_Sclerodermataceae|g_Pisolithus|s_marmoratus|ASV_496	3.177
	k_Fungi|p_Entorrhizomycota|c_|o_Branch04|f_|g_|s_|ASV_374	3.113
	k_Fungi|p_Ascomycota|c_Eurotiomycetes|o_Phaeomoniellales|f_Celotheliaceae|g_Phaeomoniella|s_|ASV_732	2.899
	k_Fungi|p_Ascomycota|c_|o_|f_|g_|s_|ASV_1910	2.705
	k_Fungi|p_Ascomycota|c_Eurotiomycetes|o_Eurotiales|f_Trichocomaceae|g_Talaromyces|s_diversus|ASV_1026	2.625
	k_Fungi|p_Ascomycota|c_|o_|f_|g_|s_|ASV_1967	2.482
	k_Fungi|p_Ascomycota|c_Eurotiomycetes|o_Eurotiales|f_|g_|s_|ASV_1633	2.471

Area	Taxa	LDA
ILF-EP 5.25 m	k_Fungi|p_Basidiomycota|c_Agaricomycetes|o_Agaricales|f_Entolomataceae|g_|s_|ASV_54	3.406
MP	k_Fungi|p_Ascomycota|c_Eurotiomycetes|o_Eurotiales|f_Aspergillaceae|g_Penicillium|s_shearii|ASV_222	3.263
	k_Fungi|p_|c_|o_|f_|g_|s_|ASV_205	3.144
	k_Fungi|p_Ascomycota|c_Dothideomycetes|o_|f_|g_|s_|ASV_243	2.845
NF	k_Fungi|p_Ascomycota|c_Sordariomycetes|o_Hypocreales|f_Clavicipitaceae|g_Metarhizium|s_|ASV_129	3.817
	k_Fungi|p_|c_|o_|f_|g_|s_|ASV_189	3.619
	k_Fungi|p_Ascomycota|c_|o_|f_|g_|s_|ASV_278	3.553
	k_Fungi|p_|c_|o_|f_|g_|s_|ASV_233	3.483
	k_Fungi|p_|c_|o_|f_|g_|s_|ASV_388	3.417
	k_Fungi|p_Basidiomycota|c_|o_|f_|g_|s_|ASV_234	3.385
	k_Fungi|p_Ascomycota|c_Sordariomycetes|o_Microascales|f_Microascaceae|g_Pseudallescheria|s_angusta|ASV_149	3.382
	k_Fungi|p_|c_|o_|f_|g_|s_|ASV_271	3.304
	k_Fungi|p_Ascomycota|c_|o_|f_|g_|s_|ASV_324	3.226
	k_Fungi|p_Ascomycota|c_Eurotiomycetes|o_Eurotiales|f_Aspergillaceae|g_Aspergillus|s_citocrescens|ASV_408	3.184
	k_Fungi|p_Ascomycota|c_Sordariomycetes|o_Sordariales|f_Chaetomiaceae|g_|s_|ASV_318	3.102
	k_Fungi|p_Basidiomycota|c_Tremellomycetes|o_|f_|g_|s_|ASV_283	3.092
	k_Fungi|p_|c_|o_|f_|g_|s_|ASV_555	3.082
	k_Fungi|p_|c_|o_|f_|g_|s_|ASV_509	3.061
	k_Fungi|p_Ascomycota|c_Eurotiomycetes|o_Eurotiales|f_Aspergillaceae|g_Penicillium|s_aquadulcis|ASV_527	3.059
	k_Fungi|p_Basidiomycota|c_|o_|f_|g_|s_|ASV_619	3.036
	k_Fungi|p_Basidiomycota|c_|o_|f_|g_|s_|ASV_662	3.030
	k_Fungi|p_|c_|o_|f_|g_|s_|ASV_620	3.026
	k_Fungi|p_|c_|o_|f_|g_|s_|ASV_786	3.000
	k_Fungi|p_Ascomycota|c_Eurotiomycetes|o_Eurotiales|f_Aspergillaceae|g_|s_|ASV_612	2.990
	k_Fungi|p_Ascomycota|c_Eurotiomycetes|o_Eurotiales|f_Trichocomaceae|g_Talaromyces|s_|ASV_927	2.990
	k_Fungi|p_|c_|o_|f_|g_|s_|ASV_1322	2.986
	k_Fungi|p_Basidiomycota|c_Cystobasidiomycetes|o_Cystobasidiales|f_Cystobasidiaceae|g_Cystobasidium|s_|ASV_890	2.976
	k_Fungi|p_Ascomycota|c_Leotiomycetes|o_Helotiales|f_Dermateaceae|g_Pezicula|s_ericae|ASV_592	2.973
	k_Fungi|p_Ascomycota|c_Eurotiomycetes|o_Eurotiales|f_Trichocomaceae|g_|s_|ASV_698	2.970
	k_Fungi|p_Basidiomycota|c_|o_|f_|g_|s_|ASV_650	2.957
	k_Fungi|p_Ascomycota|c_Leotiomycetes|o_Helotiales|f_|g_Xylogone|s_|ASV_784	2.927
	k_Fungi|p_|c_|o_|f_|g_|s_|ASV_723	2.926
	k_Fungi|p_Ascomycota|c_Eurotiomycetes|o_Eurotiales|f_Aspergillaceae|g_Penicillium|s_|ASV_642	2.925
	k_Fungi|p_Basidiomycota|c_Cystobasidiomycetes|o_Cystobasidiales|f_Cystobasidiaceae|g_Cystobasidium|s_|ASV_711	2.879
	k_Fungi|p_Rozellomycota|c_|o_GS11|f_|g_|s_|ASV_767	2.878
	k_Fungi|p_Ascomycota|c_Leotiomycetes|o_Helotiales|f_|g_|s_|ASV_719	2.829
	k_Fungi|p_Basidiomycota|c_|o_|f_|g_|s_|ASV_1027	2.818
	k_Fungi|p_Ascomycota|c_Eurotiomycetes|o_Eurotiales|f_Aspergillaceae|g_Penicillium|s_ferraniaense|ASV_781	2.812
	k_Fungi|p_Ascomycota|c_Eurotiomycetes|o_Eurotiales|f_Aspergillaceae|g_|s_|ASV_1059	2.802
	k_Fungi|p_Ascomycota|c_Eurotiomycetes|o_Chaetothyriales|f_Herpotrichiellaceae|g_Cladophialophora|s_lanosa|ASV_1025	2.769

Area	Taxa	LDA
	k_Fungi|p_Ascomycota|c_|o_|f_|g_|s_|ASV_1174	2.767
	k_Fungi|p_Ascomycota|c_Leotiomycetes|o_Helotiales|f_Helotiaceae|g_Scytalidium|s_ganodermophthorum|ASV_588	2.747
	k_Fungi|p_|c_|o_|f_|g_|s_|ASV_949	2.738
	k_Fungi|p_Ascomycota|c_|o_|f_|g_|s_|ASV_1021	2.690
	k_Fungi|p_Basidiomycota|c_|o_|f_|g_|s_|ASV_1132	2.684
	k_Fungi|p_Ascomycota|c_Sordariomycetes|o_|f_|g_|s_|ASV_2140	2.667
	k_Fungi|p_Ascomycota|c_Sordariomycetes|o_Microascales|f_Microascaceae|g_Scedosporium|s_minutisporum|ASV_899	2.640
	k_Fungi|p_Ascomycota|c_Sordariomycetes|o_Hypocreales|f_Ophiocordycipitaceae|g_Tolypocladium|s_album|ASV_1441	2.639
	k_Fungi|p_Ascomycota|c_Eurotiomycetes|o_Eurotiales|f_|g_|s_|ASV_1744	2.639
	k_Fungi|p_Basidiomycota|c_|o_|f_|g_|s_|ASV_1335	2.638
	k_Fungi|p_|c_|o_|f_|g_|s_|ASV_1111	2.629
	k_Fungi|p_Rozellomycota|c_|o_GS11|f_|g_|s_|ASV_907	2.624
	k_Fungi|p_|c_|o_|f_|g_|s_|ASV_2380	2.624
	k_Fungi|p_Ascomycota|c_Dothideomycetes|o_Venturiales|f_Sympoventuriaceae|g_Sympoventuria|s_capensis|ASV_1106	2.614
	k_Fungi|p_Ascomycota|c_Eurotiomycetes|o_Eurotiales|f_Aspergillaceae|g_|s_|ASV_1353	2.612
	k_Fungi|p_Basidiomycota|c_Agaricomycetes|o_|f_|g_|s_|ASV_1629	2.606
	k_Fungi|p_Ascomycota|c_Sordariomycetes|o_Sordariales|f_Chaetomiaceae|g_Acrophialophora|s_levis|ASV_1525	2.603
	k_Fungi|p_Ascomycota|c_|o_|f_|g_|s_|ASV_1863	2.597
	k_Fungi|p_Ascomycota|c_Sordariomycetes|o_Amphisphaeriales|f_|g_|s_|ASV_1561	2.588
	k_Fungi|p_Basidiomycota|c_|o_|f_|g_|s_|ASV_1246	2.586
	k_Fungi|p_Ascomycota|c_Dothideomycetes|o_|f_|g_|s_|ASV_1124	2.585
	k_Fungi|p_Ascomycota|c_Eurotiomycetes|o_Eurotiales|f_|g_|s_|ASV_1217	2.580
	k_Fungi|p_Basidiomycota|c_|o_|f_|g_|s_|ASV_1247	2.576
	k_Fungi|p_Ascomycota|c_Eurotiomycetes|o_Eurotiales|f_Aspergillaceae|g_Aspergillus|s_|ASV_1564	2.572
	k_Fungi|p_Ascomycota|c_Dothideomycetes|o_|f_|g_|s_|ASV_1354	2.555
	k_Fungi|p_Mucoromycota|c_Umbelopsidomycetes|o_|f_|g_|s_|ASV_1331	2.532
	k_Fungi|p_Basidiomycota|c_Agaricomycetes|o_Agaricales|f_Entolomataceae|g_Entoloma|s_|ASV_917	2.527
	k_Fungi|p_Ascomycota|c_Sordariomycetes|o_Diaporthales|f_Melanconiellaceae|g_Melanconiella|s_|ASV_1684	2.527
	k_Fungi|p_|c_|o_|f_|g_|s_|ASV_1398	2.515
	k_Fungi|p_Ascomycota|c_Sordariomycetes|o_Hypocreales|f_Bionectriaceae|g_Nectriopsis|s_didymii|ASV_1885	2.510
	k_Fungi|p_Mortierellomycota|c_Mortierellomycetes|o_Mortierellales|f_Mortierellaceae|g_Lunasporangiospora|s_|ASV_1268	2.507
	k_Fungi|p_Ascomycota|c_Eurotiomycetes|o_Eurotiales|f_Trichocomaceae|g_Talaromyces|s_wortmannii|ASV_1726	2.503
	k_Fungi|p_Basidiomycota|c_Tremellomycetes|o_|f_|g_|s_|ASV_449	2.503
	k_Fungi|p_Ascomycota|c_Eurotiomycetes|o_Eurotiales|f_Trichocomaceae|g_Talaromyces|s_|ASV_1068	2.489
	k_Fungi|p_Kickxellomycota|c_|o_|f_|g_|s_|ASV_365	2.487
	k_Fungi|p_|c_|o_|f_|g_|s_|ASV_1897	2.468
	k_Fungi|p_Rozellomycota|c_|o_GS11|f_|g_|s_|ASV_2430	2.433
	k_Fungi|p_Ascomycota|c_Sordariomycetes|o_Hypocreales|f_|g_|s_|ASV_3659	2.427
	k_Fungi|p_Ascomycota|c_Sordariomycetes|o_Hypocreales|f_|g_|s_|ASV_2017	2.422
	k_Fungi|p_Ascomycota|c_|o_|f_|g_|s_|ASV_1481	2.417

Area	Taxa	LDA
	k_Fungi|p_Ascomycota|c_|o_|f_|g_|s_|ASV_1912	2.376
	k_Fungi|p_|c_|o_|f_|g_|s_|ASV_1795	2.374
	k_Fungi|p_Ascomycota|c_|o_|f_|g_|s_|ASV_1766	2.361
	k_Fungi|p_Basidiomycota|c_|o_|f_|g_|s_|ASV_2216	2.358
	k_Fungi|p_Ascomycota|c_Sordariomycetes|o_Hypocreales|f_|g_|s_|ASV_3190	2.285
	k_Fungi|p_Ascomycota|c_Dothideomycetes|o_|f_|g_Marquesius|s_|ASV_2154	2.259
	k_Fungi|p_Ascomycota|c_Sordariomycetes|o_Hypocreales|f_Ophiocordycipitaceae|g_Tolypocladium|s_tropicale|ASV_1979	2.256
	k_Fungi|p_Ascomycota|c_Sordariomycetes|o_|f_|g_|s_|ASV_2457	2.248
	k_Fungi|p_Ascomycota|c_Eurotiomycetes|o_Eurotiales|f_Aspergillaceae|g_Penicillium|s_|ASV_2731	2.243
	k_Fungi|p_Ascomycota|c_Leotiomycetes|o_Helotiales|f_Dermateaceae|g_Pezicula|s_ericae|ASV_2638	2.204
	k_Fungi|p_Ascomycota|c_Sordariomycetes|o_Amplistromatales|f_Amplistromataceae|g_Neoacrodontium|s_|ASV_1320	2.176
	k_Fungi|p_Chytridiomycota|c_|o_|f_|g_|s_|ASV_3316	2.140
	k_Fungi|p_Ascomycota|c_Dothideomycetes|o_Pleosporales|f_Didymosphaeriaceae|g_Paraconiothyrium|s_|ASV_4246	2.120
	k_Fungi|p_|c_|o_|f_|g_|s_|ASV_2395	2.091
	k_Fungi|p_Basidiomycota|c_Agaricomycetes|o_Agaricales|f_|g_|s_|ASV_1757	2.091
	k_Fungi|p_|c_|o_|f_|g_|s_|ASV_3554	2.088
	k_Fungi|p_|c_|o_|f_|g_|s_|ASV_3535	2.062
	k_Fungi|p_Ascomycota|c_Eurotiomycetes|o_Eurotiales|f_Aspergillaceae|g_Penicillium|s_aquadulcis|ASV_2361	2.031
	k_Fungi|p_Basidiomycota|c_|o_|f_|g_|s_|ASV_3850	2.006
	---------- 10-20 cm ----------	
ILF-ST 0.00 m	k_Fungi|p_Ascomycota|c_Sordariomycetes|o_Hypocreales|f_Nectriaceae|g_Fusarium|s_variasi|ASV_5	4.313
	k_Fungi|p_Rozellomycota|c_|o_GS11|f_|g_|s_|ASV_24	3.980
	k_Fungi|p_Ascomycota|c_Sordariomycetes|o_Hypocreales|f_Ophiocordycipitaceae|g_Purpureocillium|s_lilacinum|ASV_14	3.949
	k_Fungi|p_Mortierellomycota|c_Mortierellomycetes|o_Mortierellales|f_Mortierellaceae|g_Actinomortierella|s_|ASV_27	3.807
	k_Fungi|p_Ascomycota|c_Eurotiomycetes|o_Eurotiales|f_Aspergillaceae|g_Penicillium|s_shearii|ASV_39	3.762
	k_Fungi|p_Ascomycota|c_Sordariomycetes|o_Sordariales|f_Chaetomiaceae|g_Acrophialophora|s_|ASV_81	3.425
	k_Fungi|p_Ascomycota|c_Eurotiomycetes|o_Onygenales|f_Onygenaceae|g_Auxarthron|s_|ASV_193	3.318
	k_Fungi|p_Ascomycota|c_Sordariomycetes|o_Sordariales|f_Chaetomiaceae|g_Humicola|s_|ASV_167	3.266
	k_Fungi|p_Ascomycota|c_Sordariomycetes|o_Hypocreales|f_Stachybotryaceae|g_Striaticonidium|s_humicola|ASV_389	3.086
	k_Fungi|p_Ascomycota|c_Sordariomycetes|o_Hypocreales|f_Nectriaceae|g_Fusarium|s_|ASV_470	2.932
	k_Fungi|p_|c_|o_|f_|g_|s_|ASV_393	2.896
	k_Fungi|p_Ascomycota|c_Sordariomycetes|o_Hypocreales|f_|g_|s_|ASV_771	2.717
	k_Fungi|p_Ascomycota|c_Sordariomycetes|o_Hypocreales|f_|g_|s_|ASV_1102	2.662
	k_Fungi|p_Ascomycota|c_Sordariomycetes|o_|f_|g_|s_|ASV_5472	2.634
	k_Fungi|p_Ascomycota|c_Dothideomycetes|o_Pleosporales|f_Dacampiaceae|g_Aaosphaeria|s_arxii|ASV_797	2.626
	k_Fungi|p_Mortierellomycota|c_Mortierellomycetes|o_Mortierellales|f_Mortierellaceae|g_|s_|ASV_426	2.554
	k_Fungi|p_|c_|o_|f_|g_|s_|ASV_1084	2.514

Area	Taxa	LDA
ILF-ST 5.25 m	k_Fungi|p_Ascomycota|c_Sordariomycetes|o_Hypocreales|f_|g_Bulbithecium|s_pinkertoniae|ASV_16	3.926
ILF-EP 0.00 m	k_Fungi|p_Basidiomycota|c_Agaricomycetes|o_Thelephorales|f_Thelephoraceae|g_Tomentella|s_|ASV_6	4.398
	k_Fungi|p_Ascomycota|c_Archaeorhizomycetes|o_Archaeorhizomycetales|f_Archaeorhizomycetaceae|g_|s_|ASV_15	4.255
	k_Fungi|p_Basidiomycota|c_Agaricomycetes|o_Thelephorales|f_Thelephoraceae|g_|s_|ASV_33	3.867
	k_Fungi|p_Ascomycota|c_Eurotiomycetes|o_Eurotiales|f_Trichocomaceae|g_Talaromyces|s_|ASV_68	3.840
	k_Fungi|p_Entorrhizomycota|c_|o_Branch04|f_|g_|s_|ASV_374	3.122
	k_Fungi|p_Ascomycota|c_Eurotiomycetes|o_Phaeomoniellales|f_Celotheliaceae|g_Phaeomoniella|s_|ASV_732	2.925
	k_Fungi|p_Basidiomycota|c_Agaricomycetes|o_Boletales|f_Sclerodermataceae|g_Scleroderma|s_citrinum|ASV_519	2.917
	k_Fungi|p_Ascomycota|c_Eurotiomycetes|o_Eurotiales|f_Trichocomaceae|g_Talaromyces|s_diversus|ASV_1026	2.678
	k_Fungi|p_Ascomycota|c_Sordariomycetes|o_|f_|g_|s_|ASV_4697	2.478
	k_Fungi|p_Ascomycota|c_|o_|f_|g_|s_|ASV_1910	2.455
MP	k_Fungi|p_Ascomycota|c_Eurotiomycetes|o_Eurotiales|f_Aspergillaceae|g_Penicillium|s_shearii|ASV_222	3.231
	k_Fungi|p_Basidiomycota|c_|o_|f_|g_|s_|ASV_1219	2.757
NF	k_Fungi|p_Ascomycota|c_Sordariomycetes|o_Hypocreales|f_Clavicipitaceae|g_Metarhizium|s_|ASV_129	3.811
	k_Fungi|p_|c_|o_|f_|g_|s_|ASV_233	3.717
	k_Fungi|p_Basidiomycota|c_Tremellomycetes|o_|f_|g_|s_|ASV_283	3.673
	k_Fungi|p_|c_|o_|f_|g_|s_|ASV_189	3.532
	k_Fungi|p_Basidiomycota|c_Tremellomycetes|o_|f_|g_|s_|ASV_449	3.526
	k_Fungi|p_Basidiomycota|c_|o_|f_|g_|s_|ASV_234	3.495
	k_Fungi|p_Ascomycota|c_|o_|f_|g_|s_|ASV_278	3.260
	k_Fungi|p_Basidiomycota|c_Tremellomycetes|o_Tremellales|f_Trimorphomycetaceae|g_Saitozyma|s_podzolica|ASV_576	3.242
	k_Fungi|p_Ascomycota|c_Eurotiomycetes|o_Eurotiales|f_Aspergillaceae|g_Aspergillus|s_citocrescens|ASV_408	3.232
	k_Fungi|p_|c_|o_|f_|g_|s_|ASV_509	3.007
	k_Fungi|p_Ascomycota|c_Eurotiomycetes|o_Eurotiales|f_Aspergillaceae|g_|s_|ASV_612	3.003
	k_Fungi|p_Ascomycota|c_Eurotiomycetes|o_Eurotiales|f_Trichocomaceae|g_|s_|ASV_698	2.977
	k_Fungi|p_Basidiomycota|c_Cystobasidiomycetes|o_Cystobasidiales|f_Cystobasidiaceae|g_Cystobasidium|s_|ASV_711	2.953
	k_Fungi|p_Ascomycota|c_Eurotiomycetes|o_Eurotiales|f_Aspergillaceae|g_Penicillium|s_aquadulcis|ASV_527	2.915
	k_Fungi|p_Ascomycota|c_Eurotiomycetes|o_Eurotiales|f_Aspergillaceae|g_Penicillium|s_|ASV_642	2.911
	k_Fungi|p_Basidiomycota|c_|o_|f_|g_|s_|ASV_662	2.903
	k_Fungi|p_Basidiomycota|c_|o_|f_|g_|s_|ASV_650	2.898
	k_Fungi|p_Basidiomycota|c_|o_|f_|g_|s_|ASV_619	2.893
	k_Fungi|p_Ascomycota|c_Leotiomycetes|o_Helotiales|f_|g_|s_|ASV_719	2.892
	k_Fungi|p_Ascomycota|c_Leotiomycetes|o_Helotiales|f_Dermateaceae|g_Pezicula|s_ericae|ASV_592	2.865
	k_Fungi|p_Rozellomycota|c_|o_GS11|f_|g_|s_|ASV_767	2.792
	k_Fungi|p_Ascomycota|c_Leotiomycetes|o_Helotiales|f_Helotiaceae|g_Scytalidium|s_ganodermophthorum|ASV_934	2.787
	k_Fungi|p_Ascomycota|c_Eurotiomycetes|o_Eurotiales|f_Aspergillaceae|g_Penicillium|s_ferraniaense|ASV_781	2.778
	k_Fungi|p_|c_|o_|f_|g_|s_|ASV_1042	2.759

Area	Taxa	LDA
	k_Fungi|p_Chytridiomycota|c_Rhizophlyctidomycetes|o_Rhizophlyctidales|f_Rhizophlyctidaceae|g_|s_|ASV_918	2.753
	k_Fungi|p_Rozellomycota|c_|o_GS11|f_|g_|s_|ASV_907	2.710
	k_Fungi|p_Ascomycota|c_Leotiomycetes|o_Helotiales|f_|g_Xylogone|s_|ASV_784	2.703
	k_Fungi|p_|c_|o_|f_|g_|s_|ASV_855	2.700
	k_Fungi|p_|c_|o_|f_|g_|s_|ASV_1389	2.692
	k_Fungi|p_Ascomycota|c_Sordariomycetes|o_|f_|g_|s_|ASV_1365	2.654
	k_Fungi|p_Ascomycota|c_Eurotiomycetes|o_Eurotiales|f_Trichocomaceae|g_Talaromyces|s_|ASV_927	2.646
	k_Fungi|p_Basidiomycota|c_|o_|f_|g_|s_|ASV_1027	2.630
	k_Fungi|p_Ascomycota|c_Eurotiomycetes|o_Eurotiales|f_Aspergillaceae|g_|s_|ASV_1059	2.616
	k_Fungi|p_Ascomycota|c_Dothideomycetes|o_Venturiales|f_Sympoventuriaceae|g_Sympoventuria|s_capensis|ASV_1106	2.615
	k_Fungi|p_Basidiomycota|c_|o_|f_|g_|s_|ASV_1247	2.608
	k_Fungi|p_Ascomycota|c_Eurotiomycetes|o_Eurotiales|f_|g_|s_|ASV_1217	2.594
	k_Fungi|p_Basidiomycota|c_|o_|f_|g_|s_|ASV_870	2.593
	k_Fungi|p_Basidiomycota|c_|o_|f_|g_|s_|ASV_1246	2.588
	k_Fungi|p_Ascomycota|c_Sordariomycetes|o_Hypocreales|f_Nectriaceae|g_Penicillifer|s_dipa rietisporus|ASV_1239	2.580
	k_Fungi|p_Ascomycota|c_Sordariomycetes|o_|f_|g_|s_|ASV_1617	2.574
	k_Fungi|p_Ascomycota|c_|o_|f_|g_|s_|ASV_1481	2.535
	k_Fungi|p_Ascomycota|c_Sordariomycetes|o_Hypocreales|f_Ophiocordycipitaceae|g_Tolypocladium|s_album|ASV_1441	2.523
	k_Fungi|p_Basidiomycota|c_|o_|f_|g_|s_|ASV_1132	2.521
	k_Fungi|p_Ascomycota|c_Eurotiomycetes|o_Chaetothyriales|f_Herpotrichiellaceae|g_Cladophialophora|s_lanosa|ASV_1025	2.494
	k_Fungi|p_Ascomycota|c_Sordariomycetes|o_Glomerellales|f_Plectosphaerellaceae|g_Plectosphaerella|s_|ASV_1282	2.493
	k_Fungi|p_Basidiomycota|c_|o_|f_|g_|s_|ASV_1335	2.493
	k_Fungi|p_Ascomycota|c_Eurotiomycetes|o_Eurotiales|f_Aspergillaceae|g_Aspergillus|s_|ASV_1564	2.475
	k_Fungi|p_Basidiomycota|c_|o_|f_|g_|s_|ASV_603	2.473
	k_Fungi|p_Basidiomycota|c_|o_|f_|g_|s_|ASV_1559	2.451
	k_Fungi|p_Ascomycota|c_Eurotiomycetes|o_Eurotiales|f_|g_|s_|ASV_1744	2.445
	k_Fungi|p_Ascomycota|c_Eurotiomycetes|o_Eurotiales|f_Aspergillaceae|g_Aspergillus|s_|ASV_1195	2.426
	k_Fungi|p_|c_|o_|f_|g_|s_|ASV_1842	2.413
	k_Fungi|p_Ascomycota|c_Sordariomycetes|o_Amphisphaeriales|f_|g_|s_|ASV_1561	2.380
	k_Fungi|p_Ascomycota|c_|o_|f_|g_|s_|ASV_1653	2.375
	k_Fungi|p_Ascomycota|c_Eurotiomycetes|o_Eurotiales|f_Trichocomaceae|g_Talaromyces|s_wortmannii|ASV_1726	2.370
	k_Fungi|p_Ascomycota|c_Dothideomycetes|o_|f_|g_Marquesius|s_|ASV_2154	2.346
	k_Fungi|p_|c_|o_|f_|g_|s_|ASV_1897	2.332
	k_Fungi|p_Ascomycota|c_Eurotiomycetes|o_Eurotiales|f_Aspergillaceae|g_|s_|ASV_1353	2.328
	k_Fungi|p_|c_|o_|f_|g_|s_|ASV_2519	2.298
	k_Fungi|p_Ascomycota|c_|o_|f_|g_|s_|ASV_1606	2.292
	k_Fungi|p_Ascomycota|c_|o_|f_|g_|s_|ASV_2160	2.280
	k_Fungi|p_Basidiomycota|c_|o_|f_|g_|s_|ASV_3440	2.276
	k_Fungi|p_|c_|o_|f_|g_|s_|ASV_1965	2.263
	k_Fungi|p_|c_|o_|f_|g_|s_|ASV_2827	2.242
	k_Fungi|p_Ascomycota|c_Eurotiomycetes|o_|f_|g_|s_|ASV_2441	2.216

Area	Taxa	LDA
	k_Fungi|p_|c_|o_|f_|g_|s_|ASV_2989	2.208
	k_Fungi|p_Ascomycota|c_Sordariomycetes|o_Hypocreales|f_|g_|s_|ASV_2017	2.189
	k_Fungi|p_Basidiomycota|c_|o_|f_|g_|s_|ASV_2216	2.189
	k_Fungi|p_Basidiomycota|c_|o_|f_|g_|s_|ASV_2542	2.165
	k_Fungi|p_Ascomycota|c_Eurotiomycetes|o_Eurotiales|f_Aspergillaceae|g_Penicillium|s_|ASV_2731	2.128
	k_Fungi|p_|c_|o_|f_|g_|s_|ASV_2207	2.109
	k_Fungi|p_Rozellomycota|c_|o_GS11|f_|g_|s_|ASV_2065	2.101
	k_Fungi|p_Chytridiomycota|c_|o_|f_|g_|s_|ASV_3316	2.041
	k_Fungi|p_Ascomycota|c_Dothideomycetes|o_|f_|g_|s_|ASV_5682	2.028
	k_Fungi|p_Ascomycota|c_Sordariomycetes|o_|f_|g_|s_|ASV_3692	2.015
	k_Fungi|p_|c_|o_|f_|g_|s_|ASV_3896	2.007
	---------- 20-40 cm ----------	
ILF-ST 0.00 m	k_Fungi|p_Ascomycota|c_Sordariomycetes|o_Hypocreales|f_|g_|s_|ASV_1102	2.843
ILF-EP 0.00 m	k_Fungi|p_Basidiomycota|c_Agaricomycetes|o_Thelephorales|f_Thelephoraceae|g_Tomentella|s_|ASV_6	4.484
	k_Fungi|p_Basidiomycota|c_Agaricomycetes|o_Thelephorales|f_Thelephoraceae|g_|s_|ASV_33	3.865
	k_Fungi|p_Ascomycota|c_Eurotiomycetes|o_Eurotiales|f_Trichocomaceae|g_Talaromyces|s_|ASV_68	3.766
	k_Fungi|p_Entorrhizomycota|c_|o_Branch04|f_|g_|s_|ASV_374	3.308
	k_Fungi|p_Ascomycota|c_Eurotiomycetes|o_Phaeomoniellales|f_Celotheliaceae|g_Phaeomoniella|s_|ASV_732	3.059
NF	k_Fungi|p_|c_|o_|f_|g_|s_|ASV_189	3.606
	k_Fungi|p_Basidiomycota|c_|o_|f_|g_|s_|ASV_234	3.592
	k_Fungi|p_|c_|o_|f_|g_|s_|ASV_271	3.481
	k_Fungi|p_Ascomycota|c_|o_|f_|g_|s_|ASV_278	3.242
	k_Fungi|p_|c_|o_|f_|g_|s_|ASV_555	3.182
	k_Fungi|p_Basidiomycota|c_|o_|f_|g_|s_|ASV_619	3.139
	k_Fungi|p_|c_|o_|f_|g_|s_|ASV_233	3.090
	k_Fungi|p_Ascomycota|c_Eurotiomycetes|o_Eurotiales|f_Aspergillaceae|g_Penicillium|s_aquadulcis|ASV_527	3.087
	k_Fungi|p_Basidiomycota|c_|o_|f_|g_|s_|ASV_650	3.075
	k_Fungi|p_Ascomycota|c_Leotiomycetes|o_Helotiales|f_|g_Xylogone|s_|ASV_784	3.051
	k_Fungi|p_Ascomycota|c_Eurotiomycetes|o_Eurotiales|f_Aspergillaceae|g_Aspergillus|s_citocrescens|ASV_408	3.018
	k_Fungi|p_Basidiomycota|c_Tremellomycetes|o_|f_|g_|s_|ASV_283	3.003
	k_Fungi|p_Ascomycota|c_Eurotiomycetes|o_Eurotiales|f_Aspergillaceae|g_Penicillium|s_ferraniaense|ASV_781	2.980
	k_Fungi|p_|c_|o_|f_|g_|s_|ASV_855	2.954
	k_Fungi|p_Rozellomycota|c_|o_GS11|f_|g_|s_|ASV_907	2.951
	k_Fungi|p_Ascomycota|c_Leotiomycetes|o_Helotiales|f_|g_|s_|ASV_719	2.932
	k_Fungi|p_Ascomycota|c_Sordariomycetes|o_Hypocreales|f_Clavicipitaceae|g_|s_|ASV_770	2.921
	k_Fungi|p_Ascomycota|c_Sordariomycetes|o_Hypocreales|f_Nectriaceae|g_Ilyonectria|s_|ASV_964	2.916
	k_Fungi|p_Chytridiomycota|c_Rhizophlyctidomycetes|o_Rhizophlyctidales|f_Rhizophlyctidaceae|g_|s_|ASV_918	2.867
	k_Fungi|p_Ascomycota|c_Dothideomycetes|o_Venturiales|f_Sympoventuriaceae|g_Sympoventuria|s_capensis|ASV_1106	2.857
	k_Fungi|p_Basidiomycota|c_Cystobasidiomycetes|o_Cystobasidiales|f_Cystobasidiaceae|g_Cystobasidium|s_|ASV_711	2.834
	k_Fungi|p_|c_|o_|f_|g_|s_|ASV_1398	2.800

Area	Taxa	LDA
	k_Fungi|p_Basidiomycota|c_|o_|f_|g_|s_|ASV_1132	2.797
	k_Fungi|p_Basidiomycota|c_|o_|f_|g_|s_|ASV_1246	2.777
	k_Fungi|p_Basidiomycota|c_Tremellomycetes|o_|f_|g_|s_|ASV_449	2.734
	k_Fungi|p_Ascomycota|c_Eurotiomycetes|o_Eurotiales|f_|g_|s_|ASV_1217	2.726
	k_Fungi|p_Ascomycota|c_Sordariomycetes|o_Amphisphaeriales|f_Castanediellaceae|g_Castanediella|s_cagnizarii|ASV_1786	2.680
	k_Fungi|p_Ascomycota|c_|o_|f_|g_|s_|ASV_1481	2.603
	k_Fungi|p_Ascomycota|c_|o_|f_|g_|s_|ASV_1653	2.577
	k_Fungi|p_Basidiomycota|c_|o_|f_|g_|s_|ASV_1335	2.565
	k_Fungi|p_Ascomycota|c_|o_|f_|g_|s_|ASV_2792	2.399

† Significant (adjusted $p < 0.05$) taxa identified by Linear Discriminant Analysis Effect Size (LEfSe) with an LDA score threshold of ≥ 2.000. Positive LDA scores indicate significantly higher relative abundance of the taxon within the respective area compared to other treatments in that soil layer. Taxonomic levels: p, phylum; c, class; o, order; f, family; g, genus; s, species; ASV, amplicon sequence variant.

Among the prokaryotic biomarkers, the phyla *Pseudomonadota*, *Actinomycetota*, *Acidobacteriota*, and *Chloroflexota* were the most abundant, with 33.1, 20.6, 19.4, and 17.8 % of the total biomarkers, respectively. Therefore, the other eight significant phyla represented 9.1 % of the biomarkers. *Alphaproteobacteria* (phylum *Pseudomonadota*), *Ktedonobacteria* (phylum *Chloroflexota*), *Acidobacteria* (phylum *Acidobacteriota*), and *Actinobacteria* (phylum *Actinomycetota*) were the most abundant classes, with 26.9, 15.6, 15.3, and 11.9 % of the total biomarkers, while the other 16 classes summed up 30.3 %. Notably, only two *Archaea* biomarkers were observed: ASV_927, in the 0-10 and 20-40 cm layers, and ASV_932, in the 10-20 cm layer. They were both from NF and belong to the *Nitrososphaeraceae* family (phylum *Thermoproteota*).

The managed system with most prokaryotic biomarkers was ILF-ST at 0.00 m, with 8, 15, and 2 biomarkers in the 0-10, 10-20 and 20-40 cm layers, respectively, summing up 25 biomarkers, followed by ILF-EP at 5.25 m, with 5, 5, and 2 biomarkers in 0-10, 10-20 and 20-40 cm layers, respectively. Interestingly, ILF-EP presented more biomarkers at 5.25 m (12) than at 0.00 m (7). Additionally, the tree-integrated systems presented more biomarkers in the 10-20 cm layer, whereas MP and NF presented more biomarkers in the 0-10 cm layer.

In the 0-10 cm layer, the highest effect size was recorded in ILF-EP 5.25 m, dominated by an ASV from the *Xanthobacteraceae* family (ASV_1, LDA = 4.331). The native forest (NF) followed with a strong signature from another *Xanthobacteraceae* member (ASV_2, LDA = 4.089). In the MP system, the most prominent biomarker belonged to the *Micromonosporaceae* family (ASV_53, LDA = 3.337). Within the integrated systems at the tree row, ILF-EP 0.00 m was characterized by *Acidobacteriae* Subgroup 2 (ASV_179, LDA = 3.264), while ILF-ST 0.00 m was defined by a member of the *Methyloligellaceae* family

(ASV_580, LDA = 2.952). The ILF-ST 5.25 m distance was specifically marked by the genus *Acidiferrimicrobium* (ASV_1001, LDA = 2.876).

At the 10-20 cm layer, several taxa showed vertical persistence. The NF area maintained its primary biomarker (*Xanthobacteraceae*, ASV_2) with a consistently high effect size (LDA = 4.052). Similarly, ILF-EP 0.00 m continued to be characterized by *Acidobacteriae* Subgroup 2 (ASV_179, LDA = 3.292). In the ILF-EP 5.25 m system, the dominant biomarker shifted to the genus *Conexibacter* (ASV_127, LDA = 3.384). The MP system at this depth was uniquely identified by the genus *HSBOF53-F07* (*Ktedonobacteraceae*; ASV_108, LDA = 3.146). Within the ILF-ST system, the tree row (0.00 m) was marked by the 67-14 group (*Solirubrobacterales*; ASV_363, LDA = 3.077), while the 5.25 m distance was characterized by the genus *Bradyrhizobium* (ASV_122, LDA = 3.130).

In the deepest layer (20-40 cm), the genus *Acidothermus* emerged as a key biomarker for both the NF (ASV_167, LDA = 3.495) and ILF-ST 0.00 m (ASV_820, LDA = 2.884) systems. The ILF-EP 5.25 m system maintained ASV_127 (genus *Conexibacter*) as its primary biomarker, which reached its highest effect size at this depth (LDA = 3.458).

Ascomycota phyla represented 55.0 % of the fungal biomarkers, followed by *Basidiomycota* with 20.9 %. The other six identified phyla summed up 8.1 %, whereas 16.1 % of biomarkers were from indetermined phyla. Moreover, 41.4 % of the biomarkers are from unidentified classes, but *Eurotiomycetes* and *Sordariomycetes* (phylum *Ascomycota*) comprised 19.4 and 18.3 % of total fungal biomarkers. Among the managed systems, ILF-ST at 0.00 m presented the highest number of biomarkers: 16, 17, and 1 in the 0-10, 10-20 and 20-40 cm layers, respectively. The ILF-EP system, contrary to what was observed for prokaryotic biomarkers, presented higher number of fungal biomarkers at 0.00 m from the tree row: 12, 10, and 5 in the 0-10, 10-20 and 20-40 cm layers, respectively. Notably, no fungal biomarker was identified in the 20-40 cm layer for ILF-ST and ILF-EP at 5.25 m, nor for MP.

In the 0-10 cm layer, the highest effect size among integrated systems was found in ILF-EP 0.00 m, dominated by an ASV of the class *Archaeorhizomycetes* (ASV_15, LDA = 4.427). In the ILF-ST 0.00 m system, the primary biomarker was identified as *Fusarium variasi* (ASV_5, LDA = 4.324). At the 5.25 m distance, the integrated systems were characterized by *Bulbithecium pinkertoniae* (ASV_16, LDA = 3.898) in the ILF-ST area and a member of the *Entolomataceae* family (ASV_54, LDA = 3.406) in the ILF-EP area. The NF system was distinguished by the entomopathogenic genus *Metarhizium* (ASV_129, LDA = 3.817), while the MP system was defined by *Penicillium shearii* (ASV_222, LDA = 3.263).

At the 10-20 cm layer, remarkable taxonomic stability was observed for several systems. *Fusarium variasi* (ASV_5) remained the top biomarker for ILF-ST 0.00 m (LDA = 4.313), and *Bulbithecium pinkertoniae* (ASV_16) persisted as the primary biomarker for ILF-ST 5.25 m (LDA = 3.926). Similarly, the NF system maintained *Metarhizium* (ASV_129) as its principal biomarker (LDA = 3.811), and the MP system continued to be characterized by *Penicillium shearii* (ASV_222, LDA = 3.231). In contrast, the biomarker for ILF-EP 0.00 m shifted to the ectomycorrhizal genus *Tomentella* (ASV_6), which reached a high effect size (LDA = 4.398).

In the 20-40 cm layer, the genus *Tomentella* (ASV_6) remained the dominant biomarker for the ILF-EP 0.00 m system, achieving its highest effect size at this depth (LDA = 4.484). For the ILF-ST 0.00 m system, the primary biomarker was an unidentified member of the *Hypocreales* order (ASV_1102, LDA = 2.843). The native forest (NF) was identified by a highly specific but unclassified fungal ASV (ASV_189, LDA = 3.606).

The taxonomic composition analysis revealed that soil microbial communities, across both Prokaryotic and Fungal domains, are dominated by a select number of persistent phyla, regardless of management system or soil depth (Figure 2.3). Importantly, LEfSe results demonstrated that the statistically significant biomarkers for each treatment belonged, in their majority, to these high-frequency phyla.

The prokaryotic community was characterized by the predominance of *Pseudomonadota*, *Actinomycetota*, *Acidobacteriota*, and *Chloroflexota*, which together accounted for the bulk (more than 70 %) of the relative abundance across all profiles. Notably, NF exhibited a higher proportion of *Acidobacteriota* and *Pseudomonadota*, and lower proportion of *Bacillota* compared to managed systems. This pattern is maintained across soil layers.

Archaea abundance was relatively small, with less than 0.8 % in the system with the highest abundance (ILF-ST at 0.00 m), followed by MP and NF (Figure 2.4). *Thermoproteota* was the most abundant phylum, with approximately 90 % of the archaeal abundance in most treatments, except for ILF-ST in the 5.25 m distance and the 20-40 cm soil layer, which presented less than 80 % of *Thermoproteota*. Moreover, *Thermoplasmatota* was the second most abundant phyla across areas and soil layers, except for ILF-ST at 0.00 m, in all layers, and at 5.25 m in the topsoil. In these treatments, *Nanoarchaeota* was the second most abundant phylum.

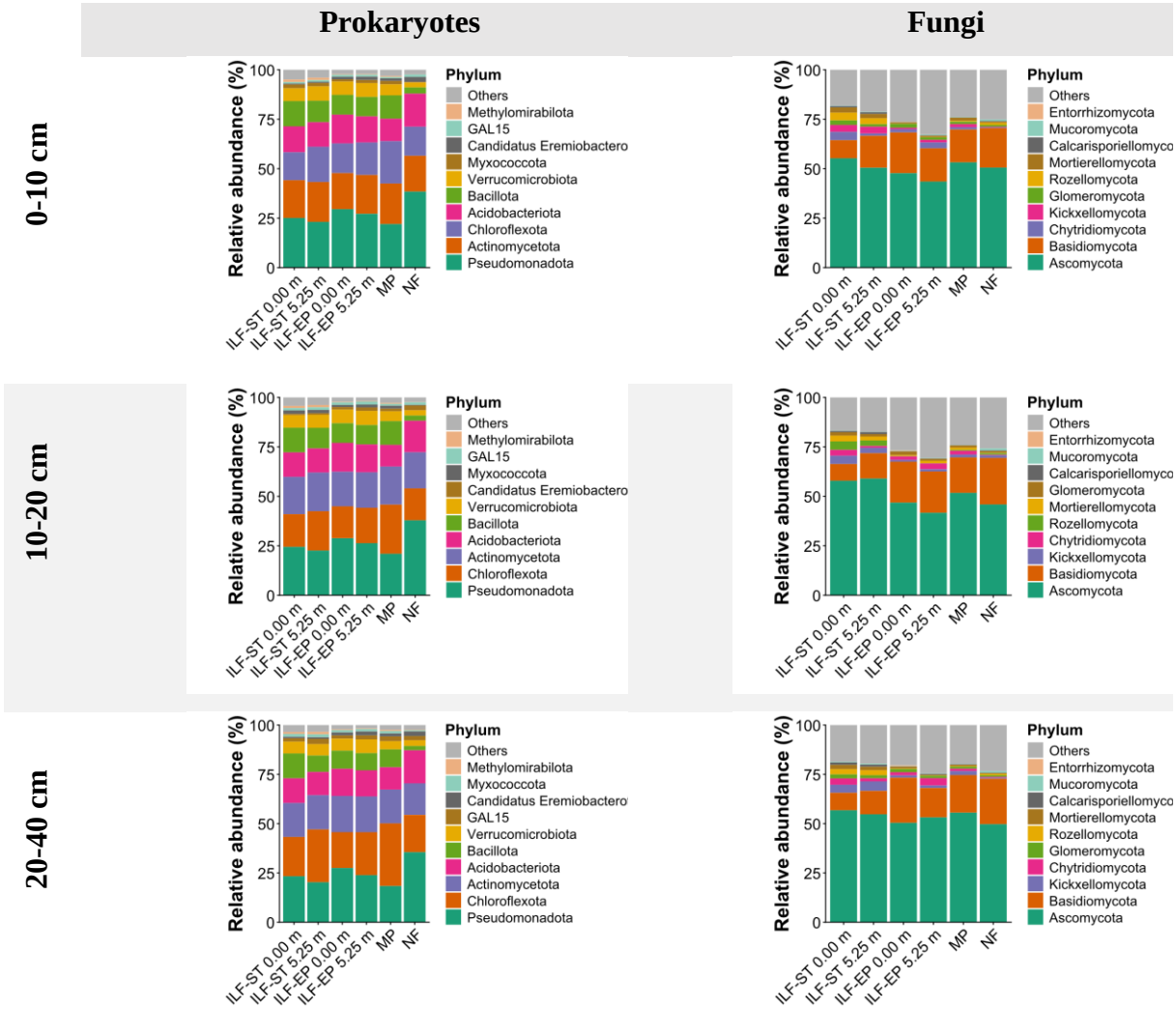

Figure 2.3 - Relative abundance of prokaryotic and fungal phyla across three soil layers (0-10, 10-20, and 20-40 cm) under different management systems. ILF-ST: integrated livestock-forestry with *Samanea tubulosa*; ILF-EP: integrated livestock-forestry with *Eucalyptus pellita*; MP: *Urochloa brizantha* 'Marandu' pasture; NF: native forest; 0.00 and 5.25 m: distance from the tree row in the ILF systems.

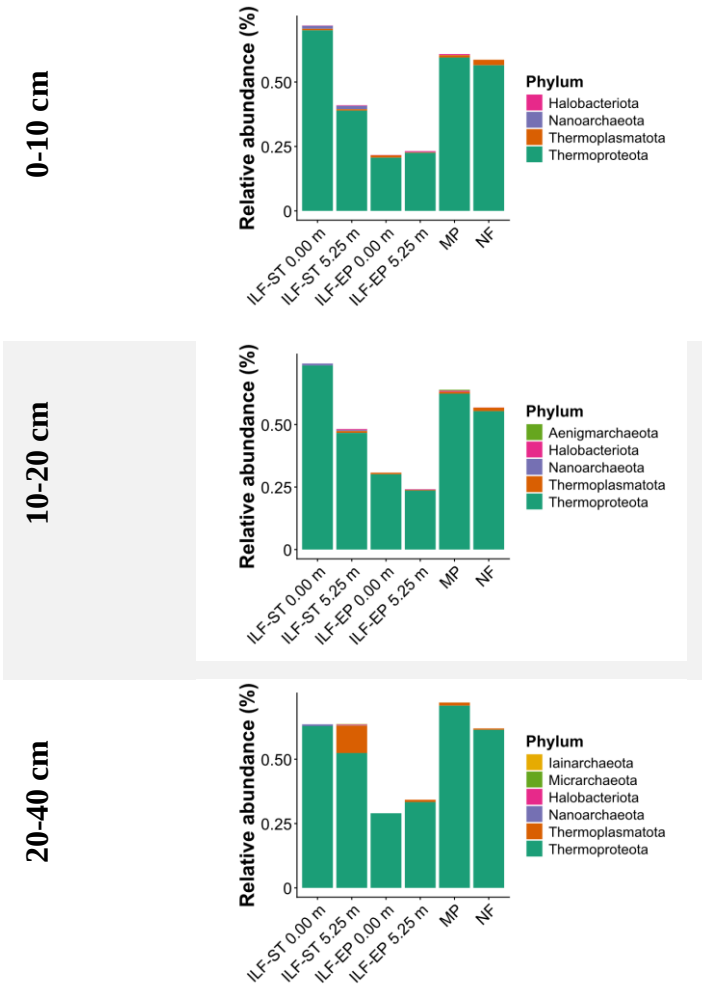

Figure 2.4 - Relative abundance of *Archaea* phyla across three soil layers (0-10, 10-20, and 20-40 cm) under different management systems. ILF-ST: integrated livestock-forestry with *Samanea tubulosa*; ILF-EP: integrated livestock-forestry with *Eucalyptus pellita*; MP: *Urochloa brizantha* 'Marandu' pasture; NF: native forest; 0.00 and 5.25 m: distance from the tree row in the ILF systems.

The fungal community was heavily dominated by *Ascomycota*, which accounted for approximately 50 % of the relative abundance, followed by *Basidiomycota*, with 10-25 % of the relative abundance, depending on the area and soil layer. Notably, the proportion of others phyla is higher in fungal than prokaryotic communities, mainly due to the contribution of unidentified phyla.

The Venn diagrams illustrate the unique and shared ASVs among areas (Figure 2.5 for prokaryotes and Figure 2.6 for fungi). Remarkably, NF and MP present the highest numbers of unique prokaryotic ASVs, each representing 12-16 % of the total ASV richness across layers. In contrast, the integrated systems (ILF-ST and ILF-EP) showed a high degree of overlap between their respective distances from the tree row (0.00 m and 5.25 m), with lower counts of exclusive ASVs compared to the reference areas.

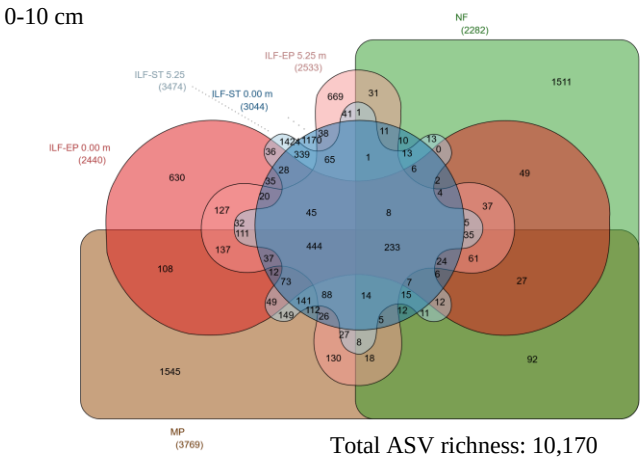

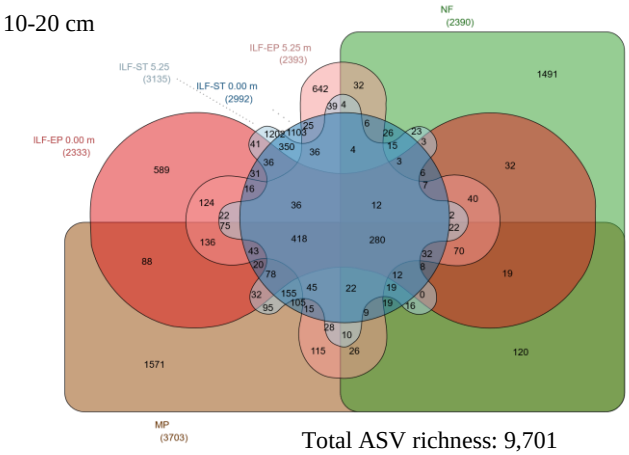

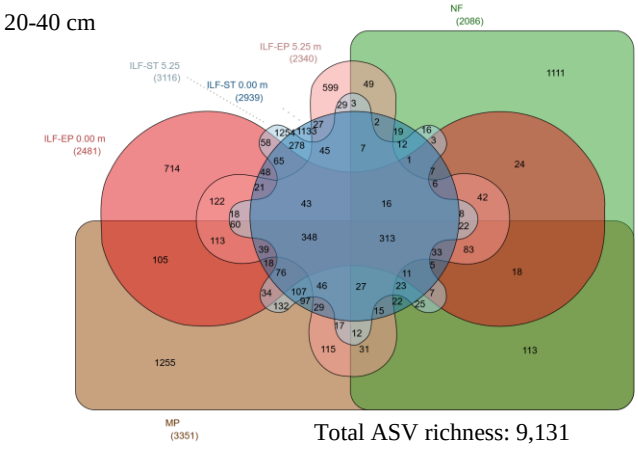

Figure 2.5 - Distribution and sharing of prokaryotic amplicon sequence variants (ASVs) across soil layers (0-10, 10-20, and 20-40 cm) under different management systems. Venn diagrams illustrate the number of unique and shared ASVs among the treatments. ILF-ST: integrated livestock-forestry with *Samanea tubulosa*; ILF-EP: integrated livestock-forestry with *Eucalyptus pellita*; MP: *Urochloa brizantha* 'Marandu' pasture; NF: native forest; 0.00 and 5.25 m: distance from the tree row in the ILF systems. Numerical values in the central overlapping areas represent the core microbiome (taxa persistent across all systems) for each respective layer. Total ASV richness for each soil layer is indicated in the bottom right corner of each panel.

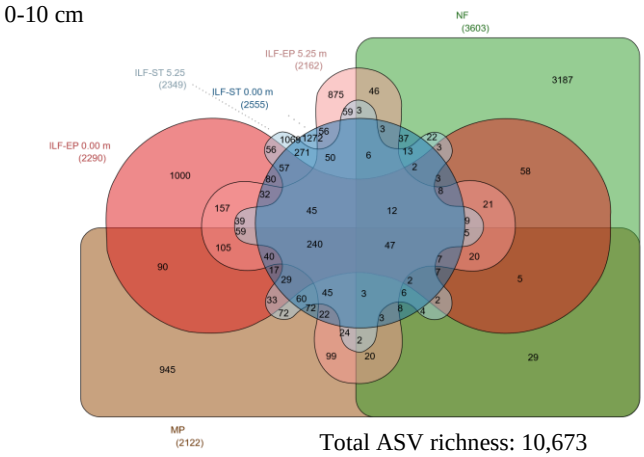

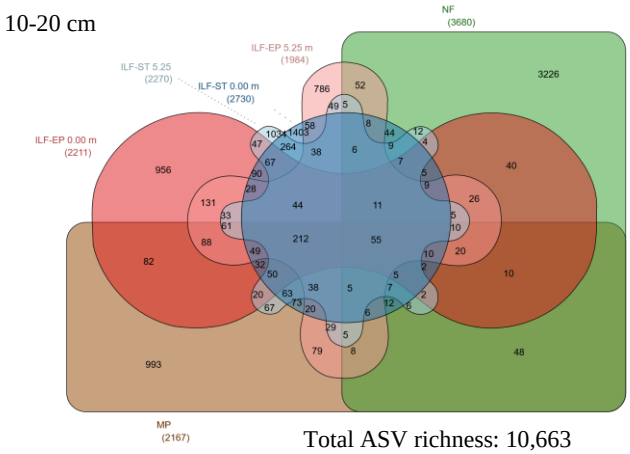

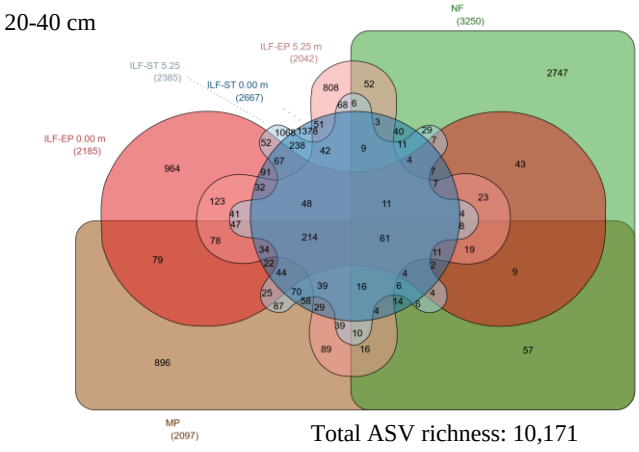

Figure 2.6 - Distribution and sharing of fungi amplicon sequence variants (ASVs) across soil layers (0-10, 10-20, and 20-40 cm) under different management systems. Venn diagrams illustrate the number of unique and shared ASVs among the treatments. ILF-ST: integrated livestock-forestry with *Samanea tubulosa*; ILF-EP: integrated livestock-forestry with *Eucalyptus pellita*; MP: *Urochloa brizantha* 'Marandu' pasture; NF: native forest; 0.00 and 5.25 m: distance from the tree row in the ILF systems. Numerical values in the central overlapping areas represent the core microbiome (taxa persistent across all systems) for each respective layer. Total ASV richness for each soil layer is indicated in the bottom right corner of each panel.

A primary distinction between prokaryotes and fungi regarding the distribution of unique and shared ASVs was observed in NF, which functioned as a significantly more specialized reservoir for fungi than for prokaryotes. While unique ASVs in the NF accounted for approximately 15 % of the total prokaryotic community, this proportion doubled to 30 % for the fungal community.

In the prokaryotic domain, the ILF-ST system presented the third-largest proportion of unique ASVs, surpassing the ILF-EP system by nearly 100 %. Furthermore, the unique prokaryotic richness in ILF-ST almost equilibrated with the MP, which remained the closest system to NF in terms of exclusive taxa. In contrast, the fungal domain showed a homogenization of unique richness among the managed systems. The differences between MP, ILF-ST, and ILF-EP were considerably smaller for fungi than for prokaryotes. Nevertheless, the ILF-ST remained the most diverse among the managed options (considering all five managed treatments).

The core microbiota, which represents the degree of community cohesion, also differed drastically between the two domains. For prokaryotes, approximately 3 % of all ASVs were shared across all six treatments. In contrast, this universal sharing dropped to 0.5 % for fungi, indicating a much lower baseline of common taxa across the entire study area. This trend was also reflected in the managed systems (excluding NF). The proportion of ASVs shared exclusively among the five managed systems decreased from 4 % in prokaryotes to less than 2 % in fungi.

The spatial sharing of ASVs between the tree row (0.00 m) and the area at 5.25 m distance from the tree row was different between the two microbial groups. For prokaryotes, in the ILF-ST system, 3 % of ASVs were shared between both distances, whereas in the ILF-EP, this sharing was 1%. For fungi, a 2 % sharing between distances was observed in the ILF-ST compared to 1 % in the ILF-EP.

2.3.4 Functional prediction and profile analysis

The functional prediction analysis using FAPROTAX identified distinct metabolic signatures across management systems and soil depths (Table 2.6). The ILF-ST at 0.00 m treatment presented the highest number of functional biomarkers across all sampled layers. In the topsoil (0-10 cm), this system was significantly enriched with anaerobic chemoheterotrophy, nitrate reduction, and aromatic compound degradation. In contrast, at the 5.25 m distance, ILF-ST was characterized by sulfur-related pathways, specifically sulfate

respiration and respiration of sulfur compounds, while the ILF-EP system at the same depth was uniquely identified by dark hydrogen oxidation. The MP system in this layer showed a distinct signature for cellulolysis.

Table 2.6 - Predicted functional biomarkers of prokaryotic communities across soil layers and management systems. The potential ecological functions were predicted using the FAPROTAX database based on 16S rRNA gene sequences. Listed functions represent significant biomarkers identified by Linear Discriminant Analysis Effect Size (LEfSe). Only functional groups with an adjusted p-value < 0.05 and a Linear Discriminant Analysis (LDA) score ≥ 2.000 are shown. Positive LDA scores indicate significantly higher relative abundance of the functional group within the respective area compared to other treatments in that soil layer. ILF-ST: integrated livestock-forestry with *Samanea tubulosa*; ILF-EP: integrated livestock-forestry with *Eucalyptus pellita*; MP: *Urochloa brizantha* 'Marandu' pasture; NF: native forest; 0.00 and 5.25 m: distance from the tree row in the ILF systems.

Layer	Area	Potential function	LDA
0-10 cm	ILF-ST 0.00 m	anaerobic_chemoheterotrophy	4.401
		nitrate_reduction	3.701
		aromatic_compound_degradation	3.491
		invertebrate_parasites	3.474
	ILF-ST 5.25 m	sulfate_respiration	3.397
		respiration_of_sulfur_compounds	3.397
	ILF-EP 5.25 m	dark_hydrogen_oxidation	4.195
	MP	cellulolysis	4.285
10-20 cm	ILF-ST 0.00 m	anaerobic_chemoheterotrophy	4.610
		chemoheterotrophy	4.403
		aromatic_compound_degradation	4.134
	NF	cellulolysis	4.487
20-40 cm	ILF-ST 0.00 m	anaerobic_chemoheterotrophy	4.300
	ILF-ST 5.25 m	nitrate_reduction	3.759
	NF	intracellular_parasites	3.619

In the intermediate layer (10-20 cm), anaerobic chemoheterotrophy remained a dominant biomarker for ILF-ST 0.00 m, reaching the highest effect size (LDA = 4.61). In the same layer, NF was characterized by cellulolysis, which was notably absent as a significant biomarker in the tree-integrated systems. At the deepest layer (20- 40 cm), the functional profile was more streamlined. ILF-ST at 0.00 m maintained its association with anaerobic chemoheterotrophy, while at 5.25 m it showed a significant presence of nitrate reduction. Interestingly, the NF system at this depth was uniquely associated with intracellular parasites, contrasting with the more metabolic-oriented biomarkers found in the managed areas.

The functional prediction analysis using the FungalTraits database revealed distinct ecological specializations among the management systems across the soil profile (Table 2.7). The ILF-EP 0.00 m treatment presented the most prominent functional signature, characterized by a strong dominance of ectomycorrhizal fungi (LDA > 4.2) across all three soil layers. This

system was also associated with specific fungal structures, such as corticioid and gasteroid fruit bodies, and various ectomycorrhizal exploration types (medium-distance smooth, long-distance, and short-distance coarse). Notably, NF presented the highest number of fungal trait biomarkers (40 out of 100), reflecting its unique fungal community composition (Figure 2.2, Table 2.3, and Figure 2.6).

Table 2.7 - Predicted functional biomarkers of fungal communities across soil layers and management systems. The potential ecological traits and guilds were predicted using the FungalTraits database based on ITS rRNA gene sequences. Listed functions represent significant biomarkers identified by Linear Discriminant Analysis Effect Size (LEfSe). Only functional groups with an adjusted p-value < 0.05 and a Linear Discriminant Analysis (LDA) score ≥ 2.000 are shown. Positive LDA scores indicate significantly higher relative abundance of the functional group within the respective area compared to other treatments in that soil layer. ILF-ST: integrated livestock-forestry with *Samanea tubulosa*; ILF-EP: integrated livestock-forestry with *Eucalyptus pellita*; MP: *Urochloa brizantha* 'Marandu' pasture; NF: native forest; 0.00 and 5.25 m: distance from the tree row in the ILF systems.

Layer	Area	Trait	LDA
0-10 cm	ILF-ST 0.00 m	Secondary_lifestyle|litter_saprotroph	3.966
		Endophytic_interaction_capability|foliar_endophyte	3.932
		Decay_type|soft_rot	3.924
		Decay_substrate|roots	3.902
		primary_lifestyle|animal_parasite	3.499
		Decay_type|keratinolytic	3.459
		Plant_pathogenic_capacity|algal_parasite	2.747
		Secondary_lifestyle|algal_parasite	2.693
	ILF-ST 5.25 m	Growth_form|filamentous_mycelium	3.994
		Aquatic_habitat|aquatic	3.978
		primary_lifestyle|dung_saprotroph	3.938
		Animal_biotrophic_capacity|arthropod_parasite	3.367
		Secondary_lifestyle|unsepcified_saprotroph	2.586
	ILF-EP 0.00 m	primary_lifestyle|ectomycorrhizal	4.232
		Hymenium_type|smooth	4.102
		Ectomycorrhiza_exploration_type|medium-distance_smooth	4.100
		Fruitbody_type|corticioid	4.016
		Fruitbody_type|gasteroid	3.839
		Fruitbody_type|gasteroid-hypogeous	3.598
		primary_lifestyle|foliar_endophyte	3.520
		Ectomycorrhiza_exploration_type|long-distance	3.416
		Ectomycorrhiza_exploration_type|short-distance_coarse	3.266
	ILF-EP 5.25 m	Decay_substrate|sugar-rich_substrates	2.999
		primary_lifestyle|nectar/tap_saprotroph	2.966
	NF	Growth_form|yeast	3.681
		Decay_substrate|fungal_material	3.669
		primary_lifestyle|mycoparasite	3.668
		Secondary_lifestyle|animal_parasite	3.655
		Animal_biotrophic_capacity|animal_parasite	3.651
		Decay_type|white_rot	3.639

Layer	Area	Trait	LDA
		Hymenium_type|poroid	3.535
		Fruitbody_type|agaricoid	3.500
		Hymenium_type|gills	3.500
		Fruitbody_type|polyporoid	3.482
		Plant_pathogenic_capacity|wood_pathogen	3.435
		Growth_form|dimorphic_yeast	3.281
		Secondary_lifestyle|fungal_decomposer	3.177
		Animal_biotrophic_capacity|arthropod-associated	3.057
		primary_lifestyle|root_endophyte	2.984
		primary_lifestyle|moss_symbiont	2.618
		Endophytic_interaction_capability|moss-associated	2.618
		Plant_pathogenic_capacity|moss-associated	2.618
		primary_lifestyle|lichen_parasite	2.611
		Secondary_lifestyle|arthropod-associated	2.597
		Secondary_lifestyle|protistan_parasite	2.578
		Ectomycorrhiza_exploration_type|unknown	2.477
10-20 cm	ILF-ST 0.00 m	Decay_substrate|soil	4.081
		Decay_substrate|animal_material	3.991
		Secondary_lifestyle|litter_saprotroph	3.964
		Decay_type|soft_rot	3.932
		Plant_pathogenic_capacity|leaf/fruit/seed_pathogen	3.921
		Decay_substrate|roots	3.916
		primary_lifestyle|plant_pathogen	3.737
		Decay_type|keratinolytic	3.730
		Secondary_lifestyle|animal_decomposer	3.599
		Animal_biotrophic_capacity|arthropod_parasite	3.437
	ILF-ST 5.25 m	primary_lifestyle|dung_saprotroph	4.138
		Aquatic_habitat|aquatic	3.978
		primary_lifestyle|foliar_endophyte	3.648
	ILF-EP 0.00 m	primary_lifestyle|ectomycorrhizal	4.280
		Ectomycorrhiza_exploration_type|medium-distance_smooth	4.205
		Hymenium_type|smooth	4.203
		Fruitbody_type|corticioid	4.167
		Fruitbody_type|gasteroid	3.602
		Fruitbody_type|gasteroid-hypogeous	3.404
		Ectomycorrhiza_exploration_type|long-distance	3.135
		Ectomycorrhiza_exploration_type|short-distance_coarse	3.107
	ILF-EP 5.25 m	Growth_form|filamentous_mycelium	4.078
	MP	Decay_type|mold	4.062
	NF	Animal_biotrophic_capacity|animal_parasite	3.831
		Secondary_lifestyle|animal_parasite	3.711
		primary_lifestyle|animal_parasite	3.645
		primary_lifestyle|mycoparasite	3.641
		Decay_substrate|fungal_material	3.636
		Decay_type|white_rot	3.554

Layer	Area	Trait	LDA
20-40 cm		Hymenium_type|gills	3.492
		Fruitbody_type|agaricoid	3.492
		Growth_form|dimorphic_yeast	3.387
		Fruitbody_type|polyporoid	3.368
		Ectomycorrhiza_exploration_type|unknown	3.127
		Secondary_lifestyle|root_endophyte	3.011
		Secondary_lifestyle|root_endophyte_dark_septate	3.011
		Endophytic_interaction_capability|root_endophyte_dark_septate	2.925
		Secondary_lifestyle|protistan_parasite	2.654
		primary_lifestyle|lichen_parasite	2.645
	ILF-ST 0.00 m	Decay_type|soft_rot	3.991
		Decay_substrate|roots	3.851
		Decay_type|keratinolytic	3.808
		Decay_substrate|fungal_material	3.669
		Animal_biotrophic_capacity|arthropod_parasite	3.561
	ILF-ST 5.25 m	primary_lifestyle|dung_saprotroph	4.054
		primary_lifestyle|foliar_endophyte	3.404
	ILF-EP 0.00 m	primary_lifestyle|ectomycorrhizal	4.307
		Ectomycorrhiza_exploration_type|medium-distance_smooth	4.141
		Hymenium_type|smooth	4.135
		Fruitbody_type|gasteroid	3.913
		Ectomycorrhiza_exploration_type|short-distance_coarse	3.650
		Ectomycorrhiza_exploration_type|long-distance	3.537
	NF	primary_lifestyle|mycoparasite	3.605
		Secondary_lifestyle|protistan_parasite	2.877

In the topsoil, functional diversity was highly niche-specific. The ILF-ST 0.00 m system was significantly enriched with litter saprotrophs, soft rot decomposers, and fungi with foliar endophyte capabilities. At the 5.25 m distance in the same system, the profile shifted toward dung saprotrophs and aquatic habitats. In NF, the community was characterized by mycoparasites, white rot decay, and a diversity of growth forms, including yeasts and dimorphic yeasts.

As depth increased, the ILF-ST 0.00 m system maintained its association with soft rot decay but also showed significant biomarkers for plant pathogens and fungi utilizing soil and roots as substrates. The MP system emerged in this layer with a specific signature for molds. The native forest (NF) continued to be characterized by animal parasites and white rot decay, along with the presence of dark septate root endophytes.

In the deepest layer, functional biomarkers became more concentrated. The ILF-EP 0.00 m system reached its highest effect size for the ectomycorrhizal lifestyle (LDA = 4.30). The

ILF-ST 0.00 m treatment remained associated with soft rot and root decay, while the ILF-ST 5.25 m distance continued to harbor dung saprotrophs. Functional biomarkers in the NF were reduced to mycoparasites and protistan parasites.

2.3.5 Co-occurrence networks

The topological properties of the microbial co-occurrence networks revealed distinct patterns of connectivity and structural complexity across management systems and soil depths (Table 2.8). In the 0-10 cm layer, the treeless pasture (MP) exhibited notably higher complexity compared to other treatments; its number of edges (34,146) and average degree (86.66) were more than three times higher than those observed in ILF-ST 5.25 m, which had the second-highest edge count. While the edge count in ILF-ST was similar to NF, it was considerably higher than in the ILF-EP system, which also recorded the lowest number of nodes.

Table 2.8 - Topological attributes of microbial (prokaryotes and fungi) co-occurrence networks across soil layers (0-10, 10-20, and 20-40 cm) and management systems. ILF-ST: integrated livestock-forestry with *Samanea tubulosa*; ILF-EP: integrated livestock-forestry with *Eucalyptus pellita*; MP: *Urochloa brizantha* 'Marandu' pasture; NF: native forest; 0.00 and 5.25 m: distance from the tree row in the ILF systems.

Network atribute[†]	**ILF-ST**		**ILF-EP**		**MP**	**NF**
	0.00 m	**5.25 m**	**0.00 m**	**5.25 m**		
	---------- 0-10 cm ----------					
Nodes	927	789	691	748	788	775
Fungal/prokaryotic ratio	0.398	0.356	0.470	0.441	0.352	0.547
Edges	11,109	10,904	5,098	7,433	34,146	10,164
Positive/negative ratio	1.103	1.462	1.058	1.048	1.019	0.941
Fungi-fungi (%)	9.200	6.700	10.906	10.628	5.750	10.324
Prokaryote-prokaryote (%)	43.372	56.750	44.704	43.657	60.378	47.252
Fungi-prokaryote (%)	47.433	36.550	44.390	45.715	33.871	42.424
Average degree	23.968	27.640	14.755	19.874	86.665	26.230
Network diameter	4	4	5	4	3	4
Density	0.026	0.035	0.021	0.027	0.110	0.034
Modularity	0.179	0.164	0.233	0.187	0.116	0.178
Average clustering coefficient	0.034	0.042	0.0250	0.030	0.130	0.045
Average path length	2.481	2.339	2.721	2.542	1.895	2.387
	---------- 10-20 cm ----------					
Nodes	1009	730	796	720	803	782
Fungal/prokaryotic ratio	0.456	0.401	0.437	0.437	0.354	0.561
Edges	14,633	10,410	14,856	5,234	6,599	6,962
Positive/negative ratio	1.200	1.107	1.132	0.861	1.313	1.114
Fungi-fungi (%)	10.613	7.368	9.922	9.935	7.334	13.904
Prokaryote-prokaryote (%)	44.864	52.728	47.429	42.988	52.508	40.621
Fungi-prokaryote (%)	44.523	39.904	42.649	47.077	40.158	45.475

Network atribute†	ILF-ST		ILF-EP		MP	NF
	0.00 m	5.25 m	0.00 m	5.25 m		
Average degree	29.005	28.521	37.327	14.539	16.436	17.806
Network diameter	4	4	3	5	5	4
Density	0.029	0.039	0.047	0.02	0.02	0.023
Modularity	0.159	0.163	0.141	0.235	0.218	0.205
Average clustering coefficient	0.033	0.05	0.054	0.024	0.023	0.027
Average path length	2.389	2.292	2.138	2.736	2.691	2.629
	---------- 20-40 cm ----------					
Nodes	964	728	765	716	738	747
Fungal/prokaryotic ratio	0.428	0.425	0.425	0.455	0.344	0.543
Edges	8,951	9,221	5,647	6,435	9,649	6,036
Positive/negative ratio	1.099	1.606	0.972	0.988	1.598	1.025
Fungi-fungi (%)	10.580	10.010	9.173	10.660	5.659	12.816
Prokaryote-prokaryote (%)	44.118	43.921	50.044	46.356	61.074	42.326
Fungi-prokaryote (%)	45.302	46.069	40.783	42.984	33.268	44.858
Average degree	18.571	25.332	14.763	17.975	26.149	16.161
Network diameter	4	4	5	4	4	5
Density	0.019	0.035	0.019	0.025	0.035	0.022
Modularity	0.203	0.165	0.228	0.205	0.172	0.221
Average clustering coefficient	0.022	0.044	0.023	0.031	0.043	0.028
Average path length	2.666	2.356	2.754	2.591	2.362	2.681

† Nodes represent individual microbial taxa (prokaryotes or fungi); edges indicate significant SparCC correlations ($r \leq -0.7$ or ≥ 0.7, $p < 0.01$ after FDR correction) between taxa; fungi/prokaryote ratio is the proportion of fungal nodes relative to prokaryotic nodes in the network; positive/negative ratio is the proportion of positive correlations relative to negative correlations; fungi-fungi, prokaryote-prokaryote, and fungi-prokaryote represent the percentage of connections within and between each domain; average degree is the mean number of connections per node; network diameter is the longest shortest path between any two nodes; density measures how close the network is to being complete (all possible edges). Modularity indicates the degree to which a network is divided into distinct clusters or modules. Average clustering coefficient measures the tendency of nodes to form tightly knit groups. Average path length is the average number of steps required to connect any two nodes in the network.

Regarding domain interactions, ILF-ST 5.25 m and MP showed a high percentage of prokaryote-prokaryote connections (56.75% and 60.37%, respectively) compared to other treatments. Although ILF-EP 0.00 m displayed considerably higher modularity (0.233), the average clustering coefficient in MP (0.13) was remarkably superior. Notably, NF was the only treatment to present a higher proportion of negative correlations relative to positive ones (0.941) and the highest fungi/prokaryote node ratio (0.547). The ILF-EP system followed with the second-highest fungi/prokaryote ratio, yet its proportion of fungi-fungi connections (10.9 %) exceeded even that of the NF.

In the 10-20 cm layer, the integrated systems at the tree row (0.00 m) stood out, with more than double the number of edges compared to the next highest treatment (NF). The number of nodes in these systems also increased considerably compared to the 0-10 cm layer,

reaching 1,009 in ILF-ST 0.00 m. A notable finding was the smallest network diameter recorded in ILF-EP 0.00 m (3), although modularity in this system decreased despite the increase in connections.

In contrast, MP showed a substantial decline in edge count (6,599) despite an increase in the number of nodes (803). However, the positive/negative ratio in MP (1.313) was much higher than in the other treatments. The lowest positive/negative ratio at this depth was observed in ILF-EP 5.25 m (0.861). Prokaryote-prokaryote connections remained most prevalent in ILF-ST 5.25 m (52.72 %) and MP (52.50 %), while NF continued to maintain the highest fungi/prokaryote ratio (0.561). Unlike the surface layer, the highest modularity values were observed in MP (0.218) and NF (0.205).

At the 20-40 cm layer, differences between treatments regarding node and edge counts were less discrepant. ILF-ST 0.00 m stood out with the highest number of nodes (964), while MP exhibited the highest average degree (26.14). Generally, ILF-ST and MP presented the highest number of edges, whereas ILF-EP 0.00 m recorded the lowest edge count (5,647) and average degree (14.76).

The positive/negative ratio at this depth was highest in ILF-ST 5.25 m (1.606), followed by MP (1.598). Conversely, the ILF-EP system (at both 0.00 m and 5.25 m) was the only area to present a higher proportion of negative correlations relative to positive ones (0.972 and 0.988, respectively). NF maintained the highest fungi/prokaryote ratio (0.543) and MP the highest percentage of prokaryote-prokaryote connections (61.07 %). Furthermore, the differences between the 0.00 m and 5.25 m distances in the ILF-ST system regarding the proportions of connection types were smaller in this layer. This magnitude of difference between distances was not observed for the ILF-EP system at any layer.

2.4 Discussion

2.4.1 Alpha diversity

The significant influence of management systems, sampling distances, and soil depths on microbial alpha diversity suggests that the integration of trees into Amazonian pastures creates distinct ecological niches that override the inherent biotic homogenization of conventional cattle ranching. The consistent superiority of the ILF-ST system in maintaining higher prokaryotic richness and Shannon diversity compared to ILF-EP, particularly at the tree row (0.00 m) across all layers, highlights the legume effect in integrated systems. *Samanea*

tubulosa, as a nitrogen-fixing legume, likely provides a more labile litter and a broader range of root exudates compared to the more recalcitrant litter of *E. pellita* (Constantinides and Fownes 1994; Duarte et al. 2013). This nutrient-rich environment supports a more even and diverse prokaryotic community, potentially facilitating faster nutrient cycling (Barros et al. 2018; Gou et al. 2023; Cai and Zhao 2024). These results corroborate the findings of Cipriani, Salman, Pellegrinetti, et al. (2025), which worked in practically the same areas in the dry season, two years early, and found higher prokaryotic diversity in ILF-ST.

The tree effect was markedly spatial. In the intermediate layer (10-20 cm), the significant increase in fungal richness at the tree row (0.00 m) compared to the area 5.25 m distant from the tree row in the ILF systems indicates that the trees can enhance local fungal habitats through root-zone interactions. In addition, for fungi, the ILF-ST system at 0.00 m was the only managed system able to reach a Shannon diversity equivalent to NF. This suggests that the microenvironment created by *S. tubulosa* mimics some of the structural complexities of the forest floor, supporting a fungal community that is as diverse as the native baseline (Beule, Guerra, et al. 2022; Vaupel et al. 2023; Dyson et al. 2025; Bässler et al. 2025).

The results revealed a divergence in the response of prokaryotes and fungi to land-use change. For prokaryotes, diversity was generally higher in the treeless pasture (MP) and lower in the NF. This often occurs in Amazonian soils where forest-to-pasture conversion increases soil pH and nutrient availability, favoring copiotrophic bacterial groups (Rocha et al. 2021; Mandro et al. 2026; Muchalak et al. 2025). For fungi, NF consistently exhibited superior richness and Shannon diversity across all depths compared to managed systems. This underscores the sensitivity of fungal communities, often dependent on specific host plants and complex organic matter, to the structural simplification that follows deforestation (Kutos et al. 2023; Balami et al. 2020).

Despite the typical decline in resources with depth, the ILF-ST system maintained significantly higher fungal richness and Shannon diversity at the 0.00 m distance even in the deepest layer (20-40 cm) compared to ILF-EP. This persistence suggests that the deep-rooting system of *S. tubulosa* and its associated rhizospheric effects extend deeper into the soil profile, a crucial factor for long-term soil health.

2.4.2 Beta diversity

The PCoA and PERMANOVA analyses revealed that land-use change exerted a deterministic selective pressure on microbial community composition, resulting in distinct

assemblies between the native forest (NF) and managed systems. The most striking pattern observed was the highly cohesive and isolated clustering of NF across all soil layers, confirming that the native vegetation supports a markedly different microbial assembly than any managed system. This isolation suggests that deforestation leads to the loss of specialized forest microbial lineages that are not recovered even in integrated production systems (Goss-Souza et al. 2022; Carmo et al. 2024; Mandro et al. 2026).

The choice of tree species was a significant driver of beta diversity, since the ILF-ST and ILF-EP systems differed significantly from each other across all soil layers. Interestingly, no significant difference was detected between the tree row (0.00 m) and its pasture (5.25 m) within the ILF-ST system at any depth. This suggests that the influence of the legume tree (*S. tubulosa*) is spatially extensive, potentially due to the widespread distribution of shade, nitrogen-rich labile litter or expansive root systems that homogenize the microbial signature across the system. In contrast, the ILF-EP system showed significant spatial variation for fungi in the 10-20 cm and 20-40 cm layers. This indicates that the impact of Eucalyptus is more localized, creating a distinct rhizospheric footprint near the trunk that differs from the pasture area within the system (Cipriani, Salman, Pellegrinetti, et al. 2025; Zandona et al. 2019; Bieluczyk et al. 2021).

The tree row (0.00 m) of both integrated systems successfully shifted the microbial composition away from the conventional pasture (MP) profile in the upper layers. However, at the 5.25 m distance, the communities often became statistically indistinguishable from the MP. This confirms that while integrated systems diversify the landscape, the restorative effect on microbial composition is a gradient that weakens as the distance from the tree increases (Rivest et al. 2020; Sarto, Borges, Sarto, Pires, et al. 2020).

Prokaryotic communities showed more pronounced segregation between management systems than fungi, as evidenced by higher R^2 values in pairwise comparisons. For instance, at 20-40 cm, the R^2 for prokaryotes in the NF vs. ILF-ST 0.00 m comparison was 0.697, whereas for fungi, it was 0.402. This suggests that bacteria and archaea are more sensitive indicators of short-term and widespread changes induced by management (such as pH and nutrient flux), while fungal communities may be more influenced by the presence of specific host plants or the quality of recalcitrant organic matter (Zagatto et al. 2026; Bier et al. 2024).

2.4.3 Taxonomic biomarkers and community composition

The LEfSe analysis did not merely identify specific taxa but revealed how different management strategies shape soil functionality by selecting microbial groups with distinct ecological niches. The dramatic vertical stratification, with only ~9 % of biomarkers shared across layers, highlights that microbial life strategies in the surface are fundamentally decoupled from those in the subsoil (Byers et al. 2023; Leewis et al. 2022; Beule and Guerra, et al. 2022).

The dominance of *Xanthobacteraceae* and *Ca. Solibacter* in NF across all layers reflects an ecosystem balanced for the acidic, nutrient-tight conditions of the Amazonian rainforest. *Xanthobacteraceae* are key players in nitrogen fixation and carbon turnover in stable forest environments (Soltysiak et al. 2025; Willms et al. 2021). Furthermore, the persistence of fungi like *Saitozyma podzolica* in the upper layers suggests a highly acidic environment and specialization in decomposing complex forest litter, acting as a hub for carbon processing that is effectively lost when the forest is cleared (Gorte et al. 2020; Feng et al. 2023; Moreira and Vale 2018).

The ILF-ST system stood out for prokaryotic biomarkers that suggest a more fertile and biologically integrated soil environment compared to other managed systems. The prominence of *Bradyrhizobium* (ASV_122) at 5.25 m indicates that the influence of the legume tree fosters plant-growth-promoting bacteria even far from the trunk. This explains why ILF-ST shows higher biological connectivity than ILF-EP between distances: the tree effectively fertilizes the soil with root exudates that support these beneficial groups (Barros et al. 2018; Santos et al. 2022).

The high abundance of *Fusarium variasi* (ASV_5) at the tree row suggests rapid cycling of the labile, nitrogen-rich organic material provided by *S. tubulosa*. While some *Fusarium* species are pathogens, many are highly efficient saprotrophs that thrive in nutrient-rich niches, marking a clear functional shift from the recalcitrant-decomposing fungi of the NF. In fact, *F. variasi* abundance is positively correlated with foliar P abundance (Petticord et al. 2026).

Unlike the ILF-ST system, the eucalyptus-integrated system creates a highly specialized and localized niche. The presence of *Tomentella* (ASV_6) and *Pisolithus* as primary biomarkers near the tree row is clear evidence of the dependency of Eucalyptus on symbioses to capture nutrients in poor soils (Wang et al. 2024; Zhong et al. 2025; Heinrich et al. 1988). These fungi are host-specific and do not extend into the pasture matrix, which explains the relatively low

sharing of ASVs between the tree row and the area at 5.25 m distance from the tree row in this system. Moreover, the enrichment of *Acidobacteriae* Subgroup 2 (ASV_179) suggests an adaptation to soils with lower nutrient availability or the presence of antimicrobial compounds like essential oils, contrasting with the more copiotrophic profile of the ILF-ST system (Goldfarb et al. 2011; Moussa et al. 2024; Muchalak et al. 2025). In MP, the dominance of fungi like *Curvularia* and *Penicillium shearii* suggests a community adapted to rapid herbaceous decomposition and the environmental fluctuations typical of open pastures (Silvestro et al. 2018; Mehta et al. 2022).

The discovery that only 0.5 % of fungal ASVs are universally shared (core microbiota) demonstrates that while prokaryotes maintain a common functional baseline (3 % sharing), fungal communities are severely fragmented by management. Each production system creates its own fungal community, suggesting that the restoration of complex functions, such as lignin decomposition, depends mainly on tree species diversity, as the pasture matrix alone cannot sustain the fungal groups found in the forest or even in the legume-based systems. This extremely low baseline of common fungal taxa indicates that fungi are significantly more sensitive to land-use fragmentation and vegetation type than prokaryotes. Consequently, fungal communities might serve as more precise indicators of management history, reflecting the specific impacts of tree integration in silvopastoral systems (Raimbault et al. 2024; Seaton et al. 2023).

2.4.4 Functional prediction and profile analysis

Functional prediction analysis (FAPROTAX and FungalTraits) revealed that the integration of trees into Amazonian pastures does not merely alter microbial taxonomy but fundamentally redirects soil metabolic pathways and ecological guilds. The ILF-ST system (legume-based) displayed the highest functional complexity, while the ILF-EP system (eucalyptus-based) showed a high degree of symbiotic specialization.

The enrichment of functions such as nitrate reduction and anaerobic chemoheterotrophy at the tree row (0.00 m) of the ILF-ST system suggests an environment with high organic substrate availability and variable oxygen dynamics. The significant presence of litter saprotrophs and soft rot decomposers indicates that *S. tubulosa* provides high-quality, nitrogen-rich litter (low C:N ratio), which is rapidly processed by the fungal community (Vaupel et al. 2025; Wang et al. 2020; Zhang et al. 2025). The unique signature for degrading aromatic compounds in the topsoil suggests a robust microbiome capable of breaking down

complex organic polymers, ensuring active carbon flux and soil resilience (Naylor et al. 2022; Fuchs et al. 2011).

In sharp contrast, the ILF-EP system exhibited a functional specialization geared toward nutrient acquisition in restricted environments. The highest effect size for the ectomycorrhizal lifestyle (LDA = 4.30) in the deepest layer (20-40 cm) at the tree row confirms that *Eucalyptus pellita* strongly shapes soil function to ensure its own nutrient uptake via symbiosis. The identification of short-distance and long-distance exploration types reflects a spatial adaptation to mine the soil for phosphorus and other limiting nutrients (Wang et al. 2024; Zhong et al. 2025; Heinrich et al. 1988).

The functionality of the native forest was characterized by white rot decay and mycoparasitism. While white rot is the hallmark of complex lignin decomposition in tropical forests, the presence of mycoparasites suggests a highly balanced microbial food web with intrinsic biological control mechanisms (Dossa et al. 2021; Wang et al. 2020; Penton et al. 2014). Conversely, the MP system was uniquely identified by cellulolysis and the presence of molds. This reflects a simplified carbon cycle based on the rapid turnover of herbaceous material (grass roots and litter), lacking the enzymatic complexity required to process forest-derived organic matter (Júnior et al. 2023; Abrão et al. 2017; Eo et al. 2021).

The functional shift from the tree row (0.00 m) to the area at 5.25 m distance from the tree row in the ILF-ST system, moving from aromatic degradation to sulfate respiration, demonstrates that the tree component creates a distinct biogeochemical zonation. The presence of sulfur-related pathways at 5.25 m suggests a shift toward anaerobic processes or specific nutrient cycling dynamics in areas further from the direct influence of the legume canopy (Santana et al. 2021; Demin et al. 2024).

The alignment between taxonomic biomarkers and predicted functional profiles demonstrates that tree integration creates specialized biogeochemical hotspots in pastures. This integration confirms that the microbial shifts observed are not merely structural but functional, directly impacting nutrient cycling and soil stability. In the ILF-ST system, the dominance of the legume tree (*S. tubulosa*) is functionally mirrored by the co-occurrence of nitrate reduction and the presence of nitrogen-fixing taxa such as *Bradyrhizobium*. The high LDA scores for litter saprotrophs and aromatic compound degradation in the topsoil (0-10 cm) explain the presence of *Fusarium variasi* as a primary biomarker. Together, these results suggest that the legume system maintains a high-energy decomposition engine, where high-quality organic matter is rapidly mineralized to support both plant growth and microbial biomass.

In the ILF-EP system, the microbial community is functionally tethered to the eucalyptus roots. The massive effect size for ectomycorrhizal functions (LDA = 4.30) in the subsoil (20-40 cm) corresponds directly to the presence of *Tomentella* and *Pisolithus*. This indicates that in deeper, nutrient-limited layers, the system shifts its functional investment from free-living decomposition to symbiotic mining. The prevalence of *Acidobacteriae* Subgroup 2 as a biomarker in this system aligns with the potential soil acidification often associated with Eucalyptus plantations, creating a functional niche that favors specialized, acid-tolerant oligotrophs over the generalists found in the pasture (Leite et al. 2010; Korchagin et al. 2019; Li et al. 2018).

In line with the results of Cipriani, Salman, Pellegrinetti et al. (2025), functions related to the N-cycle, anaerobic chemoheterotrophy, and aromatic compound degradation were identified as potential biomarkers in ILF-ST at 0.00 m, indicating their persistence over time. Conversely, the fewer differential functions identified in the current study may stem from the inclusion of the MP treatment, which likely increased the proportion of redundant functions across systems.

The highly specific functional guilds (e.g., white rot in NF vs. soft rot in ILF-ST vs. ectomycorrhiza in ILF-EP), corroborates with the community composition analyses that fungi are the primary sensors of land-use change. While prokaryotes provide a stable metabolic baseline (maintaining general chemoheterotrophy across systems), the fungal community is more specialized, changing considerably depending on the tree species. Therefore, to restore forest-like functions in Amazonian pastures, the choice of tree species in integrated systems is not just a silvicultural decision, but a fundamental driver of soil biological recovery.

2.4.5 Co-occurrence networks

The topological analysis of co-occurrence networks provided deep insights into the ecological assembly rules and stability of the soil microbiome under different management regimes. The results indicate that land-use change and tree species integration fundamentally reorganize the patterns of microbial interactions across the soil profile.

A prominent finding was that the treeless pasture (MP) exhibited significantly higher complexity in the surface layer (0-10 cm), with edge counts and average degree more than three times higher than those in the integrated systems or native forest. This high connectivity in MP suggests an intertwined community, likely driven by the rapid turnover of labile carbon from grass roots and more frequent environmental fluctuations (e.g., temperature and moisture).

While high complexity is often associated with efficiency, it can also render the network more vulnerable to cascading failures if key hub taxa are lost due to environmental stress (Wang et al. 2025; Nuwagaba et al. 2017).

The Marandu pasture (MP) and the ILF-ST system at 5.25 m exhibited remarkably high positive/negative ratios at some layers (e.g., 1.313 in MP at 10–20 cm and a peak of 1.606 in ILF-ST 5.25 m at 20–40 cm). In community ecology, a network dominated by positive correlations (where taxa rise or fall together) is often considered less stable. If an environmental stressor (such as drought or compaction) negatively affects a few key taxa, the negative impact can cascade through these positive links, potentially leading to a localized collapse of the microbial community (Kajihara et al. 2025). The high ratio in ILF-ST, especially at the 5.25 m distance, likely reflects a high availability of labile resources (legume-derived nitrogen and grass-root exudates). When resources are abundant, niche competition (negative interactions) decreases, and facilitation, where one group's metabolic byproduct feeds another, becomes the dominant structural force (Khan et al. 2019; Muscarella and O'Dwyer 2020).

On the other hand, the dominance of negative correlations in the NF at 0-10 cm suggests strong niche partitioning and competition. This creates a buffered network: if one species declines, its competitors can fill the functional void, preventing a total system failure (Kajihara et al. 2025). Similarly, the fact that ILF-EP (at 20-40 cm) returns to a near-forest ratio (0.972-0.988) is significant. It suggests that in the subsoil, the eucalyptus tree imposes environmental filters, such as lower nutrient availability or more recalcitrant carbon, that force the community back into a state of high specialization and competition, structurally mimicking the forest more closely than the cooperative legume or pasture systems (Yu et al. 2022; Alvarez et al. 2023; Muchalak et al. 2025).

The analysis of network modularity provides a window into how microbial interactions are organized into semi-independent clusters or niches. Notably, modularity fluctuated sharply with depth in all systems. For instance, modularity in the MP system jumped from a low of 0.116 at the surface to 0.218 at 10-20 cm, while ILF-EP at 0.00 m dropped from 0.233 to 0.141. In network theory, highly modular networks are more resistant to external disturbances because the impact of a stressor (e.g., localized nutrient shifts or moisture changes) tends to be contained within a specific module, preventing it from cascading throughout the entire network (Kajihara et al. 2025; Muchalak et al. 2025).

The very low modularity in the surface layer of the MP system, combined with its massive connectivity (34,146 edges), suggests a globalized network where almost every taxon

is linked to many others. While this may facilitate rapid nutrient cycling under ideal conditions, the lack of compartmentalization makes the network structurally fragile, as any disturbance can easily spread across the entire community (Kajihara et al. 2025).

The fact that ILF-EP at 0.00 m maintains a relatively high modularity even with lower number of nodes and edges in certain layers reinforces that the quality and organization of interactions are more critical than the sheer volume of links (Yu et al. 2022; Alvarez et al. 2023; Khan et al. 2019). The stable modularity in this system likely reflects a more rigid functional partitioning, possibly driven by the specific chemical environment of Eucalyptus (e.g., litter chemical composition) or its strong reliance on specialized fungal guilds (ectomycorrhizae), which create exclusion zones that define these microbial compartments (Qin et al. 2024; Pereira et al. 2019; Xu et al. 2022).

The high complexity (average degree and edge count) of the MP network at the surface represents a hyper-connected prokaryote-dominated system (~60 % of connections). By contrast, the higher fungi/prokaryotic ratio in forested systems (NF and ILF-EP) introduces fungal-bacterial antagonisms into the network. These negative links act as barriers, breaking the network into modules that prevent disturbances from spreading globally across the microbiome.

As depth increased, the discrepancies in complexity between treatments narrowed, but the nature of the interactions shifted. The dominance of prokaryote-prokaryote connections in MP contrasts with the higher integration of fungi in the NF and ILF systems. This suggests that the tree component (whether native or exotic) is essential for maintaining fungal-bacterial interactions in subsoil layers, which is critical for long-term carbon sequestration and nutrient mobilization.

2.5 Conclusion

This study demonstrates that the integration of trees into Amazonian pastures fundamentally reorganizes the soil microbiome, though the structural and functional outcomes are highly dependent on tree species and soil depth. By evaluating the hypotheses against the integrated results of diversity, biomarkers, and co-occurrence networks, it can be concluded that the *S. tubulosa* system (ILF-ST) was the primary driver of taxonomic and functional recovery. It promoted higher biological connectivity and established biodiversity hotspots characterized by nitrogen-cycling bacteria and a fungal richness that approached forest levels.

This confirms that native nitrogen-fixing trees are superior to exotic monocultures in restoring the biological quality of degraded pastures.

Unlike ILF-ST, ILF-EP (*Eucalyptus*) promoted a more specialized and restricted microbial assembly. The network analysis revealed that the eucalyptus tree row imposes a specific structural signature, which, rather than merely increasing complexity, selects for symbiotic specialists like ectomycorrhizal fungi. This suggests that the *Eucalyptus* effect is more about niche filtering than a broad restoration of forest-like network interactions.

The discovery of an extremely small universal core microbiota underscores the high sensitivity of the fungal domain to land-use management. While prokaryotic communities maintain a relatively higher functional baseline across systems, the recovery of specialized fungal guilds is entirely dependent on the presence and type of the arboreal component.

The high connectivity observed in the monoculture pasture (MP) does not necessarily translate to ecological stability. These networks are characterized by hyper-connectivity among prokaryotes and a high ratio of positive (cooperative) interactions, which may increase vulnerability to environmental stressors compared to the more partitioned and modular structures found in forested and integrated systems.

In summary, integrated livestock-forestry systems mitigate the biotic homogenization typical of conventional pastures. However, for producers and policymakers aiming at soil biological health and nutrient cycling resilience, the use of native species like *S. tubulosa* offers a more robust pathway for restoring the intricate microbial networks essential for sustainable agriculture in Western Amazonia.

References

Abarenkov, Kessy, Allan Zirk, Timo Piirmann, et al. 2025. UNITE General FASTA Release for Fungi. UNITE Community, February 19. Application/gzip. https://doi.org/10.15156/BIO/3301229.

Abrão, Flávia Oliveira, Eduardo Robson Duarte, Moisés Sena Pessoa, et al. 2017. Notable Fibrolytic Enzyme Production by Aspergillus Spp. Isolates from the Gastrointestinal Tract of Beef Cattle Fed in Lignified Pastures. *PLOS ONE* 12 (8): e0183628. https://doi.org/10.1371/journal.pone.0183628.

Alvares, Clayton Alcarde, José Luiz Stape, Paulo Cesar Sentelhas, José Leonardo de Moraes Gonçalves, and Gerd Sparovek. 2013. Köppen's Climate Classification Map for Brazil. *Meteorologische Zeitschrift* 22 (6): 711–28. https://doi.org/10.1127/0941-2948/2013/0507.

Alvarez, Dasiel Obregon, Leandro Fonseca de Souza, Lucas William Mendes, et al. 2023. Shifts in Functional Traits and Interactions Patterns of Soil Methane-Cycling Communities Following Forest-to-Pasture Conversion in the Amazon Basin. *Molecular Ecology* 32 (12): 3257–75. https://doi.org/10.1111/mec.16912.

Azevedo, Alcinei Mistico. 2022. *Tratamentos.Ad: Pacote Para Analise De Experimentos Com Testemunhas Adicionais*. V. 0.2.4. Released September 13. https://cran.r-project.org/web/packages/Tratamentos.ad/index.html.

Balami, S., M. Vašutová, D. Godbold, P. Kotas, and P. Cudlín. 2020. Soil Fungal Communities across Land Use Types. Forest Soil Science. *iForest - Biogeosciences and Forestry* 13 (6): 548. World. https://doi.org/10.3832/ifor3231-013.

Barros, Felipe Martins do Rêgo, Giselle Gomes Monteiro Fracetto, Felipe José Cury Fracetto, José Petrônio Mendes Júnior, Victor Lucas Vieira Prudêncio de Araújo, and Mario Andrade Lira Junior. 2018. Silvopastoral Systems Drive the Nitrogen-Cycling Bacterial Community in Soil. *Ciência e Agrotecnologia* 42: 281–90. https://doi.org/10.1590/1413-70542018423031117.

Bässler, Claus, Petr Baldrian, Jörg Müller, et al. 2025. Enhancing Experimentally the Structural Heterogeneity of Forests Increase Soil Fungal Diversity but Functional Lifestyles in Contrasting Ways. Preprint, bioRxiv, September 2. https://doi.org/10.1101/2025.08.29.673114.

Bastian, Mathieu, Sebastien Heymann, and Mathieu Jacomy. 2009. Gephi: An Open Source Software for Exploring and Manipulating Networks. *Proceedings of the International AAAI Conference on Web and Social Media* 3 (1): 1. https://doi.org/10.1609/icwsm.v3i1.13937.

Bentes-Gama, Michelliny de Matos, Guido Sanick Leal, Joelson de Oliveira Barros, Raimunda Herculano Lopes, Giovana Fiorella Zamora López, and Juliane Cardoso da Silveira. 2009. *Características Da Estrutura de Uma Floresta de Terra Firme Em Porto Velho, Rondônia*. Embrapa Rondônia. Circular Técnica 109. Embrapa Rondônia. https://ainfo.cnptia.embrapa.br/digital/bitstream/item/24747/1/ct109-floresta.pdf.

Berry, David, and Stefanie Widder. 2014. Deciphering Microbial Interactions and Detecting Keystone Species with Co-Occurrence Networks. *Frontiers in Microbiology* 5 (May). https://doi.org/10.3389/fmicb.2014.00219.

Beule, Lukas, Victor Guerra, Ena Lehtsaar, and Anna Vaupel. 2022. Digging Deeper: Microbial Communities in Subsoil Are Strongly Promoted by Trees in Temperate Agroforestry Systems. *Plant and Soil* 480 (1): 423–37. https://doi.org/10.1007/s11104-022-05591-2.

Beule, Lukas, and Petr Karlovsky. 2020. Improved Normalization of Species Count Data in Ecology by Scaling with Ranked Subsampling (SRS): Application to Microbial Communities. *PeerJ* 8 (August): e9593. https://doi.org/10.7717/peerj.9593.

Beule, Lukas, Anna Vaupel, and Virna Estefania Moran-Rodas. 2022. Abundance, Diversity, and Function of Soil Microorganisms in Temperate Alley-Cropping Agroforestry Systems: A Review. *Microorganisms* 10 (3): 616. https://doi.org/10.3390/microorganisms10030616.

Bieluczyk, Wanderlei, Marisa De Cássia Piccolo, João Vitor Matos Gonçalves, et al. 2024. Fine Root Production and Decomposition of Integrated Plants under Intensified Farming Systems in Brazil. *Rhizosphere* 31 (September): 100930. https://doi.org/10.1016/j.rhisph.2024.100930.

Bieluczyk, Wanderlei, Marisa de Cássia Piccolo, Marcos Gervasio Pereira, et al. 2021. Eucalyptus Tree Influence on Spatial and Temporal Dynamics of Fine-Root Growth in an Integrated Crop-Livestock-Forestry System in Southeastern Brazil. *Rhizosphere* 19 (September): 100415. https://doi.org/10.1016/j.rhisph.2021.100415.

Bier, Raven L., Melinda Daniels, Diana Oviedo-Vargas, et al. 2024. Agricultural Soil Microbiomes Differentiate in Soil Profiles with Fertility Source, Tillage, and Cover Crops. *Agriculture, Ecosystems & Environment* 368 (July): 109002. https://doi.org/10.1016/j.agee.2024.109002.

Brewer, Kelsey M., and Amélie C. M. Gaudin. 2020. Potential of Crop-Livestock Integration to Enhance Carbon Sequestration and Agroecosystem Functioning in Semi-Arid Croplands. *Soil Biology and Biochemistry* 149 (October): 107936. https://doi.org/10.1016/j.soilbio.2020.107936.

Byers, Alexa K., Loretta G. Garrett, Charlotte Armstrong, Fiona Dean, and Steve A. Wakelin. 2023. Soil Depth as a Driver of Microbial and Carbon Dynamics in a Planted Forest (*Pinus Radiata*) Pumice Soil. *SOIL* 9 (1): 55–70. https://doi.org/10.5194/soil-9-55-2023.

Cai, Siyuan, and Xu Zhao. 2024. Responses of Bacterial Communities and Nitrogen-Cycling Microbiomes to the Conversion from Cereals to Legumes in the Rice-Based System. *Applied Soil Ecology* 195 (March): 105241. https://doi.org/10.1016/j.apsoil.2023.105241.

Callahan, Benjamin J., Paul J. McMurdie, Michael J. Rosen, Andrew W. Han, Amy Jo A. Johnson, and Susan P. Holmes. 2016. DADA2: High Resolution Sample Inference from Illumina Amplicon Data. *Nature Methods* 13 (7): 581–83. https://doi.org/10.1038/nmeth.3869.

Caporaso, J. Gregory, Christian L. Lauber, William A. Walters, et al. 2011. Global Patterns of 16S rRNA Diversity at a Depth of Millions of Sequences per Sample. Colloquium Paper. *Proceedings of the National Academy of Sciences* 108 (Supplement 1): 4516–22. https://doi.org/10.1073/pnas.1000080107.

Carmo, Kellen Banhos do, Raquel Dias, Patricia Dorr de Quadros, et al. 2024. Assessment of Soil Bacterial Communities in Integrated Crop Production Systems within the Amazon Biome, Brazil: A Comparative Study. *Brazilian Journal of Microbiology*, ahead of print, May 2. https://doi.org/10.1007/s42770-024-01352-8.

Cipriani, Henrique Nery, Ana Karina Dias Salman, Pedro Gomes da Cruz, Elaine Coimbra de Souza, and Siu Mui Tsai. 2025. Atributos Químicos, Físicos e Microbiológicos Do Solo Em Áreas de IPF, ILP, ILPF, Pastagens e Floresta No Campo Experimental de Porto Velho, Em Duas Estações (Seca e Chuvosa). Redape. https://doi.org/10.48432/QC7QW0.

Cipriani, Henrique Nery, Ana Karina Dias Salman, Thierry Alexandre Pellegrinetti, Elaine Coimbra Souza, Pedro Gomes Cruz, and Siu Mui Tsai. 2025. Native Tree Species in Silvopastoral System Outperforms Eucalyptus in Enhancing Soil Health. SSRN Scholarly Paper No. 5195852. Social Science Research Network, March 27. https://doi.org/10.2139/ssrn.5195852.

Cipriani, Henrique Nery, Ana Karina Dias Salman, Carlos Henrique Semper Da Silva, Murilo Luz Rodrigues, Emily Soares Dos Santos, and Pedro Gomes Da Cruz. 2023. Crescimento Inicial de Samanea Tubulosa e Eucalyptus Pellita Em Sistemas de Integração Pecuária-Floresta Em Porto Velho, Rondônia. *Série Técnica IPEF* 26 (48): 310–14. https://doi.org/10.18671/sertec.v26n48.061.

Climate-Data.org. 2022. Clima Porto Velho: Temperatura, Tempo e Dados Climatológicos. May. https://pt.climate-data.org/america-do-sul/brasil/rondonia/porto-velho-3120/#google_vignette.

Constantinides, M., and J. H. Fownes. 1994. Nitrogen Mineralization from Leaves and Litter of Tropical Plants: Relationship to Nitrogen, Lignin and Soluble Polyphenol Concentrations. *Soil Biology and Biochemistry* 26 (1): 49–55. https://doi.org/10.1016/0038-0717(94)90194-5.

Costa, Romario Martins, Mayanna Karlla Lima Costa, Sandra Mara Barbosa Rocha, et al. 2024. Soil Management Shapes Bacterial and Archaeal Communities in Soybean Rhizosphere: Comparison of No-Tillage and Integrated Crop-Livestock Systems. *Rhizosphere* 30 (June): 100886. https://doi.org/10.1016/j.rhisph.2024.100886.

Danielson, Rachel E., and Jorge L. Mazza Rodrigues. 2022. Impacts of Land-Use Change on Soil Microbial Communities and Their Function in the Amazon Rainforest. In *Advances in Agronomy*, vol. 175. Academic Press. https://doi.org/10.1016/bs.agron.2022.04.001.

Demin, Konstantin A., Evgeniya V. Prazdnova, Tatiana M. Minkina, and Andrey V. Gorovtsov. 2024. Sulfate-Reducing Bacteria Unearthed: Ecological Functions of the Diverse Prokaryotic Group in Terrestrial Environments. *Applied and Environmental Microbiology* 90 (4): e01390-23. https://doi.org/10.1128/aem.01390-23.

Deng, Pengfei, Wei Fan, Huiling Wang, Jianhang Ti, and Xiaoniu Xu. 2022. Chinese Torreya Agroforestry Alters the Rhizosphere Soil Bacterial Communities and Potential Functions. *Applied Soil Ecology* 177 (September): 104504. https://doi.org/10.1016/j.apsoil.2022.104504.

Dossa, Gbadamassi G. O., Yun-Qiang Yang, Weiming Hu, et al. 2021. Fungal Succession in Decomposing Woody Debris across a Tropical Forest Disturbance Gradient. *Soil Biology and Biochemistry* 155 (April): 108142. https://doi.org/10.1016/j.soilbio.2021.108142.

Duarte, Edivânia M. G., Irene M. Cardoso, Thomas Stijnen, et al. 2013. Decomposition and Nutrient Release in Leaves of Atlantic Rainforest Tree Species Used in Agroforestry Systems. *Agroforestry Systems* 87 (4): 835–47. https://doi.org/10.1007/s10457-013-9600-6.

Dyson, Bronwyn Lira, Vendula Brabcová, Petr Baldrian, Jörg Müller, Michael Junginger, and Claus Bässler. 2025. Experimentally Manipulating Forest Structure to Mimic Management Strategies: Effects on Deadwood Fungal Diversity and Related Ecosystem Processes. Preprint, bioRxiv, September 4. https://doi.org/10.1101/2025.08.30.673211.

Eo, Jinu, Myung-Hyun Kim, Min-Kyeong Kim, and Soon-Kun Choi. 2021. Shift of Dominant Species in Plant Community and Soil Chemical Properties Shape Soil Bacterial Community Characteristics and Putative Functions: A Case Study on Topographic Variation in a Mountain Pasture. *Microorganisms* 9 (5): 961. https://doi.org/10.3390/microorganisms9050961.

Feitosa, Izabela de Lima, Marcelo Silva de Oliveira, Rafael Lemos Bastos, Alexandre Martins Abdão dos Passos, and Henrique Nery Cipriani. 2022. Spatial Distribution of Agronomic Attributes of Corn Plants in Integrated Production Systems in Brazilian Amazonia. *International Journal of Advanced Engineering Research and Science* 9 (12): 382–88. https://doi.org/10.22161/ijaers.912.42.

Feitosa, Izabela de Lima, Alexandre Martins Abdão dos Passos, Henrique Nery Cipriani, Marcelo Silva de Oliveira, Alaerto Luiz Marcolan, and Gustavo Mattos Vasques. 2019. Spatial Variability of Soil Physical Attributes in Integrated Production Systems in the Amazon Region. *Pesquisa Agropecuária Brasileira* 54 (November). https://doi.org/10.1590/S1678-3921.pab2019.v54.00324.

Feng, Shunli, Yihan Guo, Yulu Ran, et al. 2023. Production of Microbial Lipids by Saitozyma Podzolica Zwy2-3 Using Corn Straw Hydrolysate, the Analysis of Lipid Composition, and the Prediction of Biodiesel Properties. *Energies* 16 (18): 6630. https://doi.org/10.3390/en16186630.

Friedman, Jonathan, and Eric J. Alm. 2012. Inferring Correlation Networks from Genomic Survey Data. *PLOS Computational Biology* 8 (9): e1002687. https://doi.org/10.1371/journal.pcbi.1002687.

Fuchs, Georg, Matthias Boll, and Johann Heider. 2011. Microbial Degradation of Aromatic Compounds — from One Strategy to Four. *Nature Reviews Microbiology* 9 (11): 803–16. https://doi.org/10.1038/nrmicro2652.

Gilbert, Jack A., Janet K. Jansson, and Rob Knight. 2014. The Earth Microbiome Project: Successes and Aspirations. *BMC Biology* 12 (1): 69. https://doi.org/10.1186/s12915-014-0069-1.

Goldfarb, Katherine C., Ulas Karaoz, China A. Hanson, et al. 2011. Differential Growth Responses of Soil Bacterial Taxa to Carbon Substrates of Varying Chemical Recalcitrance. *Frontiers in Microbiology* 2 (May). https://doi.org/10.3389/fmicb.2011.00094.

Gong, Ying, Langqin Yu, and Lei Zhao. 2022. ECOLOGICAL NETWORKS IN AGROECOSYSTEMS: APPROACHES AND APPLICATIONS. *ENGINEERING Agriculture* 9 (4): 523. https://doi.org/10.15302/J-FASE-2022466.

Gorte, Olga, Michaela Kugel, and Katrin Ochsenreither. 2020. Optimization of Carbon Source Efficiency for Lipid Production with the Oleaginous Yeast Saitozyma Podzolica DSM 27192 Applying Automated Continuous Feeding. *Biotechnology for Biofuels* 13 (1): 181. https://doi.org/10.1186/s13068-020-01824-7.

Goss-Souza, Dennis, Siu Mui Tsai, Jorge Luiz Mazza Rodrigues, et al. 2022. Biogeographic Responses and Niche Occupancy of Microbial Communities Following Long-Term Land-Use Change. *Antonie van Leeuwenhoek* 115 (9): 1129–50. https://doi.org/10.1007/s10482-022-01761-5.

Gou, Xiaomei, Peter B. Reich, Liping Qiu, et al. 2023. Leguminous Plants Significantly Increase Soil Nitrogen Cycling across Global Climates and Ecosystem Types. *Global Change Biology* 29 (14): 4028–43. https://doi.org/10.1111/gcb.16742.

Heberle, Henry, Gabriela Vaz Meirelles, Felipe R. da Silva, Guilherme P. Telles, and Rosane Minghim. 2015. InteractiVenn: A Web-Based Tool for the Analysis of Sets through Venn Diagrams. *BMC Bioinformatics* 16 (1): 169. https://doi.org/10.1186/s12859-015-0611-3.

Heinrich, P. A., D. R. Mulligan, and J. W. Patrick. 1988. The Effect of Ectomycorrhizas on the Phosphorus and Dry Weight Acquisition of Eucalyptus Seedlings. *Plant and Soil* 109 (1): 147–49. https://doi.org/10.1007/BF02197597.

IUSS Working Group WRB. 2022. *World Reference Base for Soil Resources 2022: International Soil Classification System for Naming Soils and Creating Legends for Soil Maps*. 4th ed. International Union of Soil Sciences. https://files.isric.org/public/documents/WRB_fourth_edition_2022-12-18.pdf.

Júnior, Valdo Soares Martins, Eduardo Robson Duarte, Kellerson Luiz da Silva, Cláudio Eduardo Silva Freitas, Flávia Oliveira Abrão Pessoa, and Patrícia Natalícia Mendes de Almeida. 2023. Seleção de Fungos Celulolíticos do Intestino Grosso de Borregos e Ovelhas Criados em Pastagens Tropicais. *Ensaios e Ciência: Ciências Biológicas, Agrárias e da Saúde* 27 (2): 167–71. https://doi.org/10.17921/1415-6938.2023v27n2p167-171.

Kajihara, Kacie T., Mengting Yuan, Anthony S. Amend, et al. 2025. Diversity, Connectivity and Negative Interactions Define Robust Microbiome Networks across Land, Stream, and Sea. Preprint, bioRxiv, January 10. https://doi.org/10.1101/2025.01.07.631746.

Karimi, Battle, Pierre Alain Maron, Nicolas Chemidlin-Prevost Boure, Nadine Bernard, Daniel Gilbert, and Lionel Ranjard. 2017. Microbial Diversity and Ecological Networks as Indicators of Environmental Quality. *Environmental Chemistry Letters* 15 (2): 265–81. https://doi.org/10.1007/s10311-017-0614-6.

Kerdraon, Deirdre, Julia Drewer, Biancolini Castro, Abby Wallwork, Jefferson S. Hall, and Emma J. Sayer. 2019. Litter Traits of Native and Non-Native Tropical Trees Influence Soil Carbon Dynamics in Timber Plantations in Panama. *Forests* 10 (3): 209. https://doi.org/10.3390/f10030209.

Khan, M. A. Wadud, Brendan J. M. Bohannan, Klaus Nüsslein, et al. 2019. Deforestation Impacts Network Co-Occurrence Patterns of Microbial Communities in Amazon Soils. *FEMS Microbiology Ecology* 95 (2): fiy230. https://doi.org/10.1093/femsec/fiy230.

Korchagin, Jackson, Edson Campanhola Bortoluzzi, Diovane Freire Moterle, Claudia Petry, and Laurent Caner. 2019. Evidences of Soil Geochemistry and Mineralogy Changes Caused by Eucalyptus Rhizosphere. *CATENA* 175 (April): 132–43. https://doi.org/10.1016/j.catena.2018.12.001.

Kurtz, Zachary D., Christian L. Müller, Emily R. Miraldi, Dan R. Littman, Martin J. Blaser, and Richard A. Bonneau. 2015. Sparse and Compositionally Robust Inference of Microbial Ecological Networks. *PLOS Computational Biology* 11 (5): e1004226. https://doi.org/10.1371/journal.pcbi.1004226.

Kutos, Steve, Elle M. Barnes, and J. D. Lewis. 2023. Soil Fungal Communities Vary More with Soil Characteristics than Tree Diversity at a Local Scale. *Canadian Journal of Forest Research* 53 (1): 14–24. https://doi.org/10.1139/cjfr-2021-0360.

Leewis, Mary-Cathrine, Corey R. Lawrence, Marjorie S. Schulz, et al. 2022. The Influence of Soil Development on the Depth Distribution and Structure of Soil Microbial Communities. *Soil Biology and Biochemistry* 174 (November): 108808. https://doi.org/10.1016/j.soilbio.2022.108808.

Leite, Fernando Palha, Ivo Ribeiro Silva, Roberto Ferreira Novais, Nairam Félix de Barros, and Júlio César Lima Neves. 2010. Alterations of Soil Chemical Properties by Eucalyptus Cultivation in Five Regions in the Rio Doce Valley. *Revista Brasileira de Ciência Do Solo* 34: 821–31. https://doi.org/10.1590/S0100-06832010000300024.

Li, Jiayu, Jiayi Lin, Chenyu Pei, Kaitao Lai, Thomas C. Jeffries, and Guangda Tang. 2018. Variation of Soil Bacterial Communities along a Chronosequence of Eucalyptus Plantation. *PeerJ* 6 (September): e5648. https://doi.org/10.7717/peerj.5648.

Liu, Chi, Yaoming Cui, Xiangzhen Li, and Minjie Yao. 2021. Microeco: An R Package for Data Mining in Microbial Community Ecology. *FEMS Microbiology Ecology* 97 (2): fiaa255. https://doi.org/10.1093/femsec/fiaa255.

Louca, Stilianos, Laura Wegener Parfrey, and Michael Doebeli. 2016. Decoupling Function and Taxonomy in the Global Ocean Microbiome. *Science* 353 (6305): 1272–77. https://doi.org/10.1126/science.aaf4507.

Mandro, Jéssica Adriele, Júlia Brandão Gontijo, Fernanda Mancini Nakamura, et al. 2026. From Deforestation to Regeneration: How Do Land-Use Changes Shape Soil Microbes and Methane-Cycling Genes in the Eastern Amazon? *Total Environment Microbiology*, February 12, 100069. https://doi.org/10.1016/j.temicr.2026.100069.

Maracaípe, Ingrid Da Silva Moreira, Maiza Mota Rodrigues, Laila Fernanda Conceição De Paiva, et al. 2025. SISTEMA DE INTEGRAÇÃO LAVOURA-PECUÁRIA-FLORESTA (ILPF): SUSTENTABILIDADE, PRODUTIVIDADE E DESAFIOS. In *Agropecuária e Meio Ambiente: Uma Visão Integrada*, 1st ed., with Antonia Francisca Lima Cardoso, Sharles Gabriel De Souza Borges, Shirlenne Ferreira Silva, and Francisco Helio Alves De Andrade. Editora Científica Digital. https://doi.org/10.37885/250319061.

McMurdie, Paul J., and Susan Holmes. 2013. Phyloseq: An R Package for Reproducible Interactive Analysis and Graphics of Microbiome Census Data. *PLOS ONE* 8 (4): e61217. https://doi.org/10.1371/journal.pone.0061217.

Mehta, Tushar, Mukesh Meena, and Adhishree Nagda. 2022. Bioactive Compounds of Curvularia Species as a Source of Various Biological Activities and Biotechnological Applications. *Frontiers in Microbiology* 13 (December). https://doi.org/10.3389/fmicb.2022.1069095.

Moreira, Geisianny Augusta Monteiro, and Helson Mario Martins Do Vale. 2018. Occurrence of Yeast Species in Soils under Native and Modified Vegetation in an Iron Mining Area. *Revista Brasileira de Ciência Do Solo* 42 (0). https://doi.org/10.1590/18069657rbcs20170375.

Moussa, Hakim Haj, Benamara Sara, Hadia Benhalima, Fouzia Benaliouche, Ibtissem Sbartai, e Hana Sbartai. 2024. "Chemical Characterization of Eucalyptus (*Eucalyptus Globulus*) Leaf Essential Oil and Evaluation of Its Antifungal, Antibacterial and Antioxidant Activities". *Cellular and Molecular Biology* 70 (12): 1–9. https://doi.org/10.14715/cmb/2024.70.12.1.

Muchalak, Franciele, Anderson Santos de Freitas, Luís Felipe Guandalin Zagatto, et al. 2025. Plant-Soil Microbiome Feedback under Post-Pasture Tropical Ecotone Forest Regeneration. *Applied Soil Ecology* 214 (October): 106381. https://doi.org/10.1016/j.apsoil.2025.106381.

Muscarella, Mario E., and James P. O'Dwyer. 2020. Species Dynamics and Interactions via Metabolically Informed Consumer-Resource Models. *Theoretical Ecology* 13 (4): 503–18. https://doi.org/10.1007/s12080-020-00466-7.

Naylor, Dan, Ryan McClure, and Janet Jansson. 2022. Trends in Microbial Community Composition and Function by Soil Depth. *Microorganisms* 10 (3): 540. https://doi.org/10.3390/microorganisms10030540.

Nuwagaba, Savannah, Feng Zhang, and Cang Hui. 2017. Robustness of Rigid and Adaptive Networks to Species Loss. *PLOS ONE* 12 (12): e0189086. https://doi.org/10.1371/journal.pone.0189086.

Oliveira, Maniele Mendonça de, Ana Karina Dias Salman, Henrique Nery Cipriani, Amanda Ribeiro de Moura, and Odilene de Souza Teixeira. 2021. Desempenho Inicial de Espécies Arbóreas Para Sombreamento Natural Em Sistema de Integração Pecuária-Floresta. *Anais...*, 36–41. https://www.alice.cnptia.embrapa.br/bitstream/doc/1139635/1/cpafro-18701.pdf.

Oliveira, Patricia Christiana S. de S., Alex Mota dos Santos, and Nilson Clementino Ferreira. 2019. MODELAGEM DINÂMICA DO DESMATAMENTO NO SUL DA AMAZÔNIA OCIDENTAL. *Boletim de Geografia* 37 (3): 189–207. https://doi.org/10.4025/bolgeogr.v37i3.42643.

Peng, Yumei, Huasen Xu, Jia Shi, et al. 2024. Soil Microbial Composition, Diversity, and Network Stability in Intercropping versus Monoculture Responded Differently to Drought. *Agriculture, Ecosystems & Environment* 365 (May): 108915. https://doi.org/10.1016/j.agee.2024.108915.

Penton, C. Ryan, V. V. S. R. Gupta, James M. Tiedje, et al. 2014. Fungal Community Structure in Disease Suppressive Soils Assessed by 28S LSU Gene Sequencing. *PLOS ONE* 9 (4): e93893. https://doi.org/10.1371/journal.pone.0093893.

Pereira, Arthur P. A., Ademir Durrer, Thiago Gumiere, et al. 2019. Mixed *Eucalyptus* Plantations Induce Changes in Microbial Communities and Increase Biological Functions in the Soil and Litter Layers. *Forest Ecology and Management* 433 (February): 332–42. https://doi.org/10.1016/j.foreco.2018.11.018.

Perez-Alvarez, Ricardo, Julián Chará, Lauren D. Snyder, Michelle Bonatti, Stefan Sieber, and Emily A. Martin. 2023. Global Meta-Analysis Reveals Overall Benefits of Silvopastoral Systems for Biodiversity. Preprint, bioRxiv, July 31. https://doi.org/10.1101/2023.07.30.551160.

Petticord, Daniel F., Ran Zhi, Elizabeth H. Boughton, et al. 2026. Foliar Phosphorus Concentrations in Bahiagrass Are Well-Predicted by the Abundance of a Fusarium Taxa. *Soil Biology and Biochemistry* 214 (March): 110049. https://doi.org/10.1016/j.soilbio.2025.110049.

Piontekowski, Valderli Jorge, Fabiana Piontekowski Ribeiro, Eraldo Aparecido Trondoli Matricardi, Ilvan Medeiros Lustosa Junior, Angela Pereira Bussinguer, and Alcides Gatto. 2019. Modeling Deforestation in the State of Rondônia. *Floresta e Ambiente* 26: e20180441. https://doi.org/10.1590/2179-8087.044118.

Põlme, Sergei, Kessy Abarenkov, R. Henrik Nilsson, et al. 2020. FungalTraits: A User-Friendly Traits Database of Fungi and Fungus-like Stramenopiles. *Fungal Diversity* 105 (1): 1–16. https://doi.org/10.1007/s13225-020-00466-2.

Qin, Fangcuo, Fucheng Yang, Angang Ming, et al. 2024. Mixture Enhances Microbial Network Complexity of Soil Carbon, Nitrogen and Phosphorus Cycling in *Eucalyptus* Plantations. *Forest Ecology and Management* 553 (February): 121632. https://doi.org/10.1016/j.foreco.2023.121632.

Quast, Christian, Elmar Pruesse, Pelin Yilmaz, et al. 2013. The SILVA Ribosomal RNA Gene Database Project: Improved Data Processing and Web-Based Tools. *Nucleic Acids Research* 41 (Database issue): D590-596. https://doi.org/10.1093/nar/gks1219.

Raimbault, Alexandre, Antoine Brin, Sophie Manzi, et al. 2024. Influence of Habitat Fragmentation and Habitat Amount on Soil Fungi Communities in Ancient Forests. *Landscape Ecology* 39 (2): 19. https://doi.org/10.1007/s10980-024-01821-3.

Revell, Liam J. 2024. Phytools 2.0: An Updated R Ecosystem for Phylogenetic Comparative Methods (and Other Things). *PeerJ* 12 (January): e16505. https://doi.org/10.7717/peerj.16505.

Rivest, Maxime, Joann K. Whalen, and David Rivest. 2020. Variation of Soil Microbial and Earthworm Communities along an Agricultural Transect with Tree Windbreak. *Agroforestry Systems* 94 (5): 1639–49. https://doi.org/10.1007/s10457-019-00476-3.

Rocha, Fernando Igne, Thiago Gonçalves Ribeiro, Marcelo Antoniol Fontes, et al. 2021. Land-Use System and Forest Floor Explain Prokaryotic Metacommunity Structuring and Spatial Turnover in Amazonian Forest-to-Pasture Conversion Areas. *Frontiers in Microbiology* 12 (April). https://doi.org/10.3389/fmicb.2021.657508.

Rodrigues, Jorge L. M., Vivian H. Pellizari, Rebecca Mueller, et al. 2013. Conversion of the Amazon Rainforest to Agriculture Results in Biotic Homogenization of Soil Bacterial Communities. *Proceedings of the National Academy of Sciences of the USA* 110 (3): 988–93. https://doi.org/10.1073/pnas.1220608110.

Santana, Margarida M., Teresa Dias, Juan M. Gonzalez, and Cristina Cruz. 2021. Transformation of Organic and Inorganic Sulfur– Adding Perspectives to New Players in Soil and Rhizosphere. *Soil Biology and Biochemistry* 160 (September): 108306. https://doi.org/10.1016/j.soilbio.2021.108306.

Santos, Adriana Bezerra dos, Giselle Gomes Monteiro Fracetto, Felipe José Cury Fracetto, and Mario Andrade Lira Junior. 2022. Rhizobial Diversity in Shrub-Tree Legume-Based Silvopastoral Systems. *Bragantia* 81: e2622. https://doi.org/10.1590/1678-4499.20210336.

Santos, Humberto Gonçalves dos, Paulo Klinger Tito Jacomine, Lúcia Helena Cunha dos Anjos, et al. 2025. *Sistema Brasileiro de Classificação de Solos*. 6th ed. Embrapa, 2025. http://www.infoteca.cnptia.embrapa.br/handle/doc/1176834.

Sarto, Marcos V. M., Wander L. B. Borges, Jaqueline R. W. Sarto, Carlos A. B. Pires, Charles W. Rice, and Ciro A. Rosolem. 2020. Soil Microbial Community and Activity in a Tropical Integrated Crop-Livestock System. *Applied Soil Ecology* 145 (January): 103350. https://doi.org/10.1016/j.apsoil.2019.08.012.

Schliep, Klaus Peter. 2011. Phangorn: Phylogenetic Analysis in R. *Bioinformatics* 27 (4): 592–93. https://doi.org/10.1093/bioinformatics/btq706.

Seaton, Fiona M., Rob I. Griffiths, Tim Goodall, Inma Lebron, and Lisa R. Norton. 2023. Soil Bacterial and Fungal Communities Show within Field Heterogeneity That Varies by Land Management and Distance Metric. *Soil Biology and Biochemistry* 177 (February): 108920. https://doi.org/10.1016/j.soilbio.2022.108920.

Segata, Nicola, Jacques Izard, Levi Waldron, et al. 2011. Metagenomic Biomarker Discovery and Explanation. *Genome Biology* 12 (6): R60. https://doi.org/10.1186/gb-2011-12-6-r60.

Shi, Xinyuan, and Ashley Conway-Anderson. 2022. Assessing the Sustainability of Silvopasture Systems. *CABI Reviews* 2022 (November). https://doi.org/10.1079/cabireviews202217047.

Silvestro, L. B., F. Biganzoli, S. A. Stenglein, H. Forjan, L. Manso, and M. V. Moreno. 2018. Mixed Cropping Regimes Promote the Soil Fungal Community under Zero Tillage. *Antonie van Leeuwenhoek* 111 (7): 1055–64. https://doi.org/10.1007/s10482-017-1005-5.

Soil Survey Staff. 2022. *Keys to Soil Taxonomy*. 13th ed. USDA Natural Resources Conservation Service. https://www.nrcs.usda.gov/sites/default/files/2022-09/Keys-to-Soil-Taxonomy.pdf.

Soltysiak, Maximillian P. M., Amogh P. Jalihal, Caroline E. Christophersen, et al. 2025. Expansion and Revision of the Genus Xanthobacter and Proposal of Roseixanthobacter Gen. Nov. *International Journal of Systematic and Evolutionary Microbiology* 75 (9): 006909. https://doi.org/10.1099/ijsem.0.006909.

Tahir, Ashar, Yingying Zhang, Chuan Yang, et al. 2026. Rubber Based Agroforestry Systems Enhance Soil Organic Carbon Sequestration through Changes in Soil Properties and Microbial Community Structure. *Applied Soil Ecology* 220 (April): 106842. https://doi.org/10.1016/j.apsoil.2026.106842.

Teixeira, Paulo Cesar, Guilherme Kangussu Donagema, Ademir Fontana, and Wenceslau Geraldes Teixeira, eds. 2017. *Manual de Métodos de Análise de Solo*. 3rd ed. Embrapa. http://ainfo.cnptia.embrapa.br/digital/bitstream/item/181717/1/Manual-de-Metodos-de-Analise-de-Solo-2017.pdf.

Valente, Moacir Azevedo, Raimundo Cosme de Oliveira Júnior, Tarcísio Ewerton Rodrigues, João Marcos Lima da Silva, and Paulo Lacerda dos Santos. 1998. *Levantamento Semidetalhado Dos Solos Do Campo Experimental de Porto Velho, RO*. Belém: Embrapa Trópico Úmido. (Documentos, 136). http://ainfo.cnptia.embrapa.br/digital/bitstream/item/57557/1/CPATU-Doc136.pdf.

Vaupel, Anna, Zita Bednar, Nadine Herwig, Bernd Hommel, Virna Estefania Moran-Rodas, and Lukas Beule. 2023. Tree-Distance and Tree-Species Effects on Soil Biota in a Temperate Agroforestry System. *Plant and Soil* 487 (1): 355–72. https://doi.org/10.1007/s11104-023-05932-9.

Vaupel, Anna, Max Küsters, Julia Toups, Nadine Herwig, Benedikt Bösel, and Lukas Beule. 2025. Trees Shape the Soil Microbiome of a Temperate Agrosilvopastoral and Syntropic Agroforestry System. *Scientific Reports* 15 (1): 1550. https://doi.org/10.1038/s41598-025-85556-4.

Venturini, Andressa M., Júlia B. Gontijo, Jéssica Adriele Mandro, et al. 2023. Soil Microbes under Threat in the Amazon Rainforest. *Trends in Ecology & Evolution* 38 (8): 693–96. https://doi.org/10.1016/j.tree.2023.04.014.

Wang, Huaxiang, Dian Tian, Jizhao Cao, et al. 2024. Eucalyptus and Native Broadleaf Mixed Cultures Boost Soil Multifunctionality by Regulating Soil Fertility and Fungal Community Dynamics. *Journal of Fungi* 10 (10): 709. https://doi.org/10.3390/jof10100709.

Wang, Wenbo, Dongsheng Chen, Qian Zhang, Xiaomei Sun, and Shougong Zhang. 2020. Effects of Mixed Coniferous and Broad-Leaved Litter on Bacterial and Fungal Nitrogen Metabolism Pathway during Litter Decomposition. *Plant and Soil* 451 (1): 307–23. https://doi.org/10.1007/s11104-020-04523-2.

Wang, Ye, Aming Li, and Long Wang. 2025. Stability of Complex Communities with Environmental Feedbacks. *Proceedings of the Royal Society A: Mathematical, Physical and Engineering Sciences* 481 (2310): 20240872. https://doi.org/10.1098/rspa.2024.0872.

Welke, Selmir, Ana Karina Dias Salman, Henrique Nery Cipriani, Laércio Cavalcante Monteiro Filho, Odilene de Souza Teixeira, and Giovanna Moreira Ghedin. 2022. Duas Espécies Arbóreas Para Sombreamento de Pastagem Em Sistema de Integração Pecuária-Floresta. *Anais...* 39–44. https://www.alice.cnptia.embrapa.br/alice/bitstream/doc/1146390/1/Anais-EIPER-2022-1-39-44.pdf.

White, T., Tom Bruns, Steven Lee, et al. 1990. Amplification and Direct Sequencing of Fungal Ribosomal RNA Genes for Phylogenetics. In *Pcr Protocols: A Guide to Methods and Applications*, vol. 31.

Willms, Inka M., Simon H. Bolz, Jingyue Yuan, et al. 2021. The Ubiquitous Soil Verrucomicrobial Clade 'Candidatus Udaeobacter' Shows Preferences for Acidic pH. *Environmental Microbiology Reports* 13 (6): 878–83. https://doi.org/10.1111/1758-2229.13006.

Xu, Yuxing, Chao Li, Yuanli Zhu, et al. 2022. The Shifts in Soil Microbial Community and Association Network Induced by Successive Planting of *Eucalyptus* Plantations. *Forest Ecology and Management* 505 (February): 119877. https://doi.org/10.1016/j.foreco.2021.119877.

Yu, Jingjing, Wei Cong, Yi Ding, Lixiao Jin, Jing Cong, and Yuguang Zhang. 2022. Interkingdom Plant–Soil Microbial Ecological Network Analysis under Different Anthropogenic Impacts in a Tropical Rainforest. *Forests* 13 (8): 1167. https://doi.org/10.3390/f13081167.

Zagatto, Luís Felipe Guandalin, Valerie L. Kalle, Tanja Bakx-Schotman, et al. 2026. Land Use Influences Prokaryotes More than Fungi in Adjacent Hedgerow Soils. *Agriculture, Ecosystems & Environment* 400 (April): 110238. https://doi.org/10.1016/j.agee.2026.110238.

Zandona, Ana Paula, Arnaldo Colozzi, and Laíse da Silveira Pontes. 2019. Effects of Trees and Nitrogen Supply on the Soil Microbiological Attributes on Integrated Crop-Livestock Systems. *Revista Ceres* 66: 226–34. https://doi.org/10.1590/0034-737X201966030009.

Zhang, Mengmeng, Ying Lu, Guangze Jin, and Biao Zhu. 2025. Bacterial Communities in Litter Are More Sensitive to High Nitrogen Addition than Fungal Communities in a Korean Pine (Pinus Koraiensis) Plantation. *Journal of Forestry Research* 37 (1): 23. https://doi.org/10.1007/s11676-025-01961-5.

Zhong, Jundi, Hanyuan Xu, Zina Chen, Kaiyan Yang, Shenghong Xiao, and Xunzhi Ouyang. 2025. Influence of Eucalyptus Plantation on Soil Microbial Characteristics in Severely Degraded Land of Leizhou Peninsula. *Forests* 16 (10): 1602. https://doi.org/10.3390/f16101602.

3 INTEGRATION OF CHEMICAL, PHYSICAL AND BIOLOGICAL INDICATORS FOR ASSESSMENT OF SOIL QUALITY IN INTEGRATED PRODUCTION AND PASTURE SYSTEMS

ABSTRACT

The intensification of livestock systems in the Amazon through integrated production models is a key strategy for sustainable land use. This study aimed to evaluate soil quality in Western Amazonia by integrating chemical, physical, and biological indicators into composite soil quality indices (SQIs). The research was conducted over two years (2023 and 2024) in Porto Velho (Rondônia State, Brazil), across different systems: integrated crop-livestock (ICL), integrated crop-livestock-forestry (ICLF), integrated livestock-forestry (ILF) with native (*Samanea tubulosa*) and exotic (*Eucalyptus pellita*) trees, and treeless pastures (Ipyporã hybrid and *U. humidicola* monocultures), besides a native forest (NF) fragment. A knowledge-based minimum data set (MDS) was established to evaluate six soil functions from the three soil health dimensions (chemical, physical, and biological): acidity regulation, based on pH and potential acidity (H+Al); nutrient availability, comprising available phosphorus (P) and exchangeable bases (K + Ca + Mg); water availability and root support, including gravimetric moisture (θ_w) and soil resistance to penetration (RP); support biological activity, using soil organic matter (OM) and the enzymes acid phosphatase (AP), arylsulfatase (AS), and beta-glucosidase (BG). We hypothesized that composite SQIs would provide a more accurate assessment of soil health than individual attributes and that native species would offer greater stability. Results showed that all managed systems maintained high functional stability, with no significant interannual degradation, contrasting with the typical degradation patterns in the region. ICL and ICLF showed better chemical quality. However, by 2024, the ILF with *S. tubulosa* (ILF-ST) emerged as the most resilient model, showing superior acidity regulation and organic matter scores while avoiding the localized soil compaction (root support deficit) observed under the ILF with *E. pellita*. Furthermore, well-managed treeless pastures (Ipyporã) demonstrated competitive soil quality, indicating their viability for sustainable intensification. All managed systems presented lower soil physical quality than NF due to lower capacity to support root growth (increased RP). The influence of distance from the trees on soil quality indices and indicators varies with year and system. Likewise, most indicators presented interannual variations among systems, but interannual variation of SQIs was less frequent. The application of composite SQIs proved to be a more effective diagnostic tool than the analysis

of individual indicators, as it simplified the interpretation of complex interactions and provided a more coherent assessment of soil health. Furthermore, the study concludes that while ICLF offers immediate chemical gains from crop residuals, the integration of native legumes like *S. tubulosa* provides a more balanced and spatially stable soil environment over time, effectively decoupling livestock production from soil exhaustion in the Amazon.

Keywords: *Samanea tubulosa*, silvopastoral systems, soil health, soil quality index, spatial variability.

3.1 Introduction

Livestock significantly contributes to the economic development of the Brazilian Amazon region, primarily through cattle ranching, which has become a dominant agribusiness sector. The region hosts over 50 million cattle, utilizing more than 40 million hectares of pasture, which has facilitated economic integration into national and global markets (Dias-Filho 2026; Valentim et al. 2010; Araujo et al. 2026). However, this integration has historically led to deforestation, driven by the expansion of cattle herds and the organization of commodity chains (Barbanti 2015; Pacheco and Poccard-Chapuis 2012). Recent trends indicate a shift towards low-carbon cattle ranching, where intensification of livestock production can mitigate environmental impacts while enhancing productivity, thus avoiding further deforestation (Dias-Filho 2026; Skidmore et al. 2022; Silva et al. 2018; Valentim et al. 2010).

Research on the application of soil quality indexes (SQIs) in cattle ranching systems has emerged as a critical area of inquiry due to its implications for sustainable land management and ecosystem conservation. Soil quality, defined as the capacity of soil to function within ecosystem limits to sustain biological productivity and maintain environmental quality, is essential for supporting plant growth, nutrient cycling, and water regulation (Lima et al. 2016; Humeniuk and Hrubinko 2025; Simon et al. 2022). Over recent decades, studies have evolved from assessing individual soil attributes to integrating physical, chemical, and biological indicators into composite SQIs to better capture soil health dynamics under varying land uses (Bravo-Medina et al. 2021; Simon et al. 2022; Marion et al. 2022).

Conceptually, SQIs integrate multiple soil attributes – physical, chemical, and biological – to provide a holistic measure of soil health and functionality (El Behairy et al. 2024; Bünemann et al. 2016; Bhaduri et al. 2025). These indexes serve as tools to evaluate the impact of land use changes and management practices on soil sustainability, linking soil condition to

ecosystem services and agricultural productivity. The framework positions SQIs as essential for monitoring soil responses in cattle ranching landscapes and native forest fragments, guiding sustainable land use decisions (Lima et al. 2016; Bermeo 2022; Bravo-Medina et al. 2021).

Despite advances, knowledge gaps persist regarding the sensitivity and applicability of SQIs across diverse agroecosystems, especially in tropical and subtropical regions (Rosales et al. 2018; Valani et al. 2022; Bravo-Medina et al. 2021). Moreover, the spatial variability of soil quality under silvopastoral and agroforestry systems remains underexplored (Marçal et al. 2022; M. A. Santos et al. 2023; Valani et al. 2021). This is particularly true in integrated livestock-forestry (ILF) systems (or silvopastoralism) with native to Amazon tree species, since most attention is given to eucalyptus (Nunes et al. 2020; Behling et al. 2021).

Samanea tubulosa (raintree), a native leguminous tree, shows significant potential for integration into ILF systems due to its multifaceted benefits for sustainable livestock production (P. E. R. Carvalho 2007). It has been identified as a promising species for reforestation and ILF systems, offering shade, wood, edible fruits, and improved pasture quality around the trees (Andrade et al. 2012; T. K. de Oliveira and Luz 2012; de Morais et al. 2025). This aligns with the broader benefits of ILF systems, which include improved animal welfare, enhanced forage quality, and reduced greenhouse gas emissions (Pérez-Márquez et al. 2025; de Morais et al. 2025; Olival et al. 2021).

Therefore, the aim of this study was to evaluate the integration of chemical, physical, and biological indicators in the assessment of soil quality within integrated production and monoculture pasture systems in Western Amazonia. It was hypothesized that the integration of these indicators into composite SQIs provides a more accurate assessment of soil health compared to evaluations based on individual soil attributes.

Furthermore, the implementation of ILF systems is expected to significantly improve soil quality indicators in comparison to traditional cattle ranching systems. These SQIs are also expected to demonstrate high sensitivity not only to changes in land use and management practices but also to interannual variations, providing an effective framework for monitoring the temporal dynamics of soil health in tropical and subtropical agroecosystems. Finally, the study posits that there is significant spatial variability in soil quality indicators within tree-integrated systems, and that this spatial distribution is modulated by the sampling year, with native species like *S. tubulosa* providing more stable or progressive benefits to soil health over time compared to non-native species.

3.2 Materials and Methods

3.2.1 Site description

Samples were taken from six cattle ranching experimental areas and a native forest (NF) fragment located within the Empresa Brasileira de Pesquisa Agropecuária (Embrapa) experimental field in Porto Velho, Rondônia State, Brazil (8° 48’ S, 63° 51’ W; 95 m altitude). According to the Köppen climate classification system, the climate is Am, or tropical monsoon (Alvares et al. 2013). The area has an average annual rainfall of 2,216 mm, with average annual maximum and minimum temperatures of 30.4 °C and 23.3 °C, respectively (Climate-Data.org 2022).

The predominant soil in the area is classified as a Latossolo Vermelho-Amarelo distrófico (LVAd) according to the Brazilian soil classification system (Valente et al. 1998; Santos et al. 2025), which corresponds to a Ferralsol in the World Reference Base (WRB) soil classification system (IUSS Working Group WRB 2022), or a Hapludox under the USDA Soil Taxonomy (Soil Survey Staff 2022). The soil has a predominant clay texture.

3.2.1.1 Integrated livestock-forestry (ILF) systems

The experiments were initiated in February 2018 with the establishment of trees in a palisade grass pasture [*Urochloa brizantha* (Hochst. Ex A. Rich.) R. Webster ‘Marandu’], resulting in two low-tree-density integrated livestock–forestry (ILF) systems: one with *Eucalyptus pellita* F. Muell (ILF-EP) and another with *Samanea tubulosa* (Benth.) Barneby & J.W. Grimes (ILF-ST).

In each ILF system, trees were planted in a single tree strip functioning primarily as a windbreak, composed of two rows approximately 300 m long, with spacing of 6.0 m between rows and 3.5 m between trees within rows, oriented along an azimuth of 320° (NW–SE). Considering the total area of each ILF system (12.8 ha), the initial tree density was approximately 13 trees ha^{-1}, with 171 trees planted in each system. The *E. pellita* and *S. tubulosa* strips were separated by approximately 240 m (Figure 2.1).

The planting was done manually, using post hole diggers and 30 cm-tall cuttings (*E. pellita*) and seedlings (*S. tubulosa*), 30 days after desiccating the pasture in the strip area with glyphosate. Fertilization was done with chemical NPK + micronutrients fertilizer (350 g $plant^{-1}$) applied in the holes, just before planting, and as top-dressing applications (twice

annually in 2018 and 2019, and once annually from 2020 to 2023). The mean total height of the trees was 5.9 m (*S. tubulosa*), and 19.8 m (*E.* pellita), and mean canopy diameter was 8.4 m (*S. tubulosa*), and 5.8 m (*E. pellita*), at the time of soil sampling (Cipriani et al. 2023; Oliveira et al. 2021; Welke et al. 2022).

The palisade grass was established before 1970, i.e., more than 40 years before tree planting, and its grazing management was carried out using 4 paddocks of 3.2 ha. The animals used were of the Girolando breed (dry cows and heifers) with ad libittum intake of salt and water. Grazing management followed a mob grazing strategy, in which animals were maintained at high stocking density for short occupation periods followed by adequate pasture recovery intervals. Average annual stocking rate was approximately two animal units per hectare in both ILF-ST and ILF-EP systems. Whole-area pasture fertilization and liming were rare, with the most recent application occurring five years before the planting of the trees.

3.2.1.2 Integrated crop-livestock (ICL) and integrated crop-livestock-forestry (ICLF) systems

From earlier than 1970 to 2008, the area where the ICL and ICLF systems were established (approximately 6 ha each) was occupied by a variety of pastures, such as *Andropogon gayanus* Kunth, *U. humidicola,* Mombaça grass [*Megathyrsus maximus* (Jacq.) BKSimon & SWL Jacobs] and Marandu grass. From 2008 to 2012, the areas served for experiments on no-till and cover crop succession, including, maize, rice, soybean, sorghum and *U. ruziziensis* (Townsend et al. 2013). From 2012 to 2020 the soybean/maize+*Urochloa* succession was used annually or every two years (Ribeiro, Passos, Aker 2020). In 2020, *U. brizantha* x *U. ruziziensis* 'Ipyporã' pasture was established on no-till, remaining until soil sampling date.

The ICLF was established in March 2013, with the planting of *Eucalyptus* spp. cuttings in seven strips, with four rows of 240 m each. Three tree arrangements (subsystems) were adopted, with 18, 30, and 42 m between strips, following an azimuth of 210° (NE–SW) (Feitosa et al. 2019, 2022). From late 2018 to early 2019, the eucalyptus trees were harvested and *E. pellita* seedlings were planted in between-rows, resulting in seven strips with two rows of trees each, and tree densities of 267, 180, and 136 trees ha^{-1}, for the subsystems with 18, 30, and 42 m between strips, respectively. Nevertheless, only the subsystem with 42 m between strips (136 trees ha^{-1}) was considered in the present study.

Soil preparation and fertilization for tree planting were as described for the ILF systems. The alleys between strips were managed as the ICL. The mean total height of the trees was

between 10.2 and 12.4 m, and mean diameter at 1.30 m from the soil (DBH) was between 13.9 and 16.5 cm at the time of soil sampling.

3.2.1.3 Treeless pastures

Two treeless pasture systems were assessed, which are differentiated mainly by the variety of pasture: *U. humidicola* (HP) and Ipyporã grass (IP). The establishment date of HP occurred 40 to 30 years before soil sampling. The Ipyporã grass was planted in 2019 on an area formerly occupied by Marandu grass and *U. humidicola.* The two treeless pasture areas can be considered moderately managed, receiving liming and fertilization sporadically and with mean grazing intensity.

3.2.1.4 Native forest fragment (NF)

An unmanaged NF fragment from the same experimental field was included as a reference area to represent baseline conditions without human intervention. The fragment spans 41 ha of primary tropical rainforest, containing 99 woody species and 258 individuals per hectare. *Sclerolobium paniculatum*, *Psidium araca*, *Eschweilera grandiflora*, *Licania heteromorpha*, and *Protium puncticulatum* comprise 35 % of the relative density in the fragment (Bentes-Gama et al. 2009). The NF soil was assigned the same classification as the ILFSs.

3.2.2 Soil sampling

Soil samples were collected with augers in March 2023 and April 2024 (rainy season) from the 0-10 and 10-20 cm layers. In the ILF and ICLF systems, samples were taken at three distances from the tree rows: 0.00 m (the planting line), 5.25 m, and 21.00 m. The 5.25 and 21.00 m distances were chosen for standardization, as they correspond to one-eighth and one-half of the 42 m inter-row spacing used in previous studies conducted within the same ICLF system (Feitosa et al. 2019, 2022). Furthermore, these distances are representative of intermediate and distal zones among those adopted by studies assessing the influence of trees on pasture and soil attributes in integrated systems.

The spatial distribution of sampling points was planned to ensure representativeness and minimize edge effects within the experimental areas. In NF, the five sampling points were

established along a transect parallel to the boundary road, with each point located more than 30 m from the edge to avoid external influences. Successive samples were collected approximately every 30 m along this transect to ensure spatial independence. In the treeless systems (ICL and pastures), the five sampling points were distributed randomly across the area, while maintaining a minimum distance of 30 m from the edges and between points. In the ILF and ICLF systems, the five sampling points for each distance (0.00 m, 5.25 m and 21.00 m) were positioned along the tree rows. A 30 m buffer zone was maintained from both the start and the end of the rows. Samples were collected at intervals of approximately 30 m along the row, alternating the collection between the NE and SW sides of the planting line.

Five composite samples (prepared from two simple samples each) were taken per area, depth and distance, summing up 130 composite samples per year. Specifically, the NF, ICL and pasture areas (HP and IP) contributed with 10 samples each (2 depths x 5 replicates), while the two ILF and the ICLF areas contributed with 30 samples each, factoring in the three distance levels (3 distances x 2 depths x 5 replicates). Subsamples for soil enzyme activity assays were placed in a cooler and stored at 7 °C. Soil samples for chemical analysis were air-dried, ground, sieved (2 mm) and stored at room temperature.

3.2.3 Analysis of soil attributes

A knowledge-based minimum data set (MDS) was established by selecting indicators based on their functional relevance, widespread use in soil health protocols (Mendes et al. 2024) and with high diagnostic feasibility.

3.2.3.1 Chemical and physical attributes and organic matter

The soil chemical attributes analyses were conducted following the methodology described in (Teixeira et al. 2017). Soil pH was measured in a 1:2.5 soil:water suspension. Exchangeable aluminum (Al), calcium (Ca), and magnesium (Mg) were extracted with 1 mol L^{-1} of KCl. Exchangeable Ca and Mg were determined by atomic absorption spectrometry, and Al by acid-base titration. Soil phosphorus and potassium were extracted using the Mehlich-1 method, with available P determined by visible spectrophotometry and K by flame atomic emission spectrometry. Potential acidity (H+Al) was determined using the 0.5 mol L^{-1} of calcium acetate method at pH 7.0. Exchangeable bases (EB) are the sum of Ca, Mg, and K. Soil organic matter (OM) was measured using the Walkley and Black (1934)

method, as modified by Jackson (1982). Gravimetric moisture (θ_w) was determined as the mass of water per mass of soil oven-dried at 105°C for 72 h (dag kg^{-1}). These attributes were analyzed at Laboratório de Solos e Plantas, Embrapa Rondônia, Porto Velho, Brazil (samples from 2023) and Laboratório Qualita Agroambiental, Ji-Paraná, Rondônia State, Brazil (samples from 2024). The values from 0-10 and 10-20 cm layers were averaged to obtain 0-20 cm layer values.

Soil resistance to penetration (RP) was measured in the field with an impact penetrometer, Model IAA-Planalsucar-Stolf (Stolf et al. 1983). The data from the penetrometer was converted to MPa for the 0-20 cm layer using equations in Excel spreadsheets (Stolf et al. 2014). Five measurements were taken per area, close to the soil sampling points.

3.2.3.2 Soil enzyme activity assays

Acid phosphatase (AP), β-glucosidase (BG), and arylsulfatase (AS) activities were determined in the 0-10 cm layer samples using the method described by (Tabatabai 1994), with minor modifications. Briefly, 1 g of fresh soil was incubated with 1 mL of a 0.05 mol L^{-1} substrate (p-nitrophenyl phosphate, p-nitrophenyl β-D-glucopyranoside or p-nitrophenyl sulfate) solution in 4 mL buffer at 37 °C for 1 h. Following incubation, the reaction was stopped by adding 4 mL of 0.5 mol L^{-1} NaOH and 1 mL of 0.5 mol L^{-1} $CaCl_2$. Blank samples (containing soil and buffer but no substrate) were run concurrently to correct for background absorbance. These analyses were carried out in Laboratório de Biologia Celular e Molecular, USP/CENA, Piracicaba, São Paulo State, Brazil

The liberated p-nitrophenol was quantified by measuring the absorbance at 405 nm using a spectrophotometer. A standard curve of p-nitrophenol was used for quantification. Results were expressed as micromoles of p-nitrophenol released per gram of soil per hour (μmol p-nitrophenol g^{-1} soil h^{-1}), on an oven-dry soil basis.

3.2.3.3 Soil quality index

A Soil Quality Index (SQI) and its subindices ($SQI_{chemical}$, $SQI_{physical}$, and $SQI_{biological}$) were calculated to assess soil quality (Cherubin et al. 2016). Reference values were obtained from Alvarez V. et al. (1999) for chemical attributes and organic matter (OM), or from the dataset itself for physical and biological attributes. Indicators were scaled proportionally relative to the reference values, which received score 1 (maximum allowed score). The index was calculated for the 0-20 cm layer, except for AP, AS and BG, for which only the 0-10 cm

layer values were used (Lopes et al. 2013). The more is better approach was applied to all indicators, except for H+Al and soil resistance to penetration (RP), for which less is better. The SQI was calculated as the weighted average of the nine indicators, with equal weights for subindices and individual indicators (Table 3.1).

Table 3.1 - Subindices, soil functions and indicators, with their respective weights and reference values, used in the soil quality index (SQI) calculation. H+Al: potential acidity; P: available phosphorus; EB: exchangeable bases; θ_w: gravimetric moisture; RP: soil resistance to penetration; OM: organic matter; AP: acid phosphatase activity; AS: arylsulfatase activity; BG: betaglucosidase activity.

SQI subindex	Weight I†	Soil function	Weight II‡	Indicator	Weight III§	Reference value
Chemical	1/3	Acidity regulation	1/2	pH	1/2	5.5 (Alvarez V et al. 1999)
				H+Al	1/2	2.50 $cmol_c\ dm^{-3}$ (Alvarez V et al. 1999)
		Nutrient availability	1/2	P	1/2	12.1 mg dm^{-3} (Alvarez V et al. 1999)
				EB	1/2	3.61 $cmol_c\ dm^{-3}$ (Alvarez V et al. 1999)
Physical	1/3	Water availability	1/2	θ_w	1	42.08 (2023) and 42.00 (2024) dag kg^{-1} (highest values in dataset)
		Support root growth	1/2	RP	1	1.02 (2023) and 0.95 (2024) MPa (lowest values in dataset)
Biological	1/3	Sustain biological activity	1/2	OM	1	4.01 dag kg^{-1} (Alvarez V et al. 1999)
		Nutrient cycling	1/2	AP	1/3	10.07 (2023) and 13.90 (2024) µmol p-nitrophenol g^{-1} soil h^{-1} (highest values in dataset)
				AS	1/3	8.25 (2023) and 1.59 (2024) µmol p-nitrophenol g^{-1} soil h^{-1} (highest values in dataset)
				BG	1/3	2.16 (2023) and 0.64 (2024) µmol p-nitrophenol g^{-1} soil h^{-1} (highest values in dataset)

† Subindex weight for SQI calculation. ‡Soil function weight within the respective subindex. § Indicator weight within the respective soil function.

3.2.4 Statistical analysis

The statistical analyses were performed according to a completely randomized design (CRD), arranged in a split-plot in time scheme. The main plots consisted of 13 treatments: a 3 x 3 factorial [3 tree-integrated systems (ILF-EP, ILF-ST, and ICLF) x 3 distances from the trees (0.00, 5.25, and 21.00 m)] + 4 additional treatments (ICL, IP, HP, and NF), with 5 replicates. The sub-plots consisted of the evaluation years (2023 and 2024).

After checking for the assumptions of homoscedasticity and normality, outlier removal, and application of the Box-Cox transformation (or Johnson transformation when Box-Cox was

ineffective), the means of soil physical (θ_w and RP) and chemical (pH, H+Al, P, EB and OM) attributes, enzyme activity assays (AP, AS and BG) and SQI were subjected to ANOVA. A partition of the treatment x year interaction (slicing) was performed to compare years within each treatment and to compare treatments within each year.

Regression analysis was then performed to evaluate the effect of distance within the tree-integrated systems. The choice between linear and quadratic models was based on the significance of the regression coefficients and the lack-of-fit test. The quadratic model was selected whenever the linear lack-of-fit was significant and the second-degree term contributed significantly to the model; otherwise, the linear model was preferred if significant. In cases where neither model showed significance, the distance effect was considered non-significant.

Comparisons among ILFs and ICLF, within distances, were made using Tukey's test. For comparisons among the additional treatments (treeless systems and NF), Tukey's test was also used. To compare the combinations of tree-integrated systems and distances relative to the treeless systems and NF, Dunnett's test was applied. The 5 % significance level was adopted in all analyses. Statistical procedures were performed using Sisvar 5.8 (Ferreira 2011), Minitab 22, and the Tratamentos.ad package for R (Azevedo 2022).

3.3 Results

3.3.1 Soil chemical quality indicators

The soil chemical quality indicators were significantly influenced by the management systems, sampling distances, and evaluation years. In 2023 and 2024, the soil pH was significantly lower in ILF-EP compared to ILF-ST and ICLF at the 0.00 m distance, but higher in the ICLF system compared to ILF-ST and ILF-EP at the 5.25 and 21.00 m distances (Table 3.2). The native forest (NF) consistently exhibited the most acidic conditions in both years (3.97 in 2023 and 4.46 in 2024), being statistically inferior to all managed systems, except for ILF-EP at 0.00 m (4.33 in 2023 and 4.98 in 2024).

When comparing integrated systems to the treeless systems in 2023, the pH values in ICL system was superior to ILF-ST and ILF-EP at all distances, and to ICLF at the 0.00 m distance. Ipyporã pasture pH was higher than ILF-EP at 0.00 m and lower than ICLF at 5.25 m. On the other hand, HP showed lower values than ILF-ST and ILF-EP at 5.25 m, and ICLF at 21.00 m. Moreover, among the treeless pastures, ICL and IP showed higher mean pH than HP.

Table 3.2 - Soil chemical quality indicators (mean ± standard deviation) according to the distance from the trees (in tree-integrated systems), area and sampling year (2023 and 2024). H+Al: potential acidity; P: available phosphorus; EB: exchangeable bases; ILF-ST: integrated livestock-forestry with *Samanea tubulosa*; ILF-EP: integrated livestock-forestry with *Eucalyptus pellita*; ICLF: integrated crop-livestock-forestry; ICL: integrated crop-livestock; IP: *Urochloa brizantha* x *U. ruziziensis* 'Ipyporã' pasture; HP: *U. humidicola* pasture; NF: native forest.

Distance	**Area**	**pH**	**H+Al**	**P**	**EB**
m			$cmol_c\ dm^{-3}$	$mg\ dm^{-3}$	$cmol_c\ dm^{-3}$
		---------- 2023 ----------			
0.00	ILF-ST	4.84±0.38 ABβ†¶	9.79±1.52 Aα¶	1.90±0.42 Bα†	2.49±1.17 ABα†¶
	ILF-EP	4.33±0.34 Bβ†‡	9.12±0.59 Aα¶	1.90±0.22 Bα†	1.30±1.20 Bα†‡
	ICLF	5.01±0.15 Aβ†¶	8.08±1.23 Aα§¶	3.60±1.56 Aα†	3.46±0.72 Aα†¶
5.25	ILF-ST	5.24±0.11 Bβ§¶	10.61±0.99 Aα¶	1.88±0.65 Bα†‡§	3.11±0.73 Bα†¶
	ILF-EP	5.00±0.31 Bα†¶	8.84±1.54 ABα§¶	2.20±0.27 Bα†	1.88±0.88 Bα†
	ICLF	5.66±0.11 Aβ‡§¶	7.63±0.22 Bα‡§¶	13.80±7.43 Aα‡§¶	4.87±0.88 Aα§¶
21.00	ILF-ST	4.96±0.53 Bβ†¶	11.52±1.79 Aα¶	3.50±2.83 Bα†	3.05±2.02 Bα†¶
	ILF-EP	5.03±0.17 Bα†¶	8.20±0.70 Bα§¶	1.40±0.22 Cα†‡§¶	2.45±0.77 Bα†¶
	ICLF	5.34±0.08 Aβ§¶	7.56±1.65 Bα‡§¶	9.80±3.17 Aα‡§¶	4.70±0.71 Aα§¶
	ICL	5.37±0.21 aβ	9.47±0.98 bα	9.80±4.86 aα	5.22±0.52 aα
	IP	5.19±0.12 aβ	10.10±1.57 bα	3.00±0.79 bα	3.35±1.06 bα
	HP	4.84±0.16 bβ	11.41±0.98 bα	2.90±0.65 bα	2.04±0.39 bα
	NF	3.97±0.06 cβ	15.79±3.67 aα	2.70±0.76 bα	0.31±0.09 cα
		---------- 2024 ----------			
0.00	ILF-ST	5.79±0.11 Aα¶	2.99±0.09 Bβ¶	2.48±0.67 Aα‡§	3.12±0.68 Aα¶
	ILF-EP	4.98±0.41 Bα†‡	4.74±1.21 Aβ†‡¶	2.22±0.36 Aα‡	1.54±0.60 Bα†
	ICLF	5.76±0.07 Aα¶	3.01±0.07 Bβ¶	2.25±0.62 Aα‡	3.14±0.53 Aα¶
5.25	ILF-ST	5.48±0.43 Bα¶	3.51±0.88 Aβ¶	1.60±1.16 Bα†‡	2.21±1.19 Bα¶
	ILF-EP	5.10±0.34 Bα†‡¶	4.42±1.00 Aβ†‡¶	0.88±0.18 Bβ†	1.57±0.59 Bα†
	ICLF	5.98±0.02 Aα§¶	2.56±0.08 Bβ†‡§¶	5.87±3.02 Aβ‡§¶	3.45±0.37 Aβ‡§¶
21.00	ILF-ST	5.37±0.52 Bα¶	4.45±1.74 Aβ¶	1.01±0.48 Bβ†	2.06±1.09 Bβ¶
	ILF-EP	5.34±0.25 Bα†¶	4.42±0.80 Aβ†‡¶	0.86±0.43 Bβ†¶	1.86±0.52 Bα†¶
	ICLF	6.03±0.06 Aα†‡§¶	2.66±0.14 Bβ§¶	4.74±2.43 Aβ‡§¶	3.68±0.28 Aβ§¶
	ICL	5.87±0.06 aα	2.88±0.09 cβ	3.55±0.97 aβ	3.10±0.42 aβ
	IP	5.70±0.22 abα	3.10±0.52 bcβ	0.76±0.34 cβ	2.52±0.44 abα
	HP	5.34±0.44 bα	4.00±1.17 bβ	1.19±0.15 bβ	2.00±0.83 bα
	NF	4.46±0.08 cα	9.30±0.82 aβ	1.63±0.28 bβ	0.43±0.05 cα

Data were analyzed by factorial ANOVA at the 5 % significance level. Tukey's test was used to compare tree-integrated systems within distances (capital letters), treeless systems and NF among themselves (lowercase letters), and years within systems (Greek letters). Systems sharing the same letters do not differ statistically. Treeless systems and NF were compared with tree-integrated systems using Dunnett's test. The symbols †, ‡, §, and ¶ indicate a significant difference relative to ICL, IP, HP and NF, respectively.

By 2024, a general increase in pH occurred, including NF. Soil pH in ICLF system at the 21.00 m distance was superior to all other areas. Mean pH in ICL was similar to IP, but higher than HP and ILF-EP at all distances. Moreover, soil pH in IP and HP were lower than ICLF at the 5.25 m distance at 5.25 m and 21.00 m.

Potential acidity (H+Al) exhibited an inverse trend to pH, with NF showing the highest levels in 2023 and 2024 (15.79 and 9.30 $cmol_c$ dm^{-3}, respectively). In 2023, no significant difference was observed among tree-integrated systems at the 0.00 m distance, but ILFS-ST showed the highest mean H+Al at 5.25 and 21.00 m. Moreover, the tree-integrated systems at the 21.00 m distance presented H+Al levels (range 7.56-11.52 $cmol_c$ dm^{-3}) that were statistically equivalent to the ICL system (9.47 $cmol_c$ dm^{-3}). Potential acidity in HP soil was significantly higher than ICLF at all distances and ILF-EP at 5.25 and 21.00 m; and IP showed higher H+Al levels than ICLF at 5.25 and 21.00 m. In turn, no significant difference was observed among treeless systems.

However, a significant temporal reduction in H+Al was noted in 2024. At the 0.00 m distance, ILF-EP showed the highest mean H+Al among the tree-integrated systems (4.74 $cmol_c$ dm^{-3}), whereas, at 5.25 and 21.00 m, the lowest mean values were observed in the ICLF system (2.56 and 2.66 $cmol_c$ dm^{-3}). Among the treeless systems, H+Al in ICL was statistically lower than HP, ILF-EP at all distances and ICLF at 5.25 m; IP also showed lower mean H+Al than ILF-EP at all distances and ICLF at 5.25 m; and HP showed higher mean H+Al than ICLF at 5.25 and 21.00 m.

Available phosphorus (P) concentrations generally decreased from 2023 to 2024, except for ILF-ST at the 0.00 m distance, which showed no significant difference between years. The highest mean available P were observed in the ICL and ICLF (at 5.25 m and 21.00 m) systems, which significantly exceeded the levels of all other managed systems and NF in both 2023 and 2024. On the other hand, in 2023, the treatment with the lowest average P was ILF-EP at 21.00 m (1.40 mg dm^{-3}). In 2024, IP, ILF-ST (at 21.00 m) and ILF-EP (at 5.25 and 21.00 m) shared the lowest P values. Moreover, in 2023, available P in IP and HP was higher than ILF-ST at the 5.25 m distance (1.88 mg dm^{-3}). In 2024, available P in HP was higher than IP, but lower than ILFS-ST at 0.00 m, which, in turn was also higher than IP.

Mean exchangeable bases (EB) showed some significant differences between years, with lower values for ICL, ICLF (at the 5.25 and 21.00 m distances) and ILF-ST (at the 5.25 m distance) in 2024, compared to 2023. Among the tree-integrated systems, EB in ICLF was superior to ILF-ST at 5.25 and 21.00 m, and to ILF-EP at all distances, in 2023, and to ILF-ST and ILF-EP at all distances in 2024. Among the treeless systems, in 2023, EB in ICL

(5.22 $cmol_c$ dm^{-3}) was higher than every other treatment, except for ICLF at 5.25 and 21.00 m (4.87 and 4.70 $cmol_c$ dm^{-3}). In 2024, EB in ICL (3.10 $cmol_c$ dm^{-3}) was higher than ILF-EP (at all distances), HP and NF. In 2023, IP presented superior EB than ILF-EP (at 0.00 m) and inferior EB than ICL. In 2024, IP presented lower EB than ICLF at 5.25 and 21.00 m. Mean EB in HP was significantly lower than ICL and ICLF at 5.25 and 21.00 m in both years. Moreover, across both years, except for ILF-EP (at 0.00 and 5.25 m), all managed systems presented significantly higher EB concentrations than NF (0.31 $cmol_c$ dm^{-3}in 2023 and 0.43 $cmol_c$ dm^{-3} in 2024).

The regression analysis revealed distinct spatial patterns for soil chemical indicators across the tree-integrated systems, which varied significantly between the sampling years (Table 3.3). In 2023, soil pH followed a significant quadratic behavior across all three integrated systems (ILF-ST, ILF-EP, and ICLF). These models indicate that pH values initially increased as distance from the tree row increased, reaching estimated maximums at intermediate distances before showing a downward trend toward the 21.00 m position. However, this spatial dynamic shifted to a linear response in 2024 for ILF-ST and ILF-EP. Specifically, pH in the ILF-ST system exhibited a linear decrease as distance from the trees increased, while the ILF-EP system showed a linear increase. No significant regression adjustment for pH was observed for the ICLF system in the second year.

Potential acidity (H+Al) only showed a significant spatial response in 2024 within the ILF-ST system. In this instance, a linear model demonstrated that potential acidity increased as distance from the *Samanea tubulosa* tree row increased. For all other systems and years, H+Al remained non-significant regarding distance from the trees.

The available phosphorus (P) exhibited significant regression adjustments solely for the ICLF system across both evaluated years. In 2023 and 2024, P levels in the ICLF system followed a quadratic model indicating higher nutrient concentrations at intermediate distances from the tree component.

Finally, the status of EB was significantly influenced by distance in the ILF-ST system during the 2024 sampling year. The data adjusted to a linear model, representing a reduction in basic cations as sampling moved further from the trees into the pasture area. For the remaining systems in 2024 and all systems in 2023, the regression for exchangeable bases was non-significant.

Table 3.3 - Regression equations and determination coefficients (R^2) for soil chemical quality indicators as a function of distance from trees in tree-integrated systems and sampling year (2023 and 2024)[†]. H+Al: potential acidity; P: available phosphorus; EB: exchangeable bases; ILF-ST: integrated livestock-forestry with *Samanea tubulosa*; ILF-EP: integrated livestock-forestry with *Eucalyptus pellita*; ICLF: integrated crop-livestock-forestry; ns: non-significant.

Indicator	Area	Equation	$R^{2‡}$
		---------- 2023 ----------	
pH	ILF-ST	$Y = 4.840 + 0.100x - 0.005x^2$	1.000
	ILF-EP	$Y = 4.330 + 0.159x - 0.006x^2$	1.000
	ICLF	$Y = 5.010 + 0.160x - 0.007x^2$	1.000
P (mg dm^{-3})	ILF-ST	ns	--
	ILF-EP	ns	--
	ICLF	$Y = 5.298 + 0.128x - 0.005x^2$	1.000
		---------- 2024 ----------	
pH	ILF-ST	$Y = 5.695 - 0.017x$	0.723
	ILF-EP	$Y = 4.996 + 0.017x$	0.992
	ICLF	ns	--
H+Al ($cmol_c\ dm^{-3}$)	ILF-ST	$Y = 3.060 + 0.067x$	0.985
	ILF-EP	ns	--
	ICLF	ns	--
P (mg dm^{-3})	ILF-ST	ns	--
	ILF-EP	ns	--
	ICLF	$Y = 2.254 + 0.879x - 0.036x^2$	1.000
EB ($cmol_c\ dm^{-3}$)	ILF-ST	$Y = 2.821 - 0.041x$	0.611
	ILF-EP	ns	--
	ICLF	ns	--

[†] For each sampling year, only indicators with a significant effect of distance ($p < 0.05$) in at least one management system are presented. [‡] The R^2 values of 1.000 for quadratic models result from the number of distance levels ($n = 3$) being equal to the number of estimated model parameters.

3.3.2 Soil physical quality indicators

The soil physical indicators were significantly influenced by the management systems and their spatial configuration relative to the tree component (Table 3.4). In 2023, gravimetric moisture (θ_w) at the 0.00 and 5.25 m distances was significantly higher in ILF-ST and ILF-EP systems compared to the ICLF system. When comparing tree-integrated to treeless systems, the moisture levels in ICLF were significantly lower than those found in the IP pasture, while ILF-ST and ILF-EP presented higher moisture levels than ICL, and ILF-ST (at 21.00 m) higher levels than NF. By 2024, a reduction in soil moisture was observed in ILF-ST and ILF-EP, and the ICLF system no longer differed from the forestry-integrated systems across all distances. Moreover, IP presented the highest overall mean θ_w, and no difference was observed among other treeless systems or NF.

Table 3.4 - Soil physical quality indicators (mean ± standard deviation) according to the distance from the trees (in tree-integrated systems), area and sampling year (2023 and 2024). θw: gravimetric moisture; RP: soil resistance to penetration; ILF-ST: integrated livestock-forestry with *Samanea tubulosa*; ILF-EP: integrated livestock-forestry with *Eucalyptus pellita*; ICLF: integrated crop-livestock-forestry; ICL: integrated crop-livestock; IP: *Urochloa brizantha* x *U. ruziziensis* 'Ipyporã' pasture; HP: *U. humidicola* pasture; NF: native forest.

Distance	**Area**	**θ_w**	**RP**
m		dag kg^{-1}	MPa
		---------- 2023 ----------	
0.00	ILF-ST	33.31±5.44 Aα†	3.68±0.43 Aα¶
	ILF-EP	32.06±3.52 Aα†	4.31±0.65 Aα¶
	ICLF	24.30±3.28 Bα‡	4.12±1.07 Aα¶
5.25	ILF-ST	30.35±4.55 Aα	3.94±1.17 Aα¶
	ILF-EP	30.34±1.80 Aα	3.45±0.41 ABα¶
	ICLF	26.67±2.25 Aα‡	2.61±0.57 Bα
21.00	ILF-ST	34.80±3.13 Aα†¶	4.20±1.34 Aα¶
	ILF-EP	32.45±3.28 Aα†	3.00±0.27 Aα¶
	ICLF	24.40±1.56 Bβ‡	3.03±0.45 Aα¶
	ICL	24.30±0.86 bβ	3.96±0.77 aα
	IP	33.09±4.57 aα	3.72±1.50 aα
	HP	29.97±5.82 abα	3.15±0.90 aα
	NF	28.45±3.01 abα	1.28±0.20 bα
		---------- 2024 ----------	
0.00	ILF-ST	27.56±1.67 Aβ‡	3.27±1.83 Bα¶
	ILF-EP	25.82±2.01 Aβ‡	5.22±0.99 Aα†‡§¶
	ICLF	26.46±2.11 Aα‡	3.33±0.65 Bα¶
5.25	ILF-ST	26.23±3.50 Aβ‡	3.57±0.62 Aα¶
	ILF-EP	25.20±3.07 Aβ‡	3.70±0.73 Aα¶
	ICLF	27.46±0.72 Aα‡	2.63±0.65 Aα
21.00	ILF-ST	28.78±2.14 Aβ‡	3.66±1.07 Aα¶
	ILF-EP	27.97±1.09 Aβ‡	3.66±0.76 Aα¶
	ICLF	27.53±1.34 Aα‡	2.74±0.67 Aα¶
	ICL	29.53±2.12 bα	3.06±0.88 aα
	IP	34.32±5.22 aα	3.46±0.25 aα
	HP	29.62±3.37 bα	2.93±0.51 aα
	NF	27.30±2.53 bα	1.19±0.31 bα

Data were analyzed by factorial ANOVA at the 5 % significance level. Tukey's test was used to compare tree-integrated systems within distances (capital letters), treeless systems and NF among themselves (lowercase letters), and years within systems (Greek letters). Systems sharing the same letters do not differ statistically. Treeless systems and NF were compared with tree-integrated systems using Dunnett's test. The symbols †, ‡, §, and ¶ indicate a significant difference relative to ICL, IP, HP and NF, respectively.

Soil resistance to penetration (RP) also exhibited distinct spatial variations. In 2023, at the 5.25 m distance, the ICLF system presented significantly lower RP (2.61 MPa) than the ILF-ST system (3.94 MPa). The native forest (NF) consistently displayed the lowest resistance values (1.19 to 1.28 MPa), differing significantly from nearly all managed systems in both years, except for ICLF at 5.25 m. In 2024, the ILF-EP system at the 0.00 m distance reached the highest recorded RP value (5.22 MPa), which was significantly superior to the ICLF and ILF-ST systems at the same position, as well as significantly higher than all treeless controls (ICL, IP, and HP). For the same system, no significant difference was observed between 2023 and 2024 mean RP values.

The spatial dynamics of soil physical quality, specifically soil RP, were significantly influenced by the distance from the tree row primarily within the ILF-EP system (Table 3.5). In 2023, RP in the ILF-EP system exhibited a linear decrease as the distance from the *E. pellita* trees increased, indicating higher compaction levels in closer proximity to the arboreal component. During the same period, no significant spatial trends for RP were observed in the ILF-ST and ICLF systems.

Table 3.5 - Regression equations and determination coefficients (R^2) for soil physical quality indicators as a function of distance from trees in tree-integrated systems and sampling year (2023 and 2024)[†]. RP: soil resistance to penetration; ILF-ST: integrated livestock-forestry with *Samanea tubulosa*; ILF-EP: integrated livestock-forestry with *Eucalyptus pellita*; ICLF: integrated crop-livestock-forestry; ns: non-significant.

Indicator	Area	Equation	$R^{2‡}$
		---------- 2023 ----------	
RP (MPa)	ILF-ST	ns	--
	ILF-EP	$Y = 4.064 - 0.055x$	0.807
	ICLF	ns	--
		---------- 2024 ----------	
RP (MPa)	ILF-ST	ns	--
	ILF-EP	$Y = 5.222 - 0.363x + 0.014x^2$	1.000
	ICLF	ns	--

[†] For each sampling year, only indicators with a significant effect of distance ($p < 0.05$) in at least one management system are presented. [‡] The R^2 values of 1.000 for quadratic models result from the number of distance levels ($n = 3$) being equal to the number of estimated model parameters.

By the 2024 sampling period, the spatial behavior of RP in the ILF-EP system transitioned to a significant quadratic model. This model reflects a more complex distribution of soil resistance, where the highest estimated values remain near the tree row (0.00 m), followed by a reduction at intermediate distances and a slight increase toward the 21.00 m position. Consistent with the previous year, the ILF-ST and ICLF systems did not show significant regression adjustments for RP as a function of distance in 2024.

3.3.3 Soil biological quality indicators

Soil biological quality was significantly influenced by the management systems and the presence of the arboreal component, showing marked variations between sampling years (Table 3.6). Soil organic matter (OM) content was consistently higher in the ILF-ST system compared to the other integrated systems. In 2023, at 21.00 m, the ILF-ST system reached 4.61 dag kg^{-1} of OM, which was significantly higher than the levels found in ILF-EP (2.86 dag kg^{-1}) and ICLF (2.56 dag kg^{-1}). This pattern of superiority for ILF-ST regarding OM content was maintained in 2024 across all evaluated distances. Furthermore, the ILF-ST system frequently presented OM levels superior to those of the native forest (NF) and treeless pastures.

Regarding enzymatic activities, acid phosphatase (AP) showed important variations among systems. In 2023, the ILF-ST and ILF-EP systems exhibited AP activities that were superior to the ICLF system. By 2024, the difference among tree-integrated systems was restricted to the 21.00 m distance. In addition, HP presented the highest mean AP activity (8.20 µmol p-nitrophenol g^{-1} soil h^{-1}) among treeless systems and NF, and a reduction was observed in IP (7.61 µmol p-nitrophenol g^{-1} soil h^{-1}, 2023, to 2.33 µmol p-nitrophenol g^{-1} soil h^{-1}, in 2024).

Few significant differences in arylsulfatase (AS) and beta-glucosidase (BG) activities among areas were detected. In 2023, AS activity differed only at 21.00 m, with ICLF presenting lower values than ILF-ST and ILF-EP. Moreover, BG activity was highest in ICL and IP. However, in 2024, AS and BG activities underwent drastic reductions across all systems, with BG values ranging between 0.23 and 0.45 µmol p-nitrophenol g^{-1} soil h^{-1} without marked statistical differences among systems. Notably, the native forest (NF) presented lower BG activities than the treeless pastures (ICL and IP) in 2023 but became similar to the managed systems in 2024.

Table 3.6 - Soil biological quality indicators (mean ± standard deviation) according to the distance from the trees (in tree-integrated systems), area and sampling year (2023 and 2024). OM: organic matter; AP: acid phosphatase activity; AS: arylsulfatase activity; BG: betaglucosidase activity; ILF-ST: integrated livestock-forestry with *Samanea tubulosa*; ILF-EP: integrated livestock-forestry with *Eucalyptus pellita*; ICLF: integrated crop-livestock-forestry; ICL: integrated crop-livestock; IP: *Urochloa brizantha* x *U. ruziziensis* 'Ipyporã' pasture; HP: *U. humidicola* pasture; NF: native forest.

Distance	Area	OM	AP	AS	BG
m		dag kg^{-1}	µmol p-nitrophenol g^{-1} soil h^{-1}		
		---------- 2023 ----------			
0.00	ILF-ST	4.10±0.51 Aα¶	7.55±2.35 Aα	3.57±2.07 Aα	0.61±0.26 Aα†‡
	ILF-EP	2.98±0.18 Bα‡§	6.25±1.20 ABα	2.90±2.03 Aα	0.60±0.40 Aα†‡
	ICLF	2.78±0.26 Bα†‡§	4.55±1.41 Bα‡§	2.95±2.18 Aα	0.54±0.27 Aα‡
5.25	ILF-ST	4.41±0.30 Aα†¶	7.42±1.67 Aα	3.61±2.36 Aα	0.80±0.38 Aα
	ILF-EP	3.54±0.24 Bα	6.70±0.90 Aα	2.73±1.81 Aα	0.49±0.21 Aα†‡
	ICLF	3.46±0.40 Bα	4.43±1.17 Bα‡§	2.52±1.17 Aα	0.71±0.26 Aα†‡
21.00	ILF-ST	4.61±0.36 Aα†‡§¶	7.30±1.68 Aα	2.69±2.31 ABα	0.60±0.30 Aα†‡
	ILF-EP	2.86±0.26 Bα‡§	7.78±1.60 Aα	4.45±2.24 Aα	0.76±0.44 Aα‡
	ICLF	2.56±0.41 Bα†‡§	3.83±0.81 Bα‡§	1.02±0.39 Bα	0.84±0.31 Aα
	ICL	3.47±0.47 abα	5.42±1.10 aα	2.08±1.51 aα	1.38±0.69 aα
	IP	3.86±0.43 aα	7.61±0.80 aα	4.18±2.66 aα	1.39±0.43 aα
	HP	3.77±0.42 abα	7.75±1.65 aα	2.57±1.72 aα	0.85±0.17 abα
	NF	3.21±0.50 bα	5.79±1.06 aα	2.01±0.63 aα	0.49±0.14 bα
		---------- 2024 ----------			
0.00	ILF-ST	3.86±0.35 Aα†‡§¶	5.01±2.65 Aβ	0.98±0.29 Aβ	0.43±0.15 Aα
	ILF-EP	3.07±0.29 Bα§	5.57±1.17 Aα	0.93±0.30 Aβ	0.43±0.13 Aα
	ICLF	2.35±0.33 Cβ¶	3.96±1.53 Aα§	0.81±0.19 Aβ	0.37±0.13 Aα
5.25	ILF-ST	3.20±0.26 Aβ‡§	5.96±2.53 Aα‡	0.81±0.24 Aβ	0.29±0.12 Aβ
	ILF-EP	2.75±0.15 ABβ	5.12±1.32 Aα	0.72±0.24 Aβ‡	0.29±0.07 Aα
	ICLF	2.28±0.11 Bβ¶	3.29±0.50 Aα§	0.67±0.12 Aβ‡	0.26±0.04 Aβ
21.00	ILF-ST	4.24±0.73 Aα†‡§¶	5.16±3.58 ABα	1.01±0.37 Aα	0.37±0.13 Aα
	ILF-EP	2.83±0.34 Bα§	6.34±0.74 Aα‡	0.84±0.13 ABβ	0.32±0.09 Aβ
	ICLF	2.32±0.29 Bα¶	2.62±1.03 Bα§	0.55±0.11 Bβ‡	0.26±0.08 Aβ
	ICL	2.66±0.38 abβ	3.44±1.86 bα	0.64±0.31 bβ	0.45±0.15 aβ
	IP	2.45±0.19 bβ	2.33±1.64 bβ	1.15±0.24 aβ	0.39±0.17 abβ
	HP	2.12±0.15 bβ	8.20±3.45 aα	0.69±0.19 bβ	0.23±0.05 bβ
	NF	3.13±0.63 aα	4.49±1.85 bα	0.70±0.18 bβ	0.41±0.15 abα

Data were analyzed by factorial ANOVA at the 5 % significance level. Tukey's test was used to compare tree-integrated systems within distances (capital letters), treeless systems and NF among themselves (lowercase letters), and years within systems (Greek letters). Systems sharing the same letters do not differ statistically. Treeless systems and NF were compared with tree-integrated systems using Dunnett's test. The symbols †, ‡, §, and ¶ indicate a significant difference relative to ICL, IP, HP and NF, respectively.

The spatial distribution OM exhibited significant trends as a function of distance from the trees, although these patterns varied between systems and sampling years (Table 3.7). In 2023, significant quadratic responses were observed for the ILF-EP and ICLF systems. During this initial period, the ILF-ST system did not show a significant spatial adjustment for OM. By 2024, the spatial dynamics shifted, and a significant quadratic effect was detected exclusively in the ILF-ST system. This model for *Samanea tubulosa* indicates higher OM levels near the tree row and at the furthest sampling point, with a slight reduction at intermediate distances. Conversely, the ILF-EP and ICLF systems, which had shown significant spatial variation in the previous year, presented non-significant responses to distance in 2024.

Table 3.7 - Regression equations and determination coefficients (R^2) for soil biological quality indicators as a function of distance from trees in tree-integrated systems and sampling year (2023 and 2024)[†]. OM: organic matter; ILF-ST: integrated livestock-forestry with *Samanea tubulosa*; ILF-EP: integrated livestock-forestry with *Eucalyptus pellita*; ICLF: integrated crop-livestock-forestry; ns: non-significant.

Indicator	Area	Equation	$R^{2‡}$
		---------- 2023 ----------	
OM (dag kg^{-1})	ILF-ST	ns	--
	ILF-EP	$Y = 2.984 + 0.144x - 0.007x^2$	1.000
	ICLF	$Y = 2.780 + 0.176x - 0.009x^2$	1.000
		---------- 2024 ----------	
OM (dag kg^{-1})	ILF-ST	$Y = 3.858 - 0.174x + 0.009x^2$	1.000
	ILF-EP	ns	--
	ICLF	ns	--

[†] For each sampling year, only indicators with a significant effect of distance ($p < 0.05$) in at least one management system are presented. [‡] The R^2 values of 1.000 for quadratic models result from the number of distance levels (n = 3) being equal to the number of estimated model parameters.

3.3.4 Soil quality index

3.3.4.1 Chemical

The soil chemical quality, represented by the $SQI_{chemical}$ and its underlying soil functions, revealed significant differences driven by the integrated management systems and their spatial configurations (Table 3.8). In 2023, the ICLF system consistently exhibited superior chemical quality compared to the forestry-integrated systems (ILF-ST and ILF-EP) across all distances. At the 5.25 m distance, the ICLF system reached an $SQI_{chemical}$ of 0.79, which was significantly higher than the values for ILF-ST 0.55 and ILF-EP 0.48. This superiority was directly linked to the enhanced Acidity regulation and Nutrient availability functions in the ICLF system, which was statistically higher than in the ILF systems and NF across all evaluated positions in both years. In addition, the ICL system presented the second

highest $SQI_{chemical}$ (0.74 in 2023 and 0.75 in 2024), being statistically superior to almost every other system and NF in both years. On the other hand, NF presented the lowest chemical quality (0.30 in 2023 and 0.33 in 2024).

Table 3.8 - Soil chemical quality subindex ($SQI_{chemical}$) and related soil functions (mean ± standard deviation) according to the distance from the trees (in tree-integrated systems), area and sampling year (2023 and 2024). ILF-ST: integrated livestock-forestry with *Samanea tubulosa*; ILF-EP: integrated livestock-forestry with *Eucalyptus pellita*; ICLF: integrated crop-livestock-forestry; ICL: integrated crop-livestock; IP: *Urochloa brizantha* x *U. ruziziensis* 'Ipyporã' pasture; HP: *U. humidicola* pasture; NF: native forest.

Distance (m)	Area	$SQI_{chemical}$	Acidity regulation	Nutrient availability
		---------- 2023 ----------		
0.00	ILF-ST	0.50±0.11 ABβ†¶	0.57±0.05 ABβ¶	0.42±0.16 ABα†¶
	ILF-EP	0.39±0.10 Bβ†¶	0.53±0.04 Bβ†‡¶	0.26±0.16 Bα†‡
	ICLF	0.61±0.02 Aβ¶	0.61±0.04 Aβ¶	0.60±0.03 Aα†¶
5.25	ILF-ST	0.55±0.06 Bα†¶	0.59±0.02 Bβ¶	0.51±0.10 Bα†¶
	ILF-EP	0.48±0.09 Bα†¶	0.60±0.05 Bβ¶	0.35±0.12 Bα†
	ICLF	0.79±0.07 Aα‡§¶	0.66±0.00 Aβ‡§¶	0.91±0.13 Aα‡§¶
21.00	ILF-ST	0.53±0.16 Bα†¶	0.56±0.06 Bβ¶	0.50±0.27 Bα†¶
	ILF-EP	0.50±0.06 Bα†¶	0.61±0.03 ABβ¶	0.40±0.10 Bα†¶
	ICLF	0.77±0.05 Aα‡§¶	0.66±0.05 Aβ§¶	0.88±0.08 Aα‡§¶
	ICL	0.74±0.05 aα	0.62±0.01 aβ	0.86±0.10 aα
	IP	0.57±0.06 bα	0.60±0.03 abβ	0.55±0.09 bα
	HP	0.48±0.03 bα	0.55±0.02 bβ	0.40±0.06 bα
	NF	0.30±0.03 cα	0.44±0.02 cβ	0.15±0.04 cα
		---------- 2024 ----------		
0.00	ILF-ST	0.72±0.05 Aα§¶	0.92±0.01 Aα¶	0.52±0.08 Aα§¶
	ILF-EP	0.52±0.10 Bα†¶	0.73±0.11 Bα†‡¶	0.31±0.08 Bα†
	ICLF	0.72±0.04 Aα§¶	0.92±0.01 Aα¶	0.52±0.07 Aα§¶
5.25	ILF-ST	0.61±0.12 Bα¶	0.86±0.10 Bα¶	0.36±0.14 Bα†¶
	ILF-EP	0.51±0.09 Bα†¶	0.76±0.10 Bα†‡¶	0.25±0.08 Bα†
	ICLF	0.85±0.08 Aα‡§¶	0.99±0.01 Aα†‡§¶	0.71±0.16 Aβ‡§¶
21.00	ILF-ST	0.56±0.16 Bα†¶	0.79±0.15 Bα¶	0.33±0.16 Bβ†¶
	ILF-EP	0.53±0.06 Bα†¶	0.77±0.07 Bα†¶	0.29±0.09 Bα†
	ICLF	0.83±0.07 Aα‡§¶	0.97±0.02 Aα§¶	0.69±0.12 Aβ‡§¶
	ICL	0.75±0.05 aα	0.93±0.01 aα	0.57±0.09 aβ
	IP	0.64±0.06 abα	0.91±0.06 abα	0.38±0.06 abβ
	HP	0.57±0.11 bα	0.81±0.12 bα	0.33±0.11 bα
	NF	0.33±0.00 cα	0.54±0.01 cα	0.13±0.02 cα

Data were analyzed by factorial ANOVA at the 5 % significance level. Tukey's test was used to compare tree-integrated systems within distances (capital letters), treeless systems and NF among themselves (lowercase letters), and years within systems (Greek letters). Systems sharing the same letters do not differ statistically. Treeless systems and NF were compared with tree-integrated systems using Dunnett's test. The symbols †, ‡, §, and ¶ indicate a significant difference relative to ICL, IP, HP and NF, respectively.

The Acidity regulation and Nutrient availability functions also varied among systems and sampling years, following a similar pattern than $SQI_{chemical}$ across areas. However, in 2024, a generalized improvement in acidity regulation was observed across all integrated systems compared to 2023. Noticeably, the overall scores for nutrient availability across managed systems is low (0.25 to 0.60), with exception of ICLF (0.52 to 0.91) and ICL (0.57 in 2024 and 0.86 in 2023).

The spatial distribution of soil chemical quality indices and their underlying functions were significantly influenced by the distance from the tree rows, with distinct patterns emerging across management systems and sampling years (Table 3.9). In 2023, the ICLF system exhibited a significant quadratic response for both the overall $SQI_{chemical}$ and the Nutrient availability function. During the same period, the ILF-EP system showed a significant quadratic trend for Acidity regulation, while no significant spatial variation was detected for the ILF-ST system in any chemical parameter in the first year. All quadratic trends indicate higher values at an intermediate distance from the trees.

By 2024, the spatial dynamics evolved significantly. The ICLF system maintained its quadratic behavior for both the $SQI_{chemical}$ and Nutrient availability. Notably, the ILF-ST system transitioned to a significant linear response during the second year, where both Acidity regulation and Nutrient availability decreased linearly as the distance from the *S. tubulosa* trees increased. This indicates a localized improvement in chemical fertility closer to the legume tree over time. In contrast, the ILF-EP system showed no significant spatial effects for $SQI_{chemical}$ and its related functions in 2024.

Table 3.9 - Regression equations and determination coefficients (R^2) for soil chemical quality subindex ($SQI_{chemical}$) and related soil functions as a function of distance from trees in tree-integrated systems and sampling year (2023 and 2024)[†]. ILF-ST: integrated livestock-forestry with *Samanea tubulosa*; ILF-EP: integrated livestock-forestry with *Eucalyptus pellita*; ICLF: integrated crop-livestock-forestry; ns: non-significant.

Variable	Area	Equation	$R^{2‡}$
		---------- 2023 ----------	
$SQI_{chemical}$	ILF-ST	ns	--
	ILF-EP	ns	--
	ICLF	$Y = 0.609 + 0.042x - 0.002x^2$	1.000
Acidity regulation	ILF-ST	ns	--
	ILF-EP	$Y = 0.531 + 0.016x - 0.001x^2$	1.000
	ICLF		
Nutrient availability	ILF-ST	ns	--
	ILF-EP	ns	--
	ICLF	$Y = 0.604 + 0.073x - 0.003x^2$	1.000

		2024	
$SQI_{chemical}$	ILF-ST	ns	--
	ILF-EP	ns	--
	ICLF	$Y = 0.718 + 0.031x - 0.001x^2$	1.000
Acidity regulation	ILF-ST	$Y = 0.904 - 0.006x$	0.921
	ILF-EP	ns	--
	ICLF	ns	--
Nutrient availability	ILF-ST	$Y = 0.470 - 0.008x$	0.643
	ILF-EP	ns	--
	ICLF	$Y = 0.521 + 0.045x - 0.002x^2$	1.000

† For each sampling year, only variables with a significant effect of distance ($p < 0.05$) in at least one management system are presented. ‡ The R^2 values of 1.000 for quadratic models result from the number of distance levels (n = 3) being equal to the number of estimated model parameters.

3.3.4.2 Physical

The soil physical quality, assessed through the $SQI_{physical}$ and the functions of Water availability and Support root growth, exhibited distinct spatial and temporal variations among the integrated management systems (Table 3.10). In 2023, the forestry-integrated systems generally outperformed the ICLF system in physical quality near the tree row. At the 0.00 m distance, the ILF-ST (0.54) and ILF-EP (0.50) systems presented significantly higher $SQI_{physical}$ values than the ICLF system (0.42). This superiority was largely driven by the Water availability function, which was significantly higher in ILF-ST (0.79) and ILF-EP (0.76) compared to ICLF (0.58) at the same position.

Table 3.10 - Soil physical quality subindex ($SQI_{physical}$) and related soil functions (mean ± standard deviation) according to the distance from the trees (in tree-integrated systems), area and sampling year (2023 and 2024). ILF-ST: integrated livestock-forestry with *Samanea tubulosa*; ILF-EP: integrated livestock-forestry with *Eucalyptus pellita*; ICLF: integrated crop-livestock-forestry; ICL: integrated crop-livestock; IP: *Urochloa brizantha* x *U. ruziziensis* 'Ipyporã' pasture; HP: *U. humidicola* pasture; NF: native forest.

Distance (m)	**Area**	**$SQI_{physical}$**	**Water availability**	**Support root growth**
		2023		
0.00	ILF-ST	0.54±0.07 Aα¶	0.79±0.13 Aα†	0.28±0.03 Aα¶
	ILF-EP	0.50±0.04 ABα¶	0.76±0.08 Aα†	0.24±0.04 Aα¶
	ICLF	0.42±0.06 Bα‡¶	0.58±0.08 Bα‡	0.26±0.07 Aα¶
5.25	ILF-ST	0.50±0.05 Aα¶	0.72±0.11 Aα	0.28±0.08 Bα¶
	ILF-EP	0.51±0.03 Aα¶	0.72±0.04 Aα	0.30±0.04 ABα¶
	ICLF	0.52±0.05 Aα¶	0.63±0.05 Aα‡	0.40±0.07 Aα¶
21.00	ILF-ST	0.54±0.04 Aα†¶	0.83±0.07 Aα†¶	0.26±0.07 Aα¶
	ILF-EP	0.56±0.05 Aα†¶	0.77±0.08 Aα†	0.34±0.03 Aα¶
	ICLF	0.46±0.02 Aα¶	0.58±0.04 Bβ‡	0.34±0.05 Aα¶

	ICL	0.42±0.02 cβ	0.58±0.02 bβ	0.27±0.05 bα
	IP	0.56±0.13 bα	0.79±0.11 aα	0.34±0.20 bα
	HP	0.53±0.12 bcα	0.71±0.14 abα	0.35±0.11 bα
	NF	0.74±0.07 aα	0.68±0.07 abα	0.81±0.13 aα
		---------- 2024 ----------		
0.00	ILF-ST	0.51±0.08 Aα¶	0.66±0.04 Aβ‡	0.37±0.18 Aα¶
	ILF-EP	0.40±0.03 Bβ†‡§¶	0.61±0.05 Aβ‡	0.19±0.03 Bα¶
	ICLF	0.46±0.05 ABα¶	0.63±0.05 Aα‡	0.29±0.05 ABα¶
5.25	ILF-ST	0.45±0.06 Aα¶	0.62±0.08 Aβ‡	0.27±0.05 Aα¶
	ILF-EP	0.43±0.03 Aβ‡¶	0.60±0.07 Aβ‡	0.26±0.05 Aα¶
	ICLF	0.52±0.05 Aα¶	0.65±0.02 Aα‡	0.38±0.09 Aα¶
21.00	ILF-ST	0.48±0.05 Aα¶	0.69±0.05 Aβ‡	0.28±0.08 Aα¶
	ILF-EP	0.47±0.04 Aβ¶	0.67±0.03 Aβ‡	0.27±0.05 Aα¶
	ICLF	0.51±0.05 Aα¶	0.66±0.03 Aα‡	0.36±0.08 Aα¶
	ICL	0.52±0.09 bα	0.70±0.05 bα	0.34±0.13 bα
	IP	0.55±0.07 bα	0.82±0.12 aα	0.28±0.02 bα
	HP	0.52±0.06 bα	0.71±0.08 bα	0.33±0.06 bα
	NF	0.74±0.11 aα	0.65±0.06 bα	0.83±0.18 aα

Data were analyzed by factorial ANOVA at the 5 % significance level. Tukey's test was used to compare tree-integrated systems within distances (capital letters), treeless systems and NF among themselves (lowercase letters), and years within systems (Greek letters). Systems sharing the same letters do not differ statistically. Treeless systems and NF were compared with tree-integrated systems using Dunnett's test. The symbols †, ‡, §, and ¶ indicate a significant difference relative to ICL, IP, HP and NF, respectively.

By 2024, a decline in physical quality was observed for the ILF-EP system, becoming significantly lower than the ILF-ST at 0.00 m. This reduction in ILF-EP is reflect of the Support root growth function, which reached its lowest value (0.19) in the tree row, being statistically inferior to the other integrated systems. This decline in 2024 suggests a cumulative impact on soil structure, likely associated with the increased soil resistance to penetration observed near eucalyptus trees in the second year of sampling.

When compared to the native forest (NF) baseline, the integrated systems showed mixed results. In both years, NF consistently maintained the highest scores for Support root growth (0.81 in 2023 and 0.83 in 2024) and the overall $SQI_{physical}$ (0.74 in both years), differing significantly from all managed systems. Regarding the Water availability function, few differences were observed across systems. In 2023, ICL presented the overall lowest mean (0.58), whereas IP presented the highest mean in 2024 (0.82), being statistically superior to all other areas.

The soil physical quality was significantly affected by the distance from trees only in the crop-livestock-forestry system during the first year of study (Table 3.11). In 2023, the ICLF system exhibited significant quadratic responses for both the overall $SQI_{physical}$ and the Support root growth function. These models indicate that physical quality peaked at intermediate distances from the tree rows within the ICLF arrangement.

Table 3.11 - Regression equations and determination coefficients (R^2) for soil physical quality subindex ($SQI_{physical}$) and related soil functions as a function of distance from trees in tree-integrated systems†. ILF-ST: integrated livestock-forestry with *Samanea tubulosa*; ILF-EP: integrated livestock-forestry with *Eucalyptus pellita*; ICLF: integrated crop-livestock-forestry; ns: non-significant.

Variable	Area	Equation	$R^{2‡}$
		---------- 2023 ----------	
$SQI_{physical}$	ILF-ST	ns	--
	ILF-EP	ns	--
	ICLF	$Y = 0.420 + 0.024x - 0.001x^2$	1.000
Support root growth	ILF-ST	ns	--
	ILF-EP	ns	--
	ICLF	$Y = 0.262 + 0.035x - 0.001x^2$	1.000

† Only variables with a significant effect of distance ($p < 0.05$) in at least one management system are presented. No significant effect of distance was observed in 2024. ‡ The R^2 values of 1.000 for quadratic models result from the number of distance levels (n = 3) being equal to the number of estimated model parameters.

3.3.4.3 Biological

The soil biological quality was significantly influenced by the management systems and their respective tree components (Table 3.12). Across both sampling years, the ILF-ST system consistently demonstrated superior biological quality compared to the other integrated arrangements. In 2023, at the 0.00 m distance, the ILF-ST system reached an $SQI_{biological}$ of 0.73, which was significantly higher than the values for ILF-EP (0.58) and ICLF (0.52). This trend was largely driven by the Sustain biological activity function, where the ILF-ST system achieved scores of 0.96 to 1.00 across all distances, significantly outperforming the ICLF system at every position.

Table 3.12 - Soil biological quality subindex ($SQI_{physical}$) and related soil functions (mean ± standard deviation) according to the distance from the trees (in tree-integrated systems), area and sampling year (2023 and 2024). ILF-ST: integrated livestock-forestry with *Samanea tubulosa*; ILF-EP: integrated livestock-forestry with *Eucalyptus pellita*; ICLF: integrated crop-livestock-forestry; ICL: integrated crop-livestock; IP: *Urochloa brizantha* x *U. ruziziensis* 'Ipyporã' pasture; HP: *U. humidicola* pasture; NF: native forest.

Distance (m)	Area	$SQI_{biological}$	Sustain biological activity	Nutrient cycling
		---------- 2023 ----------		
0.00	ILF-ST	0.73±0.10 Aα¶	0.96±0.06 Aα¶	0.49±0.17 Aα
	ILF-EP	0.58±0.07 Bα‡	0.74±0.05 Bα‡§	0.42±0.11 Aα‡
	ICLF	0.52±0.06 Bα†‡§	0.69±0.06 Bα†‡§	0.35±0.11 Aα‡
5.25	ILF-ST	0.76±0.08 Aα¶	1.00±0.00 Aα¶	0.51±0.16 Aα
	ILF-EP	0.65±0.03 ABα	0.88±0.06 ABα	0.41±0.05 Aα‡
	ICLF	0.61±0.08 Bα‡§	0.86±0.10 Bα	0.36±0.08 Aα‡
21.00	ILF-ST	0.72±0.06 Aα¶	1.00±0.00 Aα¶	0.44±0.12 ABα
	ILF-EP	0.63±0.10 Aα‡	0.71±0.06 Bα†‡§	0.55±0.16 Aα
	ICLF	0.47±0.07 Bα†‡§	0.64±0.10 Bα†‡§¶	0.30±0.05 Bα‡
	ICL	0.67±0.11 abα	0.86±0.12 abα	0.48±0.14 abα
	IP	0.79±0.10 aα	0.94±0.08 aα	0.64±0.12 aα
	HP	0.70±0.09 abα	0.92±0.08 abα	0.49±0.14 abα
	NF	0.57±0.08 bα	0.80±0.12 bα	0.35±0.05 bα
		---------- 2024 ----------		
0.00	ILF-ST	0.75±0.11 Aα†‡§	0.94±0.06 Aα†‡§¶	0.55±0.17 Aα
	ILF-EP	0.66±0.07 Aα§	0.77±0.07 Bα‡§	0.55±0.13 Aα
	ICLF	0.52±0.09 Bα	0.59±0.08 Cβ¶	0.46±0.11 Aα
5.25	ILF-ST	0.63±0.10 Aβ	0.80±0.07 Aβ†‡§	0.46±0.15 Aα
	ILF-EP	0.56±0.03 ABα	0.69±0.04 Aβ§	0.42±0.07 Aα
	ICLF	0.46±0.03 Bβ¶	0.57±0.03 Bβ¶	0.36±0.05 Aα
21.00	ILF-ST	0.74±0.11 Aα†‡§	0.96±0.06 Aα†‡§¶	0.53±0.22 Aα
	ILF-EP	0.60±0.07 Bα	0.71±0.08 Bα§	0.49±0.07 ABα
	ICLF	0.45±0.04 Cα¶	0.58±0.07 Cα¶	0.32±0.04 Bα
	ICL	0.55±0.11 aβ	0.66±0.10 abβ	0.45±0.18 aα
	IP	0.56±0.07 aβ	0.61±0.05 bcβ	0.50±0.12 aα
	HP	0.49±0.07 aβ	0.53±0.04 cβ	0.46±0.14 aα
	NF	0.63±0.13 aα	0.78±0.16 aα	0.47±0.11 aα

Data were analyzed by factorial ANOVA at the 5 % significance level. Tukey's test was used to compare tree-integrated systems within distances (capital letters), treeless systems and NF among themselves (lowercase letters), and years within systems (Greek letters). Systems sharing the same letters do not differ statistically. Treeless systems and NF were compared with tree-integrated systems using Dunnett's test. The symbols †, ‡, §, and ¶ indicate a significant difference relative to ICL, IP, HP and NF, respectively.

By 2024, the ILF-ST system maintained its higher biological status, particularly at the 0.00 m and 21.00 m distances, where its $SQI_{biological}$ (0.75 and 0.74, respectively) remained significantly superior to the ICLF system (0.52 and 0.45). Notably, almost all managed systems showed a significant temporal decline in their biological quality, specifically in their ability to

Sustain biological activity, from 2023 to 2024. The Nutrient cycling function showed fewer statistical differences between the systems, with IP presenting the highest mean in 2023, while, in 2024, a significant difference was observed only between ILF-ST (0.53) and ICLF (0.32) at 21.00 m. Compared to NF, in 2023, most managed systems, especially ILF-ST, showed comparable or higher biological quality indices. However, in 2024, fewer differences from NF were observed.

Soil biological quality was significantly influenced by the distance from tree rows, revealing distinct patterns that evolved between sampling years (Table 3.13). In 2023, the ICLF system exhibited significant quadratic responses for both the overall $SQI_{biological}$ and the Sustain biological activity function, with higher values at an intermediate distance from the tree row. During the same period, the ILF-EP system also showed a quadratic response for Sustain biological activity and a significant linear increase in Nutrient cycling as distance from the eucalyptus trees increased. No significant spatial trends were observed for the ILF-ST system in 2023.

Table 3.13 - Regression equations and determination coefficients (R^2) for soil biological quality subindex ($SQI_{biological}$) and related soil functions as a function of distance from trees in tree-integrated systems and sampling year (2023 and 2024)[†]. ILF-ST: integrated livestock-forestry with *Samanea tubulosa*; ILF-EP: integrated livestock-forestry with *Eucalyptus pellita*; ICLF: integrated crop-livestock-forestry; ns: non-significant.

Variable	Area	Equation	R^2[‡]
		---------- 2023 ----------	
$SQI_{biological}$	ILF-ST	ns	--
	ILF-EP	ns	--
	ICLF	$Y = 0.523 + 0.023x - 0.001x^2$	1.000
Sustain biological activity	ILF-ST	ns	--
	ILF-EP	$Y = 0.744 + 0.036x - 0.002x^2$	1.000
	ICLF	$Y = 0.693 + 0.044x - 0.002x^2$	1.000
Nutrient cycling	ILF-ST	ns	--
	ILF-EP	$Y = 0.396 + 0.007x$	0.914
	ICLF	ns	--
		---------- 2024 ----------	
$SQI_{biological}$	ILF-ST	$Y = 0.745 - 0.029x + 0.001x^2$	1.000
	ILF-EP	ns	--
	ICLF	ns	--
Sustain biological activity	ILF-ST	$Y = 0.942 - 0.037x + 0.002x^2$	1.000
	ILF-EP	ns	--
	ICLF	ns	--

[†] For each sampling year, only variables with a significant effect of distance ($p < 0.05$) in at least one management system are presented. [‡] The R^2 values of 1.000 for quadratic models result from the number of distance levels ($n = 3$) being equal to the number of estimated model parameters.

By 2024, the spatial dynamics shifted predominantly toward ILF-ST. The ILF-ST system transitioned to significant quadratic models for both the $SQI_{biological}$ and the Sustain biological activity function. These models indicate higher biological quality near the *S. tubulosa* rows and at the furthest sampling points, with a slight reduction at intermediate distances. In contrast, the ICLF and ILF-EP systems, which had shown significant spatial variation in the previous year, presented non-significant responses to distance in 2024.

3.3.4.4 Overall SQI

The overall soil quality index (SQI), which synthesizes the chemical, physical, and biological status of the soil, was significantly affected by the management systems (Table 3.14). In 2023, at the 0.00 m distance, the ILF-ST system presented a higher SQI (0.59) compared to the ILF-EP system (0.49), while the ICLF system maintained an intermediate value (0.52). At the 5.25 m distance, the ICLF system achieved the highest recorded score (0.64), being significantly superior to the ILF-EP system (0.54). No significant differences between the integrated systems were found at the 21.00 m distance during the first year.

Table 3.14 - Mean ± standard deviation of soil quality index (SQI) according to the distance from the trees (in tree-integrated systems), area and sampling year (2023 and 2024). ILF-ST: integrated livestock-forestry with *Samanea tubulosa*; ILF-EP: integrated livestock-forestry with *Eucalyptus pellita*; ICLF: integrated crop-livestock-forestry; ICL: integrated crop-livestock; IP: *Urochloa brizantha* x *U. ruziziensis* 'Ipyporã' pasture; HP: *U. humidicola* pasture; NF: native forest.

Distance (m)	**Area**	**SQI**	
		2023	2024
0.00	ILF-ST	0.59±0.08 Aα	0.66±0.07 Aα§
	ILF-EP	0.49±0.04 Bα†‡	0.53±0.05 Bα
	ICLF	0.52±0.03 ABα†‡	0.57±0.04 Bα
5.25	ILF-ST	0.60±0.06 ABα	0.56±0.08 ABα
	ILF-EP	0.54±0.04 Bα‡	0.50±0.04 Bα†
	ICLF	0.64±0.05 Aα¶	0.61±0.04 Aα
21.00	ILF-ST	0.60±0.04 Aα	0.59±0.07 Aα
	ILF-EP	0.56±0.06 Aα	0.53±0.02 Aα
	ICLF	0.57±0.03 Aα	0.59±0.04 Aα
	ICL	0.61±0.04 abα	0.61±0.07 aα
	IP	0.64±0.07 aα	0.58±0.06 aα
	HP	0.57±0.07 abα	0.53±0.05 aα
	NF	0.54±0.04 bα	0.57±0.07 aα

Data were analyzed by factorial ANOVA at the 5 % significance level. Tukey's test was used to compare tree-integrated systems within distances (capital letters), treeless systems and NF among themselves (lowercase letters), and years within systems (Greek letters). Systems sharing the same letters do not differ statistically. Treeless systems and NF were compared with tree-integrated systems using Dunnett's test. The symbols †, ‡, §, and ¶ indicate a significant difference relative to ICL, IP, HP and NF, respectively.

By 2024, the ILF-ST system maintained its superiority at the tree row (0.00 m) with an SQI of 0.66, which was significantly higher than both the ILF-EP (0.53) and ICLF (0.57) systems. At intermediate distances (5.25 m), the ICLF system remained the most effective (0.61), differing statistically from ILF-EP (0.50). The SQI remained relatively stable between years, with no significant difference between 2023 and 2024 within systems.

In comparison to the treeless controls and the native forest (NF), the integrated systems generally matched or exceeded the SQI values of NF, which presented values of 0.54 in 2023 and 0.57 in 2024. Interestingly, the ICLF system at 5.25 m in 2023 and IP reached significantly higher SQIs than NF. Among the treeless pastures, in 2023, the ICL and IP systems performed better than tree-integrated systems at some distances. However, in 2024, few statistically significant differences among areas were observed, with HP presenting lower SQI than ILF-ST at 0.00 m, and ICL presenting higher SQI than ILF-EP at 5.25 m.

The spatial behavior of SQI showed significant variations depending on the management system and the sampling period (Table 3.15). In 2023, a significant quadratic response was observed exclusively in the ICLF system. The model indicates that the highest overall soil quality during the first year of sampling occurred at intermediate distances within the crop-livestock-forestry arrangement. In contrast, the ILF systems did not exhibit significant spatial adjustments for the SQI in 2023.

Table 3.15 - Regression equations and determination coefficients (R^2) for soil quality index (SQI) as a function of distance from trees in tree-integrated systems and sampling year (2023 and 2024)[†]. ILF-ST: integrated livestock-forestry with *Samanea tubulosa*; ILF-EP: integrated livestock-forestry with *Eucalyptus pellita*; ICLF: integrated crop-livestock-forestry; ns: non-significant.

Variable	Area	Equation	$R^{2\dagger}$
SQI_{2023}	ILF-ST	ns	--
	ILF-EP	ns	--
	ICLF	$Y = 0.517 + 0.030x - 0.001x^2$	1.000
SQI_{2024}	ILF-ST	$Y = 0.659 - 0.024x + 0.001x^2$	1.000
	ILF-EP	ns	--
	ICLF	ns	--

[†] The R^2 values of 1.000 for quadratic models result from the number of distance levels (n = 3) being equal to the number of estimated model parameters.

By 2024, the spatial pattern shifted from ICLF to ILF-ST, following a quadratic model, where the highest SQI values are concentrated near the tree row (0.00 m) and at the furthest point (21.00 m), with a slight reduction at the intermediate distance. No significant spatial effects were recorded for the ILF-EP and ICLF systems in the second year of evaluation.

3.4 Discussion

3.4.1 Soil chemical quality indicators

The soil pH, H+Al, P and EB results reveal complex interactions between management systems, tree proximity, and temporal dynamics. The native forest (NF) consistently exhibited the most acidic conditions. Naturally, Amazon soils are highly weathered and characterized by high acidity, largely due to the leaching of base cations such as calcium, magnesium, and potassium, which are replaced by protons and aluminum ions, a process exacerbated by the region's substantial rainfall (Patiño et al. 2024; Mantovanelli et al. 2016). The acidic conditions are further compounded by the accumulation of organic acids from decomposing plant material under undisturbed conditions (Ritchie and Dolling 1985).

Among integrated systems, ICL and ICLF demonstrated superior pH management, particularly at intermediate (5.25 m) and far distances (21.00 m) from tree rows. This represents a significant improvement over both ILF systems and approaches optimal ranges for tropical pasture productivity (pH 5.5-6.5). Since the last lime application occurred more than five years before sampling for all managed systems, the elevated pH in ICLF can be attributed to enhanced base cation cycling through diverse plant residues and improved nutrient management from integrated crop-livestock activities (Martins et al. 2014, 2016).

The spatial gradient in pH observed in tree-integrated systems (ILF-ST, ILF-EP, ICLF) demonstrates the localized influence of tree rows. Lower pH and EB values at 0.00 m distance, particularly in ILF-EP, suggest that *E. pellita* may contribute to soil acidification through uptake and immobilization of base cations in woody biomass, production of acidic root exudates, decomposition of acidic litter, and enhanced nitrification in the rhizosphere (Soumare et al. 2015; Regasa et al. 2024; Korchagin et al. 2019).

In contrast, *S. tubulosa* (ILF-ST) showed less acidification and base depletion at 0.00 m, possibly reflecting its lower demand for nutrients and more favorable litter chemistry (Rwibasira et al. 2021; Chaer et al. 2011). Lower acidity in ILF-ST compared to ILF-EP was also observed by Cipriani et al. (2025) in 2022. The temporal improvement in pH and H+Al in

virtually all systems and NF from 2023 to 2024 requires further investigation. Since no relevant intervention was made, an unmeasured natural alkalinization process (e.g., decreased acid rain, interannual temperature and rainfall oscillation) could be the cause (Yaulilahua-Huacho et al. 2024; Shen et al. 2021).

Phosphorus availability emerged as a critical differentiating factor among systems, with ICLF and ICL demonstrating markedly superior P status compared to all other systems and NF. This advantage became even more pronounced at 5.25 m and 21.00 m distances, where ICLF reached 5.88-7.20 mg dm^{-3}, representing 3-8 times the P levels in other systems. The exceptional P availability in ICLF reflects the residual P accumulation from repeated crop-livestock rotations, as well as higher-quality (low C/N ratio) residues (Assis et al. 2022).

The extremely low P availability in native forest (0.91-1.08 mg dm^{-3}) represents the highly weathered Oxisols dominant in the Amazon, which present inherently low P reserves, strong P fixation by iron and aluminum oxides at low pH, tight biological cycling where nearly all available P is immobilized in biomass with minimal soil reserves, and lack of anthropogenic inputs that characterize managed systems (Cunha et al. 2022).

The low P in ILF systems (1.54-2.90 mg dm^{-3} range) despite tree integration indicates that forestry components alone do not significantly enhance P availability without fertilization (Moreira et al. 2018). Trees may compete with pasture for limited P, and P immobilization in woody biomass reduces soil P pools (George et al. 1996). The slight spatial variation in ICLF, with marginally higher P at intermediate distances, suggests optimal zones where tree root competition is reduced but tree benefits (organic matter, microclimate) are maintained. Ipyporã and *U. humidicola* pastures (IP and HP) showed the lowest P among pasture systems, also indicating P depletion under moderate grazing without replenishment (Gatiboni et al. 2025; Coad et al. 2014).

3.4.2 Soil physical quality indicators

During the first year of evaluation (2023), the ICLF and ICL systems showed the poorest overall hydric performance which may be associated with a lower water-holding capacity of the remaining mulch in those systems (Fér et al. 2022; Zhang et al. 2021). However, by 2024, the most managed systems reached an equilibrium with NF, revealing interannual variation in soil moisture among systems. Similarly, to what was observed by Feitosa et al. (2019) in the same ICLF, the trees did not influence soil moisture in the ICLF or ILF systems.

A consistent result across both years was the performance of the Ipyporã pasture (IP), which maintained the highest levels of gravimetric moisture. In 2023, it stood out positively, and by 2024, it became the only treatment statistically superior to all others. This behavior indicates that the Ipyporã cultivar possesses a better soil cover capacity or a root architecture that favors water infiltration and maintenance in relation to Marandu and *U. humidicola* grasses (Policarpo et al. 2023; Merloti et al. 2023).

The spatial variation in soil resistance to penetration (RP) observed exclusively in the ILF-EP system suggests that the tree component's architecture and the associated management play a decisive role in soil physical quality. The linear reduction of RP with distance in 2023, followed by a quadratic pattern in 2024, indicates a higher concentration of soil compaction near the *E. pellita* rows. This localized increase in RP (reaching 5.22 MPa at 0.00 m in 2024) likely results from the behavior of grazing animals. In integrated systems, trees often serve as shade havens, leading to a higher frequency of animal permanence and, consequently, increased trampling intensity in the areas closest to the tree rows (Sartor et al. 2020; Assis et al. 2015).

Interestingly, the ILF-ST and ICLF systems did not show a significant spatial trend for RP, maintaining more stable physical conditions across the distances. In the case of ILF-ST, this may be attributed to the canopy architecture of *S. tubulosa*, which provides a broader and more diffuse shade compared to the vertical shade of eucalyptus, leading to a more even distribution of animals (Silva et al. 2025; Andrade et al. 2012; Mattos et al. 2020). Similarly, although the ICLF also utilizes eucalyptus, its lack of spatial variation in RP likely stems from its higher tree density compared to the ILF-EP system (136 vs. 13 trees ha^{-1}). This higher density promotes a more balanced distribution of animals throughout the area, preventing the concentrated trampling typically observed in systems with more isolated or sparse shade (Feitosa et al. 2019; Souza et al. 2020).

A general reduction in RP values was observed in the present study when compared with those reported by Cipriani et al. (2025), who conducted research in the same ILF areas in 2022. This discrepancy is primarily attributed to the sampling period: the dry season in Cipriani et al. (2025) versus the rainy season in the current study. Furthermore, the previous study reported higher RP in ILF-ST (10.37 MPa) than in ILF-EP (6.96 MPa) at 5.25 m from the trees, highlighting the marked seasonal and temporal sensitivity of RP as a soil quality indicator.

3.4.3 Soil biological quality indicators

The superiority of the ILF-ST system in soil organic matter (OM) content must be evaluated considering the distinct animal behavior observed in these areas. While soil physical data indicate that cattle concentrate near the tree rows in Eucalyptus-based systems (ILF-EP and ICLF), the OM levels in these systems remained significantly lower than ILF-ST at the same distance. Furthermore, while Cipriani et al. (2025) found virtually no significant differences in OM between ILF-ST, ILF-EP, and NF in 2022, the current findings suggest a clear temporal divergence in organic matter accumulation across these systems.

Moreover, this suggests that high density of animals in the *Eucalyptus* lines is leading to increased soil compaction and overgrazing near the trees, which limits the development of the pasture's root system and, consequently, reduces the input of organic carbon into the soil (Sarto et al. 2020b; Hamza and Anderson 2005; Pegoraro et al. 2011). In contrast, the more scattered distribution of cattle in the ILF-ST system appears to favor a more balanced nutrient cycling. By spreading their presence across the plot, the animals promote a more uniform distribution of excreta and avoid localized degradation, allowing the shading and nitrogen-fixing benefits of *S. tubulosa* to effectively translate into higher OM accumulation across the evaluated distances (Santos et al. 2024; Carpinelli et al. 2020).

The significant quadratic response for OM in the ILF-ST system in 2024 reinforces this hypothesis. The peak at 21.00 m (4.24 dag kg^{-1}) likely reflects the success of the pasture component in an area with lower animal pressure and optimal light availability, while the high values near the trees (3.86 dag kg^{-1} at 0.00 m) benefit from the high-quality legume litter without the excessive trampling observed in the *Eucalyptus* systems. Therefore, the higher biological quality of the soil in the ILF-ST system is not just a result of the tree species, but of how the tree architecture and shade quality promote a grazing behavior that preserves soil physical and chemical integrity.

The soil chemical profile provides a critical context for the biological patterns observed, particularly regarding enzymatic regulation and interannual variations. A clear example is the negative feedback mechanism observed for acid phosphatase (AP) activity. In 2023, the ICLF system exhibited significantly lower AP activity compared to ILF-ST and ILF-EP. This is directly explained by the phosphorus (P) levels: the ICLF system had a substantially higher P content (up to 13.80 mg dm^{-3} at 5.25 m) compared to the very low levels (1.88 to 1.90 mg dm^{-3}) found in the other systems. Since microorganisms and plants secrete acid phosphatase primarily under P-limitation to mineralize organic P, the high availability of inorganic P in the ICLF

system, likely due to residual fertilization from the crop component, suppressed the need for high AP secretion (Pereira et al. 2023; Campdelacreu Rocabruna et al. 2024).

The interannual dynamics of enzymatic activities between 2023 and 2024 were also likely influenced by the significant increase in soil pH across all systems. In 2023, the systems were more acidic (pH ranging from 4.33 to 5.66), whereas in 2024, pH levels rose significantly (reaching up to 6.03 in ICLF). This shift toward neutrality may explain some of the enzymatic variations. As its name suggests, AP enzyme has an optimal activity level in acidic conditions (Campdelacreu Rocabruna et al. 2024). The increase in pH in 2024 may have contributed to the observed reduction in its activity in several systems, such as the decline seen in IP.

The activities of arylsulfatase (AS) and beta-glucosidase (BG) revealed a soil biological environment that, in 2023, was more influenced by the herbaceous component and management intensity than by the presence of trees. For AS, the lack of significant differences among most areas suggests a relative uniformity in sulfur cycling during the first year of sampling, with a specific exception at the 21.00 m distance where ILF-EP outperformed ICLF. Moreover, the treeless controls, ICL and IP, exhibited higher BG activity compared to the native forest (NF).

Furthermore, these pastures frequently surpassed the tree-integrated systems; for instance, IP showed higher BG activity than all three integrated systems at 0.00 m. This suggests that the high root turnover and constant biomass input from the *Urochloa* grasses in open pastures provide a more accessible carbon source for the microbial community than the more complex litter found in the forest or the potentially shaded understory of the integrated systems (Lai et al. 2014; Pereira et al. 2023; Sarto et al. 2020; Santos et al. 2022). It can also be attributed to differences in grass variety (Marandu in ILF-ST and ILF-EP vs. Ipyporã in ICL and ICLF) (Ventura et al. 2021; Campdelacreu Rocabruna et al. 2024; Janusckiewicz et al. 2019). Interestingly, the lack of significant differences among ILF-ST, ILF-EP, and ICLF indicates that, at this stage (5 years), the specific tree species or row density had not yet created distinct carbon-cycling niches for this enzyme (Ventura et al. 2021; Vieira et al. 2023).

By 2024, the drastic reduction in AS and BG activities largely eliminated the distinctions observed in the previous year. In this second year, AS activity showed only isolated differences, such as IP outperforming other controls and ILF-ST becoming superior to ICLF at the 21.00 m distance. For BG, the only remaining significant difference was between ICL and HP.

The synchronization of this enzymatic decline with the sharp increase in soil pH (from acidic in 2023 to near-neutral in 2024) and the reduction in potential acidity H+Al suggests a

shift in the chemical-biological equilibrium. While the integrated systems, particularly ILF-ST, maintained higher organic matter levels during this period, the actual rate of carbon and sulfur cycling (as measured by BG and AS) was likely constrained by these broader chemical shifts and potential climatic stressors, which affected managed and natural systems alike. In summary, the biological quality in these systems is regulated by a complex interplay: the animal distribution and organic matter accumulation by the presence of trees; chemical inhibition (e.g. high P suppressing AP); and grass cultivars.

3.4.4 Soil quality index

3.4.4.1 Chemical

The transformation of chemical data into SQIchemical reveals that integrated systems are not just better than the forest but are specifically engineered environments that still struggle to reach agronomic stability. By using fixed literature references, the index highlights a significant performance gap. While the ICLF system achieved scores near 0.80-0.90 for nutrient availability, the ILF-ST and ILF-EP systems hovered around 0.30-0.50. This confirms that the biological inputs from trees (litterfall) and animals (excreta) in ILF systems are insufficient to meet the chemical demands of high-productivity tropical soils within five years (Kamboj et al. 2024). The index clearly distinguishes between subsistence cycling in ILF and the high-input fertility of ICLF, which carries the chemical legacy of the crop phase.

The acidity regulation function (pH and H+A) showed the most significant spatial improvement, particularly in the ILF-ST system, which reached a score of 0.92 near the trees in 2024. Unlike the results seen in ILF-EP, the superior performance of *S. tubulosa* in moving the soil closer to the agronomic ideal (pH 5.5) can be attributed to its physiology as a slow-growing native species compared to *Eucalyptus*. While fast-growing species like eucalyptus demand intense cation uptake, often accelerating soil acidification through the release of H^+ and the decomposition of specific recalcitrant residues, *S. tubulosa* likely exerts less pressure on the soil's base stocks. Consequently, the zone near the *S. tubulosa* rows does not undergo the same intensity of biological acidification (Rwibasira et al. 2021; Chaer et al. 2011).

This high fertility in ICL and ICLF is predominantly attributed to the residual effect of lime and fertilizer applications performed during the crop succession phase (soybean/maize + *Urochloa*). These inputs elevated P and EB levels to values near the literature's optimal

references. In the case of ILF-ST, although it shows lower scores than ICLF, there is a clear linear decay in fertility as the distance from the tree increases. This effect suggests that at 5 years, the system is still spatially fragmented; the preservation of nutrients near *S. tubulosa* stems likely from the lower nutrient extraction rates of this native species combined with localized animal excreta, rather than a homogeneous improvement across the entire paddock.

Notably NF consistently presents the lowest $SQI_{chemical}$. While NF is often seen as the gold standard for ecology, the index (calibrated for agronomic production) proves it is a chemically restrictive environment, which remains limited by natural acidification processes without management intervention. The managed systems, especially ICLF and ILF-ST, are successfully improving the soil's chemical capacity.

The index proves that the transition from forest to integrated system is not a degradation but a chemical optimization for food production. However, nutrient availability scores were consistently low across most systems (0.25-0.60), with exceptions of ICLF (0.52-0.91) and ICL (0.57-0.86). This finding highlights that phosphorus limitation remains the primary constraint in Amazonian agricultural systems, and cattle ranching systems face progressive nutrient depletion without replenishment strategies.

3.4.4.2 Physical

The analysis of the $SQI_{physical}$ provides a more critical perspective than raw data alone, as the scores normalize the gap between current management and the experimental potential of the environment. While raw data shows fluctuations in moisture and resistance, the indices reveal specific functional failures within each system.

The transformation of moisture data into scores highlighted a significant hydrologic deficiency in the ICLF and ICL systems in 2023. The fact that both ICLF and ICL presented the lowest scores suggests that this poor hydrologic performance is not driven by tree competition. Instead, it is likely linked to the crop succession history (soybean/maize) or intrinsic characteristics of the Ipyporã cultivar under intensive management. Furthermore, there might be localized physical soil limitations in those experimental blocks (such as shallower soil depth or textural variations), which the quality scores make more evident by penalizing these treatments relative to the ideal observed in the rest of the study area.

The less is better transformation of soil resistance to penetration (RP) data exposes the structural vulnerability of integrated systems to livestock pressure. By assigning the highest score to NF (the lowest RP), the index reveals that no managed system, with or without trees,

can maintain structural integrity near its natural state. However, the scores allow for a clear distinction in animal impact: in 2024, the collapse of the ILF-EP score at the tree row (0.00 m) demonstrates that cattle concentration under Eucalyptus degrades the root support function more severely than the more distributed grazing observed in the ILF-ST system.

The comparison between raw data and indices demonstrates that physical quality is the Achilles' heel of intensified systems. The index reveals that ICLF, despite its high chemical fertility (via crop residual effects), faces physical constraints regarding water. Meanwhile, ILF-ST stands out for maintaining a better physical balance than ILF-EP in 2024, suggesting that the choice of tree species (native vs. exotic) indirectly preserves soil structure by mediating animal behavior.

3.4.4.3 Biological

The analysis of the $SQI_{biological}$ demonstrates that biological quality is the most volatile subindex, undergoing drastic changes between sampling years. The transformation into scores is essential here because it uses two different benchmarks. The sustain biological activity function (OM) was evaluated against fixed literature targets (4.01 dag kg^{-1}). The scores confirmed the role of *S. tubulosa* in building real soil fertility. In both 2023 and 2024, ILF-ST approached the ideal OM score, frequently outperforming Eucalyptus systems. The slow growth and lower nutritional demand of this native legume allow for more preserved carbon accumulation, which the index translates as a higher biological carrying capacity.

For the nutrient cycling function (soil enzymatic activity), a score of 1.0 represents the maximum metabolic rate observed in the field. The scores highlight a significant advantage for the treeless Ipyporã pasture (IP) in 2023. The IP system achieved significantly higher nutrient cycling scores than the Native Forest (NF) and both ILF-EP (at 0.00 and 5.25 m) and ICLF (at all distances). This suggests that the hybrid Ipyporã grass, when managed without tree competition or the disturbance of recent crop successions, provides a more active environment for microbial enzymes. Moreover, despite its high chemical scores, the ICLF system showed the lowest nutrient cycling scores. This confirms that the higher nutrient availability and pH suppressed soil enzymatic activity, effectively lowering the overall biological cycling score compared to more nutrient-limited systems.

By 2024, the biological distinctions largely stabilized, with no significant drop in scores compared to 2023. The only remaining spatial distinction was the superiority of ILF-ST over ICLF at 21.00 m. This reinforces the idea that the ILF-ST system (*S. tubulosa*) creates a more

balanced biological environment over time, maintaining enzymatic flux even at the edges of the system where ICLF continues to lag.

The lack of significant differences in the nutrient cycling function during 2024, compared to the clear distinctions in 2023, should not be interpreted as a lack of sensitivity of the enzymes (AP, AS, and BG). On the contrary, soil enzymes are highly sensitive real-time sensors of the soil's biochemical equilibrium. The homogenization of enzymatic scores in 2024 suggests that broader environmental drivers, such as the generalized increase in soil pH and potential climatic stressors, exerted a stronger influence on microbial metabolism than the management systems themselves (Wang et al. 2023; Campdelacreu Rocabruna et al. 2024; Mendes et al. 2024).

While the enzymes showed low discriminating power in 2024, the $SQI_{biological}$ remained effective because it integrates these volatile signals with OM. The fact that ILF-ST maintained a superior biological index at 21.00 m despite the enzymatic convergence proves that the index is robust: it captures the steady-state quality (OM) even when the metabolic flux (enzymes) is temporarily suppressed or leveled by environmental shifts.

Therefore, the enzymes were sensitive enough to capture a system-wide shift in soil health between years, but this very sensitivity means that in years of environmental transition, their power to discriminate between specific treatments decreases. This highlights the importance of the Integrated SQI approach: by combining sensitive, fast-acting indicators (enzymes) with stable ones (OM), the index provides a reliable diagnostic of soil quality that survives interannual volatility.

By integrating OM and enzymes, ILF-ST stands out as the most resilient system. In 2024, while ILF-EP and ICLF showed biological quality declines due to animal pressure and acidity, ILF-ST maintained more robust scores. Moreover, while raw enzyme data showed little difference between systems in 2024, the $SQI_{biological}$ highlights that ILF-ST compensates for momentary low enzymatic activity with a consistently high OM score. The index reveals that this system provides a more stable biological environment, less dependent on metabolic spikes than the *Eucalyptus*-integrated systems (ILF-EP and ICLF).

3.4.4.4 Overall SQI

The integrated SQI provides a holistic view of soil health. The high scores across managed systems, which often showed few significant differences compared to NF, suggest that these integrated and well-managed systems are effectively conserving soil functions. The

data challenges the assumption that monoculture pastures are detrimental to soil quality in the Amazon. The Ipyporã pasture (IP), for instance, outperformed the NF in 2023 and was superior to ILF-EP and ICLF at several distances. This indicates that treeless pastures, when managed with productive cultivars and adequate stocking rates, can be as sustainable as tree-integrated systems from a soil quality perspective.

By 2024, the spatial significance shifted to the ILF-ST system, which maintained its quality while other systems faced localized challenges. Near the tree rows (0.00 m), ILF-ST achieved higher overall quality than both ILF-EP and ICLF. This reinforces the role of *S. tubulosa* in mitigating the soil quality seen under *Eucalyptus* canopies. While the ICL and ICLF remained competitive, the underperformance of ILF-EP and the lower scores of HP relative to ILF-ST (at 0.00 m) highlight that the choice of the tree species and the grass cultivar becomes more decisive as the system matures.

The integrated SQI results show that both tree-integrated and well-managed open pastures are viable pathways for sustainable land use in the Amazon. The ILF-ST system emerges as the most spatially resilient model by the second year, balancing the chemical benefits of the native legume with a more stable physical and biological environment. Most importantly, the lack of interannual degradation proves that these systems are successfully decoupling livestock production from the traditional cycle of soil exhaustion in the region.

3.5 Conclusion

This study demonstrates that the integration of chemical, physical, and biological indicators into a composite soil quality index (SQI) provides a superior and more holistic framework for assessing soil health in Western Amazonia than the evaluation of individual attributes. The use of SQIs successfully captured the complexity of soil functions, confirming the first hypothesis and establishing the index as a reliable tool for monitoring agroecosystem sustainability.

The implementation of integrated systems, particularly the ILF-ST, significantly improved key soil functions such as acidity regulation and organic matter accumulation. However, the treeless Ipyporã pasture demonstrated high water availability and competitive soil quality scores, proving that well-managed monocultures can be sustainable.

The hypothesis regarding high sensitivity to temporal and management changes was partially confirmed. SQI effectively discriminated between management systems and captured the spatial evolution of soil health. However, the lack of significant interannual degradation

across all systems suggests that these intensified models are successfully decoupling livestock production from the traditional cycle of soil exhaustion in the Amazon region.

Finally, the study confirms that soil quality within tree-integrated systems is highly spatialized and modulated by the sampling year. The ICLF system provided a chemical quality peak at intermediate distances in 2023, but the ILF-ST system emerged as the most resilient and stable model by 2024. The native species *S. tubulosa* proved to be superior to the exotic *E. pellita* in maintaining soil physical integrity and biological stability, primarily by mediating animal behavior and exerting less soil compaction and depletion of base stocks. Therefore, the integration of native legumes like *S. tubulosa* is a strategic pathway for long-term soil health and climate-resilient cattle ranching in the tropics.

References

Alvares, Clayton Alcarde, José Luiz Stape, Paulo Cesar Sentelhas, José Leonardo de Moraes Gonçalves, and Gerd Sparovek. 2013. Köppen's Climate Classification Map for Brazil. *Meteorologische Zeitschrift* 22 (6): 711–28. https://doi.org/10.1127/0941-2948/2013/0507.

Alvarez V, Victor Hugo, Roberto Ferreira Novais, Nairam Félix de Barros, Reinaldo Bertola Cantarutti, and Alfredo Scheid Lopes. 1999. Interpretação Dos Resultados Das Análises de Solos. In *Recomendações Para o Uso de Corretivos e Fertilizantes Em Minas Gerais - 5ª Aproximação*, edited by Antonio Carlos Ribeiro, Paulo Tácito Gontijo Guimarães, and Victor Hugo Alvarez V. CFSEMG/DPS-UFV.

Andrade, Carlos Maurício Soares de, Ana Karina Dias Salman, and Tadário Kamel de Oliveira. 2012. *Guia Arbopasto: Manual de Identificação e Seleção de Espécies Arbóreas Para Sistemas Silvipastoris*. Embrapa.

Araujo, Rafael, Francisco Costa, and Marcelo Sant'Anna. 2026. Efficient Conservation of the Brazilian Amazon: Estimates from a Dynamic Model. *The Review of Economic Studies* 93 (1): 72–105. https://doi.org/10.1093/restud/rdaf031.

Assis, Júlia de, Luciano Pinzon Brauwers, Lóren Pacheco Duarte, et al. 2022. Phosphorus Lability in a Subtropical Acrisol under Long-Term Integrated Crop-Livestock System: Impacts of Grazing Management and Cropping System. *Rev. Bras. Ciênc. Solo* 46 (September). https://www.rbcsjournal.org/wp-content/plugins/xml-to-html/include/lens/index.php?xml=1806-9657-rbcs-46-e0220066.xml&lang=en.

Assis, Paula C. R., Luís F. Stone, João C. Medeiros, Beata E. Madari, Janína de M. Oliveira, and Flávio J. Wruck. 2015. Atributos físicos do solo em sistemas de integração lavoura-pecuária-floresta. *Revista Brasileira de Engenharia Agrícola e Ambiental* 19: 309–16. https://doi.org/10.1590/1807-1929/agriambi.v19n4p309-316.

Azevedo, Alcinei Mistico. 2022. *Tratamentos.Ad: Pacote Para Analise De Experimentos Com Testemunhas Adicionais*. V. 0.2.4. Released September 13. https://cran.r-project.org/web/packages/Tratamentos.ad/index.html.

Barbanti, Olympio. 2015. Economic Cycles, Deforestation and Social Impacts in the Brazilian Amazon. *Agrarian South: Journal of Political Economy* 4 (2): 169–96. https://doi.org/10.1177/2277976015597121.

Behling, Maurel, Gladys Beatriz Martínez, Arystides Resende Silva, Tadário Kamel de Oliveira, and Henrique Nery Cipriani. 2021. O Eucalipto Em Sistemas de Integração Lavoura-Pecuária-Floresta (ILPF) Na Amazônia. In *O Eucalipto e a Embrapa: Quatro Décadas de Pesquisa e Desenvolvimento*, by Edilson Batista de Oliveira and José Elidney Pinto Júnior. Embrapa. https://ainfo.cnptia.embrapa.br/digital/bitstream/item/222877/1/Livro-Eucalipto.pdf.

Bentes-Gama, Michelliny de Matos, Guido Sanick Leal, Joelson de Oliveira Barros, Raimunda Herculano Lopes, Giovana Fiorella Zamora López, and Juliane Cardoso da Silveira. 2009. *Características Da Estrutura de Uma Floresta de Terra Firme Em Porto Velho, Rondônia*. Embrapa Rondônia. Circular Técnica 109. Embrapa Rondônia. https://ainfo.cnptia.embrapa.br/digital/bitstream/item/24747/1/ct109-floresta.pdf.

Bermeo, Juan Pablo Chavarro. 2022. Evaluating Soil Quality in Silvopastoral Systems by the Soil Management Assessment Framework (SMAF) in the Colombian Amazon. *Revista Ciência Agronômica* 53: 1–11.

Bhaduri, Debarati, Manimala Mahato, and Sophia Swain. 2025. Next-Generation Agriculture Plays a Decisive Role in Changing Dimension of Monitoring Soil Quality. *Discover Soil* 2 (1): 81. https://doi.org/10.1007/s44378-025-00107-7.

Bravo-Medina, C., F. Goyes-Vera, Y. Arteaga-Crespo, Y. García-Quintana, and D. Changoluisa. 2021. A Soil Quality Index for Seven Productive Landscapes in the Andean-Amazonian Foothills of Ecuador. *Land Degradation & Development* 32 (6): 2226–41. https://doi.org/10.1002/ldr.3897.

Bünemann, Else K., Paul Mäder, Jens Wohlfahrt, et al. 2016. *Concepts and Indicators of Soil Quality – a Review*. Report No. 04. iSQAPER, 3.1. FIBL, WUR, ISRIC. https://ec.europa.eu/research/participants/documents/downloadPublic?documentIds=080166e5ae63cb0e&appId=PPGMS.

Campdelacreu Rocabruna, Patrícia, Xavier Domene, Catherine Preece, and Josep Peñuelas. 2024. Relationship among Soil Biophysicochemical Properties, Agricultural Practices and Climate Factors Influencing Soil Phosphatase Activity in Agricultural Land. *Agriculture* 14 (2): 288. https://doi.org/10.3390/agriculture14020288.

Carpinelli, Sandoval, Adriel Ferreira da Fonseca, Pedro Henrique Weirich Neto, Santos Henrique Brant Dias, and Laíse da Silveira Pontes. 2020. Spatial and Temporal Distribution of Cattle Dung and Nutrient Cycling in Integrated Crop–Livestock Systems. *Agronomy* 10 (5): 672. https://doi.org/10.3390/agronomy10050672.

Carvalho, Paulo Ernani Ramalho. 2007. Bordão-de-Velho Samanea Tubulosa: Taxonomia e Nomenclatura. *Embrapa Circular Técnica*, Circular Técnica, 6.

Chaer, G. M., A. S. Resende, E. F. C. Campello, S. M. De Faria, and R. M. Boddey. 2011. Nitrogen-Fixing Legume Tree Species for the Reclamation of Severely Degraded Lands in Brazil. *Tree Physiology* 31 (2): 139–49. https://doi.org/10.1093/treephys/tpq116.

Cherubin, Maurício R., Douglas L. Karlen, Carlos E. P. Cerri, et al. 2016. Soil Quality Indexing Strategies for Evaluating Sugarcane Expansion in Brazil. *PLOS ONE* 11 (3): e0150860. https://doi.org/10.1371/journal.pone.0150860.

Cipriani, Henrique Nery, Ana Karina Dias Salman, Thierry Alexandre Pellegrinetti, Elaine Coimbra Souza, Pedro Gomes Cruz, and Siu Mui Tsai. 2025. Native Tree Species in Silvopastoral System Outperforms Eucalyptus in Enhancing Soil Health. SSRN Scholarly Paper No. 5195852. Social Science Research Network, March 27. https://doi.org/10.2139/ssrn.5195852.

Cipriani, Henrique Nery, Ana Karina Dias Salman, Carlos Henrique Semper Da Silva, Murilo Luz Rodrigues, Emily Soares Dos Santos, and Pedro Gomes Da Cruz. 2023. Crescimento Inicial de Samanea Tubulosa e Eucalyptus Pellita Em Sistemas de Integração Pecuária-Floresta Em Porto Velho, Rondônia. *Série Técnica IPEF* 26 (48): 310–14. https://doi.org/10.18671/sertec.v26n48.061.

Climate-Data.org. 2022. Clima Porto Velho: Temperatura, Tempo e Dados Climatológicos. May. https://pt.climate-data.org/america-do-sul/brasil/rondonia/porto-velho-3120/#google_vignette.

Coad, Jessica, Lucy Burkitt, Warwick Dougherty, and Leigh Sparrow. 2014. Decrease in Phosphorus Concentrations When P Fertiliser Application Is Reduced or Omitted from Grazed Pasture Soils. *Soil Research* 52 (3): 282–92. https://doi.org/10.1071/SR13243.

Cunha, Hellen Fernanda Viana, Kelly M. Andersen, Laynara Figueiredo Lugli, et al. 2022. Direct Evidence for Phosphorus Limitation on Amazon Forest Productivity. *Nature* 608 (7923): 558–62. https://doi.org/10.1038/s41586-022-05085-2.

Dias-Filho, Moacyr Bernardino. 2026. *Transformation of Brazilian Amazon Cattle Ranching: A Historical and Sustainable Perspective*. Embrapa Amazônia Oriental. Documentos 504. Embrapa Amazônia Oriental. https://www.infoteca.cnptia.embrapa.br/infoteca/bitstream/doc/1184166/1/TransformationBrazilianAmazon.pdf.

El Behairy, Radwa A., Hasnaa M. El Arwash, Ahmed A. El Baroudy, et al. 2024. How Can Soil Quality Be Accurately and Quickly Studied? A Review. *Agronomy* 14 (8): 1682. https://doi.org/10.3390/agronomy14081682.

Feitosa, Izabela de Lima, Alexandre Martins Abdão dos Passos, Henrique Nery Cipriani, Marcelo Silva de Oliveira, Alaerto Luiz Marcolan, and Gustavo Mattos Vasques. 2019. Spatial Variability of Soil Physical Attributes in Integrated Production Systems in the Amazon Region. *Pesquisa Agropecuária Brasileira* 54 (November). https://doi.org/10.1590/S1678-3921.pab2019.v54.00324.

Fér, Miroslav, Antonín Nikodem, Sára Trejbalová, Aleš Klement, Lenka Pavlů, and Radka Kodešová. 2022. How Various Mulch Materials Can Affect the Soil Hydro-Physical Properties. *Journal of Hydrology and Hydromechanics* 70 (3): 269–75. https://doi.org/10.2478/johh-2022-0016.

Ferreira, Daniel Furtado. 2011. Sisvar: A Computer Statistical Analysis System. *Ciência e Agrotecnologia* 35 (6): 1039–42.

Gatiboni, Luke, Amy L. Shober, Nicole Fiorellino, Deanna Osmond, and Lauren R. Mosesso. 2025. Drawdown of Soil Phosphorus by Crop Removal: A Meta-Analysis of 56 Fields with Interrupted Fertilization. *Agricultural & Environmental Letters* 10 (1): e70007. https://doi.org/10.1002/ael2.70007.

George, Suman Jacob, B. Mohan Kumar, P. A. Wahid, and N. V. Kamalam. 1996. Root Competition for Phosphorus between the Tree and Herbaceous Components of Silvopastoral Systems in Kerala, India. *Plant and Soil* 179 (2): 189–96. https://doi.org/10.1007/BF00009328.

Hamza, M. A., and W. K. Anderson. 2005. Soil Compaction in Cropping Systems: A Review of the Nature, Causes and Possible Solutions. *Soil and Tillage Research* 82 (2): 121–45. https://doi.org/10.1016/j.still.2004.08.009.

Humeniuk, H. B., and V. V. Hrubinko. 2025. Soil Quality As An Indicator Of Sustainable Development. *Scientific Issue Ternopil Volodymyr Hnatiuk National Pedagogical University. Series: Biology* 85 (1–2): 67–72. https://doi.org/10.25128/2078-2357.25.1-2.9.

IUSS Working Group WRB. 2022. *World Reference Base for Soil Resources 2022: International Soil Classification System for Naming Soils and Creating Legends for Soil Maps*. 4th ed. International Union of Soil Sciences. https://files.isric.org/public/documents/WRB_fourth_edition_2022-12-18.pdf.

Jackson, M. L. 1982. *Análisis químico de suelos*. Ediciones Omega.

Janusckiewicz, E. R., E. Raposo, B. M. P. R. Martins, et al. 2019. Atividade enzimática do solo de pastos de Brachiaria manejados sob ofertas de forragem. *Boletim de Indústria Animal* 76. https://doi.org/10.17523/bia.2019.v76.e1460.

Kamboj, Dimple, Rameshwar Choudhary, Anand Kumar Diwakar, and Shraddha Maurya. 2024. Integrated Nutrient Management for Improving the Soil Sustainability and Crop Productivity: A Review. *Journal of Advances in Biology & Biotechnology* 27 (11): 1053–62. https://doi.org/10.9734/jabb/2024/v27i111690.

Korchagin, Jackson, Edson Campanhola Bortoluzzi, Diovane Freire Moterle, Claudia Petry, and Laurent Caner. 2019. Evidences of Soil Geochemistry and Mineralogy Changes Caused by Eucalyptus Rhizosphere. *CATENA* 175 (April): 132–43. https://doi.org/10.1016/j.catena.2018.12.001.

Lai, Roberto, Alessandra Lagomarsino, Luigi Ledda, and Pier Paolo Roggero. 2014. Variation in Soil C and Microbial Functions across Tree Canopy Projection and Open Grassland Microenvironments. *Turkish Journal of Agriculture and Forestry* 38 (1): 62–69. https://doi.org/10.3906/tar-1303-82.

Lima, Gabriela C., Marx L. N. Silva, Diego A. F. de Freitas, Bernardo M. Cândido, Nilton Curi, and Marcelo S. de Oliveira. 2016. Spatialization of Soil Quality Index in the Sub-Basin of Posses, Extrema, Minas Gerais. *Revista Brasileira de Engenharia Agrícola e Ambiental* 20: 78–84. https://doi.org/10.1590/1807-1929/agriambi.v20n1p78-84.

Lopes, André Alves de Castro, Djalma Martinhão Gomes de Sousa, Guilherme Montandon Chaer, Fábio Bueno dos Reis Junior, Wenceslau J. Goedert, and Iêda de Carvalho Mendes. 2013. Interpretation of Microbial Soil Indicators as a Function of Crop Yield and Organic Carbon. *Soil Science Society of America Journal* 77 (2): 461–72. https://doi.org/10.2136/sssaj2012.0191.

Mantovanelli, BRUNO Campos, Milton César Costa Campos, Leandro Coutinho Alho, Uilson Franciscon, Maílson Ferreira Nascimento, Luís Antônio Coutrim dos Santos. 2016. Distribuição Espacial Dos Componentes Da Acidez Do Solo Em Área De Campo Natural Na Região De Humaitá, Amazonas. *Revista de Ciências Agro-Ambientais* 14 (1). https://doi.org/10.5327/rcaa.v14i1.817.

Marçal, Maria Fernanda Magioni, Zigomar Menezes de Souza, Rose Luiza Moraes Tavares, et al. 2022. Potential Use of Quartzipisamment under Agroforestry and Silvopastoral System for Large-Scale Production in Brazil. *Agronomy* 12 (4): 905. https://doi.org/10.3390/agronomy12040905.

Marion, Luis Fernando, Robson Schneider, Maurício Roberto Cherubin, et al. 2022. Development of a Soil Quality Index to Evaluate Agricultural Cropping Systems in Southern Brazil. *Soil and Tillage Research* 218 (April): 105293. https://doi.org/10.1016/j.still.2021.105293.

Martins, Amanda P., Diego Cecagno, José Bernardo M. Borin, et al. 2016. Long-, Medium- and Short-Term Dynamics of Soil Acidity in an Integrated Crop–Livestock System under Different Grazing Intensities. *Nutrient Cycling in Agroecosystems* 104 (1): 67–77. https://doi.org/10.1007/s10705-015-9759-5.

Martins, Amanda Posselt, Sérgio Ely V. G. de Andrade Costa, Ibanor Anghinoni, et al. 2014. Soil Acidification and Basic Cation Use Efficiency in an Integrated No-till Crop–Livestock System under Different Grazing Intensities. *Agriculture, Ecosystems & Environment* 195 (October): 18–28. https://doi.org/10.1016/j.agee.2014.05.012.

Mattos, Eduardo M. de, Dan Binkley, Otavio C. Campoe, Clayton A. Alvares, and Jose L. Stape. 2020. Variation in Canopy Structure, Leaf Area, Light Interception and Light Use Efficiency among Eucalyptus Clones. *Forest Ecology and Management* 463 (May): 118038. https://doi.org/10.1016/j.foreco.2020.118038.

Mendes, Ieda Carvalho, Guilherme Montandon Chaer, Fábio Bueno dos Reis Junior, et al. 2024. Soil Bioanalysis (SoilBio): A Sensitive, Calibrated, and Simple Assessment of Soil Health for B Razil. In *Soil Health Series: Volume 3 Soil Health and Sustainable Agriculture in Brazil*. John Wiley & Sons, Ltd. https://doi.org/10.1002/9780891187448.ch10.

Merloti, Luis Fernando, João William Bossolani, Lucas William Mendes, et al. 2023. Investigating the Effects of Brachiaria (Syn. Urochloa) Varieties on Soil Properties and Microbiome. *Plant and Soil*, ahead of print, August 23. https://doi.org/10.1007/s11104-023-06225-x.

Morais, Jozivaldo Prudêncio Gomes de, Adibe Luiz Abdalla, Alexandre de Azevedo Olival, Mariana Campana, Francine Basso Facco, and Tiago Antonio Del Valle. 2025. Amazonian Fruit (Samanea Tubulosa) in Dairy Cattle Diets: In Vitro Fermentation, Gas Production, and Digestibility. *Ruminants* 5 (4): 64. https://doi.org/10.3390/ruminants5040064.

Moreira, Guilherme Musse, Júlio César Lima Neves, Ciro Augusto de Souza Magalhães, et al. 2018. Soil Chemical Attributes In Response To Tree Distance And Sun-Exposed Faces After The Implantation Of An Integrated Crop-Livestock-Forestry System. *Revista Árvore* 42: e420405. https://doi.org/10.1590/1806-90882018000400005.

Nunes, Sâmia, Markus Gastauer, Rosane B. L. Cavalcante, et al. 2020. Challenges and Opportunities for Large-Scale Reforestation in the Eastern Amazon Using Native Species. *Forest Ecology and Management* 466 (June): 118120. https://doi.org/10.1016/j.foreco.2020.118120.

Olival, Alexandre de Azevedo, Saulo Eduardo Xavier Franco de Souza, Jozivaldo Prudêncio Gomes de Moraes, and Mariana Campana. 2021. Effect of Amazonian Tree Species on Soil and Pasture Quality in Silvopastoral Systems. *Acta Amazonica* 51 (December): 281–90. https://doi.org/10.1590/1809-4392202004692.

Oliveira, Maniele Mendonça de, Ana Karina Dias Salman, Henrique Nery Cipriani, Amanda Ribeiro de Moura, and Odilene de Souza Teixeira. 2021. Desempenho Inicial de Espécies Arbóreas Para Sombreamento Natural Em Sistema de Integração Pecuária-Floresta. *Anais...*, 36–41. https://www.alice.cnptia.embrapa.br/bitstream/doc/1139635/1/cpafro-18701.pdf.

Oliveira, Tadário Kamel de, and Samuel Almeida da Luz. 2012. *Influência Do Bordão-de-Velho (Samanea Tubulosa (Bentham) Barnedy; Grimes) Na Pastagem e No Solo Em Sistema Silvipastoril No Acre*. Embrapa Acre. Boletim de Pesquisa e Desenvolvimento 49. Embrapa Acre. https://ainfo.cnptia.embrapa.br/digital/bitstream/item/76723/1/bp49-final-140213.pdf.

Pacheco, Pablo, and Rene Poccard-Chapuis. 2012. The Complex Evolution of Cattle Ranching Development Amid Market Integration and Policy Shifts in the Brazilian Amazon. *Annals of the Association of American Geographers* 102 (6): 1366–90. https://doi.org/10.1080/00045608.2012.678040.

Patiño, Gelber Rosas, Edgar Alvaro Avila Pedraza, and Verenice Sánchez Castillo. 2024. La Acidez Del Suelo Limita La Producción Agrícola: Una Revisión Enfocada En La Amazonia Colombiana. *Revista de Investigación Agraria y Ambiental* 16 (1): 185–211. https://doi.org/10.22490/21456453.7857.

Pegoraro, Rodinei Facco, Ivo Ribeiro da Silva, Roberto Ferreira de Novais, Nairam Felix de Barros, Sebastião Fonseca, and Carlos Silva Dambroz. 2011. Estoques de carbono e nitrogênio nas frações da matéria orgânica em argissolo sob eucalipto e pastagem. *Ciência Florestal* 21 (2): 261–73. https://doi.org/10.5902/198050983230.

Pereira, Arthur Prudêncio de Araujo, Ademir Sérgio Ferreira Araujo, Maiele Cintra Santana, et al. 2023. Enzymatic Stoichiometry in Tropical Soil under Pure and Mixed Plantations of Eucalyptus with N_2-Fixing Trees. *Scientia Agricola* 80: e20210283. https://doi.org/10.1590/1678-992X-2021-0283.

Pérez-Márquez, Simón, Vagner Ovani, Vanderson Eliel Meira, et al. 2025. Assessing the Impact of Samanea Tubulosa Trees on Methane Emissions and Its Potential as a Feed Supplement for Ruminants in Silvopastoral Systems. *Agroforestry Systems* 99 (6): 135. https://doi.org/10.1007/s10457-025-01231-7.

Policarpo, Victor Hugo Custodio, Rones Dias da Costa, Hemython Luis Bandeira Nascimento, Rose Luiza Moraes Tavares, Camila Jorge Barnabé Ferreira, and Paulo Fernandes Boldrin. 2023. Parâmetros de raiz e atributos físicos do solo com cultivo de forrageiras dos gêneros Panicum e Urochloa. *Evidência* 23 (2): 113–28. https://doi.org/10.18593/evid.32576.

Regasa, Abu, Wassie Haile, and Girma Abera. 2024. Soil Acidity and Fertility Status of Surface Soils under Different Land Uses in Sayo District of Oromia, Western Ethiopia. *PLOS ONE* 19 (12): e0316009. https://doi.org/10.1371/journal.pone.0316009.

Ritchie, GSP, and PJ Dolling. 1985. The Role of Organic Matter in Soil Acidification. *Australian Journal of Soil Research* 23 (4): 569–76. https://doi.org/10.1071/SR9850569.

Rosales, Hernán R. B., Silvino V. Hernández, Digna I. G. Aguiar, Diego C. Rosero, Luis C. Perez, and Marcelo I. Rosero. 2018. Assessment of Soil Quality in Andosols Using Silvopastoral Systems. *The Open Agriculture Journal* 12 (1): 207–14. https://doi.org/10.2174/1874331501812010207.

Rwibasira, Peter, Francois Xavier Naramabuye, Donat Nsabimana, and Monique Carnol. 2021. Long-Term Effects of Forest Plantation Species on Chemical Soil Properties in Southern Rwanda. *Soil Systems* 5 (4): 59. https://doi.org/10.3390/soilsystems5040059.

Santos, Amanda Maria Gallindo dos, Jose Carlos Batista Dubeux Jr, Mércia Virginia Ferreira dos Santos, et al. 2024. The Distance from Tree Legumes in Silvopastoral Systems Modifies the Litter in Grass-Composed Pastures. *The Journal of Agricultural Science* 162 (1): 59–66. https://doi.org/10.1017/S0021859624000200.

Santos, Humberto Gonçalves dos, Paulo Klinger Tito Jacomine, Lúcia Helena Cunha dos Anjos, et al. 2025. *Sistema Brasileiro de Classificação de Solos.* 6th ed. Embrapa, 2025. http://www.infoteca.cnptia.embrapa.br/handle/doc/1176834.

Santos, João Vitor dos, Lucas Raimundo Bento, Joana Dias Bresolin, et al. 2022. The Long-Term Effects of Intensive Grazing and Silvopastoral Systems on Soil Physicochemical Properties, Enzymatic Activity, and Microbial Biomass. *CATENA* 219 (December): 106619. https://doi.org/10.1016/j.catena.2022.106619.

Santos, Melissa Alexandre, Carolina dos Santos Batista Bonini, Vitor Corrêa de Mattos Barretto, José Augusto Liberato de Souza, and Aline Marchetti Silva Matos. 2023. Soil physical quality using an agroforestry system with an agroecological basis. *Periódico Eletrônico Fórum Ambiental da Alta Paulista* 19 (1). https://doi.org/10.17271/1980082719120233255.

Sarto, Marcos V. M., Wander L. B. Borges, Jaqueline R. W. Sarto, Carlos A. B. Pires, Charles W. Rice, and Ciro A. Rosolem. 2020. Soil Microbial Community and Activity in a Tropical Integrated Crop-Livestock System. *Applied Soil Ecology* 145 (January): 103350. https://doi.org/10.1016/j.apsoil.2019.08.012.

Sarto, Marcos V. M., Wander L. B. Borges, Jaqueline R. W. Sarto, Charles W. Rice, and Ciro A. Rosolem. 2020. Deep Soil Carbon Stock, Origin, and Root Interaction in a Tropical Integrated Crop–Livestock System. *Agroforestry Systems* 94 (5): 1865–77. https://doi.org/10.1007/s10457-020-00505-6.

Sartor, Laércio Ricardo, Jessica Ramão, Vanderley Porfírio da Silva, Luis Cesar Cassol, and Eleandro José Brun. 2020. Resistência mecânica do solo à penetração em sistema silvipastoril após onze anos de implantação. *Ciência Florestal* 30 (1): 231–41. https://doi.org/10.5902/1980509831205.

Shen, Yuye, Zhongqi Zhang, and Yue Xue. 2021. Study on the New Dynamics and Driving Factors of Soil pH in the Red Soil, Hilly Region of South China. *Environmental Monitoring and Assessment* 193 (5): 304. https://doi.org/10.1007/s10661-021-09080-4.

Silva, Joélia Natália Bezerra da, Jéssica Laís Bezerra Silva, Maria Leidiane Ferreira, and Josiclêda Domiciano Galvíncio. 2025. Estimativas do sequestro de carbono em espécies predominantes na vegetação de caatinga: compreendendo a dinâmica do carbono em um bioma semiárido. *Revista Brasileira de Meio Ambiente* 13 (2). https://www.revistabrasileirademeioambiente.com/index.php/RVBMA/article/view/1879.

Silva, Marraiane A., Mendelson Lima, Carlos A. Silva Junior, Gerlane M. Costa, and Carlos A. Peres. 2018. Achieving Low-Carbon Cattle Ranching in the Amazon: 'Pasture Sudden Death' as a Window of Opportunity. *Land Degradation & Development* 29 (10): 3535–43. https://doi.org/10.1002/ldr.3087.

Simon, Carla da Penha, Taciana Figueiredo Gomes, Thaís Nascimento Pessoa, et al. 2022. Soil Quality Literature in Brazil: A Systematic Review. *Revista Brasileira de Ciência Do Solo* 46 (April). https://doi.org/10.36783/18069657rbcs20210103.

Skidmore, Marin Elisabeth, Kaitlyn M. Sims, Lisa L. Rausch, and Holly K. Gibbs. 2022. Sustainable Intensification in the Brazilian Cattle Industry: The Role for Reduced Slaughter Age. *Environmental Research Letters* 17 (6): 064026. https://doi.org/10.1088/1748-9326/ac6f70.

Soil Survey Staff. 2022. *Keys to Soil Taxonomy*. 13th ed. USDA Natural Resources Conservation Service. https://www.nrcs.usda.gov/sites/default/files/2022-09/Keys-to-Soil-Taxonomy.pdf.

Soumare, Abdoulaye, Anicet Manga, Saliou Fall, Mohamed Hafidi, Ibrahima Ndoye, and Robin Duponnois. 2015. Effect of Eucalyptus Camaldulensis Amendment on Soil Chemical Properties, Enzymatic Activity, Acacia Species Growth and Roots Symbioses. *Agroforestry Systems* 89 (1): 97–106. https://doi.org/10.1007/s10457-014-9744-z.

Souza, Jéssica Fernanda Dias, Carolina dos Santos Batista Bonini, Gustavo Pavan Mateus, et al. 2020. Compactação do solo em sistemas de integração lavoura-pecuáriafloresta após cinco anos de implantação e uso. *Revista de Ciências Agroveterinárias* 19 (3): 348–53. https://doi.org/10.5965/223811711932020348.

Stolf, Rubismar, José Fernandes, and Victório Laerte Furlani Neto. 1983. Penetrômetro de Impacto Modelo IAA/Planalsucar-Stolf: Recomendação Para Seu Uso. *STAB* 1 (3): 18–23.

Stolf, Rubismar, Jorge Hiroshi Murakami, Caetano Brugnaro, Luiz Gabriel Silva, Luiz Carlos Ferreira da Silva, and Luiz Antonio Correia Margarido. 2014. Penetrômetro de impacto stolf - programa computacional de dados em EXCEL-VBA. *Revista Brasileira de Ciência do Solo* 38 (June): 774–82. https://doi.org/10.1590/S0100-06832014000300009.

Tabatabai, M. A. 1994. Soil Enzymes. In *Methods of Soil Analysis*, edited by R. W. Weaver, Scott Angle, Peter Bottomley, et al. John Wiley & Sons, Ltd. https://doi.org/10.2136/sssabookser5.2.c37.

Teixeira, Paulo Cesar, Guilherme Kangussu Donagema, Ademir Fontana, and Wenceslau Geraldes Teixeira, eds. 2017. *Manual de Métodos de Análise de Solo*. 3rd ed. Embrapa. http://ainfo.cnptia.embrapa.br/digital/bitstream/item/181717/1/Manual-de-Metodos-de-Analise-de-Solo-2017.pdf.

Valani, Gustavo Pereira, Aline Fachin Martíni, José Ricardo Macedo Pezzopane, Alberto Carlos de Campos Bernardi, and Miguel Cooper. 2022. Soil Physical Quality in the Topsoil of Integrated and Non-Integrated Grazing Systems in a Brazilian Ferralsol. *Soil and Tillage Research* 220 (June): 105357. https://doi.org/10.1016/j.still.2022.105357.

Valani, Gustavo Pereira, Aline Fachin Martíni, Laura Fernanda Simões da Silva, Renata Cristina Bovi, and Miguel Cooper. 2021. Soil Quality Assessments in Integrated Crop–Livestock–Forest Systems: A Review. *Soil Use and Management* 37 (1): 22–36. https://doi.org/10.1111/sum.12667.

Valente, Moacir Azevedo, Raimundo Cosme de Oliveira Júnior, Tarcísio Ewerton Rodrigues, João Marcos Lima da Silva, and Paulo Lacerda dos Santos. 1998. *Levantamento Semidetalhado Dos Solos Do Campo Experimental de Porto Velho, RO*. Embrapa-CPATU. Documentos 136. Embrapa-CPATU. http://ainfo.cnptia.embrapa.br/digital/bitstream/item/57557/1/CPATU-Doc136.pdf.

Valentim, Judson Ferreira, Carlos Mauricio Soares de Andrade, and Luís Gustavo Barioni. 2010. *Reconciling Cattle Ranching and Environmental Conservation in the Legal Brazilian Amazon*. Embrapa Acre. Policy Brief. Embrapa Acre. http://www.infoteca.cnptia.embrapa.br/infoteca/handle/doc/1109631.

Ventura, Matheus Vinicius Abadia, Hellen Regina Fernandes Batista-Ventura, Edson Luiz Souchie, Marco Aurélio Carbone Carneiro, and Darliane De Castro Santos. 2021. Biological Attributes in Soils with Cover Crops in the Soybean Direct Seeding System in Southwest of Goiás, Brazil. *International Journal of Agriculture and Biology* 30 (5). https://doi.org/10.17957/IJAB/15.2088.

Vieira, Matheus Emannuel Oliveira, Lucas Dantas Lopes, France Mário Costa, Viviane Talamini, Edson Patto Pacheco, and Marcelo Ferreira Fernandes. 2023. Different No-till Grain Production Systems with Urochloa Spp. Affect Soil Microbial Community Structure, Biomass and Activity in a Tropical Ultisol. *Soil Ecology Letters* 6 (1): 230191. https://doi.org/10.1007/s42832-023-0191-5.

Walkley, A., and I. Armstrong Black. 1934. An Examination of the Degtjareff Method for Determining Soil Organic Matter, and a Proposed Modification of the Chromic Acid Titration Method. *Soil Science* 37 (1): 29.

Wang, Li, Chantal Hamel, Peina Lu, et al. 2023. Using Enzyme Activities as an Indicator of Soil Fertility in Grassland - an Academic Dilemma. *Frontiers in Plant Science* 14 (July). https://doi.org/10.3389/fpls.2023.1175946.

Welke, Selmir, Ana Karina Dias Salman, Henrique Nery Cipriani, Laércio Cavalcante Monteiro Filho, Odilene de Souza Teixeira, and Giovanna Moreira Ghedin. 2022. Duas Espécies Arbóreas Para Sombreamento de Pastagem Em Sistema de Integração Pecuária-Floresta. *Anais...*, 39–44. https://www.alice.cnptia.embrapa.br/alice/bitstream/doc/1146390/1/Anais-EIPER-2022-1-39-44.pdf.

Yaulilahua-Huacho, Russbelt, Liliana Asunción Sumarriva-Bustinza, Ligia Isaida Rosaura Gutierrez-Deza, et al. 2024. Examining the Adaptability of Soil pH to Soil Dynamics Using Different Methodologies: A Concise Review. *Journal of Experimental Biology and Agricultural Sciences* 12 (4): 573–87. https://doi.org/10.18006/2024.12(4).573.587.

Zhang, Yichuan, Lifang Qiao, Chaoping Chen, Li Tian, and Xiaozhen Zheng. 2021. Effects of Organic Ground Covers on Soil Moisture Content of Urban Green Spaces in Semi-Humid Areas of China. *Alexandria Engineering Journal* 60 (1): 251–59. https://doi.org/10.1016/j.aej.2020.08.001.

4 SOIL CARBON SEQUESTRATION POTENTIAL IN INTEGRATED PRODUCTION AND PASTURE SYSTEMS IN WESTERN AMAZONIA

ABSTRACT

The expansion of extensive cattle ranching in the Amazon is a primary driver of deforestation and soil degradation. Integrated crop-livestock-forestry systems emerge as a sustainable alternative to enhance soil carbon sequestration. This study aimed to assess the potential of different cattle production systems for soil C sequestration in Western Amazonia, comparing them with a native forest (NF) fragment. The experimental areas included integrated livestock-forestry with *Samanea tubulosa* (ILF-ST) and *Eucalyptus pellita* (ILF-EP), integrated crop-livestock-forestry (ICLF), integrated crop-livestock (ICL), and three treeless pastures (*Urochloa humidicola*, 'Marandu', and 'Ipyporã'). Soil samples were collected up to 40 cm depth to determine soil C content (SCC), soil C stocks (SCS), isotopic composition ($\delta^{13}C$) soil organic carbon (SOC), permanganate oxidizable carbon (POXC), organic matter humification index (H_{LIFS}) and the carbon management index (CMI). Results indicated that changes in SCC and SCS among areas were more pronounced in deeper layers (10-20 and 20-40 cm). The ILF-ST system, particularly at 21 m from the tree line, exhibited the highest SCC (4.35 dag kg^{-1}) and SCS (95.3 t ha^{-1}) among all managed areas, outperforming the NF (78.1 t ha^{-1}). Conversely, ICLF and *U. humidicola* pasture generally showed the lowest carbon performance. Moreover, SOC was more sensitive to management than SCC, detecting more differences among areas, but followed similar trend (higher values for ILF-ST and NF, besides 'Marandu', and lower values for ICLF and *U. humidicola* pasture). Soil carbon turnover is faster in ICLF compared to ILF-ST and ILF-EP, as indicated by ($\delta^{13}C$). Humification index (H_{LIFS}) was higher in ICLF, ICL and 'Ipyporã' pasture, indicating a higher proportion of recalcitrant organic matter in comparison to the other systems. On the other hand, POXC was lower in ICLF and *U. humidicola* pasture, and higher in ILF-ST and NF. The CMI revealed that while ILF-ST could reach or surpass the carbon management quality of native forests (CMI $\geq$ 100), other managed systems like ICLF and *U. humidicola* pasture fell short. Additionally, differences from NF are mainly due to carbon lability than to carbon pool. The findings underscore that the choice of tree species (notably native legumes like *S. tubulosa*) and pasture management are critical for optimizing C sequestration in integrated systems in the Amazon.

Keywords: carbon management index, H_{LIFS}, *Samanea tubulosa*, silvopastoral systems, soil organic matter stability.

4.1 Introduction

The Amazon rainforest, a critical global carbon sink, faces significant land degradation primarily driven by deforestation and forest degradation (Lapola et al. 2023). Livestock production, particularly extensive cattle ranching, is a major contributor to these processes. The reckless expansion of cattle ranching in the Amazon is closely linked to deforestation, as vast areas of forest are cleared to create pastures (Carvalho et al. 2020; Rivero et al. 2009). This not only leads to the loss of biodiversity and carbon storage but also contributes to greenhouse gas emissions (Rodrigues et al. 2023; Van Der Werf et al. 2009). The demand for beef and leather in both domestic and international markets further exacerbates this issue, as it incentivizes the expansion of cattle ranching into forested areas (Pendrill et al. 2019; Persson et al. 2014).

Sustainable practices, such as integrated crop-livestock-forestry (ICLF) systems, can enhance soil carbon sequestration while mitigating the adverse effects of livestock production on the Amazon rainforest's ecosystem (Conceição et al. 2017; Monteiro et al. 2024; Oliveira et al. 2018). By integrating trees, crops, and livestock, ICLF systems create a synergistic environment that supports soil health and fertility, which are crucial for sustainable livestock production (Cardoso and Gimenes 2024; Marchão et al. 2024; Oliveira et al. 2024). However, the successful implementation of ICLF systems requires careful planning and management to optimize their benefits, particularly in terms of carbon sequestration (Conceição et al. 2017). This requires studies to evaluate the effectiveness of ICLF systems in increasing soil carbon stocks in various regions, including Western Amazonia.

Long-term soil carbon stock enhancement depends not only on the quantity of soil organic carbon content, but also on the lability of that carbon to remain stable in the soil (Xu et al. 2018). The organic matter humification index (H_{LIFS}) is a useful metric for assessing the stability of soil organic carbon, serving as an alternative to the classic chemical fractionation (Segnini et al. 2019; Bento et al. 2025). Likewise, the carbon management index (CMI) conciliates total soil carbon pool with the degree of oxidation, measured by the permanganate oxidizable carbon (POXC), providing a more robust assessment of management practices on soil carbon dynamics. Particularly in the context of ICLF practices (Blair et al. 1995; Piano et al. 2020; Sodhi et al. 2009).

Therefore, the objective of this study was to assess the potential of different cattle production systems for soil carbon sequestration in Western Amazonia, by comparing them with a native forest (NF) reference area. In view of this, three main hypotheses were established: (i) The integrated systems (ICLF and ILF) would exhibit a higher carbon sequestration capacity, reflected in elevated soil carbon content (SCC) and stock (SCS) values, compared to monoculture pastures, due to diversification and the continuous input of tree biomass and/or crop residues; (ii) The choice of the arboreal component is critical, and therefore, integration with the native leguminous species (*Samanea tubulosa*) would result in greater soil carbon accumulation than with the exotic species (*Eucalyptus pellita*); and (iii) The most efficient management systems, particularly the ILF with *S. tubulosa*, would be capable of recovering the carbon stock, reaching or surpassing the levels observed in NF.

4.2 Materials and Methods

4.2.1 Site description

Samples were taken from seven cattle ranching experimental areas and a native forest (NF) fragment located within the Empresa Brasileira de Pesquisa Agropecuária (Embrapa) experimental field in Porto Velho, Rondônia State, Brazil (8° 48’ S, 63° 51’ W; 95 m altitude). According to the Köppen climate classification system, the climate is Am, or tropical monsoon (Alvares et al. 2013). The area has an average annual rainfall of 2,216 mm, with average annual maximum and minimum temperatures of 30.4 °C and 23.3 °C, respectively (Climate-Data.org 2022).

The predominant soil in the area is classified as a Latossolo Vermelho-Amarelo distrófico (LVAd) according to the Brazilian soil classification system (Valente et al. 1998; Santos et al. 2025), which corresponds to a Ferralsol in the World Reference Base (WRB) soil classification system (IUSS Working Group WRB 2022), or a Hapludox under the USDA Soil Taxonomy (Soil Survey Staff 2022). The soil has a predominant clay texture (Table 4.1).

Table 4.1 - Mean ± standard deviation of soil pH_{H2O}, available phosphorus (P), base saturation (BS), bulk density (BD), and sand and clay content for soil layers (0-10, 10-20 and 20-40 cm) in the studied land-use systems[†]. ILF-ST: integrated livestock-forestry with *Samanea tubulosa*. ILF-EP: integrated livestock-forestry with *Eucalyptus pellita*. ICLF: integrated crop-livestock-forestry. ICL: integrated crop-livestock. IP: *Urochloa brizantha* x *U. ruziziensis* 'Ipyporã' pasture. MP: *U. brizantha* 'Marandu' pasture. HP: *U. humidicola* pasture. NF: native forest.

Distance[‡]	Area	pH_{H2O}	P	BS	BD	Sand	Clay
m			mg dm^{-3}	%	g cm^{-3}	dag kg^{-1}	
		---------- 0-10 cm ----------					
0.00	ILF-ST	5.84±0.09	2.56±0.80	52.52±5.81	1.02±0.09	28.00±6.61	56.50±11.26
	ILF-EP	5.11±0.47	2.36±0.30	29.93±13.28	1.07±0.04	17.50±10.22	67.50±8.29
	ICLF	5.85±0.06	2.68±0.92	53.48±4.83	1.12±0.03	33.50±6.22	42.50±4.68
5.25	ILF-ST	5.56±0.42	1.60±1.17	41.02±14.95	1.11±0.15	27.50±3.26	54.50±6.94
	ILF-EP	5.35±0.43	0.83±0.37	35.88±13.97	1.10±0.09	20.00±8.91	63.50±5.76
	ICLF	6.02±0.03	7.83±4.42	60.42±4.19	1.10±0.03	32.50±5.70	42.50±5.00
21.00	ILF-ST	5.46±0.50	1.31±0.71	38.07±17.82	0.98±0.10	28.50±11.51	54.50±7.98
	ILF-EP	5.59±0.15	1.12±1.09	42.40±5.07	1.01±0.07	20.00±10.81	66.00±7.62
	ICLF	6.03±0.07	6.47±3.92	59.94±3.72	1.02±0.10	32.00±2.85	46.50±4.18
	ICL	5.90±0.10	4.48±2.18	53.49±5.38	0.97±0.14	26.00±1.12	59.50±10.22
	IP	5.91±0.07	0.83±0.45	52.02±3.80	0.71±0.26	31.50±7.62	46.50±11.12
	MP	4.90±0.58	1.39±0.47	22.25±16.44	0.98±0.20	26.50±2.09	59.50±4.47
	HP	5.68±0.53	1.67±0.44	43.77±17.31	1.00±0.11	29.00±5.76	43.00±5.97
	NF	4.46±0.09	1.74±0.34	4.46±0.24	0.83±0.14	34.00±3.35	54.00±3.35
		---------- 10-20 cm ----------					
0.00	ILF-ST	5.74±0.13	2.41±0.66	48.59±6.95	0.98±0.09	23.00±3.54	61.50±4.18
	ILF-EP	4.85±0.40	2.08±0.52	21.60±12.28	1.02±0.11	16.44±4.85	71.90±3.52
	ICLF	5.67±0.09	1.83±0.39	47.70±4.67	1.12±0.11	31.50±5.18	44.50±3.71
5.25	ILF-ST	5.40±0.47	1.60±1.15	34.50±18.36	1.05±0.09	24.00±3.79	58.50±5.48
	ILF-EP	4.85±0.38	0.93±0.23	19.04±11.72	1.03±0.09	16.50±9.45	66.50±6.98
	ICLF	5.95±0.02	3.91±1.82	54.01±2.43	1.13±0.06	31.50±3.35	43.00±3.26
21.00	ILF-ST	5.28±0.63	0.71±0.35	30.00±23.01	0.96±0.13	29.00±10.09	50.00±7.71
	ILF-EP	5.10±0.39	0.60±0.27	20.47±10.75	0.95±0.11	14.00±6.75	68.50±6.02
	ICLF	6.03±0.05	3.00±1.21	55.84±3.35	1.12±0.04	29.00±6.52	51.00±5.18
	ICL	5.83±0.03	2.62±0.63	49.61±3.49	1.04±0.04	24.50±2.85	60.50±10.22
	IP	5.48±0.37	0.68±0.41	37.99±11.71	0.81±0.21	26.50±10.98	54.50±11.65
	MP	4.92±0.44	1.15±0.66	18.84±16.71	1.04±0.05	24.00±3.26	63.00±2.74
	HP	5.00±0.48	0.72±0.34	25.12±15.78	0.99±0.20	25.00±8.18	44.50±5.70
	NF	4.45±0.08	1.53±0.27	4.39±0.76	0.90±0.08	28.50±4.81	58.50±4.18
		---------- 20-40 cm ----------					
0.00	ILF-ST	5.55±0.36	2.20±0.57	41.73±12.20	1.03±0.14	18.50±3.71	67.50±3.06
	ILF-EP	4.83±0.39	1.74±0.68	15.58±12.00	1.07±0.11	13.84±5.14	72.40±6.43
	ICLF	5.42±0.20	1.88±0.33	37.49±5.92	1.02±0.30	26.50±4.54	46.50±3.79
5.25	ILF-ST	4.94±0.51	1.17±0.47	20.73±18.30	1.12±0.13	20.50±5.59	65.50±4.11
	ILF-EP	4.69±0.12	0.83±0.55	9.27±3.15	1.16±0.18	13.00±7.71	70.00±5.30

Distance‡	Area	pH_{H2O}	P	BS	BD	Sand	Clay
m			mg dm^{-3}	%	g cm^{-3}	dag kg^{-1}	
21.00	ICLF	5.84±0.18	2.43±1.01	50.99±5.67	1.14±0.10	30.00±3.71	48.00±3.71
	ILF-ST	5.08±0.56	0.91±0.39	25.82±19.16	1.04±0.14	18.00±5.86	67.00±8.37
	ILF-EP	4.71±0.10	0.42±0.16	7.61±2.72	1.04±0.14	11.84±5.64	75.40±4.63
	ICLF	5.95±0.04	1.99±0.84	52.15±2.89	1.18±0.03	30.50±3.95	50.00±4.33
	ICL	5.82±0.13	1.85±0.34	48.89±4.76	1.00±0.06	20.50±2.50	56.00±2.24
	IP	5.23±0.44	1.30±0.41	30.17±14.05	0.87±0.18	19.50±9.78	59.00±11.12
	MP	4.69±0.08	1.08±0.37	9.90±5.42	1.01±0.06	23.50±3.79	63.50±6.75
	HP	4.65±0.09	1.04±0.39	12.40±6.44	1.16±0.08	25.00±7.37	46.00±8.02
	NF	4.40±0.02	1.25±0.11	5.04±0.50	0.87±0.09	22.50±2.09	50.00±7.71

† The soil properties were determined by the methods described in Teixeira et al. (2017). Clay contents for ILF-ST, ILF-EP and NF from Cipriani, Salman, da Cruz, et al. (2025), whereas MP values were directly measured. ‡ Distance from the trees in the tree-integrated systems.

4.2.1.1 Integrated livestock-forestry (ILF) systems

The experiments were initiated in February 2018 with the establishment of trees in a palisade grass pasture [*Urochloa brizantha* (Hochst. Ex A. Rich.) R. Webster 'Marandu'], resulting in two low-tree-density integrated livestock–forestry (ILF) systems: one with *Eucalyptus pellita* F. Muell (ILF-EP) and another with *Samanea tubulosa* (Benth.) Barneby & J.W. Grimes (ILF-ST).

In each ILF system, trees were planted in a single tree strip functioning primarily as a windbreak, composed of two rows approximately 300 m long, with spacing of 6.0 m between rows and 3.5 m between trees within rows, oriented along an azimuth of 320° (NW–SE). Considering the total area of each ILF system (12.8 ha), the initial tree density was approximately 13 trees ha^{-1}, with 171 trees planted in each system. The *E. pellita* and *S. tubulosa* strips were separated by approximately 240 m (Figure 2.1).

The planting was done manually, using post hole diggers and 30 cm-tall cuttings (*E. pellita*) and seedlings (*S. tubulosa*), 30 days after desiccating the pasture in the strip area with glyphosate. Fertilization was done with chemical NPK + micronutrients fertilizer (350 g $plant^{-1}$) applied in the holes, just before planting, and as top-dressing applications (twice annually in 2018 and 2019, and once annually from 2020 to 2023). The mean total height of the trees was 5.9 m (*S. tubulosa*), and 19.8 m (*E.* pellita), and mean canopy diameter was 8.4 m (*S. tubulosa*), and 5.8 m (*E. pellita*), at the time of soil sampling (Cipriani et al. 2023; Oliveira et al. 2021; Welke et al. 2022).

The palisade grass was established before 1970, i.e., more than 40 years before tree planting, and its grazing management was carried out using 4 paddocks of 3.2 ha. The animals used were of the Girolando breed (dry cows and heifers) with ad libittum intake of salt and water. Grazing management followed a mob grazing strategy, in which animals were maintained at high stocking density for short occupation periods followed by adequate pasture recovery intervals. Average annual stocking rate was approximately two animal units per hectare in both ILF-ST and ILF-EP systems. Whole-area pasture fertilization and liming were rare, with the most recent application occurring five years before the planting of the trees.

4.2.1.2 Integrated crop-livestock (ICL) and integrated crop-livestock-forestry (ICLF) systems

From earlier than 1970 to 2008, the area where the ICL and ICLF was established (approximately 6 ha each) was occupied by a variety of pastures, such as *Andropogon gayanus* Kunth, *U. humidicola*, Mombaça grass [*Megathyrsus maximus* (Jacq.) BK Simon & SWL Jacobs] and Marandu grass. From 2008 to 2012, the areas served for experiments on no-till and cover crop succession, including, maize, rice, soybean, sorghum and *U. ruziziensis* (Townsend et al. 2013). From 2012 to 2020 the soybean/maize+*Urochloa* succession was used annually or every two years (Ribeiro et al. 2020). In 2020, *U. brizantha* x *U. ruziziensis* 'Ipyporã' pasture was established on no-till, remaining until soil sampling date.

The ICLF was established in March 2013, with the planting of *Eucalyptus* spp. cuttings in seven strips, with four rows of 240 m each. Three tree arrangements (subsystems) were adopted, with 18, 30, and 42 m between strips, following an azimuth of 210° (NE–SW) (Feitosa et al. 2019, 2022). From late 2018 to early 2019, the eucalyptus trees were harvested and *E. pellita* seedlings were planted in between-rows, resulting in seven strips with two rows of trees each, and tree densities of 267, 180, and 136 trees ha^{-1}, for the subsystems with 18, 30, and 42 m between strips, respectively. Nevertheless, only the subsystem with 42 m between strips (136 trees ha^{-1}) was considered in the present study.

Soil preparation and fertilization for tree planting were as described for the ILF systems. The alleys between strips were managed as the ICL. The mean total height of the trees was between 10.2 and 12.4 m, and mean diameter at 1.30 m from the soil (DBH) was between 13.9 and 16.5 cm at the time of soil sampling.

4.2.1.3 Treeless pastures

Three treeless pasture systems were assessed, which are differentiated mainly by the variety of pasture: *U. humidicola* (HP), Marandu grass (MP) and Ipyporã grass (IP). The establishment date of HP and MP occurred 40 to 30 years before soil sampling. The Ipyporã grass was planted in 2019 on an area formerly occupied by Marandu grass and *U. humidicola.* The three treeless pasture areas can be considered moderately managed, rarely receiving liming and fertilization and with moderate grazing intensity.

4.2.1.4 Native forest fragment (NF)

An unmanaged NF fragment from the same experimental field was included as a reference area to represent baseline conditions without human intervention. The fragment spans 41 ha of primary tropical rainforest, containing 99 woody species and 258 individuals per hectare. *Sclerolobium paniculatum*, *Psidium araca*, *Eschweilera grandiflora*, *Licania heteromorpha*, and *Protium puncticulatum* comprise 35 % of the relative density in the fragment (Bentes-Gama et al. 2009).

4.2.2 Soil sampling

Soil samples were collected with a Dutch auger in April 2024 (rainy season) from the 0-10, 10-20, and 20-40 cm layers. In the ILF and ICLF systems, samples were taken at three distances from the tree rows: 0.00 m (the planting line), 5.25 m, and 21.00 m. The 5.25 and 21.00 m distances were chosen for standardization, as they correspond to one-eighth and one-half of the 42 m inter-row spacing used in previous studies conducted within the same ICLF system (Feitosa et al. 2019, 2022). Furthermore, these distances are representative of intermediate and distal zones among those adopted by studies assessing the influence of trees on pasture and soil attributes in integrated systems.

The spatial distribution of sampling points was planned to ensure representativeness and minimize edge effects within the experimental areas. In NF, the five sampling points were established along a transect parallel to the boundary road, with each point located more than 30 m from the edge to avoid external influences. Successive samples were collected approximately every 30 m along this transect to ensure spatial independence. In the treeless systems (ICL and pastures), the five sampling points were distributed randomly across the area, while maintaining

a minimum distance of 30 m from the edges and between points. In the ILF and ICLF systems, the five sampling points for each distance (0.00 m, 5.25 m and 21.00 m) were positioned along the tree rows. A 30 m buffer zone was maintained from both the start and the end of the rows. Samples were collected at intervals of approximately 30 m along the row, alternating the collection between the NE and SW sides of the planting line. Subsamples for soil permanganate oxidizable carbon (POXC) analysis were placed in a cooler and stored at 7 °C. Soil samples for other analysis were air-dried, ground, sieved (2 mm) and stored at room temperature.

Five composite samples (prepared from two simple samples each) were taken per area, depth and distance, summing up 210 composite samples. Specifically, the NF, ICL and pasture areas (HP, IP and MP) contributed with 15 samples each (3 depths x 5 replicates), while the two ILF and the ICLF areas contributed with 45 samples each, factoring in the three distance levels (3 distances x 3 depths x 5 replicates).

4.2.3 Total soil C content, stock and isotopic composition

For the analyses of soil C and ^{13}C, approximately 5 g subsamples were macerated and homogenized to pass through a 0.250 mm sieve. The analyses were conducted with an elemental analyzer coupled with a mass spectrometer (Thermo Scientific, EA IsoLink™ CN IRMS System; Bremen, Germany) at the Laboratório de Isótopos Estáveis, Centro de Energia Nuclear na Agricultura of Universidade de São Paulo (USP/CENA), Piracicaba, São Paulo state, Brazil. The stable isotope results were reported as $\delta^{13}C$ (‰), using the international standard Vienna PeeDee Belemnite (V-PDB; NBS19 and NBS22), and were calculated using the equation proposed by (Farquhar; O'Leary; Berry, 1982):

$$\delta^{13}C = \left(\frac{R_{sample}}{R_{standard}} - 1\right) \times 1000 \quad (1)$$

where: R_{sample} is the $^{13}C/^{12}C$ ratio of the samples; $R_{standard}$ is the $^{13}C/^{12}C$ ratio of the standards.

Soil C stocks (SCS) were calculated by multiplying bulk density, layer thickness, and soil C contents (SCC), with correction for bulk density differences by an equivalent mass method (Ellert and Bettany 1995), using NF as reference. Soil C contents were expressed in dag kg^{-1}, and C stocks were expressed in t ha^{-1}.

4.2.4 Soil organic and active carbon

Soil organic carbon (SOC) content (dag kg^{-1}) was determined using the Walkley-Black wet oxidation method (Walkley and Black 1934), assuming a correction factor of 1.33 to account for the incomplete oxidation inherent in the Walkley-Black procedure (Jackson 1982).

Permanganate oxidizable carbon (POXC), an indicator of active soil carbon, was determined according to the method described by (Weil et al. 2003), with minor modifications. Briefly, 2.5 g of fresh soil were reacted with 20 mL of a 0.02 mol L^{-1} potassium permanganate ($KMnO_4$) solution in a 50 mL centrifuge tube. The tubes were shaken on a reciprocal shaker at 180 oscillations per minute for 2 min. After shaking, the soil-permanganate suspension was allowed to settle for 10 min. A 0.5 mL aliquot of the supernatant was then transferred to a separate tube containing 49.5 mL of deionized water to achieve a 1:100 dilution. Reference samples, containing $KMnO_4$ solution but no soil, were run concurrently. The absorbance of the diluted supernatant was measured at 540 nm using a spectrophotometer.

The amount of $KMnO_4$ reduced by the soil sample was calculated from the decrease in absorbance relative to the initial concentration of the $KMnO_4$ solution. POXC was then calculated using the following equation:

$$POX = \left(1 - \frac{ABS_{sample}}{ABS_{reference}}\right) 1{,}440 \quad (2)$$

Where POXC is the permanganate oxidizable carbon (mg C kg^{-1} soil) in the sample, ABS_{sample} and $ABS_{reference}$, are de absorbances of the samples and references, respectively, and 1,440 is a factor that accounts for the molecular weight of carbon (12 g mol^{-1}),the volume of $KMnO_4$ used (0.02 L), the concentration of $KMnO_4$ solution (0.02 mol L^{-1}), the conversion from moles to mg, and the quantity of soil used (0.0025 kg). Results were expressed on an oven-dry soil basis.

4.2.5 Organic matter humification index

Laser-induced fluorescence spectroscopy (LIFS) measurements were conducted using soil pellets, where 0.4 g of each sample was pressed with hydraulic press (5 t) for 1 min to obtain a soil pellet, with two pellets prepared per sample. The spectra acquisition utilized a continuous wave laser (maximum power of 20 mJ) with excitation at 405 nm, described by Santos et al. (2015).

The experimental parameters defined were: integration time = 650 ms; spectral averages = four per reading; boxcar = 8 (spectral smoothing parameter); four spectra collected per sample (one at each side of the pellets); and spectral area obtained from the integration of the 460 to 850 nm spectra.

The average value of the spectral integrated area was used in the calculation of the OM humification index (H_{LIFS}) proposed by (Milori et al. 2006), using the ratio of emission area under fluorescence spectrum and total carbon content as follows:

$$H_{LIFS} = \frac{A_{LIFS}}{C_{total}} \quad (3)$$

Where H_{LIFS} is the OM humification index (nondimensional), A_{LIFS} is the average area under fluorescence spectrum, and C_{total} is the total carbon content (mg C kg^{-1} soil) of the sample, determined by an elemental analyzer, as previously described.

4.2.6 Carbon management index

The Carbon Management Index (CMI) was used to evaluate changes in soil carbon quality and quantity due to different land-use systems. The CMI was calculated following the methodology proposed by Blair et al. (1995), for the 0-40 cm soil layer. The native forest (NF) was selected as the reference area, with its CMI set at 100.

The CMI is derived from two key components: the Carbon Pool Index (CPI) and the Lability Index (LI). The CPI was calculated to assess the quantity of total soil carbon relative to the reference area using the following equation:

$$CPI_i = \frac{SCC_i}{SCC_{NF}} \quad (4)$$

Where CPI_i is the carbon pool index of a given system, SCCi is the total soil carbon content of a given system and SCC_{NF} is the total carbon content in NF soil, determined by an elemental analyzer, as previously described.

The Lability Index (LI) was used to quantify the qualitative changes in soil carbon pools. It was calculated as the ratio of the lability of a given system to the lability of the reference area. Lability (L) was defined as the ratio of labile carbon to non-labile carbon, calculated as follows:

$$L = \frac{Labile\ carbon}{Non - labile\ carbon} \quad (5)$$

Permanganate oxidizable carbon (POXC) was used as the indicator of the labile carbon fraction. The non-labile carbon fraction was determined by subtracting the POXC from the total C (SCC - POXC). The LI was then calculated using the following equation:

$$LI_i = \frac{L_i}{L_{NF}} \quad (6)$$

Where LI_i is the Lability Index of a given system, L_i is the lability of a given system and L_{NF} is the lability of NF.

Finally, CMI for each system was calculated using the following equation:

$$CMI_i = CPI_i \times LI_i \times 100 \quad (7)$$

Where CMI_i is the carbon management index of a given system, CPI_i is the Lability Index of that system and 100 is a factor to express CMI_i as a percentage relative to NF.

4.2.7 Statistical analysis

The statistical analyses were performed using the following experimental design: 3 tree-integrated systems (ILF-EP, ILF-ST and ICLF) × 3 distances from the trees (0.00, 5.25 and 21.00 m) + 5 additional treatments (ICL, IP, MP, HP and NF), with 5 replicates. Each soil layer (0-10, 10-20 and 20-40 cm) was analyzed separately, except for carbon stock (SCS) and carbon management index (CMI), which corresponded to the 0-40 cm layer.

After checking for the assumptions of homoscedasticity and normality, outlier removal, and application of the Box-Cox transformation (when necessary), the means of soil C contents, stocks and isotopes, and CPI, LI and CMI were subjected to ANOVA. Regression analysis was then performed to evaluate the effect of distance within the tree-integrated systems. Comparisons among ILFs and ICLF, within distances, were made using Tukey's test. For comparisons among the treeless systems and NF (additional treatments), Tukey's test was also used. To compare the combinations of tree-integrated systems and distances relative to treeless systems and NF, Dunnett's test was applied. To compare the CPI, LI and CMI means of each system with NF, the two-tailed one-sample t-test with FDR correction for multiple comparisons (Benjamini-Hochberg procedure) was used.

For POXC and H_{LIFS}, since Box-Cox transformation was ineffective, the Dunn’s test with FDR correction post hoc Kruskal-Wallis was used for comparisons among ILF and ICLF systems, within distances; among the treeless systems (additional treatments); and to compare

the combinations of tree-integrated systems and distances relative to the treeless systems and NF (totaling 64 pairwise comparisons). For distances within tree-integrated systems, firstly the aligned rank transformation (ART) was used to test the significance of the factor Distance and the interaction System x Distance (Wobbrock et al. 2011). If significant (the main factor or the interaction), a robust regression analysis was then performed to evaluate the effect of distance within the tree-integrated systems, using a median-based linear model (Siegel repeated medians).

To account for potential textural variations among the experimental areas, an analysis of covariance (ANCOVA) was performed using clay content as a covariate. For most variables (SCC, SCS, SOC, POXC, HLIFS, and CMI), clay content did not show a significant effect; for $\delta^{13}C$ in the 20-40 cm layer, the significance was marginal ($p = 0.048$). These results indicate that the observed differences in soil carbon dynamics were primarily driven by management practices rather than soil texture. The 5 % significance level was adopted in all analyses. Analyses were performed with the aid of Minitab 22 software and R packages: Tratamentos.ad (Azevedo 2022), dunn.test (Dinno 2024), ARTool (Kay et al. 2025) and mblm (Komsta 2019). Graphics were constructed with Origin 2025 software.

4.3 Results

4.3.1 Soil C content and isotopic composition

In the superficial layer (0-10 cm), the differences in SCC were less pronounced compared to the deeper layers (Table 4.2). Among tree-integrated systems, the ICLF system showed the lowest SCC levels (2.25 dag kg^{-1} on average). Conversely, SCC tended to increase with increasing distance in ILF-ST (Table 4.3), resulting in the ILF-ST at 21.00 m from the tree line exhibiting the highest SCC among all managed areas (4.35 dag kg^{-1}). Notably, except for the ILF-ST at 21.00 m treatment, the SCC in native forest (2.72 dag kg^{-1}) was not significantly different from most pasture or integrated systems.

Table 4.2 - Soil carbon content (SCC) and Isotopic composition ($\delta^{13}C$) for soil layers (0-10, 10-20 and 20-40 cm) across different land-use systems (mean ± standard deviation). ILF-ST: integrated livestock-forestry with *Samanea tubulosa*. ILF-EP: integrated livestock-forestry with *Eucalyptus pellita*. ICLF: integrated crop-livestock-forestry. ICL: integrated crop-livestock. IP: *Urochloa brizantha* x *U. ruziziensis* 'Ipyporã' pasture. MP: *U. brizantha* 'Marandu' pasture. HP: *U. humidicola* pasture. NF: native forest.

Variable	Distance	Area	Layer		
	m		0-10 cm	10-20 cm	20-40 cm
SCC (dag kg^{-1})	0.00	ILF-ST	3.06±0.22 A	2.96±0.30 A†‡§	3.01±0.32 A$^{\dagger\ddagger\#\S\P}$
		ILF-EP	3.04±0.15 A	2.86±0.18 A§	2.61±0.30 A†§
		ICLF	2.25±0.32 B	1.79±0.39 B$^{\#\P}$	1.35±0.23 B$^{\ddagger\#}$
	5.25	ILF-ST	3.11±0.29 A	2.91±0.27 A§	2.43±0.35 A§
		ILF-EP	2.98±0.26 A§	2.72±0.32 A§	2.32±0.48 A§
		ICLF	2.13±0.08 B	1.83±0.12 B$^{\#\P}$	1.35±0.23 B$^{\ddagger\#}$
	21.00	ILF-ST	4.35±1.03 A$^{\dagger\ddagger\#\S\P}$	3.66±0.95 A†‡§¶	2.85±0.29 A†§¶
		ILF-EP	3.12±0.65 A	3.05±0.67 AB†‡§	2.32±0.84 AB§
		ICLF	2.37±1.08 B	2.52±0.21 B$^{\#}$	1.46±0.38 B
		ICL	2.60±0.37 a	2.22±0.40 ab	1.81±0.43 ab
		IP	2.87±0.80 a	2.21±0.37 ab	2.17±0.67 a
		MP	2.75±1.04 a	2.71±0.79 a	2.15±0.42 a
		HP	2.16±0.14 a	1.71±0.18 b	1.38±0.28 b
		NF	2.83±0.75 a	2.49±0.32 a	1.93±0.34 ab
$\delta^{13}C$ (‰)	0.00	ILF-ST	-22.94±1.09 A¶	-23.40±0.75 B¶	-23.63±0.70 B¶
		ILF-EP	-22.30±1.54 A¶	-22.06±1.24 AB¶	-22.69±0.84 B¶
		ICLF	-20.68±0.95 A§¶	-20.39±1.25 A$^{\#\S\P}$	-19.99±1.30 A$^{\ddagger\#\P}$
	5.25	ILF-ST	-23.62±1.08 B¶	-23.66±0.51 B¶	-24.48±0.49 B†¶
		ILF-EP	-23.41±2.48 B¶	-22.36±1.36 B¶	-22.82±1.27 B¶
		ICLF	-19.75±0.87 A$^{\#\S\P}$	-20.42±0.93 A$^{\#\S\P}$	-19.58±1.09 A$^{\ddagger\#\S\P}$
	21.00	ILF-ST	-23.14±1.68 B¶	-23.28±1.26 B¶	-23.97±0.87 B¶
		ILF-EP	-21.50±1.58 AB¶	-22.11±1.27 AB¶	-22.90±1.17 B¶
		ICLF	-19.95±0.63 A$^{\#\S\P}$	-20.36±0.71 A$^{\#\S\P}$	-19.29±0.54 A$^{\dagger\ddagger\#\S\P}$
		ICL	-21.73±2.76 a	-21.81±2.04 a	-21.79±2.37 a
		IP	-22.58±2.08 a	-22.50±0.83 a	-24.99±2.22 b
		MP	-22.96±1.85 a	-23.54±1.82 a	-23.91±1.61 ab
		HP	-23.58±1.62 a	-23.26±1.78 a	-22.35±2.30 a
		NF	-28.04±0.34 b	-27.94±0.35 b	-27.49±0.13 c

Data were analyzed by factorial ANOVA at the 5 % significance level. Tukey's test was used to compare tree-integrated systems within distances (capital letters), and treeless systems and NF among themselves (lowercase letters). Systems sharing the same letters do not differ statistically. Dunnett's test was used to compare treeless systems with tree-integrated systems (the symbols †, ‡, $^{\#}$, § and ¶ indicate a significant difference relative to ICL, IP, MP, HP and NF, respectively).

In the intermediate (10-20 cm) and deepest (20-40 cm) layers, the differentiation among areas was clearer. ILF-ST and ILF-EP maintained the highest SCCs in these depths, while ICLF and HP generally exhibited the lowest values. The ILF-ST and ICLF systems showed a

significant distance effect at the 10-20 cm layer, with SCC significantly increasing with increasing distance from the tree line. Moreover, at the 20-40 cm layer, SCC showed a quadratic effect with distance in ICLF, decreasing at 5.25 m, but increasing farther from the tree line. Remarkably, except for ICLF and HP in the 10-20 cm layer, the differences in SCC between NF and other areas were not statistically significant, being even higher in ILF-ST in some comparisons.

Table 4.3 - Regression equations and determination coefficients (R^2) for soil carbon content (SCC) as a function of distance from trees in tree-integrated systems and soil layer (0-10, 10-20 and 20-40 cm)†. ILF-ST: integrated livestock-forestry with *Samanea tubulosa*; ILF-EP: integrated livestock-forestry with *Eucalyptus pellita*; ICLF: integrated crop-livestock-forestry; ns: non-significant.

Layer	Area	Equation	$R^{2‡}$
0-10 cm	ILF-ST	$Y = 2.932 + 0.066x$	0.956
	ILF-EP	ns	--
	ICLF	ns	--
10-20 cm	ILF-ST	$Y = 2.859 + 0.036x$	0.910
	ILF-EP	ns	--
	ICLF	$Y = 1.725 + 0.037x$	0.962
20-40 cm	ILF-ST	$Y = 3.005 - 0.144x + 0.006x^2$	1.000
	ILF-EP	ns	--
	ICLF	ns	--

† For each sampling year, only indicators with a significant effect of distance ($p < 0.05$) in at least one management system are presented. ‡ The R^2 values of 1.000 for quadratic models result from the number of distance levels ($n = 3$) being equal to the number of estimated model parameters.

The carbon isotopic composition ($\delta^{13}C$) showed significant variation across land-use systems and soil depths (Table 4.2). In all layers, the native forest (NF) fragment exhibited the most negative $\delta^{13}C$ (approximately -28 ‰), significantly different from all managed systems. Conversely, the less negative values were observed in the integrated crop-livestock-forestry (ICLF) system (approximately -20 ‰). In the 0-10 and 10-20 cm layers, average $\delta^{13}C$ values ranged from -23 to -20 ‰, approximately, among managed systems.

The values for ILF-ST and ILF-EP, in general, were significantly more negative than those of ICLF system. Differences among systems were clearer in the deepest layer (20-40 cm). ICLF consistently remained the most ^{13}C-enriched system (approximately -19.6 ‰) among the tree-integrated treatments, being statistically different from ILF-ST and ILF-EP at all distances. Also, ICL and Humidicola pasture (HP) mean $\delta^{13}C$ values (-21.8 ‰ and -22.4 ‰, respectively) were significantly higher than Ipyporã pasture (IP) mean $\delta^{13}C$ (-25.0 ‰). No significant effect of distance was observed on $\delta^{13}C$ in any layer.

4.3.2 Soil C stock

The soil carbon stock (SCS), calculated for the 0-40 cm soil layer, showed significant variation across the distinct land-use systems (Figure 4.1). Tukey's test showed that the treeless systems grouped into distinct categories: the MP system maintained the highest SCS (84.8 t ha^{-1}), being statistically similar to NF (78.1 t ha^{-1}), IP (76.4 t ha^{-1}) and ICL (74.4 t ha^{-1}); the HP system showed the lowest SCS among all systems evaluated (59.0 t ha^{-1}), being statistically lower than MP.

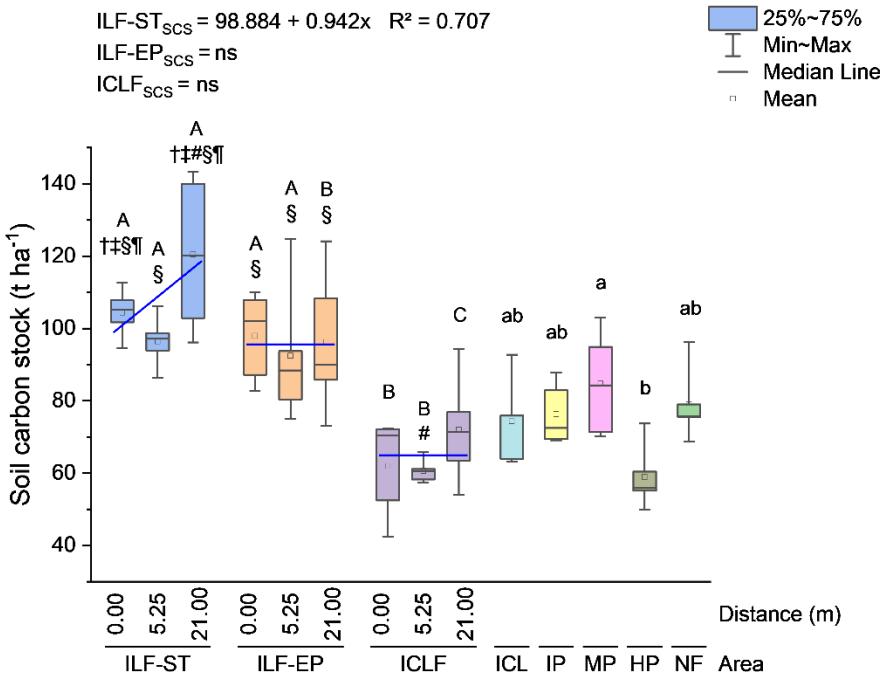

Figure 4.1 - Soil carbon stock (SCS) in the 0-40 cm layer across different land-use systems. Data were analyzed by factorial ANOVA at the 5 % significance level. Capital letters compare tree-integrated systems within the same distance. Lowercase letters compare treeless systems and NF among themselves. Systems sharing the same letters do not differ statistically, according to the Tukey's test. The symbols †, ‡, #, § and ¶ indicate a significant difference relative to ICL, IP, MP, HP and NF, respectively, according to the Dunnett's test. Blue lines and text represent the linear regression analysis used to evaluate the effect of distance from the tree line within the tree-integrated systems. The equation and R^2 are provided for significant regressions. ns: non-significant regression. ILF-ST: integrated livestock-forestry with *Samanea tubulosa*. ILF-EP: integrated livestock-forestry with *Eucalyptus pellita*. ICLF: integrated crop-livestock-forestry. ICL: integrated crop-livestock. IP: *Urochloa brizantha* x *U. ruziziensis* 'Ipyporã' pasture. MP: *U. brizantha* 'Marandu' pasture. HP*: U. humidicola* pasture. NF: native forest. SCS values are corrected for bulk density differences by an equivalent mass method, using NF as reference.

The ILF-ST system was the only system to show a significant linear effect of distance on SCS, which increased with increasing distance. The ILF-ST at 21.00 m recorded the highest average SCS of all treatments (120.5 t ha^{-1}). The ILF-EP and ICLF systems showed no

significant linear relationship between SCS and distance, recording 95.6 (ILF-EP) and 64.9 (ICLF) t ha^{-1} on average. At the 0.00 m distance (closest to the tree line), the ILF-ST and ILF-EP systems maintained the highest SCS (104.4 and 98.0 t ha^{-1}, respectively) and were statistically similar. The ICLF system showed a significantly lower SCS (62.0 t ha^{-1}). At the 21.00 m distance, the ILF-ST system maintained the highest SCS, being statistically higher than ILF-EP (96.3 t ha^{-1}), which was also statistically higher than ICLF (72.0 t ha^{-1}).

The comparison of tree-integrated systems against the treeless systems revealed the following: the ILF-ST system at 21.00 m maintained SCS values significantly higher than all treeless systems and even the NF; at 0.00 m, the ILF-ST was statistically similar only to MP; at 5.25 m, ILF-ST was statistically superior to only to HP; the ILF-EP system was also significantly higher than HP, at all distances. Conversely, the ICLF system (at all distances) showed the lowest performance among the tree-integrated systems, being statistically lower than MP at 5.25 m, but statistically similar to all treeless systems and NF at 0.00 and 21.00 m.

4.3.3 Soil organic and active carbon

The soil organic carbon (SOC) content showed significant variation across land-use systems and soil depths, with distinct patterns observed in the tree-integrated systems (Table 4.4). In the topsoil, the ILF-ST and MP systems maintained the highest SOC levels among all treatments (mean of 2.27 and 2.33 dag kg^{-1}, respectively). MP and NF exhibited the highest SOC among the treeless systems, while ICL, IP and HP showed lower values (1.62, 1.60 and 1.38, respectively), but still statistically similar to NF (1.85 dag kg^{-1}). The ILF-EP and ICLF systems, showed significantly lower SOC (mean of 1.74 and 1.52 dag kg^{-1}, respectively) than ILF-ST and MP, but statistically similar values than NF, ICL, IP and HP.

The differentiation of SOC among systems remained pronounced in the intermediate layer. ILF-ST and MP maintained the highest SOC contents (mean of 2.10 and 1.97 dag kg^{-1} respectively). ICLF showed the lowest SOC among the integrated systems (1.17 dag kg^{-1}). The NF fragment maintained the second highest SOC among the additional treatments (1.78 dag kg^{-1}). The IP and HP systems recorded the lowest SOC (1.25 and 1.07 da kg^{-1}, respectively), often being statistically similar to the lowest-performing tree-integrated system (ICLF).

In the deepest layer, the SOC content continued to reflect the differences in management, although the range of values narrowed. MP and NF maintained the highest SOC among the additional treatments (1.57 and 1.55 dag kg^{-1}, respectively), whereas IP and HP

recorded the lowest SOC (1.13 and 0.87 dag kg^{-1}, respectively). The ILF-ST system, especially at 21.00 m, in which mean SOC was 2.20 dag kg^{-1}, maintained SOC values significantly higher than most systems, whereas ICLF showed the lowest values among the tree-integrated systems (mean of 0.97 dag kg^{-1}).

Table 4.4 - Soil organic carbon (SOC) content for soil layers (0-10, 10-20 and 20-40 cm) across different land-use systems (mean ± standard deviation, dag kg^{-1}). ILF-ST: integrated livestock-forestry *with Samanea tubulosa*. ILF-EP: integrated livestock-forestry with *Eucalyptus pellita*. ICLF: integrated crop-livestock-forestry. ICL: integrated crop-livestock. IP: *Urochloa brizantha* x *U. ruziziensis* 'Ipyporã' pasture. MP: *U. brizantha* 'Marandu' pasture. HP: *U. humidicola* pasture. NF: native forest.

Distance	**Area**	**Layer**		
m		0-10 cm	10-20 cm	20-40 cm
0.00	ILF-ST	2.31±0.27 $A^{\dagger\ddagger\S}$	2.16±0.15 $A^{\dagger\ddagger\S}$	1.93±0.16 $A^{\dagger\ddagger\S}$
	ILF-EP	1.82±0.14 $B^{\#}$	1.74±0.22 $B^{\ddagger\S}$	1.50±0.30 $B^{\S}$
	ICLF	1.54±0.23 $B^{\#}$	1.19±0.22 $B^{\ddagger\P}$	0.96±0.10 $C^{\#\P}$
5.25	ILF-ST	1.97±0.17 $A^{\S}$	1.74±0.18 $A^{\ddagger\S}$	1.50±0.20 $A^{\S}$
	ILF-EP	1.67±0.09 $AB^{\#}$	1.53±0.11 $B^{\S}$	1.31±0.19 $AB^{\S}$
	ICLF	1.50±0.13 $B^{\#}$	1.15±0.04 $B^{\ddagger\P}$	1.02±0.14 $B^{\#\P}$
21.00	ILF-ST	2.51±0.40 $A^{\dagger\ddagger\S\P}$	2.40±0.46 $A^{\dagger\ddagger\S}$	2.20±0.40 $A^{\dagger\ddagger\#\S\P}$
	ILF-EP	1.75±0.26 $B^{\#}$	1.54±0.23 $B^{\S}$	1.20±0.18 B
	ICLF	1.53±0.16 $B^{\#}$	1.16±0.22 $C^{\ddagger\P}$	0.95±0.12 $B^{\#\P}$
	ICL	1.62±0.28 b	1.47±0.26 bc	1.23±0.25 ab
	IP	1.60±0.16 b	1.25±0.08 c	1.13±0.18 b
	MP	2.33±0.68 a	1.97±0.54 a	1.57±0.22 a
	HP	1.38±0.10 b	1.07±0.14 c	0.87±0.11 b
	NF	1.85±0.40 ab	1.78±0.35 ab	1.55±0.32 a

Data were analyzed by factorial ANOVA at the 5 % significance level. Tukey's test was used to compare tree-integrated systems within distances (capital letters), and treeless systems and NF among themselves (lowercase letters). Systems sharing the same letters do not differ statistically. Dunnett's test was used to compare treeless systems and NF with tree-integrated systems (the symbols †, ‡, $^{\#}$, § and ¶ indicate a significant difference relative to ICL, IP, MP, HP and NF, respectively).

The spatial distribution of SOC content was significantly influenced by the management system and soil depth, with varying regression models adjusted for each layer (Table 4.5). In the uppermost soil layer (0-10 cm), only the ILF-ST system exhibited a significant response to distance from the trees, following a quadratic model, with lower SOC content in the intermediate distance.

At the intermediate layer (10-20 cm), distinct spatial patterns emerged between the forestry-integrated systems. The ILF-ST system maintained a quadratic behavior, while the ILF-EP system showed a linear decrease in carbon content as the distance from the *Eucalyptus pellita* trees increased. Similar to the surface layer, the ICLF system did not show a significant regression adjustment for SOC at this depth. In the deepest evaluated layer (20-40 cm), significant spatial variation was exclusively observed in the ILF-ST system, where the SOC content adjusted to a quadratic model.

Table 4.5 - Regression equations and determination coefficients (R^2) for soil organic carbon (SOC) content (dag kg^{-1}) as a function of distance from trees in tree-integrated systems and soil layers (0-10, 10-20 and 20-40 cm). ILF-ST: integrated livestock-forestry with *Samanea tubulosa*; ILF-EP: integrated livestock-forestry with *Eucalyptus pellita*; ICLF: integrated crop-livestock-forestry; ns: non-significant ($p > 0.05$).

Layer	Area	Equation	$R^{2\dagger}$
0-10 cm	ILF-ST	$Y = 2.315 - 0.091x + 0.005x^2$	1.000
	ILF-EP	ns	--
	ICLF	ns	--
10-20 cm	ILF-ST	$Y = 2.161 - 0.111x + 0.006x^2$	1.000
	ILF-EP	$Y = 1.450 - 0.013x$	0.828
	ICLF	ns	--
20-40 cm	ILF-ST	$Y = 1.929 - 0.114x + 0.006x^2$	1.000
	ILF-EP	ns	--
	ICLF	ns	--

† The R^2 values of 1.000 for quadratic models result from the number of distance levels ($n = 3$) being equal to the number of estimated model parameters.

The permanganate oxidizable carbon (POXC), which represents the labile C fraction, varied significantly across land-use systems and soil depths (Table 4.6). The native forest (NF) fragment, the integrated crop-livestock system (ICL) and silvopastoral system with *S. tubulosa* (ILF-ST) consistently maintained the highest POXC content across all three soil layers (0-10, 10-20, and 20-40 cm).

In contrast, the lowest POXC values were observed in the pasture with *U. humidicola* (HP) and the integrated crop-livestock-forestry system (ICLF), particularly farther from the tree line (5.25 and 21.00 m distances). The pastures with ipyporã (IP) and marandu (MP) grasses, and and the silvopastoral system with *E. pellita* presented intermediate POXC levels. In general, observed POXC contents decreased with increasing depth (502.93, 422.92 and 360.40 mg kg^{-1} on average for the 0-10, 10-20 and 20-40 cm layers, respectively).

Table 4.6 - Permanganate oxidizable carbon (POXC) for soil layers (0-10, 10-20 and 20-40 cm) across different land-use systems (median ± interquartile range, mg kg^{-1}). ILF-ST: integrated livestock-forestry with *Samanea tubulosa*. ILF-EP: integrated livestock-forestry with *Eucalyptus pellita*. ICLF: integrated crop-livestock-forestry. ICL: integrated crop-livestock. IP: *Urochloa brizantha* x *U. ruziziensis* 'Ipyporã' pasture. MP: *U. brizantha* 'Marandu' pasture. HP: *U. humidicola pasture*. NF: native forest.

Distance	**Area**	**Layer**		
m		0-10 cm	10-20 cm	20-40 cm
0.00	ILF-ST	565.58±156.77 A§	460.97±123.90 A§	396.85±73.99 A§
	ILF-EP	590.93±125.70 A§	519.64±126.04 A‡§	395.79±101.93 A§
	ICLF	446.82±233.39 A§	370.75±125.45 A¶	261.62±65.10 A¶
5.25	ILF-ST	582.40±41.96 A§	505.03±83.17 A‡§	490.01±76.43 A§
	ILF-EP	452.50±33.67 A	362.97±92.89 A¶	308.45±112.08 B
	ICLF	355.85±49.64 B†#¶	239.26±79.52 B†#¶	225.35±81.00 B¶
21.00	ILF-ST	654.32±234.25 A‡	534.64±269.10 A‡§	529.56±193.00 A§
	ILF-EP	454.76±49.07 A	391.29±38.17 B¶	331.46±125.43 B¶
	ICLF	371.50±56.27 B†¶	278.40±61.33 B†#¶	232.81±122.78 B¶
	ICL	634.90±235.12 a	545.39±119.95 a	435.37±204.05 ab
	IP	439.96±232.53 ab	340.98±161.89 bc	358.65±176.10 ab
	MP	616.15±389.17 a	507.15±98.26 ab	308.57±230.76 ab
	HP	329.80±34.04 b	239.43±45.53 c	190.74±65.02 b
	NF	576.48±124.05 a	550.41±111.29 a	612.36±185.48 a

Data were analyzed using the Kruskal-Wallis test followed by Dunn's post hoc tests with FDR correction (Benjamini-Hochberg) at the 5 % significance level. Capital letters compare tree-integrated systems within the same distance. Lowercase letters compare the treeless systems and the native forest fragment among themselves. Systems sharing the same letters do not differ statistically. The symbols †, ‡, #, § and ¶ indicate a significant difference relative to ICL, IP, MP, HP and NF, respectively.

The median-based linear model (MBLM) analysis indicated that the distance from the tree line significantly influenced the POXC content in the 10-20 (ILF-ST, ILF-EP and ICLF) and 20-40 cm (ILF-ST and ILF-EP) (Table 4.7). In ILF-ST, POXC tended to increase with distance, whereas in ILF-EP and ICLF, POXC content significantly decreased with increasing distance from the tree line.

Table 4.7 - Regression equations (MBLM) and Kendall's rank correlation coefficient (τ) for permanganate oxidizable carbon (POXC) (mg kg^{-1}) as a function of distance from trees in tree-integrated systems and soil layers (10-20 and 20-40 cm)[†]. ILF-ST: integrated livestock-forestry with *Samanea tubulosa*; ILF-EP: integrated livestock-forestry with *Eucalyptus pellita*; ICLF: integrated crop-livestock-forestry; ns: non-significant ($p > 0.05$).

Layer	Area	Equation[‡]	τ[§]
10-20 cm	ILF-ST	Y = 461.719 + 6.100x	0.439
	ILF-EP	Y = 442.620 - 4.719x	-0.507
	ICLF	Y = 290.199 - 3.660x	-0.372
20-40 cm	ILF-ST	Y = 403.263 + 10.218x	0.597
	ILF-EP	Y = 393.373 - 5.456x	-0.575
	ICLF	ns	--

[†] No significant effect of distance was observed in the 0-10 cm layer. [‡] Regression parameters estimated by Siegel's repeated medians method. [§] Kendall's tau indicates the strength of the monotonic relationship.

4.3.4 Soil organic matter humification

The humification level of soil organic matter (H_{LIFS}) showed significant variation across the distinct land-use systems and soil layers (Table 4.8). Across all soil depths, the integrated livestock-forestry systems (ILF-ST and ILF-EP), the Marandu pasture (MP) and the native forest (NF) fragment consistently maintained the lowest H_{LIFS} values, with no statistical difference among them (1.10, 1.29, 1.77 in average for the 0-10, 10-20 and 20-40 cm layers, respectively). On the other hand, the integrated crop-livestock (ICL) and integrated crop-livestock-forestry (ICLF) systems, and Ipyporã (IP) and Humidicola (HP) pastures, presented the highest values, also with no statistical difference among them (5.62, 7.10 and 11.52 in average for the 0-10, 10-20 and 20-40 cm layers, respectively). Noticeably, H_{LIFS} values increased with increasing depth.

Table 4.8 - Humification index of soil organic matter (H_{LIFS}) for soil layers (0-10, 10-20 and 20-40 cm) across different land-use systems (median ± interquartile range). ILF-ST: integrated livestock-forestry with *Samanea tubulosa*. ILF-EP: integrated livestock-forestry with *Eucalyptus pellita*. ICLF: integrated crop-livestock-forestry. ICL: integrated crop-livestock. IP: *Urochloa brizantha* x *U. ruziziensis* 'Ipyporã' pasture. MP: *U. brizantha* 'Marandu' pasture. HP: *U. humidicola* pasture. NF: native forest.

Distance	Area	Layer		
m		0-10 cm	10-20 cm	20-40 cm
0.00	ILF-ST	0.87±0.20 B†‡§	0.79±0.26 B†‡§	0.89±0.21 B†‡§
	ILF-EP	1.30±0.60 B§	1.93±0.93 B§	1.63±1.18 B§
	ICLF	5.15±2.61 A$^{\#¶}$	7.61±4.67 A$^{\#¶}$	12.81±5.65 A$^{\#¶}$
5.25	ILF-ST	0.93±0.36 B†‡§	1.10±0.31 B†‡§	1.29±0.90 B†‡§
	ILF-EP	1.39±0.39 B§	1.76±0.80 B§	2.17±1.16 B§
	ICLF	4.83±1.40 A$^{\#}$	6.68±2.43 A$^{\#¶}$	13.13±5.84 A$^{\#¶}$
21.00	ILF-ST	0.59±0.37 B†‡§	0.89±0.35 B†‡§	0.91±0.34 B†‡§
	ILF-EP	1.53±0.87 B§	1.65±0.73 B§	2.99±2.54 B

Distance	Area	Layer		
m		0-10 cm	10-20 cm	20-40 cm
	ICLF	7.22±4.15 A$^{\#\P}$	5.03±1.82 A$^{\#}$	11.00±5.93 A$^{\#\P}$
	ICL	4.69±1.86 ab	5.65±2.95 ab	9.73±6.18 ab
	IP	4.88±3.78 ab	6.35±2.21 ab	6.59±5.61 ab
	MP	1.10±0.61 c	1.07±0.64 c	1.47±0.84 c
	HP	6.81±2.28 a	9.52±2.97 a	13.64±7.79 a
	NF	1.18±0.52 bc	1.37±0.71 bc	1.79±0.95 bc

Data were analyzed using the Kruskal-Wallis test followed by Dunn's post hoc tests with FDR correction (Benjamini-Hochberg) at the 5 % significance level. Capital letters compare tree-integrated systems within the same distance. Lowercase letters compare the treeless systems and the native forest fragment among themselves. Systems sharing the same letters do not differ statistically. The symbols †, ‡, $^{\#}$, § and ¶ indicate a significant difference relative to ICL, IP, MP, HP and NF, respectively.

When comparing the tree-integrated systems (ILF-EP, ILF-ST, and ICLF) at the same distance from the tree line, ICLF showed a significantly higher H_{LIFS} than ILF-ST and ILF-ST across all layers. The comparison of tree-integrated systems and distances relative to treeless treatments showed a pattern across layers: ILF-ST showed significantly lower values than ICL, IP and HP; ILF-EP showed lower significantly lower values than HP (except for the 21.00 m distance in the 20-40 cm layer); and ICLF showed higher values than MP and NF (except for the 5.25 and 21.00 m distances in the 0-10 and 10-20 cm layers).

The median-based linear model (MBLM) analysis showed that H_{LIFS} exhibited distinct spatial patterns across soil layers (Table 4.9). In the surface layer (0-10 cm), a significant linear decrease in the humification index was observed for the ILF-ST system as distance from the tree row increased, while no significant spatial effects were detected for ILF-EP and ICLF at this depth. Conversely, at the 10-20 cm layer, the ICLF system was the only one to show a significant spatial trend, characterized by a linear reduction in H_{LIFS} with increasing distance. In the deepest layer (20-40 cm), the spatial dynamics reversed compared to the surface; ILF-ST and ILF-EP systems showed a linear increase in the humification index as distance from the trees increased. Specifically, the ILF-EP system showed a more pronounced increase than ILF-ST. For the ICLF system at this depth, the effect of distance was non-significant.

Table 4.9 - Regression equations (MBLM) and Kendall's rank correlation coefficient (τ) for soil organic matter humification index (H_{LIFS}) as a function of distance from trees in tree-integrated systems and soil layers (0-10, 10-20 and 20-40 cm)†. ILF-ST: integrated livestock-forestry with *Samanea tubulosa*; ILF-EP: integrated livestock-forestry with *Eucalyptus pellita*; ICLF: integrated crop-livestock-forestry; ns: non-significant ($p > 0.05$).

Layer	Area	Equation†	τ‡
0-10 cm	ILF-ST	Y = 1.056 - 0.077x	-0.349
	ILF-EP	ns	--
	ICLF	ns	--
10-20 cm	ILF-ST	ns	--
	ILF-EP	ns	--
	ICLF	Y = 7.421 - 0.114x	-0.484
20-40 cm	ILF-ST	Y = 0.981 + 0.073x	0.124
	ILF-EP	Y = 1.028 + 0.571x	0.349
	ICLF	ns	--

† Regression parameters estimated by Siegel's repeated medians method. ‡ Kendall's tau indicates the strength of the monotonic relationship.

4.3.5 Carbon management index

The soil carbon dynamics, expressed through the carbon pool index (CPI), lability index (LI), and carbon management index (CMI), varied significantly among land-use systems and sampling distances (Table 4.10). Regarding the CPI, the integrated systems ILF-ST and ILF-EP maintained values superior to the ICLF and HP systems across all evaluated distances. Specifically, at the 21.00 m distance, the ILF-ST system reached the highest CPI (1.52), being statistically different from the treeless systems, as well as the native forest reference.

The lability index highlighted differences in the quality of the accumulated carbon. The ICL forestry system presented the highest LI (0.92), being statistically superior to the other managed systems (except for ICLF at the 0.00 m distance) and the only managed system with LI not significantly different from NF. No significant difference was observed among tree-integrated systems within distances.

The Carbon Management Index (CMI), which integrates both the quantity (CPI) and lability (LI) of carbon, revealed that the ILF-ST system provided the most favorable carbon management conditions being the only tree-integrated system statistically comparable to NF at all distances. Conversely, the ICLF system consistently presented the lowest CMI values among the integrated systems, ranging from 46.55 to 56.50, which were statistically inferior at certain distances, significantly lower than the ICL and IP systems, besides NF. Among the treeless pastures, the HP system showed the lowest CMI (41.77), while MP (76.32) and ICL (83.00) systems exhibited the highest management indices, statistically not different from NF.

Table 4.10 - Carbon pool index (CPI), lability index (LI) and carbon management index (CMI) across different land-use systems (mean ± standard deviation). ILF-ST: integrated livestock-forestry with *Samanea tubulosa*. ILF-EP: integrated livestock-forestry with *Eucalyptus pellita*. ICLF: integrated crop-livestock-forestry. ICL: integrated crop-livestock. IP: *Urochloa brizantha* x *U. ruziziensis* 'Ipyporã' pasture. MP: *U. brizantha* 'Marandu' pasture. HP: *U. humidicola* pasture.

Distance (m)	Area	CPI	LI	CMI
0.00	ILF-ST	1.38±0.19 A†§¶	0.63±0.13 A†¶	81.70±18.29 A§
	ILF-EP	1.26±0.19 A§	0.68±0.06 A†¶	82.14±6.43 A§¶
	ICLF	0.74±0.12 B¶	0.79±0.15 A	56.50±7.90 B†¶
5.25	ILF-ST	1.23±0.21 A§	0.74±0.09 A¶	88.58±11.88 A‡§
	ILF-EP	1.15±0.09 A§¶	0.57±0.08 A†¶	64.08±9.09 B¶
	ICLF	0.74±0.11 B¶	0.65±0.12 A†¶	46.55±5.98 B$^{†#¶}$
21.00	ILF-ST	1.52±0.24 A$^{†‡#§¶}$	0.69±0.09 A†¶	103.19±25.06 A$^{‡#§}$
	ILF-EP	1.20±0.20 A§	0.54±0.10 A†¶	60.69±2.65 B¶
	ICLF	0.85±0.15 B	0.59±0.08 A†¶	48.01±6.90 B$^{†#¶}$
	ICL	0.95±0.24 a	0.92±0.25 a	83.00±19.22 a
	IP	1.07±0.38 a	0.63±0.12 b¶	63.04±13.79 ab¶
	MP	1.12±0.36 a	0.71±0.09 b¶	76.32±21.18 a
	HP	0.75±0.17 a	0.58±0.11 b¶	41.77±7.69 b¶
	NF	1.00±0.00	1.00±0.00	100.00±0.00

Data were analyzed by factorial ANOVA at the 5 % significance level. Tukey's test was used to compare tree-integrated systems within distances (capital letters), and treeless systems among themselves (lowercase letters). Systems sharing the same letters do not differ statistically. Dunnett's test was used to compare treeless systems with tree-integrated systems (the symbols †, ‡, $^{#}$ and § indicate a significant difference relative to ICL, IP, MP, HP and NF, respectively). The symbol ¶ indicates a significant difference from NF reference (one-sample t-tests with FDR correction).

Regression analysis revealed distinct patterns for CPI, LI and CMI across the integrated systems (Table 4.11). While CPI did not exhibit a significant response to distance from the tree row in any system, the quality-related indices (LI and CMI) were significantly affected. Specifically, LI in the ICLF system followed a significant linear decrease as distance from the trees increased, whereas the ILF-ST and ILF-EP systems showed non-significant spatial variation for this parameter.

The CMI, which provides a holistic view of soil carbon quality, exhibited significant linear responses in ILF-ST and ILF-EP, though in opposite directions. In the ILF-ST system, the CMI increased linearly with distance from the *Samanea tubulosa* trees. Conversely, the ILF-EP system showed a linear reduction in CMI as distance from the *Eucalyptus pellita* row increased. No significant spatial adjustment for CMI was found in the ICLF system.

Table 4.11 - Regression equations and determination coefficients (R^2) for lability index (LI) and carbon management index (CMI) as a function of distance from trees in tree-integrated systems†. ILF-ST: integrated livestock-forestry with *Samanea tubulosa*; ILF-EP: integrated livestock-forestry with *Eucalyptus pellita*; ICLF: integrated crop-livestock-forestry; ns: non-significant.

Variable	Area	Equation	R^2
LI	ILF-ST	ns	--
	ILF-EP	ns	--
	ICLF	Y = 0.749 - 0.008x	0.776
CMI	ILF-ST	Y = 82.397 + 1.001x	0.994
	ILF-EP	Y = 76.279 - 0.835x	0.627
	ICLF	ns	--

† No significant effect of distance was observed for carbon pool index (CPI).

4.4 Discussion

4.4.1 Soil carbon content, stock and isotopic composition

The findings indicate that integrated systems, particularly ILF-ST, can significantly enhance soil carbon sequestration compared to traditional pastures and NF. It is worth noticing that SCC differences were more pronounced in the deepest layer (20-40 cm), reflecting the contribution of root biomass to carbon storage in these livestock systems (Frazão et al. 2023; Olaya-Montes et al. 2021).

Additionally, no integrated nor monoculture pasture system exhibited statistically lower values than NF, suggesting that even moderately managed monoculture pastures can achieve comparable soil carbon levels to native forests, emphasizing the importance of sustainable management practices in enhancing soil carbon stocks in the region. In fact, SCS depletion is usually observed in studies with degraded areas, but not in managed systems (Bieluczyk et al. 2025; Freitas et al. 2020; Marques et al. 2015; Mascarenhas et al. 2017). The native forest SCS was in the range of those usually reported for Rondônia Oxisols (Bernoux et al. 1998; Moquedace et al. 2024; Moraes et al. 1995), serving as a suitable baseline for evaluating the effectiveness of the livestock systems in carbon management.

The apparent negative influence of trees in ILF-ST and ICLF observed in some of the layers might be due to lower pasture biomass production of grass near the tree line, which can affect overall carbon storage dynamics (Bieluczyk et al. 2020; Pezzopane et al. 2019; Sarto et al. 2020a). Moreover, lower fine root yield from pasture or crops in the presence of trees is expected (Bieluczyk et al. 2023, 2024), which may also impact negatively on SCC and SCS. These results underscore the necessity for ongoing research to refine management strategies

that optimize carbon sequestration in integrated systems while maintaining pasture productivity and ecological balance.

The pasture species might also have influenced the results. *Urochloa humidocola* pasture (HP) showed the lowest SCC and SCS, whereas Marandu pasture (MP), the highest. Moreover, ILF-ST and ILF-EP, which are composed of Marandu pasture, demonstrated superior performance in carbon management compared to ICLF, which is composed of Ipyporã pasture, highlighting the importance of selecting appropriate species for enhancing soil carbon stocks in pasture and integrated system (Rodriguez et al. 2025; Tessema et al. 2021).

Native forest showed distinctly lower $\delta^{13}C$ values than all studied livestock systems, indicating the that the carbon sources in the managed systems are predominantly derived from C_4 plants (Sarto et al. 2020a). Remarkably, $\delta^{13}C$ among managed systems followed and inverted pattern than that of SCS and SCC, with ILF-ST and ILF-EP, showing more negative $\delta^{13}C$ values than ICLF, indicating a faster shift in carbon sources in ICLF and ICL. While this might be due to higher diversity of C_4 residues sources, such as maize and rice, this can also be attributed to native carbon depletion in ICLF and ICL, since they showed lower overall SCC and SCS (Bieluczyk et al. 2025).

4.4.2 Carbon fractions

Soil organic carbon (SOC) variations among areas were similar to those observed for SCC, but with more pronounced differences within ILF systems. In fact, the ILF-ST system exhibited higher SOC levels compared to both ILF-EP and ICLF systems. Moreover, the influence of distance to the trees varied between ILF-ST and ILF-EP in the 20-40 cm layer. In the former, SOC was higher close to the tree line, while in the latter, SOC decreased with distance. Also, active carbon (POXC) was higher in ILF-ST and was lower close to the *S. tubulosa* trees, but higher close to the eucalyptus trees in ILF-EP (in the 10-20 and 20-40 cm layers) and ICLF (in the 10-20 cm layer). These findings indicate differing dynamics in carbon storage influenced by tree species.

The humification level of soil organic matter (H_{LIFS}) highlights the influence of management and *Urochloa* species on carbon dynamics. In all assessed layers, areas can be divided by HLIFS basically into two groups: those with Ipyporã and *U. humidicola* pastures (ICLF, ICL, IP and and HP) exhibiting higher humification levels compared to those with Marandu pasture (ILF-ST, ILF-EP and MP) and NF. This can be attributed to differences in the quality of the organic residues predominating in each area, such as C:N and lignin:cellulose

ratios (Murindangabo et al. 2023; Z. Zhang et al. 2022). In addition, areas with higher content of labile carbon (such as POXC) tend to show lower humification levels, since the presence of more labile carbon indicates a higher turnover rate of organic matter and relative lower contribution of more stable organic matter for total SCC (Bento et al. 2025; Segnini et al. 2019).

4.4.3 Carbon management index

The general reduction in LI across practically all managed systems relative to the native forest indicates a fundamental shift in carbon quality following land-use conversion. Although these managed systems effectively accumulate total carbon (high CPI), the resulting carbon pools are less labile and more recalcitrant than those in undisturbed ecosystems. In addition, the lower CPI and CMI values found in the ICLF system, but not in the ICL system suggest that the presence of trees might have hindered forage biomass production, limiting the buildup of stable carbon pools over time. This negative effect of trees was not observed in ILF-ST and ILF-EP, which, besides having considerably lower tree density than ICLF (13 vs. 136 trees ha^{-1}), is composed of Marandu pasture, instead of Ipyporã pasture.

Furthermore, while ICLF and ILF-EP systems, both composed of *E. pellita*, followed a linear decrease in LI and CMI, respectively, as distance from trees increased, ILF-ST followed a reverse trend, highlighting differences in tree species influence. These results emphasize that while tree integration is a robust strategy for carbon sequestration, the specific choice of tree and forage species significantly dictate the balance between carbon quantity and its biological availability for soil health.

The CMI of ILF-ST, ICL and IP did not differ significantly from NF, indicating that these systems can effectively manage carbon levels comparable to native forest conditions. On the contrary, ICLF and HP demonstrated significantly lower CMI values, indicating a less effective carbon management performance compared to native forest systems (Baldotto et al. 2015). Therefore, by integrating labile and non-labile fractions of soil organic carbon, we can better understand the implications of different land-use systems on carbon dynamics and inform management practices that enhance soil health and sustainability, than looking only to SCC or SCS.

4.5 Conclusion

The management of soil carbon in integrated production and pasture systems in Western Amazonia presents both opportunities and challenges. The findings of this study reveal that while integrated systems, particularly those utilizing native species such as *Samanea tubulosa*, demonstrate potential for enhancing soil carbon sequestration, they do not consistently outperform traditional monoculture pastures or replicate the carbon storage capabilities of native forests. The observed variations in soil carbon content and stock across different land-use systems underscore the complexities involved in achieving effective carbon management. Additionally, the reliance on specific pasture species and the influence of tree integration on pasture biomass and soil health must be carefully evaluated to avoid undermining the ecological benefits of these systems.

The carbon management index (CMI) results suggest that many integrated systems may fall short of the carbon management performance exhibited by native forests, raising concerns about their viability as a sustainable alternative to conventional practices. Therefore, while integrated crop-livestock-forestry systems hold promise, a more nuanced approach that prioritizes the conservation of native ecosystems and explores diverse sustainable agricultural practices is essential for achieving long-term carbon management goals and preserving biodiversity in the Amazon.

References

Alvares, Clayton Alcarde, José Luiz Stape, Paulo Cesar Sentelhas, José Leonardo de Moraes Gonçalves, and Gerd Sparovek. 2013. Köppen's Climate Classification Map for Brazil. *Meteorologische Zeitschrift* 22 (6): 711–28. https://doi.org/10.1127/0941-2948/2013/0507.

Azevedo, Alcinei Mistico. 2022. *Tratamentos.Ad: Pacote Para Analise De Experimentos Com Testemunhas Adicionais*. V. 0.2.4. Released September 13. https://cran.r-project.org/web/packages/Tratamentos.ad/index.html.

Baldotto, Marihus Altoé, Erli Maciel Vieira, Dálisson de Oliveira Souza, and Lílian Estrela Borges Baldotto. 2015. Estoque e frações de carbono orgânico e fertilidade de solo sob floresta, agricultura e pecuária. *Revista Ceres* 62: 301–9. https://doi.org/10.1590/0034-737X201562030010.

Bentes-Gama, Michelliny de Matos, Guido Sanick Leal, Joelson de Oliveira Barros, Raimunda Herculano Lopes, Giovana Fiorella Zamora López, and Juliane Cardoso da Silveira. 2009. *Características Da Estrutura de Uma Floresta de Terra Firme Em Porto Velho, Rondônia*. Embrapa Rondônia. Circular Técnica 109. Embrapa Rondônia. https://ainfo.cnptia.embrapa.br/digital/bitstream/item/24747/1/ct109-floresta.pdf.

Bento, Lucas Raimundo, João Vitor dos Santos, Steffen A. Schweizer, et al. 2025. Moderate Pasture Intensification Enhances Soil Organic Carbon Stocks in a Degraded Brazilian Ferralsol. *Soil and Tillage Research* 251 (September): 106534. https://doi.org/10.1016/j.still.2025.106534.

Bernoux, Martial, Carlos Cerri, Dominique Arrouays, Claudy Jolivet, and Boris Volkoff. 1998. Bulk Densities of Brazilian Amazon Soils Related to Other Soil Properties. *Soil Science Society of America Journal* 62 (3): 743–49. https://doi.org/10.2136/sssaj1998.03615995006200030029x.

Bieluczyk, Wanderlei, Marina Pires Duarte, Guilherme Lucio Martins, et al. 2025. Slash-and-Burn Agriculture Disrupts the Carbon Storage Potential and Ecosystem Multifunctionality of Amazon's Secondary Forests. *Agriculture, Ecosystems & Environment* 381 (April): 109413. https://doi.org/10.1016/j.agee.2024.109413.

Bieluczyk, Wanderlei, Marisa De Cássia Piccolo, João Vitor Matos Gonçalves, et al. 2024. Fine Root Production and Decomposition of Integrated Plants under Intensified Farming Systems in Brazil. *Rhizosphere* 31 (September): 100930. https://doi.org/10.1016/j.rhisph.2024.100930.

Bieluczyk, Wanderlei, Marisa De Cássia Piccolo, Marcos Gervasio Pereira, et al. 2020. Integrated Farming Systems Influence Soil Organic Matter Dynamics in Southeastern Brazil. *Geoderma* 371 (July): 114368. https://doi.org/10.1016/j.geoderma.2020.114368.

Bieluczyk, Wanderlei, Marisa De Cássia Piccolo, Marcos Gervasio Pereira, et al. 2023. Fine Root Dynamics in a Tropical Integrated Crop-Livestock-Forestry System. *Rhizosphere* 26 (June): 100695. https://doi.org/10.1016/j.rhisph.2023.100695.

Blair, Gj, Rdb Lefroy, and L. Lisle. 1995. Soil Carbon Fractions Based on Their Degree of Oxidation, and the Development of a Carbon Management Index for Agricultural Systems. *Australian Journal of Agricultural Research* 46 (7): 1459–66. https://doi.org/10.1071/AR9951459.

Cardoso, Edilene Virgulina, and Régio Márcio Toesca Gimenes. 2024. Systematic Review on Sustainable Intensification Strategies in Brazilian Beef Production. *Revista de Gestão Social e Ambiental* 18 (10): e07419. https://doi.org/10.24857/rgsa.v18n10-302.

Carvalho, Raquel, Ana Paula Dutra De Aguiar, and Silvana Amaral. 2020. Diversity of Cattle Raising Systems and Its Effects over Forest Regrowth in a Core Region of Cattle Production in the Brazilian Amazon. *Regional Environmental Change* 20 (2): 44. https://doi.org/10.1007/s10113-020-01626-5.

Cipriani, Henrique Nery, Ana Karina Dias Salman, Pedro Gomes da Cruz, Elaine Coimbra de Souza, and Siu Mui Tsai. 2025. Atributos Químicos, Físicos e Microbiológicos Do Solo Em Áreas de IPF, ILP, ILPF, Pastagens e Floresta No Campo Experimental de Porto Velho, Em Duas Estações (Seca e Chuvosa). Redape. https://doi.org/10.48432/QC7QW0.

Cipriani, Henrique Nery, Ana Karina Dias Salman, Carlos Henrique Semper Da Silva, Murilo Luz Rodrigues, Emily Soares Dos Santos, and Pedro Gomes Da Cruz. 2023. Crescimento Inicial de Samanea Tubulosa e Eucalyptus Pellita Em Sistemas de Integração Pecuária-Floresta Em Porto Velho, Rondônia. *Série Técnica IPEF* 26 (48): 310–14. https://doi.org/10.18671/sertec.v26n48.061.

Climate-Data.org. 2022. Clima Porto Velho: Temperatura, Tempo e Dados Climatológicos. May. https://pt.climate-data.org/america-do-sul/brasil/rondonia/porto-velho-3120/#google_vignette.

Conceição, Marcela C. G. Da, Eduardo S. Matos, Edison D. Bidone, Renato De A. R. Rodrigues, and Renato C. Cordeiro. 2017. Changes in Soil Carbon Stocks under Integrated Crop-Livestock-Forest System in the Brazilian Amazon Region. *Agricultural Sciences* 08 (09): 904–13. https://doi.org/10.4236/as.2017.89066.

Dinno, Alexis. 2024. *Dunn.Test: Dunn's Test of Multiple Comparisons Using Rank Sums*. V. 1.3.6. Released April 12. https://cran.r-project.org/web/packages/dunn.test/index.html.

Ellert, B. H., and J. R. Bettany. 1995. Calculation of Organic Matter and Nutrients Stored in Soils under Contrasting Management Regimes. *Canadian Journal of Soil Science* 75 (4): 529–38. https://doi.org/10.4141/cjss95-075.

Feitosa, Izabela de Lima, Marcelo Silva de Oliveira, Rafael Lemos Bastos, Alexandre Martins Abdão dos Passos, and Henrique Nery Cipriani. 2022. Spatial Distribution of Agronomic Attributes of Corn Plants in Integrated Production Systems in Brazilian Amazonia. *International Journal of Advanced Engineering Research and Science* 9 (12): 382–88. https://doi.org/10.22161/ijaers.912.42.

Feitosa, Izabela de Lima, Alexandre Martins Abdão dos Passos, Henrique Nery Cipriani, Marcelo Silva de Oliveira, Alaerto Luiz Marcolan, and Gustavo Mattos Vasques. 2019. Spatial Variability of Soil Physical Attributes in Integrated Production Systems in the Amazon Region. *Pesquisa Agropecuária Brasileira* 54 (November). https://doi.org/10.1590/S1678-3921.pab2019.v54.00324.

Frazão, Leidivan Almeida, Evander Alves Ferreira, Warley Rodrigues De Oliveira, et al. 2023. *Sustainable Intensification of Agriculture Andlivestock Production in Brazil: A Meta-Analysis of Soil C Changes in Integrated Systems*. May 15. https://doi.org/10.5194/egusphere-egu23-1998.

Freitas, Igor Costa De, Juliana Martins Ribeiro, Nayara Christina Almeida Araújo, et al. 2020. Agrosilvopastoral Systems and Well-Managed Pastures Increase Soil Carbon Stocks in the Brazilian Cerrado. *Rangeland Ecology & Management* 73 (6): 776–85. https://doi.org/10.1016/j.rama.2020.08.001.

IUSS Working Group WRB. 2022. *World Reference Base for Soil Resources 2022: International Soil Classification System for Naming Soils and Creating Legends for Soil Maps*. 4th ed. International Union of Soil Sciences. https://files.isric.org/public/documents/WRB_fourth_edition_2022-12-18.pdf.

Jackson, M. L. 1982. *Análisis químico de suelos*. Ediciones Omega.

Kay, Matthew, Lisa A. Elkin, James J. Higgins, and Jacob O. Wobbrock. 2025. *ARTool: Aligned Rank Transform*. V. 0.11.2. Released April 10. https://cran.r-project.org/web/packages/ARTool/index.html.

Komsta, Lukasz. 2019. *Mblm: Median-Based Linear Models*. V. 0.12.1. Released January 26. https://cran.r-project.org/web/packages/mblm/index.html.

Lapola, David M., Patricia Pinho, Jos Barlow, et al. 2023. The Drivers and Impacts of Amazon Forest Degradation. *Science* 379 (6630): eabp8622. https://doi.org/10.1126/science.abp8622.

Marchão, Robélio Leandro, Ieda Carvalho Mendes, Lourival Vilela, et al. 2024. Integrated Crop–Livestock–Forestry Systems for Improved Soil Health, Environmental Benefits, and Sustainable Production. In *Soil Health and Sustainable Agriculture in Brazil*, 1st ed., edited by Ieda Carvalho Mendes and Maurício Roberto Cherubin. ASA, CSSA, and SSSA Books. Soil Health Series 3. Wiley. https://doi.org/10.1002/9780891187448.ch2.

Marques, Jean Dalmo de Oliveira, Flávio Jesus Luizão, Wenceslau Geraldes Teixeira, et al. 2015. Distribution Of Organic Carbon In Different Soil Fractions In Ecosystems Of Central Amazonia. *Revista Brasileira de Ciência Do Solo* 39: 232–42. https://doi.org/10.1590/01000683rbcs20150142.

Mascarenhas, Adriano Reis Prazeres, Marta Silvana Volpato Sccoti, Rafael Rodolfo Melo, et al. 2017. Atributos físicos e estoques de carbono do solo sob diferentes usos da terra em Rondônia, Amazônia Sul-Ocidental. *Pesquisa Florestal Brasileira* 37 (89): 19–27. https://doi.org/10.4336/2017.pfb.37.89.1295.

Milori, Débora Marcondes Bastos Pereira, Helder Vinicius Avanço Galeti, Ladislau Martin-Neto, et al. 2006. Organic Matter Study of Whole Soil Samples Using Laser-Induced Fluorescence Spectroscopy. *Soil Science Society of America Journal* 70 (1): 57–63. https://doi.org/10.2136/sssaj2004.0270.

Monteiro, Alyce, Luciano Barreto-Mendes, Audrey Fanchone, et al. 2024. Crop-Livestock-Forestry Systems as a Strategy for Mitigating Greenhouse Gas Emissions and Enhancing the Sustainability of Forage-Based Livestock Systems in the Amazon Biome. *Science of The Total Environment* 906 (January): 167396. https://doi.org/10.1016/j.scitotenv.2023.167396.

Moquedace, Cássio Marques, Clara Glória Oliveira Baldi, Rafael Gomes Siqueira, et al. 2024. High-Resolution Mapping of Soil Carbon Stocks in the Western Amazon. *Geoderma Regional* 36 (March): e00773. https://doi.org/10.1016/j.geodrs.2024.e00773.

Moraes, Jener L., Carlos C. Cerri, Jerry M. Melillo, et al. 1995. Soil Carbon Stocks of the Brazilian Amazon Basin. *Soil Science Society of America Journal* 59 (1): 244–47. https://doi.org/10.2136/sssaj1995.03615995005900010038x.

Murindangabo, Yves Theoneste, Marek Kopecký, Kristýna Perná, et al. 2023. Enhancing Soil Organic Matter Transformation through Sustainable Farming Practices: Evaluating Labile Soil Organic Matter Fraction Dynamics and Identifying Potential Early Indicators. *Agriculture* 13 (7): 1314. https://doi.org/10.3390/agriculture13071314.

Olaya-Montes, Andres, Maria P. Llanos-Cabrera, Maurício R. Cherubin, Wilmer Herrera-Valencia, Fausto A. Ortiz-Morea, and Adriana M. Silva-Olaya. 2021. Restoring Soil Carbon and Chemical Properties through Silvopastoral Adoption in the Colombian Amazon Region. *Land Degradation & Development* 32 (13): 3720–30. https://doi.org/10.1002/ldr.3832.

Oliveira, Dener M. S., Rafael S. Santos, Fernanda H. M. Chizzotti, et al. 2024. Crop, Livestock, and Forestry Integration to Reconcile Soil Health, Food Production, and Climate Change Mitigation in the Brazilian Cerrado: A Review. *Geoderma Regional* 37 (June): e00796. https://doi.org/10.1016/j.geodrs.2024.e00796.

Oliveira, Janaína De Moura, Beata Emoke Madari, Márcia Thaís De Melo Carvalho, et al. 2018. Integrated Farming Systems for Improving Soil Carbon Balance in the Southern Amazon of Brazil. *Regional Environmental Change* 18 (1): 105–16. https://doi.org/10.1007/s10113-017-1146-0.

Oliveira, Maniele Mendonça de, Ana Karina Dias Salman, Henrique Nery Cipriani, Amanda Ribeiro de Moura, and Odilene de Souza Teixeira. 2021. Desempenho Inicial de Espécies Arbóreas Para Sombreamento Natural Em Sistema de Integração Pecuária-Floresta. *Anais...*, 36–41. https://www.alice.cnptia.embrapa.br/bitstream/doc/1139635/1/cpafro-18701.pdf.

Pendrill, Florence, U. Martin Persson, Javier Godar, and Thomas Kastner. 2019. Deforestation Displaced: Trade in Forest-Risk Commodities and the Prospects for a Global Forest Transition. *Environmental Research Letters* 14 (5): 055003. https://doi.org/10.1088/1748-9326/ab0d41.

Persson, Martin, Sabine Henders, and Thomas Kastner. 2014. Trading Forests: Quantifying the Contribution of Global Commodity Markets to Emissions from Tropical Deforestation. *SSRN Electronic Journal*, ahead of print. https://doi.org/10.2139/ssrn.2622757.

Pezzopane, José Ricardo Macedo, Alberto Carlos de Campos Bernardi, Mariana Vieira Azenha, et al. 2019. Production and Nutritive Value of Pastures in Integrated Livestock Production Systems: Shading and Management Effects. *Scientia Agricola* 77 (September): e20180150. https://doi.org/10.1590/1678-992X-2018-0150.

Piano, Jeferson Tiago, Carlos Augusto Rocha De Moraes Rego, Andressa Perini Vengen, et al. 2020. Soil Organic Matter Fractions and Carbon Management Index under Integrated Crop-Livestock System. *Bioscience Journal* 36 (3): 743–60. https://doi.org/10.14393/BJ-v36n3a2020-47702.

Ribeiro, Rodrigo da S., Alexandre M. A. dos Passos, and Andreia M. Aker. 2020. Agronomic Performance of Soybean Crops under Integrated Production Systems in the Southwestern Brazilian Amazon Biome. *Revista Brasileira de Engenharia Agrícola e Ambiental* 24 (November): 793–99. https://doi.org/10.1590/1807-1929/agriambi.v24n12p793-799.

Rivero, Sérgio, Oriana Almeida, Saulo Ávila, and Wesley Oliveira. 2009. Pecuária e Desmatamento: Uma Análise Das Principais Causas Diretas Do Desmatamento Na Amazônia. *Nova Economia* 19 (1): 41–66. https://doi.org/10.1590/S0103-63512009000100003.

Rodrigues, Marcos, David Costa Correia Silva, and Wladimir Colman De Azevedo Junior. 2023. Agricultural Production and GHG Emissions in the Brazilian Amazon. *Novos Cadernos NAEA* 26 (3). https://doi.org/10.18542/ncn.v26i3.13083.

Rodriguez, Leonardo, Mike Bastidas, Daniel Villegas, et al. 2025. *Potential of Different Urochloa Grass Hybrids to Enhance Soil Organic Carbon Stocks in a Mollisol of Valle Del Cauca, Colombia*. May 15. https://doi.org/10.5194/egusphere-egu25-717.

Santos, Cleber H. dos, Renan A. Romano, Gustavo Nicolodelli, et al. 2015. Performance Evaluation of a Portable Laser-Induced Fluorescence Spectroscopy System for the Assessment of the Humification Degree of the Soil Organic Matter. *Journal of the Brazilian Chemical Society* 26 (April): 775–83. https://doi.org/10.5935/0103-5053.20150039.

Santos, Humberto Gonçalves dos, Paulo Klinger Tito Jacomine, Lúcia Helena Cunha dos Anjos, et al. 2025. *Sistema Brasileiro de Classificação de Solos*. 6th ed. Embrapa, 2025. http://www.infoteca.cnptia.embrapa.br/handle/doc/1176834.

Sarto, Marcos V. M., Wander L. B. Borges, Jaqueline R. W. Sarto, Charles W. Rice, and Ciro A. Rosolem. 2020. Deep Soil Carbon Stock, Origin, and Root Interaction in a Tropical Integrated Crop–Livestock System. *Agroforestry Systems* 94 (5): 1865–77. https://doi.org/10.1007/s10457-020-00505-6.

Segnini, Aline, Alfredo Augusto Pereira Xavier, Pedro Luis Otaviani-Junior, et al. 2019. Soil Carbon Stock and Humification in Pastures under Different Levels of Intensification in Brazil. *Scientia Agricola* 76 (1): 33–40. https://doi.org/10.1590/1678-992x-2017-0131.

Sodhi, G. P. S., V. Beri, and D. K. Benbi. 2009. Using Carbon Management Index to Assess the Impact of Compost Application on Changes in Soil Carbon after Ten Years of Rice–Wheat Cropping. *Communications in Soil Science and Plant Analysis* 40 (21–22): 3491–502. https://doi.org/10.1080/00103620903326024.

Soil Survey Staff. 2022. *Keys to Soil Taxonomy*. 13th ed. USDA Natural Resources Conservation Service. https://www.nrcs.usda.gov/sites/default/files/2022-09/Keys-to-Soil-Taxonomy.pdf.

Teixeira, Paulo Cesar, Guilherme Kangussu Donagema, Ademir Fontana, and Wenceslau Geraldes Teixeira, eds. 2017. *Manual de Métodos de Análise de Solo*. 3rd ed. Embrapa. http://ainfo.cnptia.embrapa.br/digital/bitstream/item/181717/1/Manual-de-Metodos-de-Analise-de-Solo-2017.pdf.

Tessema, Bezaye Gorfu, Heiko Daniel, Zenebe Adimassu, and Brian Wilson. 2021. Soil Carbon Storage Potential of Tropical Grasses: A Review. In *Botany - Recent Advances and Applications*, edited by Bimal Kumar Ghimire. IntechOpen. https://doi.org/10.5772/intechopen.97835.

Townsend, Claudio Ramalho, Alexandre Martins Abdão dos Passos, Vicente de Paulo Campos Godinho, et al. 2013. *iLPF Como Alternativa Sustentável de Recuperação de Pastagem Degradada Em Porto Velho, Rondônia*. Embrapa Rondônia. Documentos 154. Embrapa Rondônia. https://ainfo.cnptia.embrapa.br/digital/bitstream/item/125817/1/doc-154-iLPF.pdf.

Valente, Moacir Azevedo, Raimundo Cosme de Oliveira Júnior, Tarcísio Ewerton Rodrigues, João Marcos Lima da Silva, and Paulo Lacerda dos Santos. 1998. *Levantamento Semidetalhado Dos Solos Do Campo Experimental de Porto Velho, RO*. Embrapa-CPATU. Documentos 136. Embrapa-CPATU. http://ainfo.cnptia.embrapa.br/digital/bitstream/item/57557/1/CPATU-Doc136.pdf.

Van Der Werf, G. R., D. C. Morton, R. S. DeFries, et al. 2009. CO2 Emissions from Forest Loss. *Nature Geoscience* 2 (11): 737–38. https://doi.org/10.1038/ngeo671.

Walkley, A., and I. Armstrong Black. 1934. An Examination of the Degtjareff Method for Determining Soil Organic Matter, and a Proposed Modification of the Chromic Acid Titration Method. *Soil Science* 37 (1): 29.

Weil, Raymond, Melissa Stine, Joel Gruver, and Susan Samson-Liebig. 2003. Estimating Active Carbon for Soil Quality Assessment: A Simplified Method for Laboratory and Field Use. *American Journal of Alternative Agriculture* 18 (March): 3–17. https://doi.org/10.1079/AJAA200228.

Welke, Selmir, Ana Karina Dias Salman, Henrique Nery Cipriani, Laércio Cavalcante Monteiro Filho, Odilene de Souza Teixeira, and Giovanna Moreira Ghedin. 2022. Duas Espécies Arbóreas Para Sombreamento de Pastagem Em Sistema de Integração Pecuária-Floresta. *Anais...*, 39–44. https://www.alice.cnptia.embrapa.br/alice/bitstream/doc/1146390/1/Anais-EIPER-2022-1-39-44.pdf.

Wobbrock, Jacob O., Leah Findlater, Darren Gergle, and James J. Higgins. 2011. The Aligned Rank Transform for Nonparametric Factorial Analyses Using Only Anova Procedures. *Proceedings of the SIGCHI Conference on Human Factors in Computing Systems* (New York, NY, USA), CHI '11, May 7, 143–46. https://doi.org/10.1145/1978942.1978963.

Zhang, Ziliang, Jason P. Kaye, Brosi A. Bradley, Joseph P. Amsili, and Vidya Suseela. 2022. Cover Crop Functional Types Differentially Alter the Content and Composition of Soil Organic Carbon in Particulate and Mineral-associated Fractions. *Global Change Biology* 28 (19): 5831–48. https://doi.org/10.1111/gcb.16296.

5 SUMMARY AND CONCLUSIONS

This thesis provides a comprehensive evaluation of the transition from extensive land use to sustainable intensification in Western Amazonia. It starts from the premise that soils in the region, particularly in Rondônia, are characterized by high acidity and low natural fertility. Therefore, maintaining and enhancing soil quality is not only an environmental goal but a productive necessity. This research highlights that the future of Amazonian livestock production depends on management systems capable of conserving soil fertility, with the integration of the native legume *Samanea tubulosa* emerging as a superior biological strategy to overcome these natural soil limitations. By integrating microbiological, holistic soil quality, and carbon sequestration data, several key conclusions can be drawn:

First, the structure of the soil microbiome is profoundly reshaped by land-use systems. While the conversion of native forests to pastures leads to a simplification of microbial networks, the integration of trees, particularly *S. tubulosa*, acts as a catalyst for biological recovery. This native species promotes greater microbial diversity, enhances functional connectivity, and creates specialized niches for nitrogen-fixing bacteria, outperforming exotic eucalyptus systems and conventional pastures in restoring the biological complexity essential for nutrient cycling in these naturally nutrient-poor environments.

Second, soil health in the Amazon is highly resilient to intensification when appropriate management practices are applied. The use of composite soil quality indices (SQI) demonstrated that all intensified systems (ICL, ICLF, ILF, and well-managed monocultures) maintain functional stability and can decouple cattle ranching from the traditional cycle of soil exhaustion common in the region. Notably, well-managed treeless pastures (such as Ipyporã) proved to be a viable and sustainable option, showing that productivity and soil stability can be achieved even without the forest component, provided that soil fertility and grazing are correctly managed.

Third, the potential for soil carbon sequestration is significantly enhanced in integrated systems, with *S. tubulosa* again showing superior performance. The ability of this native legume to increase carbon stocks in deeper soil layers and achieve a Carbon Management Index (CMI) comparable to native forests underscores its role in climate change mitigation. The isotopic data confirms that while integrated systems accelerate carbon turnover, they also provide a pathway for building stable organic matter pools that are often lost in degraded extensive pastures.

In summary, this research concludes that sustainable intensification is not a one-size-fits-all approach but a spectrum of viable management strategies. For Western Amazonia, while well-managed monocultures ensure productive stability, the integration of native tree species represents the gold standard for multifunctional land use. To ensure the long-term resilience of the Amazonian regional economy and its ecosystems, public policies and management practices must prioritize the adoption of these intensified models, which transform naturally fragile soils into productive and stable carbon sinks. By doing so, it is possible to maintain the region's position as an agricultural powerhouse while restoring the intricate soil networks and carbon sinks that sustain the global environment.

Finally, the presence of native forest fragments remains irreplaceable. These areas serve as vital repositories of specialized microorganisms and complex ecological interactions that are not fully replicated in managed systems. This underscores the fundamental importance of permanent preservation areas (APPs) and legal reserves within rural properties as sources of biological inocula and ecosystem stability.